NASA CR-170397 - Vol - 1

YAV-8B Simulation and Modeling Volume I: Aircraft Description and Program Summary

Contract NAS4-2839
March 1983

NASA

National Aeronautics and
Space Administration

YAV-8B Simulation and Modeling Volume I: Aircraft Description and Program Summary

McDonnell Douglas Corporation
McDonnell Aircraft Company
St. Louis, Missouri 63166

NASA

TABLE OF CONTENTS

TABLE OF CONTENTS (CONT'D)

LIST OF FIGURES

LIST OF FIGURES   (CONT'D)

LIST OF FIGURES (CONT'D)

LIST OF PAGES

1. INTRODUCTION AND SUMMARY

As part of its V/STOL research program, NASA intends to conduct flight investigations of the stability, control and handling qualities of highly augmented V/STOL aircraft. Specific plans include the flight tests of a YAV-8B aircraft, Figures 1-1 and 1-2, modified to include an advanced avionics and flight control system for improved flying qualities and performance.

As an initial phase to this program, NASA will conduct flight tests of the YAV-8B vehicle in order to extract aerodynamic and propulsion characteristics, update existing simulation models, validate handling qualities and design criteria, and to improve V/STOL flight test techniques. This program will also include tests using a static test stand located at the Dryden Flight Research Center, where flight tests of the YAV-8B will take place.

In order to perform high quality parameter estimation and analysis of the YAV-8B characteristics, it is necessary to construct mathematical models of varying complexity and linearity from existing wind tunnel and flight test data.

The McDonnell Aircraft Company (MCAIR) recently completed a V/STOL simulation and modeling study under contract to NASA Dryden. This study defined and documented detailed mathematical models of varying complexity representative of the YAV-8B aircraft. These models will be used by NASA in parameter estimation and in linear analysis computer programs while investigating YAV-8B aircraft handling qualities. Both a six degree of freedom nonlinear model and a linearized three degree of freedom longitudinal and lateral directional model were developed.

The nonlinear model is based on the mathematical model used on the MCAIR YAV-8B manned flight simulator. This simulator model has undergone periodic updating based on the results of approximately 360 YAV-8B flights and 8000 hours of wind tunnel testing. Qualified YAV-8B flight test pilots have commented that the handling qualities characteristics of the simulator are quite representative of the real aircraft. These comments are validated herein by comparing data from both static and dynamic flight test maneuvers to the same obtained using the nonlinear program.

The linearized mathematical model uses stability derivatives and is formatted exactly as the models traditionally used in conventional flight dynamic analysis. Aircraft characteristics were predicted using this linearized model and compared to both the flight data and the nonlinear predictions. To document the aircraft characteristics throughout the flight envelope trim conditions and stability derivatives are provided for 24 flight conditions.

A FORTRAN batch simulation of the nonlinear model has been produced. Documentation for this simulation consists of a description of the software including top level flow charts, program structure, subroutine interfaces, modeling equations, data format, a user's guide, source listings and plots of the over 17,000 aerodynamic and propulsion data points used in the model.

This report is divided into two volumes. Volume I contains the description of the aircraft, documentation of the nonlinear and linear mathematical models, stability derivatives, the comparisons of predicted and actual flight test data which validate the nonlinear model and a discussion of models appropriate for use in parameter estimation programs. Volume II contains the source listings for the nonlinear program and plots of the aerodynamic and propulsion data used in the nonlinear program.
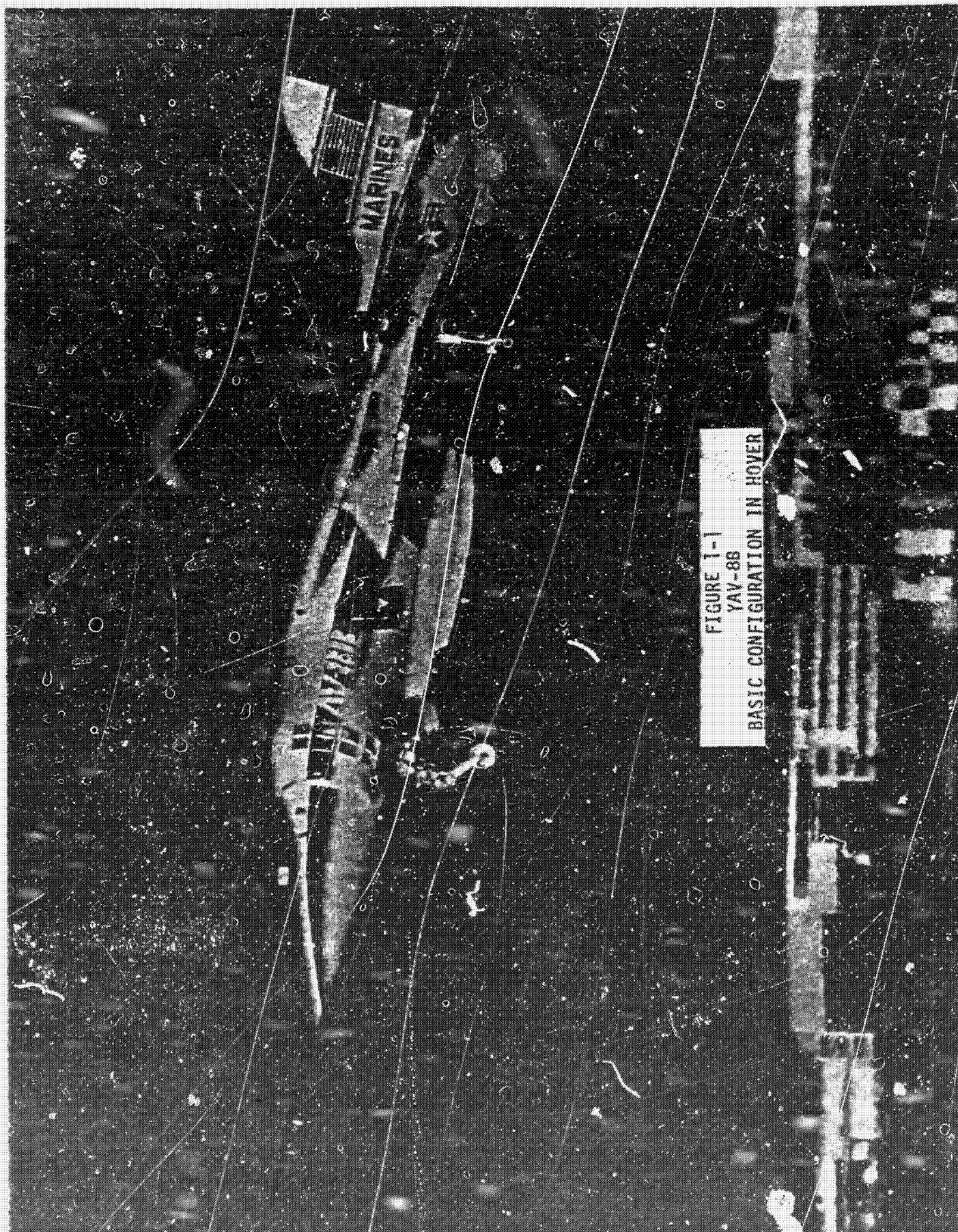
FIGURE 1-1
YAV-8B
BASIC CONFIGURATION IN HOVER
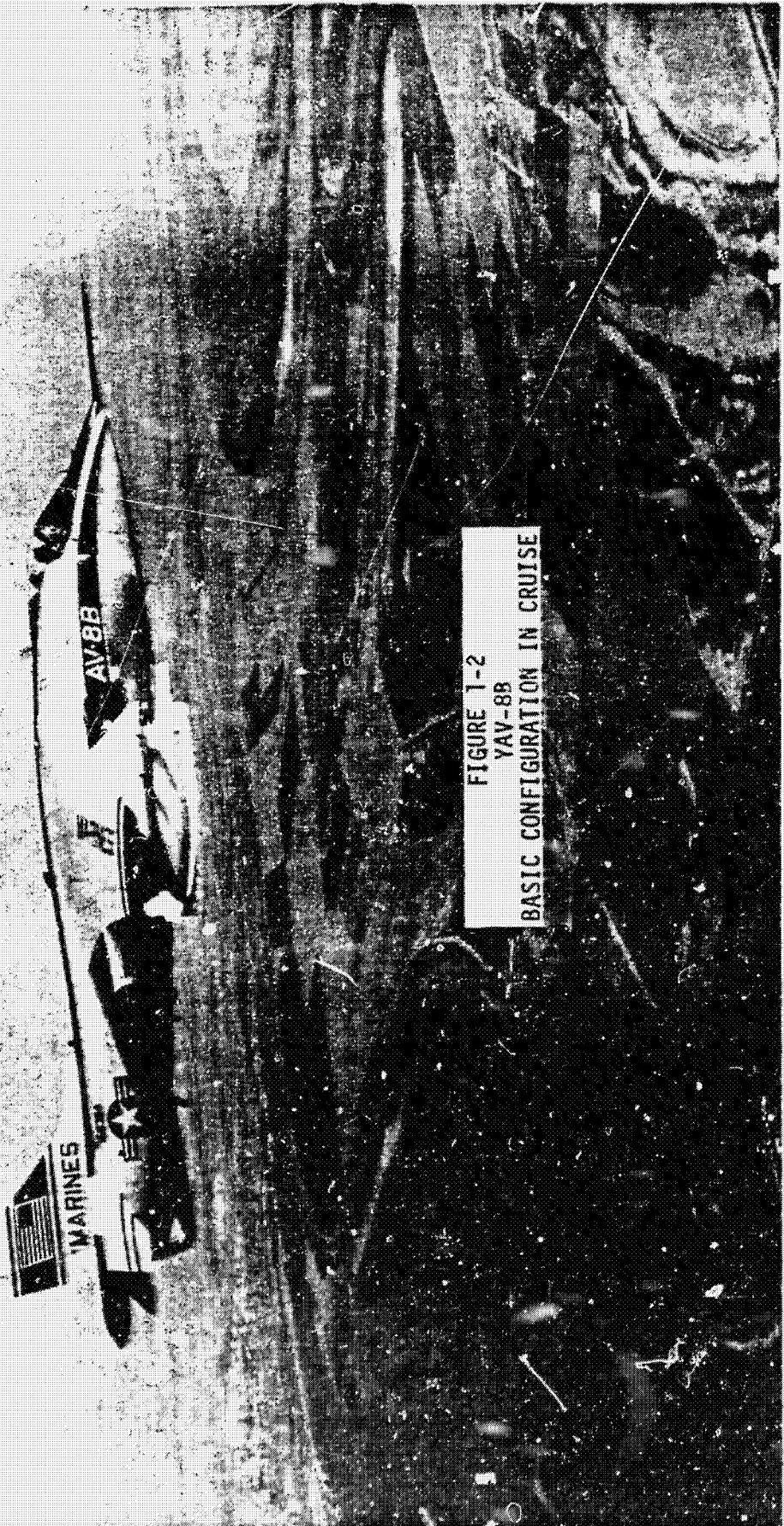
FIGURE 1-2
YAV-8B
BASIC CONFIGURATION IN CRUISE

2. AIRCRAFT DESCRIPTION

2.1 GENERAL ARRANGEMENT

The YAV-8B is a single seat transonic light attack V/STOL aircraft powered by a single YF402-RR-404 turbo-fan engine. The YAV-8B aircraft is an advanced version of the AV-8A aircraft with greatly expanded and improved capabilities. It retains the characteristic appearance of the AV-8A while incorporating an improved inlet design, a larger wing with an advanced technology airfoil, zero degree scarf of the forward nozzles, and under-fuselage modifications called Lift Improvement Devices (LIDs). A three-view general arrangement drawing of the YAV-8B is shown in Figure 2.1-1.

Conventional aerodynamic controls are utilized in wingborne flight and engine bleed air reaction controls are used in jetborne flight, with both systems operative during transition modes.

An all-movable tailplane and front and rear pitch reaction control system (RCS) valves, blowing downward, provide longitudinal control. Lateral control is provided by outboard ailerons and RCS valves, blowing down or up and down for large lateral inputs. Directional control is provided by a conventional rudder and a yaw RCS valve in the aft fuselage tail cone, blowing sideways, left or right.

In the high lift mode for VTO and STO, the ailerons are drooped 15 degrees and the flaps are interconnected with the engine nozzle control. This all is maximum longitudinal acceleration and good longitudinal control mar o be obtained during ground runs and transition to wingborne flight. Shor ndings and vertical landings can be made with either the mid 25° or the full 61.7° flap setting. Conventional landings are made with the 25° flap position.

A maneuvering flap, which can be positioned at any deflection from zero to 25°, is provided for increased maneuverability throughout the flight envelope.

The LIDs consist of a retractable fuselage fence located at the forward end of the gun pods and two fixed strakes on the gun pods. Larger strakes are provided for attachment to the fuselage when gun pods are not carried.

The YAV-8B has provisions for external store loadings on six wing stations and the fuselage centerline. In addition, guns in two pod can be attached to the fuselage. Recent flight testing of the YAV-8B has been performed using a removable Leading Edge Root Extension (LERX). This device, designed to increase the wingborne maneuverability, has only a small effect on the V/STOL flight characteristics. Since considerably more flight data exists on the aircraft without the LERX this report assumes the aircraft to be configured without the LERX in the Basic configuration of (5) pylons and (2) gun pods.

ORIGINAL PAGE IS
OF POOR QUALITY

YAV-8B THREE VIEW
FIGURE 2 1 1

2.2 DIMENSIONAL DATA

Details of YAV-8B physical characteristics are presented in this section.

2.2.0 WEIGHT AND FUEL CAPACITY

Operating Weight, Flight Test Aircraft – Lb	13847
Internal Fuel – Lb	7185

2.2.1 WING DIMENSIONAL DATA

Area (theorectical) – Ft^2	230.0
Span (projected) – Ft	30.33
Aspect Ratio	4.0
Taper Ratio	0.3

Chords (projected):

Root (theoretical) – In	139.99
Tip (theoretical) – In	42.0
Mean Aerodynamic – In	99.79

Thickness Ratio (t/c) (FIGURE 2.2-1)

Root – %	11.5
Tip – %	7.6

Incidence (with respect to FRL):

Root (exposed theoretical) – Deg.	3.0
Tip – Deg.	-5.0

Sweepback (projected):

Leading Edge – Deg.	36.0
1/4 Chord Line – Deg.	30.62

Dihedral – Deg.	-1.
Twist (FIGURE 2.2-2) – Deg.	-8
Airfoil (FIGURES 2.2-3 and 2.2-4)	Modified Supercritical

2.2.2 HORIZONTAL TAIL DIMENSIONAL DATA

Area (projected) – Ft^2	47.54
Span (projected) – Ft	13.92
Aspect Ratio	4.079
Taper Ratio	0.201

Sweepback (projected):

Leading Edge (theoretical) - Deg.	39.81
1/4 Chord Line (theoretical) - Deg.	33.91
Trailing Edge - Deg.	10.77

Dihedral - Deg.   -15.84

Chords:

Root (centerline of airplane) - In.	67.39
Tip (theoretical) - In.	13.56
Mean Aerodynamic chord - In.	46.44

Pivot Line Location: % MAC_{HT}

   (F.S. 559.05 and W.L. 22.35)   22.42

Airfoil Section: HSA Symmetric

Thickness Ratio (t/c):

Root (centerline of airplane)	.07
Tip (theoretical)	.07

Tail Length (from 25% wing MAC to 25% tail MAC) - In.   199.01
Horizontal Tail Volume Ratio   .412

Deflection (with respect to water line plane)
(Includes ± 1.5° Autostab)

Maximum Nose down - Deg.	-11.75
Maximum Nose up - Deg.	+12.75

2.2.3 VERTICAL TAIL DIMENSIONAL DATA

Area (theoretical above W.L. 126.50) - Ft^2	25.83
Span (W.L. 126.50 to W.L. 194.00) - Ft	5.63
Aspect Ratio	1.23
Taper Ratio	.268

Chord:

Root (W.L. 126.50) - In.	86.93
Tip (theoretical) (W.L. 194.00) - In	23.3
Mean Aerodynamic Chord (W.L. 153.76) - In	61.24

Airfoil Section: HSA Symmetric

Thickness Ratio (t/c):

Root (W.L. 126.50)	.082
Tip (theoretical) (W.L. 194.00)	.052

ORIGINAL PAGE IS
OF POOR QUALITY

Sweepback:

Leading Edge - Deg.	47.36
1/4 Chord - Deg.	40.37
Trailing Edge - Deg.	8.15

Tail Length (from 25% wing MAC to 25% tail MAC) - In	187.99
Vertical Tail Volume Ratio	.058

2.2.4 FUSELAGE DIMENSIONAL DATA

Length (maximum) (parallel to water line) - Ft	42.89
Width (maximum) - Ft	8.00
Depth (maximum) - Ft	5.60
Maximum Frontal Area (fuselage alone) - Ft^2	19.2
Maximum Frontal Area (including inlets) - Ft^2	31.5
Thrust Axis (zero nozzle deflection) (with respect to W.L.) - Deg.	1.50

2.2.5 FLAP DATA

Area (per side) - Ft^2	15.49
Span (per side) - In	64.54
Deflection:	
STO Mode	
$\theta_J \geq 50°$ - Deg.	61.7
$\theta_J \leq 25°$ - Deg.	25
NORMAL Mode - Leg.	0-25

2.2.6 AILERON DATA

Area (per side) - Ft^2	6.19
Span (per side) - In	58.9
Deflection (including $\pm 2°$ Autostab)	
Undrooped - Deg.	+12/-27
With 15° droop - Deg.	+27.2/-10.4
NOTE (Lateral stick travel restricted to 75% of full deflection above 250 KIAS)	

2.2.7 RUDDER DATA

Area - Ft^2	5.27
Span - In	60.75
Hinge Line Location - % W.L. Chord	
Root (W.L. 126.50)	11.87
Tip (W.L. 187.25)	33.68
Sweepback of Hinge Line - Deg	12.73
Deflection - Deg	± 15.0

2.2.8 REACTION CONTROL SYSTEM

Front Fuselage Pitch Nozzle (thrusting upward)

Position - In F.S.	137.48
W.L.	70.36
B.L.	0.00
Thrust Incidence (with respect to W.L.) - Deg	97.63
(with respect to B.L.) - Deg	0.00

Rear Fuselage Pitch Nozzle (thrusting upward)

Position - In F.S.	605.51
W.L.	114.63
B.L.	0.00
Thrust Incidence (with respect to W.L.) - Deg	82.00
(with respect to B.L.) - Deg	0.00

Rear Fuselage Yaw Nozzles (thrusting port and starboard)

Position - In F.S.	599.00
W.L.	120.50
B.L.	0.00
Thrust Incidence (with respect to B.L.) - Deg	+90.00
(with respect to W.L.) - Deg	0.00

Wing (port and starboard) roll nozzles
            (thrusting upward)

Position - In F.S.	432.45
W.L.	83.89
B.L.	177.84
Thrust Incidence (with respect to W.L.) - Deg	83.00
(with respect to B.L.) - Deg	Outbd 5.00

Wing (port and starboard) roll nozzles
            (thrusting downward)

Position - In F.S.	432.45
W.L.	83.89
B.L.	177.84
Thrust Incidence (with respect to W.L.) - Deg	263.00
(with respect to B.L.) Deg	Inbd 5.00

Reaction Control System moments versus control surface deflection or stick position

OX of maximum moment for stabilator @ 2°
100% of maximum moment for stabilator @ + 10° and -3°

OX of maximum moments for neutral lateral stick
100% of maximum downblowing moments fo: 55% (2.31 in) of maximum lateral stick deflection

OX of maximum upblowing moments for neutral to 55% (2.31 in) of maximum lateral stick deflection
100% of maximum upblowing moments for 80% (3.365 in) lateral stick deflection

OX maximum moments for rudder @ 0°
100% of maximum moments for rudder @ +10° and -10°

GP21-0992-1
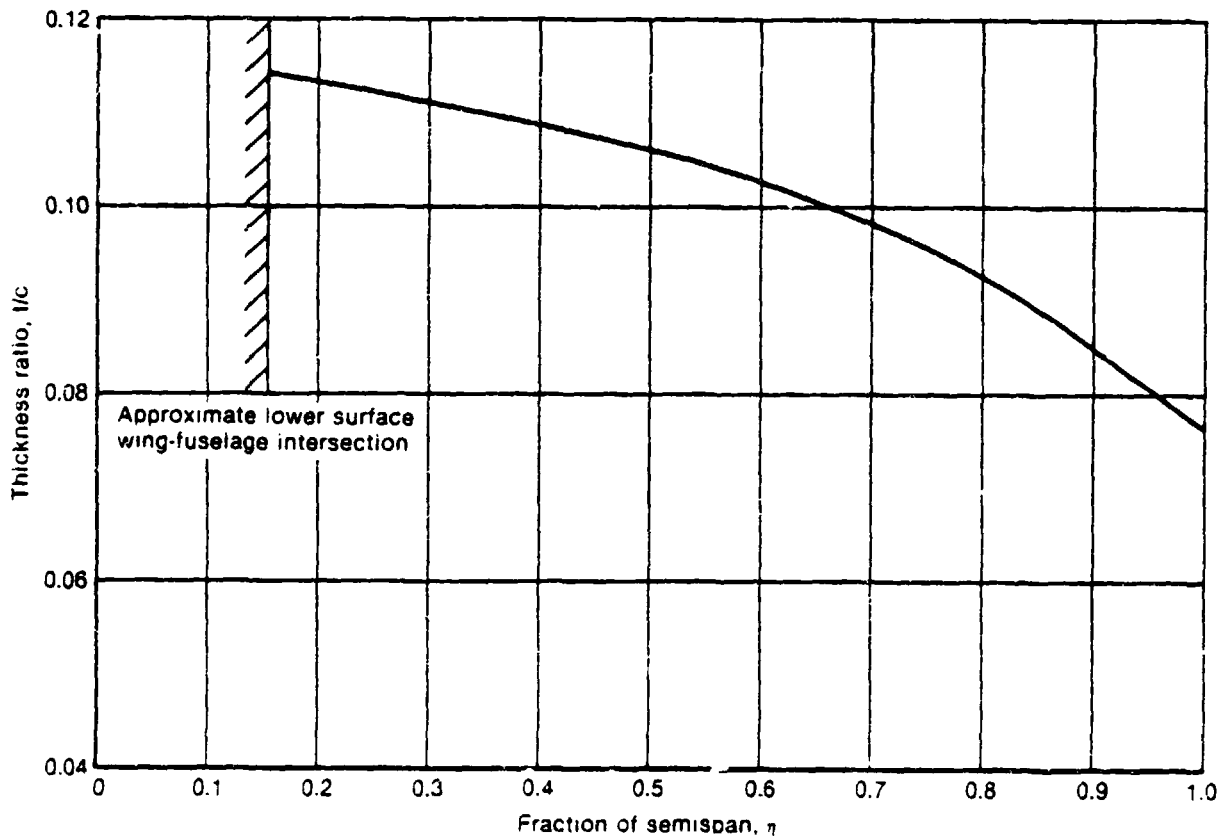
FIGURE 2.2-1
YAV-8B SPANWISE THICKNESS DISTRIBUTION COMPARISON
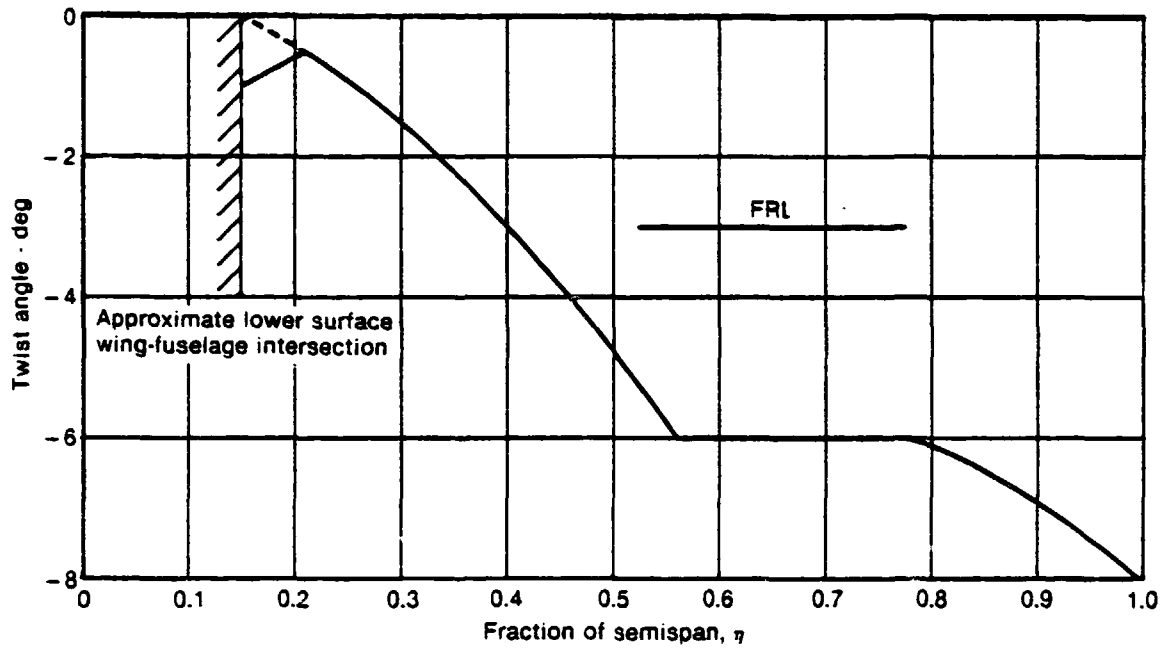
GP21-0082-2

FIGURE 2.2-2
YAV-8B GEOMETRIC TWST DISTRIBUTION
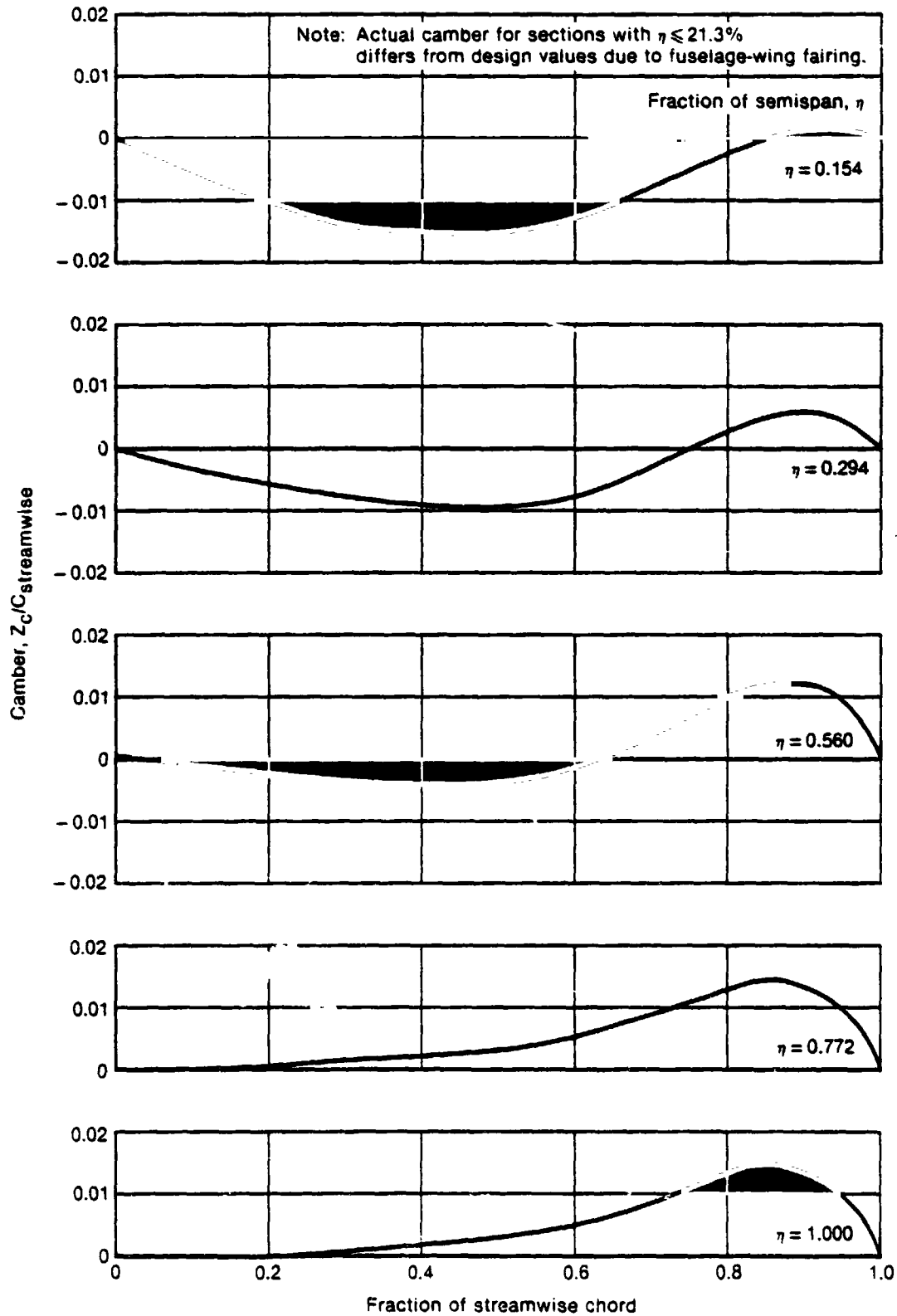
FIGURE 2.2-3
YAV-8B DESIGN STREAMWISE CAMBER DISTRIBUTION
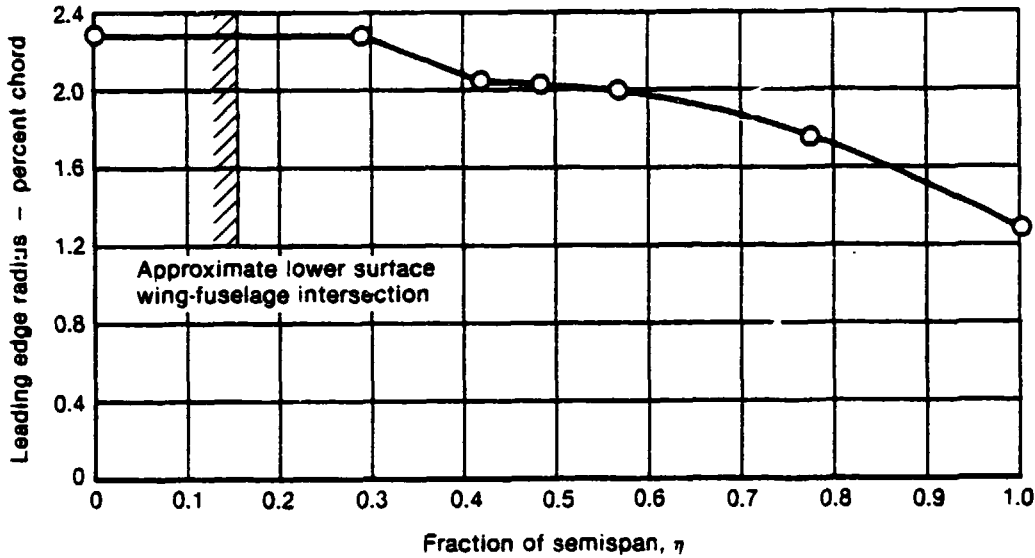
FIGURE 2.2-4
YAV-8B LEADING EDGE RADIUS DISTRIBUTION

QP21-0002-4

2.3 WEIGHT AND BALANCE DATA - Included within this section are the weight, inertia, and center of gravity data for the YAV-8B flight test configuration or clean aircraft with (2) gun pods, (2) inboard pylons, (2) intermediate pylons, and centerline rack. The moment of inertia and C.G. position data for this configuration are shown in Figure 2.3-1. In addition to the effect of pylons and gun pods, the zero fuel weight includes the pilot, oil, trapped fuel, and oxygen. A center of gravity envelope is presented in Figure 2.3-2.

GROSS WEIGHT-LB	FUEL-LB	GEAR	MOMENT OF INERTIA, SLUG-FT²				CENTER OF GRAVITY-IN		
			I_{xx} (ROLL)	I_{yy} (PITCH)	I_{zz} (YAW)	I_{xz}	FUSELAGE STATION	BUTT-LINE	WATER-LINE
1. 21527	7185	DOWN	10530	32948	39794	1871	350.7	.042	98.9
1. 21527	7185	UP	12210	33098	40262	1860	350.9	.042	99.9
2. 21032	7185	UP	10200	32788	39951	1872	349.9	.043	99.9
3. 19133	5286	UP	9624	32149	39204	1605	348.5	.048	97.7
4. 18158	4311	UP	9099	31860	38634	1499	347.7	.050	97.2
5. 16280	2433	UP	6227	31081	35157	1371	344.2	.056	96.5
6. 14657	810	UP	6010	28889	32818	1153	343.4	.062	95.7
7. 14254	407	UP	5927	28556	32460	1053	344.4	.063	96.1
8. 13847	0	UP	5832	28492	32388	1036	344.6	.066	96.6
8. 13847	0	DOWN	6152	28342	31920	1047	344.3	.066	94.9

1. Takeoff Gross Weight
2. Water Expended
3. Wing Fuel Partially Expended
4. Combat Weight (40% Fuel Expended)
5. Wing Fuel Expended
6. Fuselage Fuel Partially Expended
7. Fuselage Fuel Expended
8. Feed Tank Fuel Expended

FIGURE 2.3-1
YAV-8B FLIGHT TEST AIRCRAFT INERTIA AND C.G. DATA

1. Takeoff gross weight
2. Water expended
3. Wing fuel partially expended
4. Combat weight (40% fuel expended)
5. Wing fuel expended
6. Fuselage fuel partially expended
7. Fuselage fuel expended
8. Feed tank fuel expended
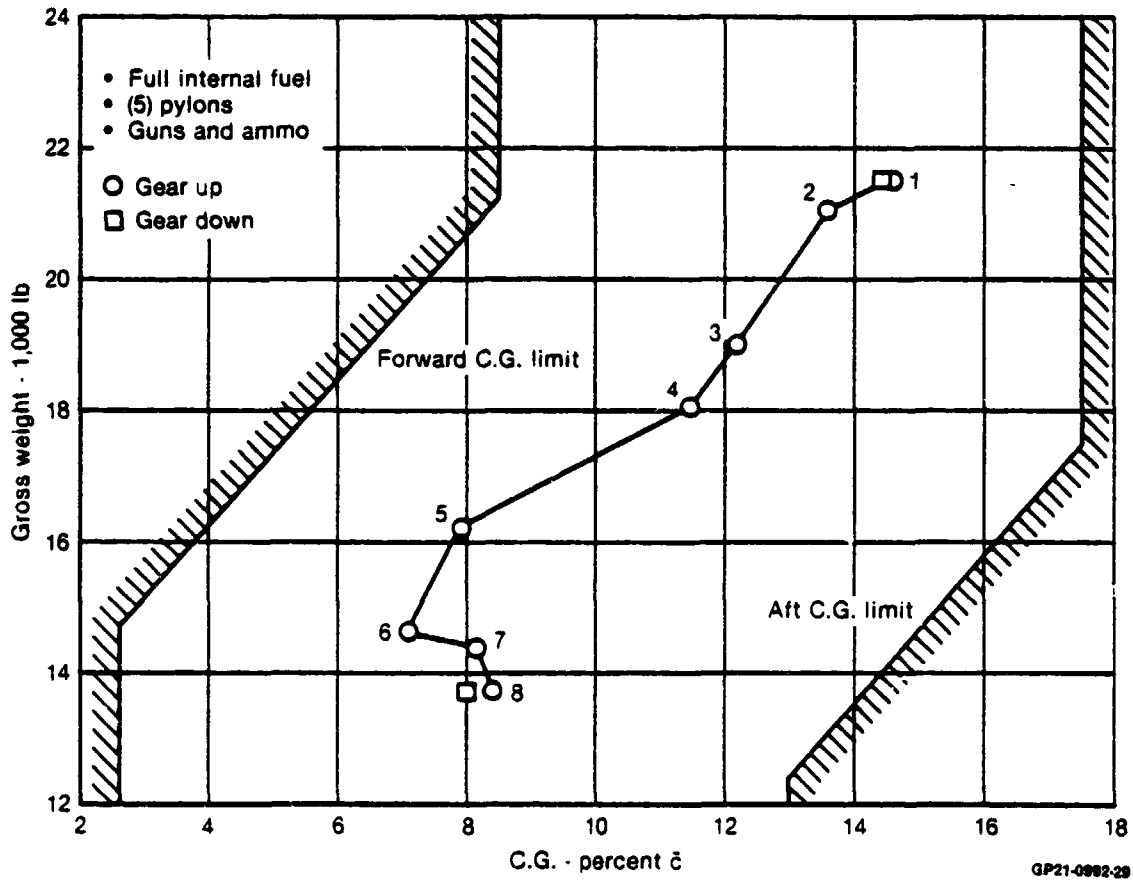
**FIGURE 2.3-2
YAV-8B FLIGHT TEST AIRCRAFT
CENTER OF GRAVITY ENVELOPE**

2.4 FLIGHT CONTROL SYSTEM

The YAV-8B flight control system consists of conventional ailerons, rudder, and stabilator, with a reaction control system (RCS) acting about all three axes during hover and transition. The stabilator and ailerons are power operated while the rudder is connected directly to the rudder pedals. In view of the ineffectiveness of aerodynamic controls at low speeds, high pressure compressor bleed air is fed to the aircraft extremities and ejected through variable shutter valves connected to the conventional controls to provide reaction control.

A single channel limited authority stability augmentation system (SAS) is provided to facilitate control in hover and transition. It may be selected "on" whenever the aircraft is flying below 250 KIAS with either the gear or flaps extended.

2.4.1 LONGITUDINAL CONTROL SYSTEM

2.4.1 LONGITUDINAL CONTROL SYSTEM - Longitudinal control of the aircraft is maintained by a combination of a stabilator and reaction control system as shown in Figure 2.4-1. Control stick movement is transferred to the stabilator as shown in Figure 2.4-2. Longitudinal feel is provided by a hydraulic q-feel unit, augmented by nonlinear backup springs and a bobweight. The bobweight contributes 1.5 lb/g at the stick, generated by vertical g forces. The stick force gradient and dynamic pressure relationship is shown in Figure 2.4-3. This q-feel unit is operative above 250 KIAS and provides a stick stiffness increasing in proportion to dynamic pressure. Longitudinal trim is obtained by electrically biasing the q-feel unit which ensures full control authority. Trim capability is from -4 to +7.5 degrees of stabilator and operates at 2.2 degrees/sec. The effect of trim range on spring force is shown in Figure 2.4-4.

Low speed pitch control is by reaction control valves at the nose and at the rear fuselage extension, the latter being fed through the same ducting as the yaw valves. The front pitch shutter is linked to the control column, and the rear shutter is linked to the stabilator. The relation of stabilator/stick position to pitch valve opening is shown in Figure 2.4-5. The pitch RCV valves thrust upward.

The pitch autostabilizer has an authority of ±1.5 degrees of stabilator and works through the forward and aft reaction control valves. The forward RCS SAS can be disengaged separately.

2.4.2 LATERAL CONTROL SYSTEM

2.4.2 LATERAL CONTROL SYSTEM - Conventional ailerons in combination with reaction controls provide lateral control as shown in Figure 2.4-6. The ailerons are power-operated with artificial feel derived from a nonlinear spring, which can be biased by an electrical trim motor. Trim capability is equivalent to 1/3 of lateral stick deflection and operates at 1 deg/sec of aileron. The aileron deflection and spring force due to stick movement are shown in Figure 2.4-7. Lateral stick travel is restricted to 75% of full deflection above 250 KIAS, but the pilot can override the limiter in an emergency.

ORIGINAL PAGE IS
OF POOR QUALITY
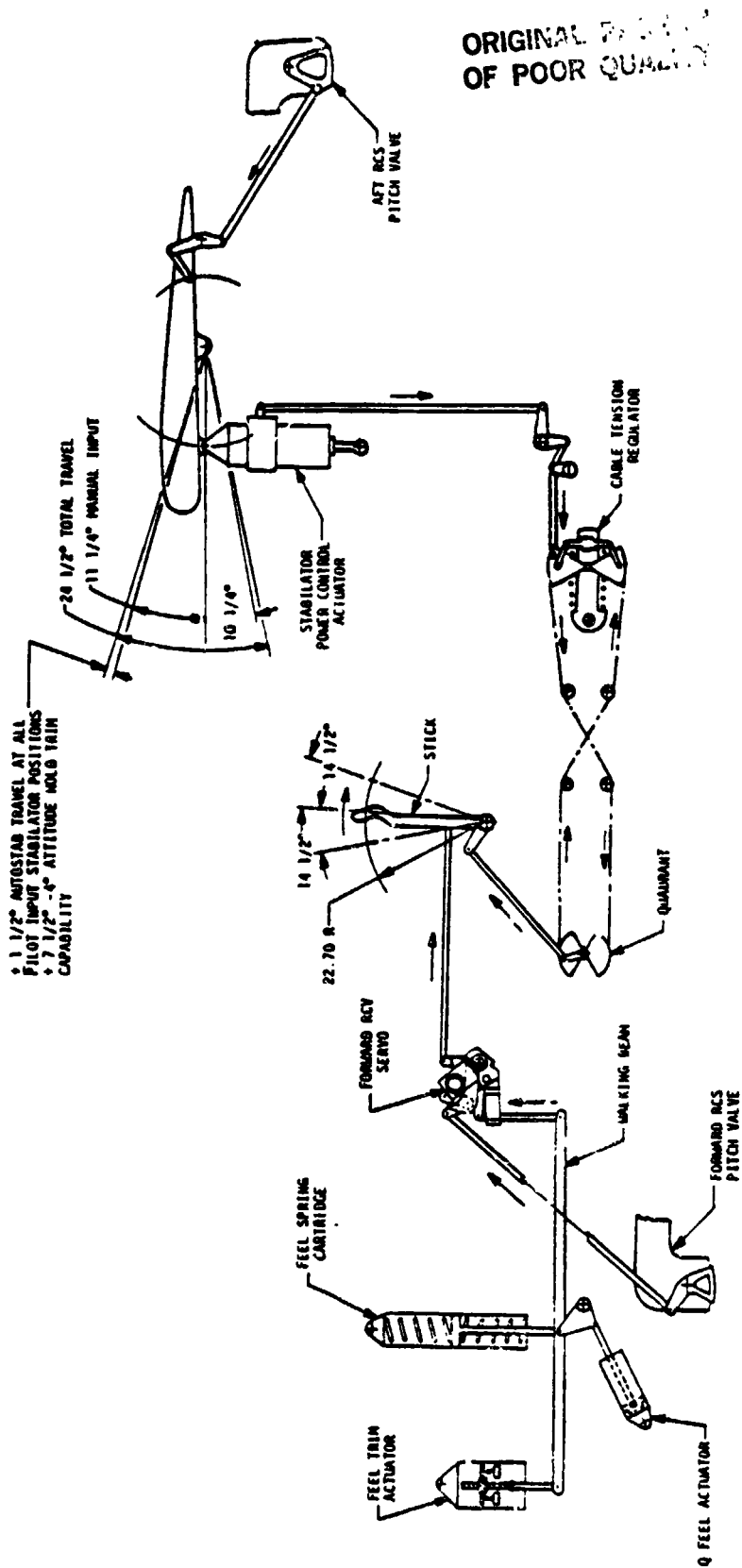
FIGURE 2.4-1
YAV-8B LONGITUDINAL CONTROL SYSTEM
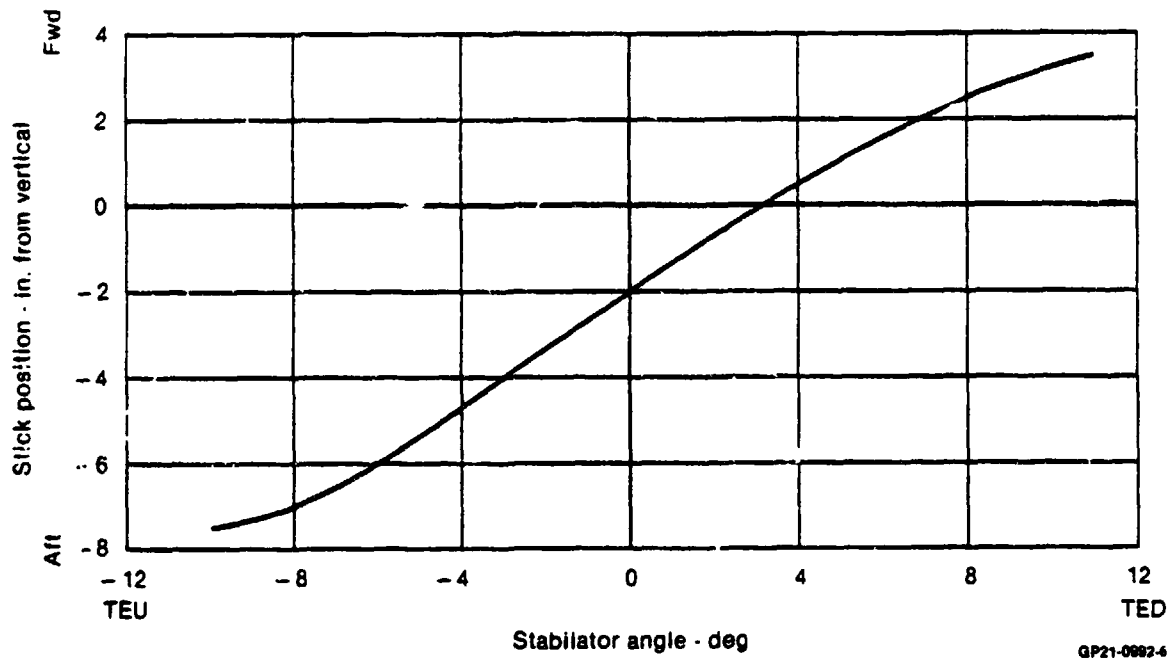
FIGURE 2.4-2
YAV-8B STABILATOR ANGLE vs STICK POSITION
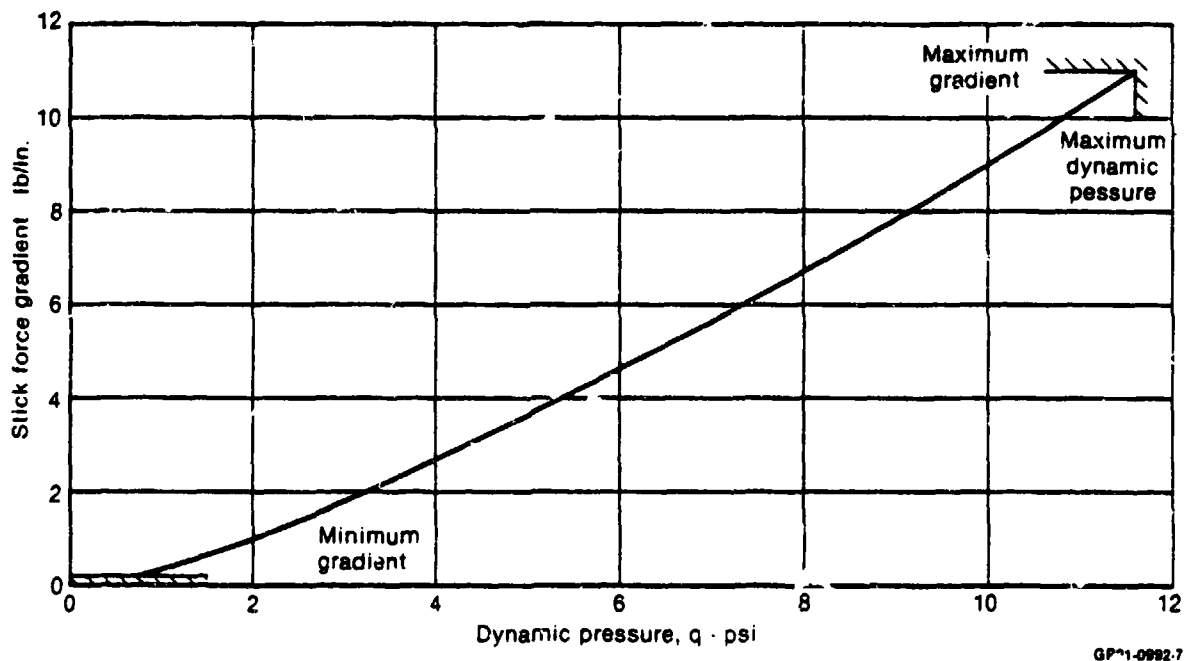
FIGURE 2.4-3
YAV-8B LONGITUDINAL Q — FEEL SYSTEM
For V_{cal} > 250 kts
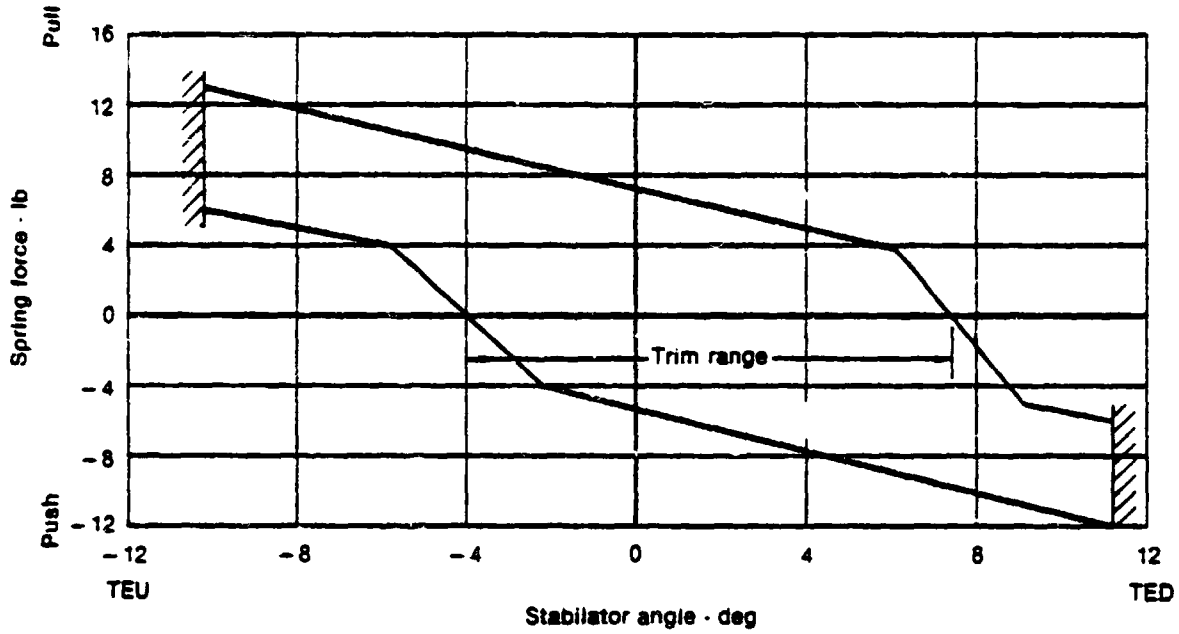
**FIGURE 2.4-4
YAV-8B EFFECT OF TRIM RANGE ON
LONGITUDINAL SPRING FORCE**
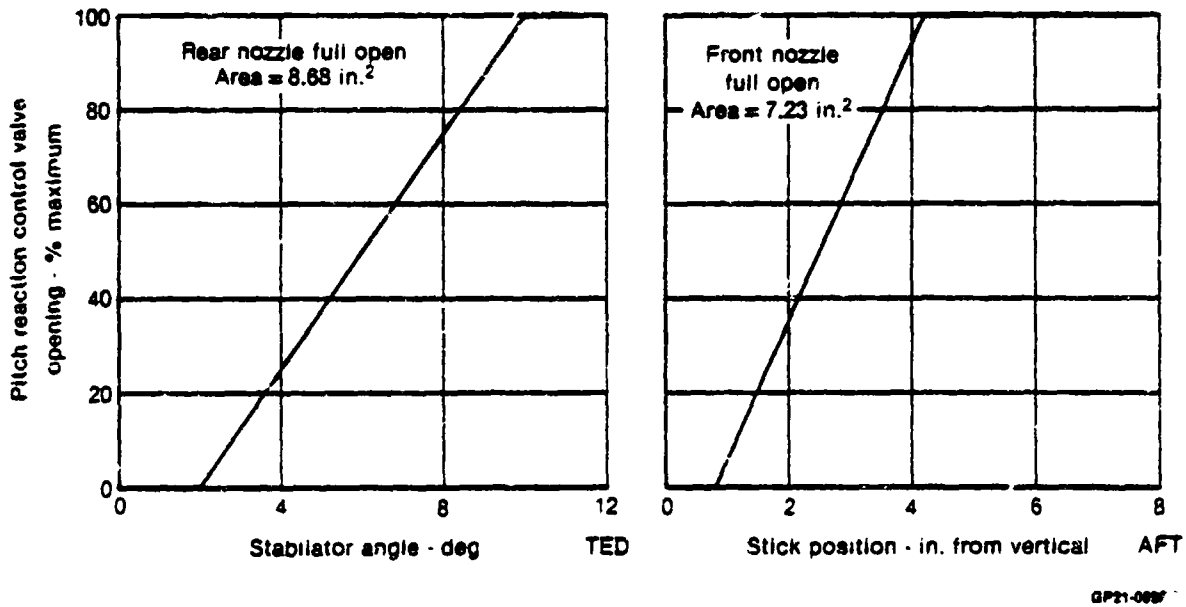
**FIGURE 2.4-5
YAV-8B LONGITUDINAL RCS VALVE OPENINGS**
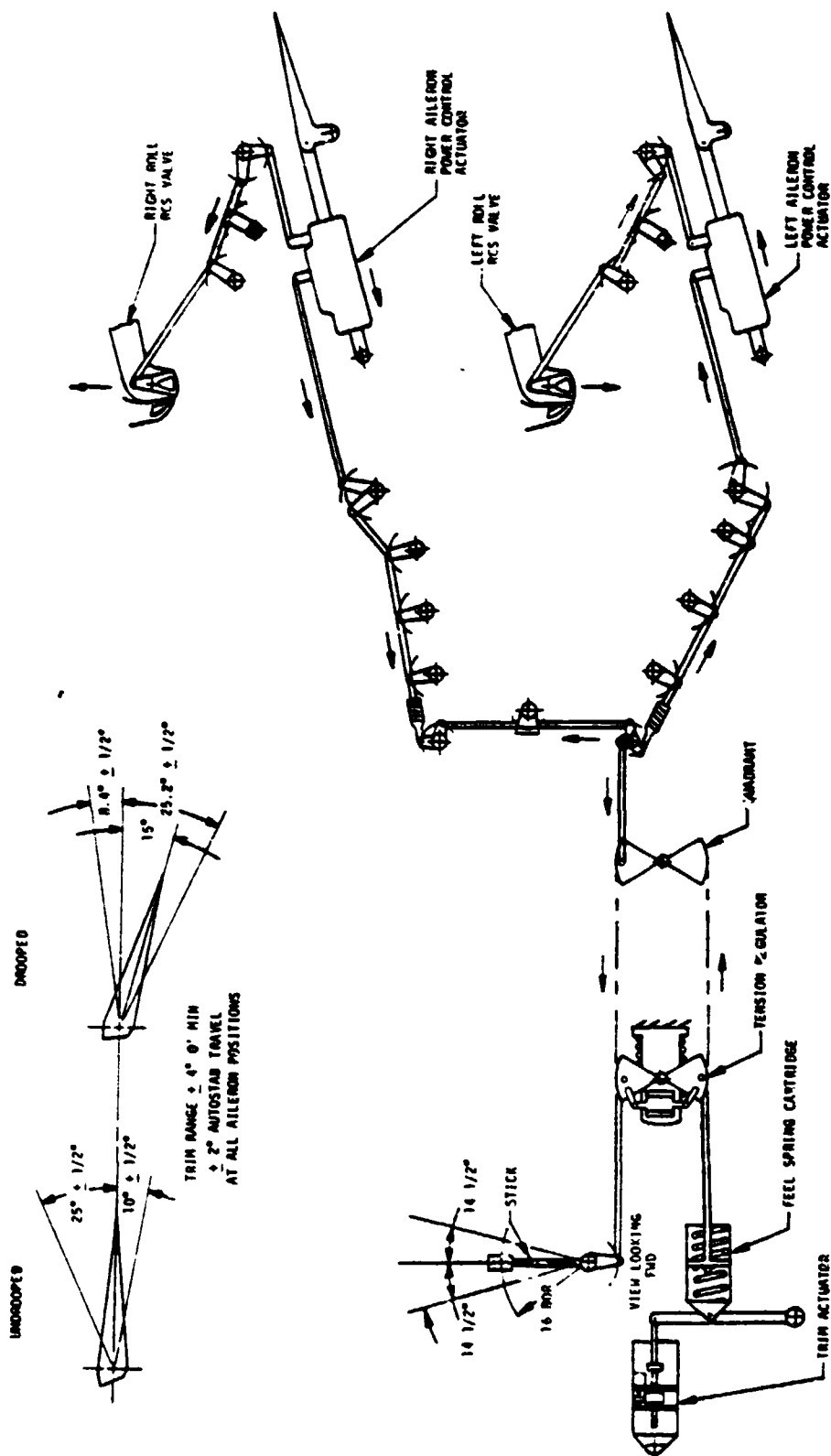
FIGURE 2.4-6
YAV-8B LATERAL CONTROL SYSTEM
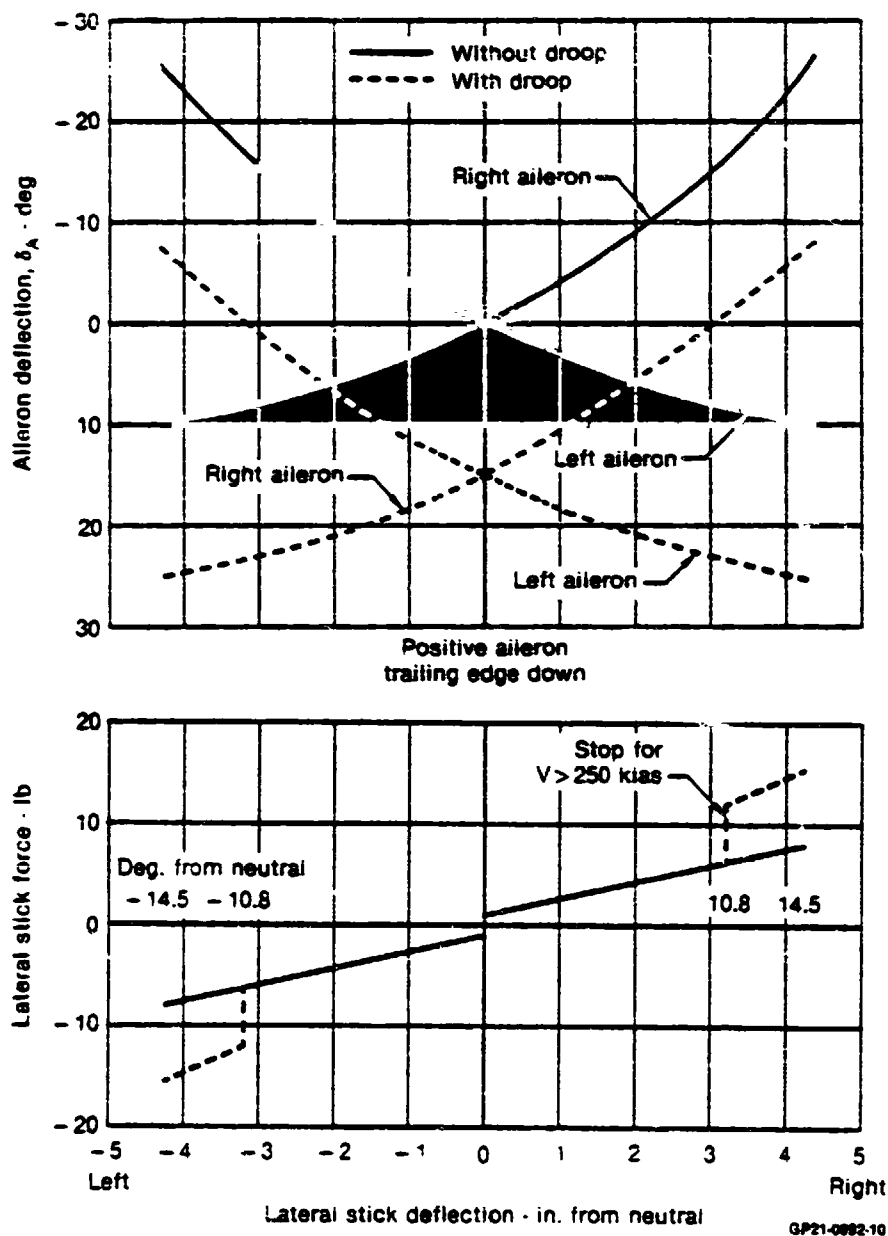
**FIGURE 2.4-7
YAV-8B LATERAL STICK CHARACTERISTICS**

Roll control valves on the wing tips are linked to the ailerons and thrust either up or down. Lateral stick position versus roll valve opening is shown in Figure 2.4-8.

A roll auto stabilizer, similar to the pitch system, is also provided in the stability augmentation system (SAS) and has an authority of $\pm2°$ of aileron.

2.4.3 DIRECTIONAL CONTROL SYSTEM - Directional control is provided by a combination of a conventional unpowered rudder and directional reaction controls as shown in Figure 2.4-9. Rudder feel is primarily aerodynamic but a centering spring is fitted to produce some feel at low speeds. Rudder deflection and spring force versus pedal deflection are shown in Figure 2.4-10. The rudder trim has a capability of $\pm9.5°$ of deflection.
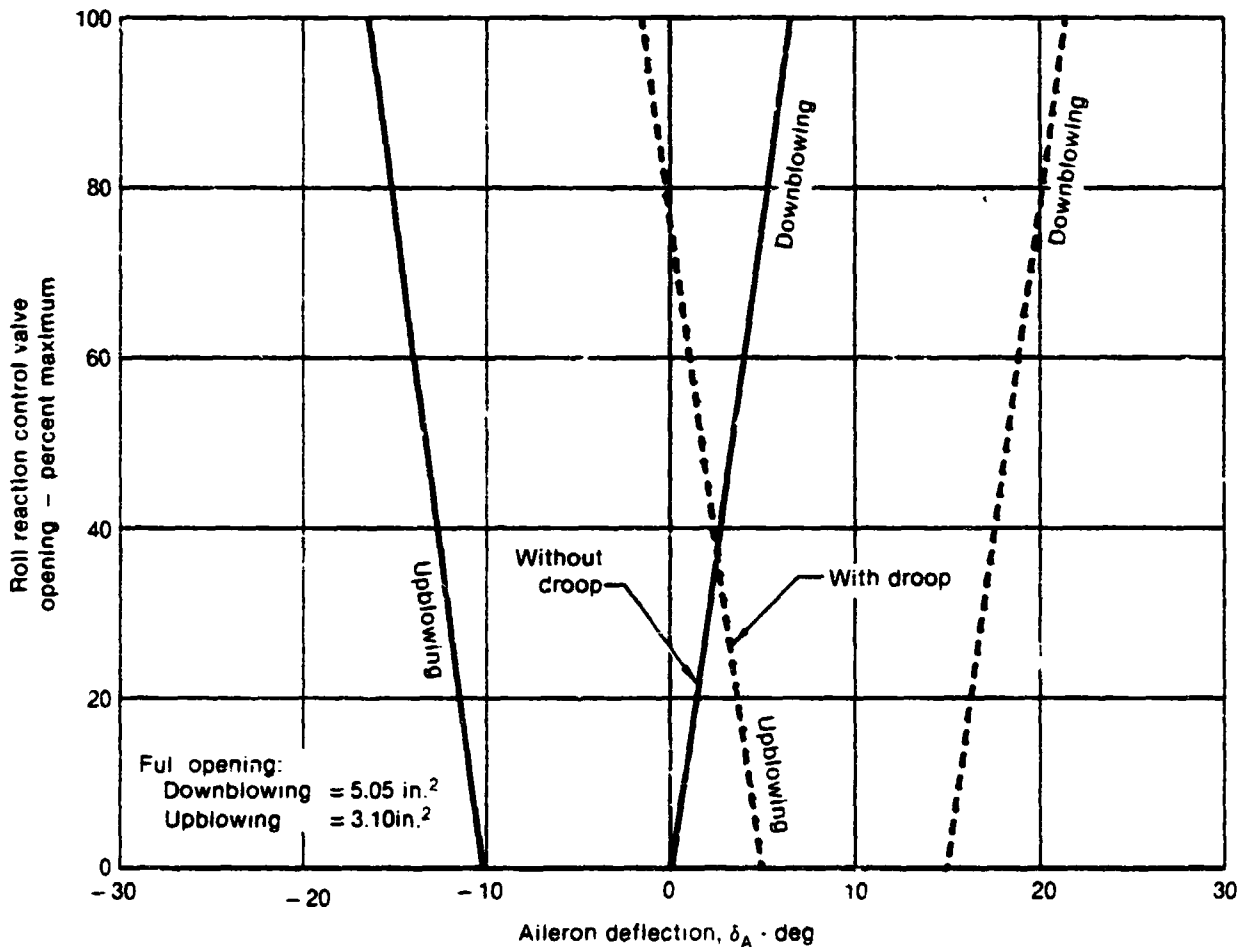
GP21-0992-11

FIGURE 2.4-8
YAV-8B LATERAL RCS VALVE OPENINGS
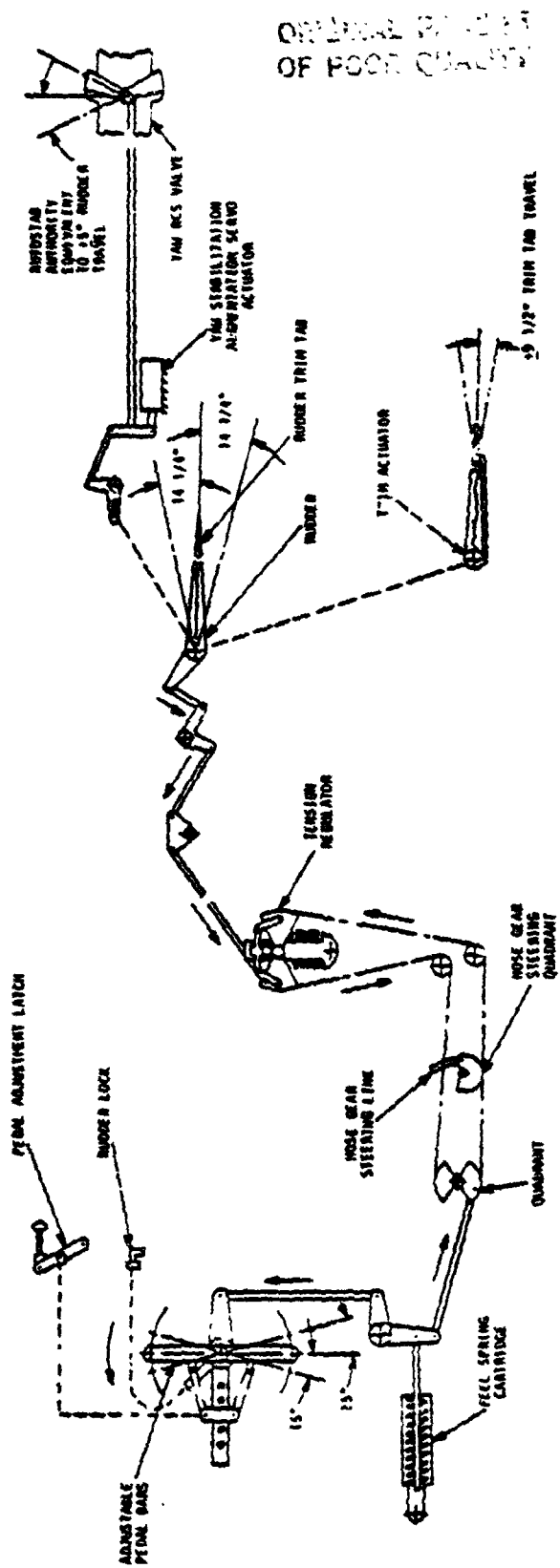
ORIGINAL PAGE IS
OF POOR QUALITY

FIGURE 2.4-9
YAV-8B DIRECTIONAL CONTROL SYSTEM
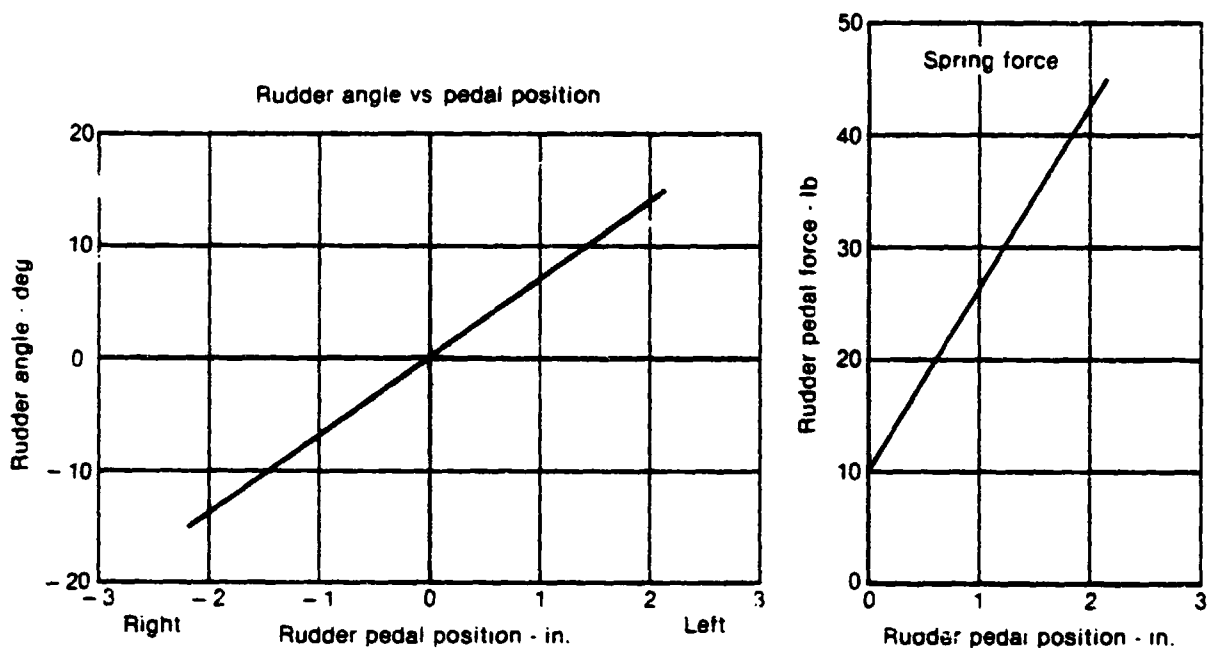
FIGURE 2.4-10
YAV-8B DIRECTIONAL CONTROL SYSTEM CHARACTERISTICS

Reaction control in yaw is by port and starboard valves in the rear fuselage extension, the shutter being opened by rudder movement as shown in Figure 2.4-11.

The yaw autostabilizer is provided in the SAS and has a yaw reaction jet authority of +5 degrees of equivalent rudder.

2.4.4 FLAPS AND DROOPED AILERONS - The YAV-8B high lift system consists of single slotted flaps and drooped ailerons. Operation of the flap and aileron droop system is controlled by three switches (flap actuation switch, flap mode switch and flap position switch). The flap switches and system logic are presented in Figure 2.4-12 and discussed below.

2.4.4.1 Flap Actuation Switch - This 3-position, toggle lever-lock, flap switch is located on the left aft console. Switch positions are ON (neutral), OFF (aft) and RESET (forward). Selection of the ON position activates the entire flap system and locks the switch out of the OFF position with the lever-lock. RESET is a momentary position which reactivates the normal modes of flap operation if the system has failed due to a transient electrical problem. Flap asymmetry must be corrected before RESETting the flap system.
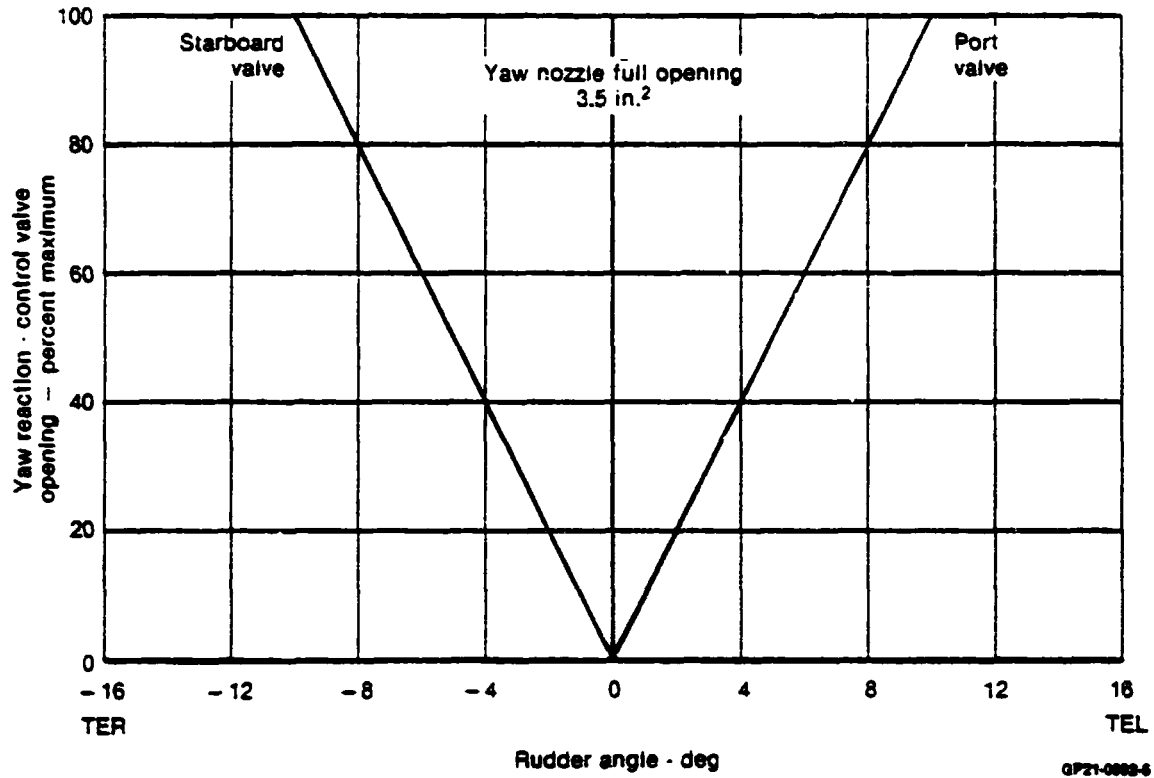
FIGURE 2.4-11
YAV-8B
DIRECTIONAL RCS NOZZLE OPENINGS
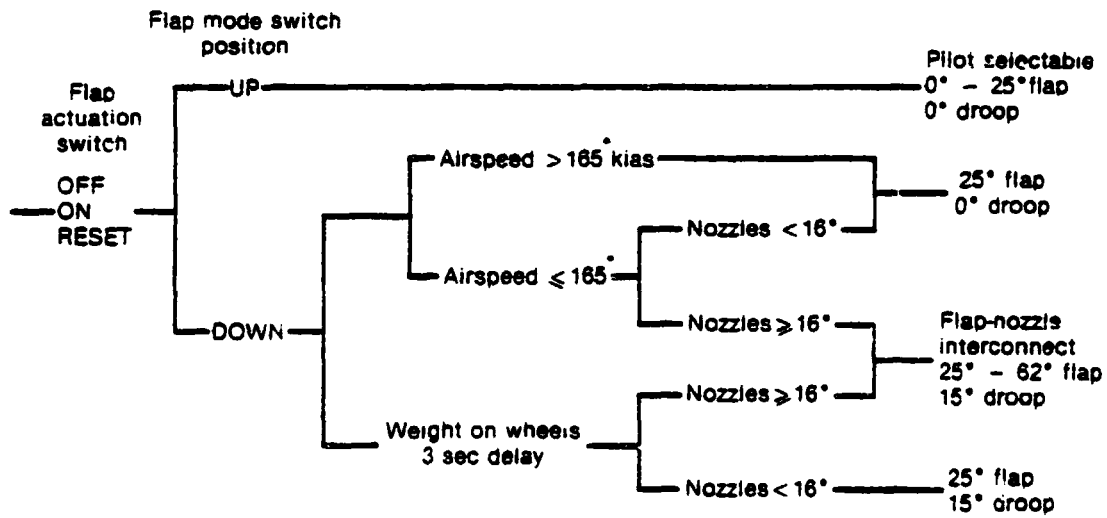
*165 kias is nominal. Hysteresis results in 155 kias
if decelerating and 175 kias if accelerating

GP21-0992-13

FIGURE 2.4-12
YAV-8B FLAP SYSTEM/AILERON DROOP LOGIC

2.4.4.2 <u>Flap Mode Switch</u> - This 2-position switch is located on the left
forward console. Switch positions are <u>DOWN</u> and <u>UP</u>. The <u>DOWN</u> position is
used for both takeoff and landing. The <u>DOWN</u> mode switch position activates
the flap-nozzle interconnect schedule (shown in Figure 2.4-13) if the air-
speed is less than approximately 165 KIAS (actual airspeed limits are 175
KIAS accelerating and 155 KIAS decelerating). The flaps move down at 45.9
degrees per second and up at 64 degrees per second (no load rates). The
flap-nozzle interconnect is overridden at higher than the above-mentioned
airspeeds, and the flaps are driven to the 25 degrees position at a 7 degree
per second no-load rate. The maximum nozzle rotation rate is about 90
degrees per second.

The <u>DOWN</u> flap mode switch position also activates the aileron droop
system, deflecting the ailerons down 15 degrees (at a no-load rate of 8
degrees per second), whenever the pilot commands the nozzles to 16 degrees or
greater and the airspeed is less than approximately 165 KIAS (actual airspeed
limits are 175 KIAS accelerating and 155 KIAS decelerating). Aileron
retraction is at 5.5 degrees per second no-load rate. Aileron droop is
available at any nozzle angle while on the ground by a weight on wheels
switch with a 3 second time delay. This system allows checkout on the
ground, and assures full droop at the moment of nozzle rotation during
short takeoffs. The 3 second time delay prevents premature droop retraction
if the aircraft becomes light on the gear during lightweight takeoffs prior
to nozzle rotation.
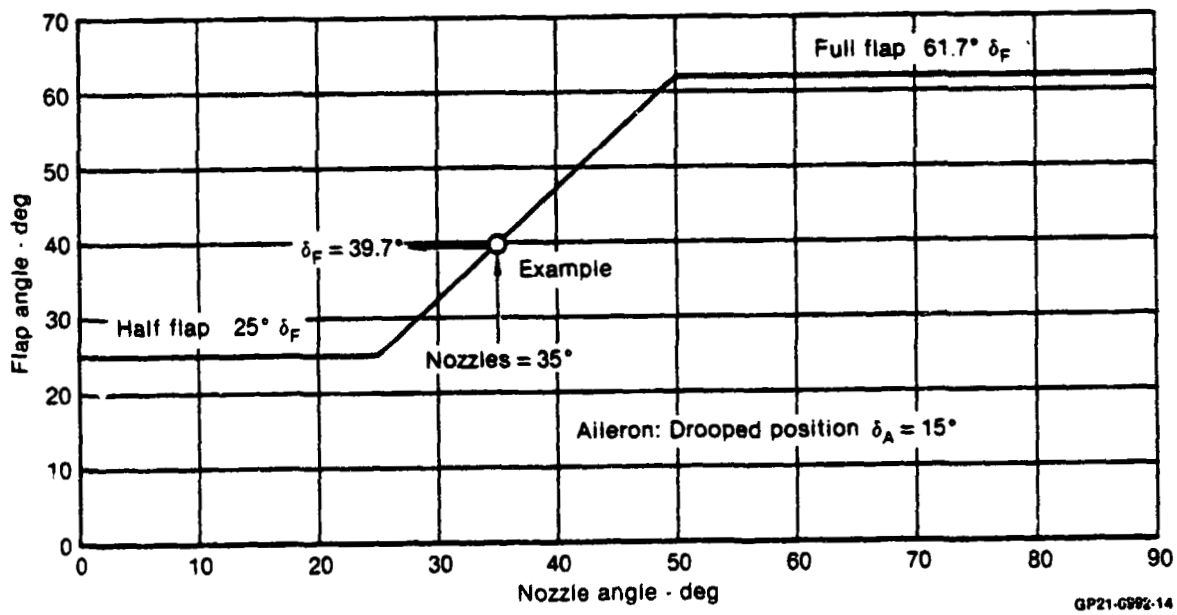
FIGURE 2.4-13
FLAP-NOZZLE INTERCONNECT SCHEDULE
Static Relative Angles
Flap Mode Switch — DOWN

When <u>UP</u>, the switch energizes the flap position switch on the throttle handle allowing pilot control of flap position. If <u>UP</u> flap mode is selected from the DOWN mode, the flaps will retract to 0° at a 7° per second no-load rate and the ailerons will undroop at a no-load rate of 5.5° per second.

2.4.4.3 <u>Flap Position Switch</u> - This 3-position switch on the throttle lever is thumb operated, momentary spring-loaded to the OFF position. Switch positions are <u>UP</u> (forward), <u>DOWN</u> (aft) and <u>OFF</u> (neutral). With the <u>UP</u> flap mode selected, this switch allows the pilot to select any flap position from 0° to 25° at a 7° per second no-load rate. Flap travel continues so long as the pilot displaces the switch in the selected direction or until 0° or 25° flap travel is reached.

2.4.4.4 <u>Flap Asymmetry</u> - If flap position asymmetry reaches 5°, the flaps stop at the failed position. The flaps can be raised by using the throttle lever switch. No asymmetry comparison is provided in this mode.

2.4.5 <u>LIFT IMPROVEMENT DEVICE SYSTEM (LIDS)</u> - The LIDS consists of a retractable fence located between and forward of the gun pods and external strakes mounted on the gun pod fairings. These strakes and fence provide lift improvement in ground effect during VTO operation and inhibit engine exhaust reingestion. Below 165 KIAS, the retractable fence extends and retracts with the landing gear. Above 165 KIAS, the fence automatically retracts.

2.4.5.1 <u>LIDS Switch</u> - A two-position LIDS switch labeled AUTO and RETRACT is on the lower left side of the main instrument panel. Below 165 KIAS with the switch in AUTO, the LIDS fence extends and retracts with the landing gear. Above 165 KIAS or with the switch in RETRACT, the LIDs fence retracts or will not extend when the landing gear is down or selected down. The LIDS switch should be in AUTO except for conventional takeoffs and landings. In emergency operation the LIDS fence extends pneumatically with the landing gear regardless of the LIDS switch position or airspeed.

2.4.6 <u>REACTION CONTROL SYSTEM (RCS)</u> - Compressor delivery (eighth stage) air is available on demand for the aircraft reaction control system. The quantity demanded is a function of pilot control inputs. The master valve is mounted on the underside of the engine, and is geared to the main nozzle rotation so that maximum airflow is provided at approximately 15° nozzle deflection. The bleed air is ducted to the nose (front pitch valve), tail (rear pitch and yaw valves) and wing tip (roll valves), as shown in Figure 2.4-14. Locations of the reaction control valves are presented in Section 2.2.8.

Yaw RCS
Valves

Aft RCS
Pitch Valve

Left Roll
RCS Valve

Right Roll
RCS Valve

Butterfly
Valve

Forward RCS
Pitch Valve
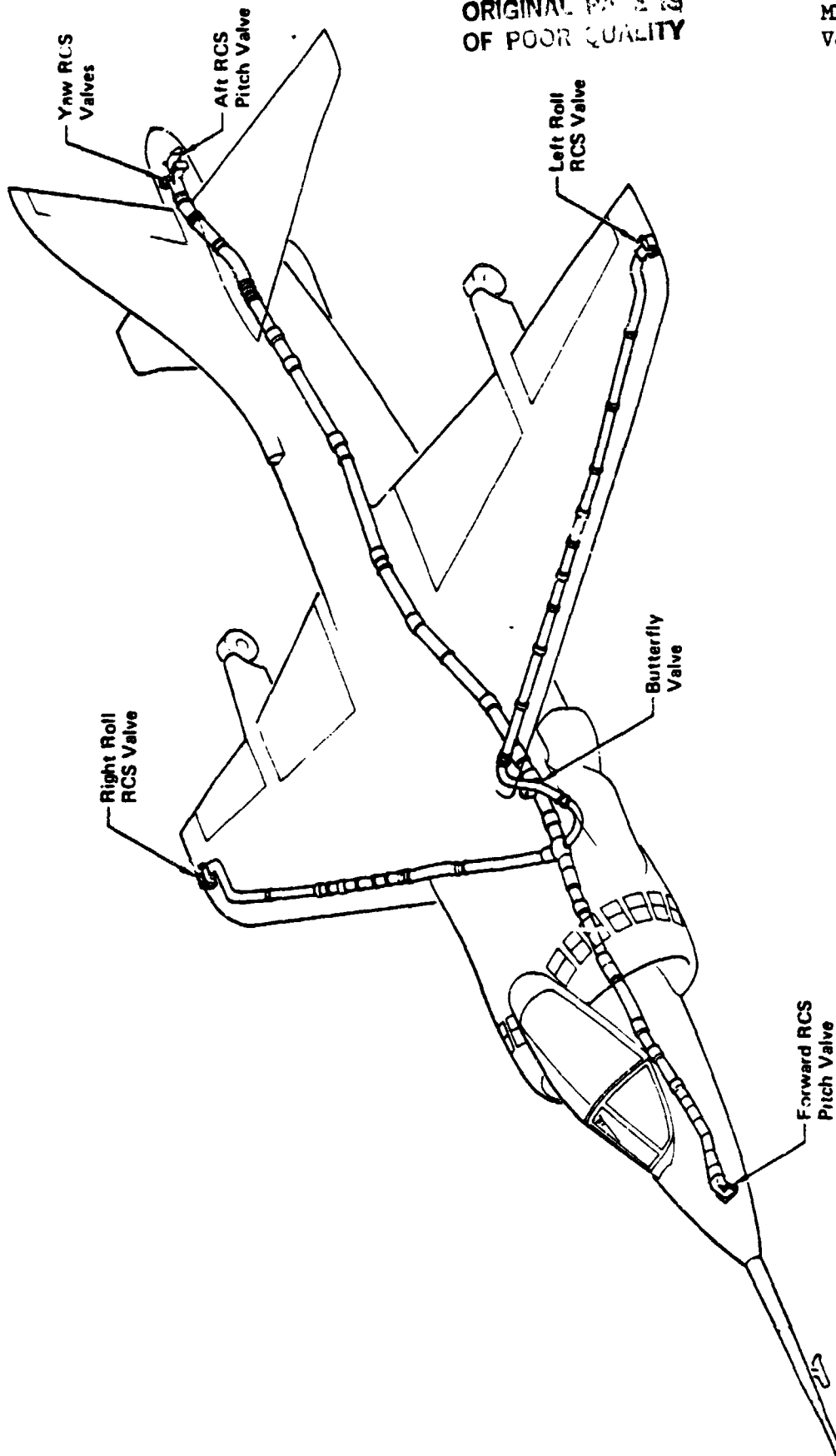
FIGURE 2.4-14
YAV-8B REACTION CONTROL SYSTEM

2.5 STABILITY AUGMENTATION SYSTEM

The Stability Augmentation System (SAS) of the YAV-8B is a limited-authority three-axis simplex autostabilization system. The SAS is provided to improve controllability in hovering and transitional flight conditions. The SAS is controlled by the AUTO STAB MASTER and AUTO STAB ENGAGE switches located on the left console. A separate switch is provided for the forward reaction control valve (RCV) series servo. Although the axes cannot be selected individually, failure of one channel does not affect operation of the others except that the yaw SAS is inoperative without the roll SAS. Position switches in the flap and landing gear linkage disengage the SAS when the flaps are selected UP, or the landing gear is retracted. When the aircraft weight is on the main gear the yaw SAS is disengaged. If the flaps are selected DOWN, the retraction of the landing gear does not disengage the SAS. Above 250 KIAS a signal from the air data computer disengages the SAS. The authority of the system about each axis is shown in Figure 2.5-1.

AXIS		SAS AUTHORITY	
		Δ CONTROL SURFACE DEG	Δ RCS OPENING % OF FULL OPEN
PITCH	FORWARD RCS	-1.5	28
	AFT RCS	+1.5	19
ROLL		±2.0	16
YAW		±5.0	50

FIGURE 2.5-1

STABILITY AUGMENTATION SYSTEM AUTHORITY

Functional block diagrams for the longitudinal and lateral-directional stability augmentation control systems are shown in Figures 2.5-2 - 2.5-4. Feedback gains are summarized in Figure 2.5-5 to 2.5-7.

Figure 2.5-2 shows the longitudinal stability augmentation control system. The pitch rate feedback loop is closed through the stabilizer actuator. The aft pitch reaction control valve is driven mechanically by the stabilizer actuator and exhausts downward only. A series servo actuator on the forward pitch RCV enhances stability augmentation when the forward RCV is demanded open and the RCS is activated such as in the hover mode or during short takeoff and accelerating transition flight.

A diagram for the roll and yaw stability augmentation system is shown in Figure 2.5-3 and 2.5-4. It consists of a rate feedback loop for roll and cancelled rate damping and turn coordination for yaw. Cancelled rate damping consists of a yaw rate feedback processed through a high-pass filter which cancels the steady state signal. This feedback is combined with a lateral acceleration feedback in a manner to improve turn coordination at the transition speeds. The yaw SAS only operates through the yaw RCV; therefore, the yaw SAS is only effective when the RCS is activated.

Selected gains for stability augmentation are summarized in Figures 2.5-5 to 2.5-7.

ORIGINAL PAGE IS
OF POOR QUALITY

FIGURE 2.9-2
YAV-8B LONGITUDINAL STABILITY AUGMENTATION SYSTEM
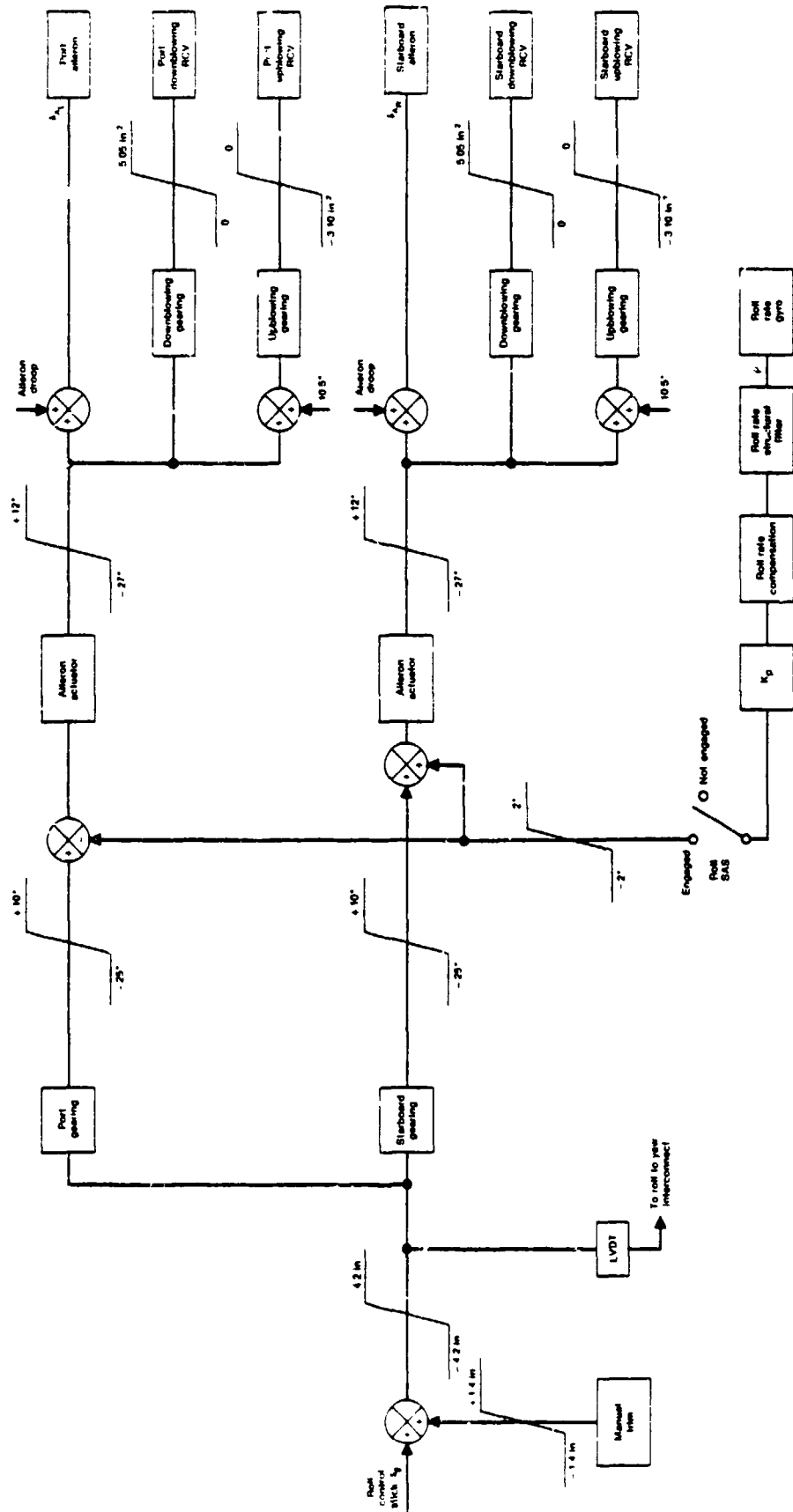
FIGURE 2.5-5
YAV-8B LATERAL STABILITY AUGMENTATION SYSTEM

FIGURE 2.5-4
YAV-8B DIRECTIONAL STABILITY AUGMENTATION SYSTEM

PARAMETER	VALUE	UNITS
AFT GEARING	$2.75 - 1.758274 \delta_\theta$ $+.09038152 \, \delta_\theta^2$ $-.01149626 \, \delta_\theta^3$	DEG/IN
AFT RCV GEARING	$1.085 \, (\delta_H - 2.0)$	IN^2/DEG
FWD GEARING	$2.126 \, (\delta_\theta - .5)$	DEG/IN
FWD RCS SERIES SERVO	$1/(1 + .0175S)$	-
FWD RCV CONVERSION	1.205	IN^2/DEG
K_q	$.22$	DEG/DEG/SEC
PITCH DEADSPACE	$\pm .06$	IN
PITCH RATE STRUCTURAL FILTER	$(1/(1 + .0222S))*$ $(1/(1 + .0448S))$	-
STABILATOR ACTUATOR	$1/(1 + .025S)$	-

FIGURE 2.5-5
LONGITUDINAL STABILITY AUGMENTATION PARAMETER VALUES

PARAMETER	VALUES	UNITS
AILERON ACTUATOR	$1/(1 + .013S)$	-
DOWNBLOWING GEARING	.778	IN^2/DEG
K_p	.346	DEG/DEG/SEC
PORT GEARING	$0 + 3.438886\phi$ $- .4106176\phi^2$ $+ .04090556\phi^3$	DEG/IN
ROLL RATE COMPENSATION	$(1 + .781S)/(1 + 1.29S)$	-
ROLL RATE STRUCTURAL FILTER	$1/(1 + .0164S)$	-
STARBOARD GEARING	$0 - 3.438886\phi$ $-.4106176\phi^2$ $-.04090556\phi^3$	DEG/IN
UPBLOWING GEARING	.477	IN^2/DEG

FIGURE 2.5-6
LATERAL STABILITY AUGMENTATION PARAMETER VALUES

PARAMETER	VALUE	UNITS
CROSS GEARING	3.05	DEG/IN
K_{AY}	.83	DEG/FT/SEC^2
K_R	.669	DEG/DEG/SEC
LATERAL ACCELERATION COMPENSATION	$(1 + .25S)/(1 + .125S)$	–
LATERAL ACCELERATION NOTCH FILTER	$(S^2 + 2.01062S + 404.26)/$ $(S^2 + 20.1062S + 404.26)$	–
LATERAL ACCELERATION STRUCTURAL FILTER	$164/(S^2 + 4S + 164)$	–
PEDAL GEARING	-7.07	DEG/IN
ROLL TO YAW COMPENSATION	$.58/(1 + .0435S)$	–
YAW RATE STRUCTURAL FILTER	$1/(1 + .0435S)$	–
YAW RATE WASHOUT	$S/(1 + 3.11S)$	–
YAW RCV GEARING	.35	IN^2/DEG
YAW RCV SERVO	$1/(1 + .0175S)$	–

FIGURE 2.5-7
DIRECTIONAL STABILITY AUGMENTATION PARAMETER VALUES

2.6 PROPULSION SYSTEM

The propulsion system of the YAV-8B aircraft consists of the YF402-RR-404
vectored thrust engine, built by Rolls Royce Limited, Aero Division-Bristol,
and an air induction system. The engine is similar to the F402-RR-402 in the
AV-8A with a number of design changes to improve performance and satisfy
increased aircraft power extraction requirements. These changes include zero
degree scarf angle front nozzles and an improved gearbox.

The air induction system retains the AV-8A basic design concept but
incorporates refinements to improve inlet performance and reduce distortion.
This section describes the physical and operational features of these propul-
sion system components.

2.6.1 YF402-RR-404 ENGINE - The YF402-RR-404 engine shown in Figure 2.6-1 is
based on long and extensive development of the Pegasus engine family which
includes Pegasus 6, 10 and 11 engines. The engine provides lift thrust for
takeoff and landing, cruise thrust for conventional wingborne flight, deflected
thrust for inflight maneuvering and compressor bleed air for the aircraft
reaction control system. This versatility has been achieved through the use
of a unique thrust-vectoring nozzle system on a conventional turbofan engine
designed for V/STOL operation. The nozzle system can direct the engine thrust
from aft (0°) through vertical (81°) to a reverse thrust position of 98.5°
relative to the engine centerline.
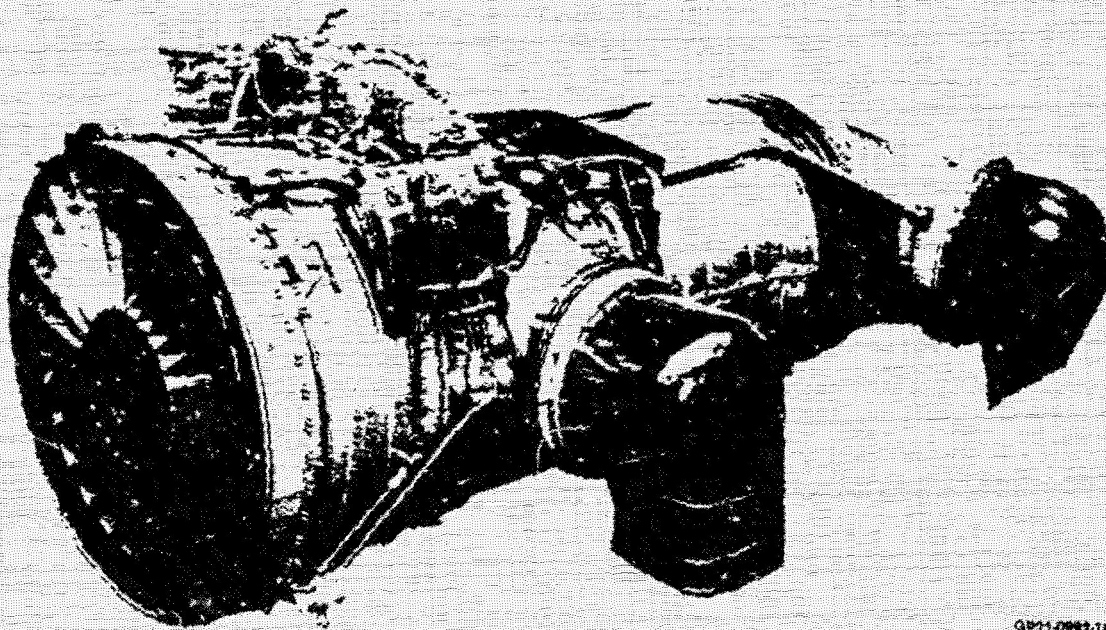
GP21-0992-18

**FIGURE 2.6-1
YAV-8B/YF402-RR-404 ENGINE**

2.6.1.1 General Description - The YF402-RR-404 engine retains the same basic
dimensions and features of the F402-RR-402. The engine consists of fan and
compressor assemblies, an annular combustor, two turbine assemblies, and
the thrust-vectoring exhaust nozzle system. The significant engine features
are:

o Non-mixed-flow turbofan

o Two-spool construction - High Pressure (HP) and Low Pressure (LP)
   rotors are contra-rotating to minimize gyroscopic effects. Four
   main bearings are used to support the two rotors (two bearings per
   rotor).

o Three-stage fan - The first two stages are overhung from the front
   fan bearing. Inlet guide vanes are not used, thus reducing Foreign
   Object Damage (FOD) susceptibility and eliminating the requirement
   for anti-icing.

o Eight-stage high-pressure compressor - Incorporates variable inlet
   guide vanes and interstage bleed valves. Aircraft services bleed
   is extracted from the 6th stage, and compressor discharge air (8th
   stage) is provided for the aircraft reaction control system (on
   demand).

o Annular combustor with J-tube vaporizing fuel injection

o Combustor water injection

o Two-stage air cooled HP turbine

o Two-stage LP turbine

These engine features are illustrated in Figure 2.6-2 and significant
design characteristics are tabulated in Figure 2.6-3.

An uprated gearbox driven by the high pressure rotor is mounted on top
of the engine. Drive pads are provided for the engine fuel pump, HP tach-
ometer generator, inlet-guide vane control, gas-turbine starter, and (2)
hydraulic pumps. A shaft geared to the low-pressure rotor is used to drive
the LP tachometer-generator.

The engine fuel control is a hydromechanical unit mounted to the accessory
gear box. The fuel control unit incorporates low pressure and high pressure
fuel pumps, a low-pressure rotor speed governor, and acceleration and flow
control units.

The engine oil system is self-contained and is of the scavenge-return
type, incorporating a fuel-cooled oil cooler. The oil tank is mounted on
the engine.
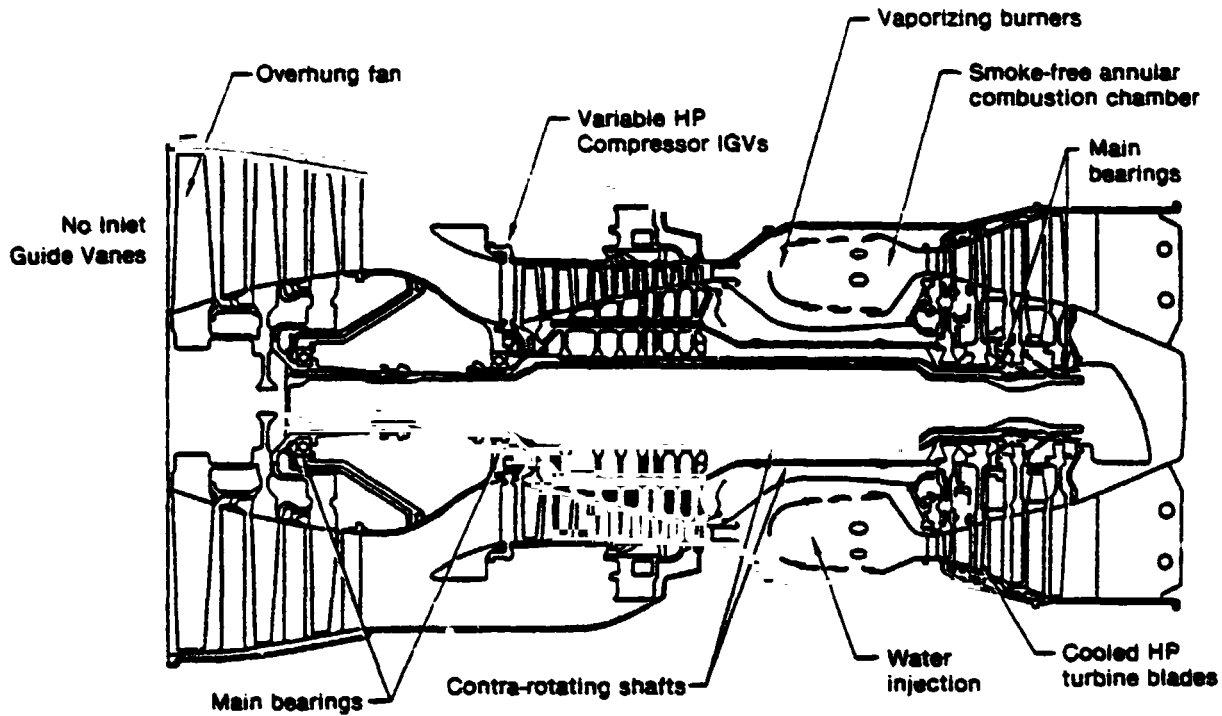
**FIGURE 2.6-2
PEGASUS ENGINE DESIGN FEATURES**

Fan stages 3
Fan airflow .... 430.7 lb/sec
Fan pressure ratio 2.29
Fan speed .... 6,500 rpm
Compressor stages 8
Compressor airflow .... 184.2 lb/sec
Compressor speed .... 11,000 rpm
Compressor pressure ratio 6.0
Overall pressure ratio 13.7
Bypass ratio 1.34
HP turbine stages 2
LP turbine stages 2

GP21-0862-20

**FIGURE 2.6-3
YF402-RR-404 SPEC ENGINE CHARACTERISTICS**
100% Corrected Fan Speed

The engine is equipped with four rotatable nozzles, two on each side of the engine. All four nozzles are a fixed area, convergent type. The nozzles are mechanically interconnected and are positioned simultaneously by an air actuated drive mechanism which provides the desired degree of thrust vectoring. The front (cold) nozzles are airframe mounted on each side of the fan delivery duct and are interchangeable between sides. They incorporate a zero degree scarf angle. This configuration was developed in an extensive test program conducted jointly by Rolls-Royce (RR) and MCAIR. It was originally conceived to reduce an adverse exhaust plume/wing/pylons interaction that exists with the AV-8A front nozzles. The zero scarf nozzle successfully demonstrated a reduction in these adverse interactions in full scale tests at NASA Ames Research Center. In developing this configuration to a flight worthy nozzle for the YAV-8B, RR has also improved the nozzle efficiency and flow characteristics. Test stand calibration of the first YAV-8B engine, conducted by Roll -Royce during April 1978, demonstrated a 200 lb. thrust improvement at the Short Lift Wet rating.

The rear (hot) nozzles are mounted on the turbine exhaust duct, are also interchangeable and are unchanged from the AV-8A/F402-RR-402. The combined effective flow areas are 389 sq. in. for both front nozzles and 530 sq. in. for both rear nozzles. Each nozzle incorporates two airfoil section turning vanes spaced equidistant across the nozzle exit.

The nozzle control system consists of a nozzle control lever mechanically connected to duplicate independent air motors which are, in turn, connected to the nozzle drive system. The nozzle system is shown in Figure 2.6-4. The YF402-RR-404 retains the current version of the Dowty hydromechanical fuel control unit, including all approved Reliability and Maintainability modifications.

Other features incorporated in the YF402-RR-404 include:

New bulkhead to match the new wing lower moldlines

Fire extinguisher pipes deleted

Simplified electrical harness

External dimensions and details of the engine are presented in Figure 2.6-5.

2.6.2 ENGINE OPERATION - Engine operation involves three basic modes; engine starting, V/STOL flight, and conventional flight. The engine is controlled through two primary systems. These are the engine fuel control and the nozzle vectoring control. The fuel control regulates engine speed and temperature (and therefore thrust) while the nozzle control system controls the direction of the engine gross thrust vector.
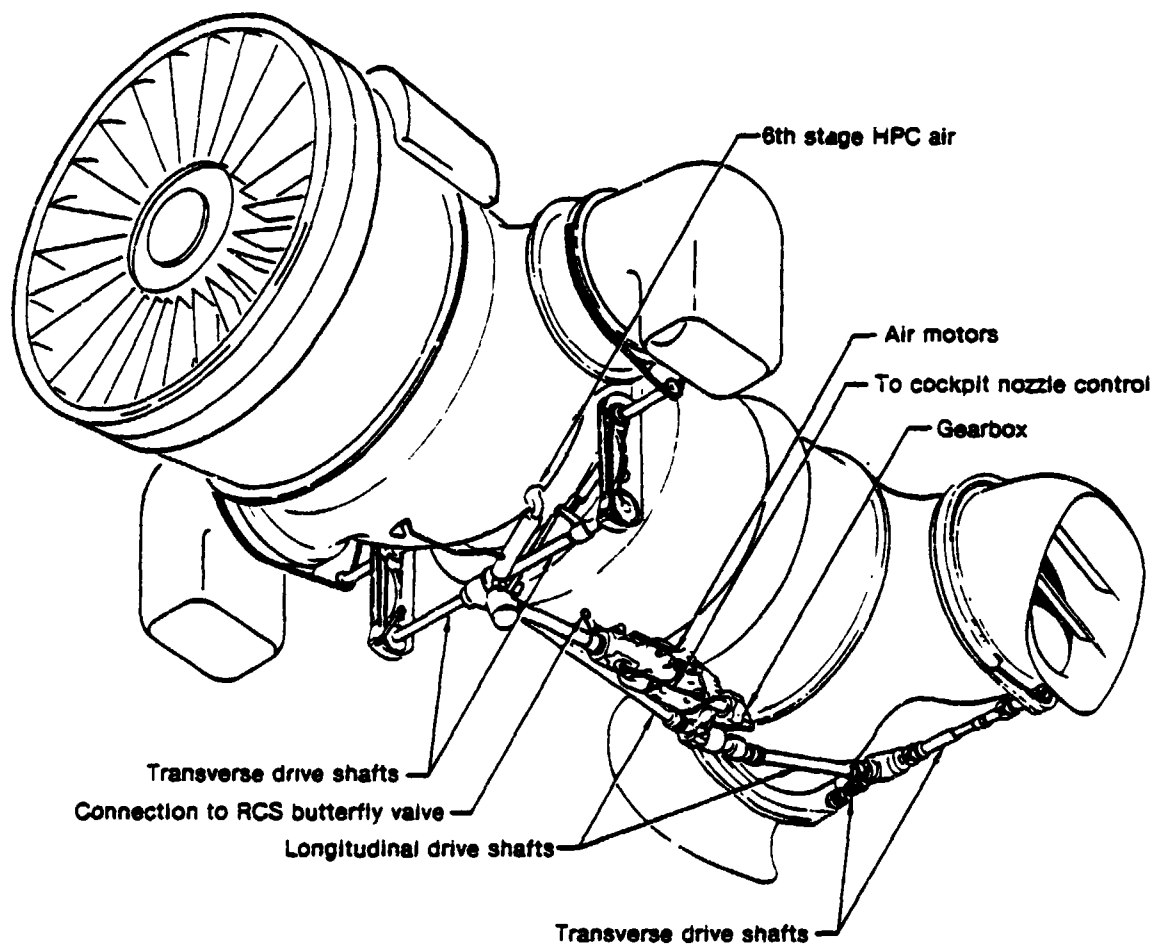
FIGURE 2.6-4
PEGASUS NOZZLE DRIVE SYSTEM

GP21-0003-21
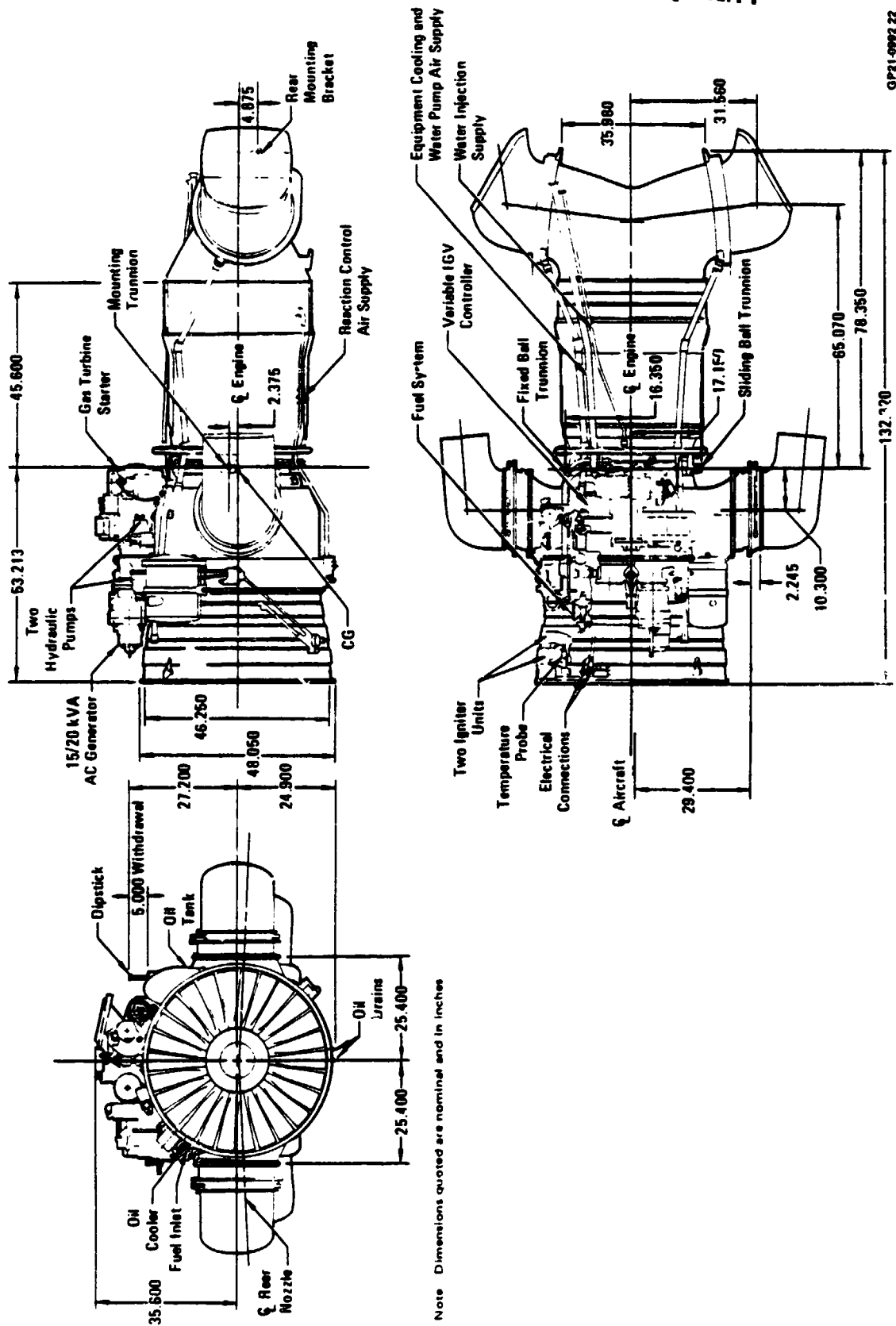
FIGURE 2.6-5
ENGINE DIMENSIONS

2.6.2.1 Fuel Control System - The YF402-RR-404 engine is controlled by a
hydromechancial fuel control system which governs fan speed and maintains
operation within selected design limits. The control system components
are: fan speed governor, limiters, pressure drop regulator for the main
metering valve, acceleration control unit, air bleed reset unit (which
provides additional fuel flow whenever reaction control system (RCS) bleed
is demanded), water bypass solenoid, fuel gallery and check valves, igniter-
jets and main-jets. Engine operating limits are maintained by a set of
limiters which operate on engine internal pressure and temperature signals.
The control system also has the capability to override the limiters and to
select an alternate manual fuel control circuit which serves as a backup
control system. Additional engine control is provided by the Inlet Guide
Vane (IGV) control unit, which regulates compressor IGV position and Blow-off
(bleed) Valve operation. The engine controls are illustrated in Figure 2.6-6.

The governing function of the control operates above 85% fan speed by
controlling the fuel metering orifice area as a function of fan speed, thus
maintaining a constant relationship between engine speed and power lever
angle. Acceleration and deceleration circuits override the governor when
an error exists between the actual fan speed and the power lever commanded
fan speed. The Acceleration Control Unit (ACU) schedules maximum fuel flow
as a function of compressor discharge pressure (P3), and fan delivery pres-
sure (P13) through positioning of the main metering valve. At less than 85%
fan speed the throttle position directly selects a metering orifice area
independent of fan speed, thus directly controlling fuel flow. In this
regime, the fuel flow is independent of altitude and ambient temperature.
The engine speed is determined by the fuel flow with no control or feedback
into the governing system. Fan speed will vary at a given throttle position
as ambient conditions vary.

o Limiters - The limiters sense pressure and temperatures and compare
the observed values against reference limit values (termed datums). When
a limit is reached or exceeded the fuel control reduces fuel flow as
necessary to maintain engine operation within the specified limits. The
limits used to control the engine are exhaust gas temperature (EGT),
compressor discharge pressure, and HP compressor pressure ratio.

The EGT limiter is an electronic control unit which senses EGT. When
the EGT exceeds datum level, the limiter acts through the fan speed governor
to reduce fan speed until the corresponding EGT is within the proper limits.
The EGT limiter has three temperature datums, Short Lift Wet (SLW), Short
Lift Dry (SLD) and Maximum Thrust. The specified datum to which the limiter
operates is dependent on the aircraft mode of operation. The EGT datums are
interlocked with the nozzle position and landing gear electrical circuits
so that the V/STOL datums, SLW and SLD, can only be used when either the
landing gear is selected down or the nozzles are rotated to greater than 16°.

FCU Inputs

P_{13}	EGT
P_3	PLA
P_{RCS}	H_2O
N_F	N_H

IGV Inputs

N_H
T_2

IGV control

Blow-off
valve control

W_F control

T_2 N_F P_{13}

P_3

EGT

H_2O

P_{RCS}

Pilot Selection — Water Injection
RCS Bleed

GP21-0902-23
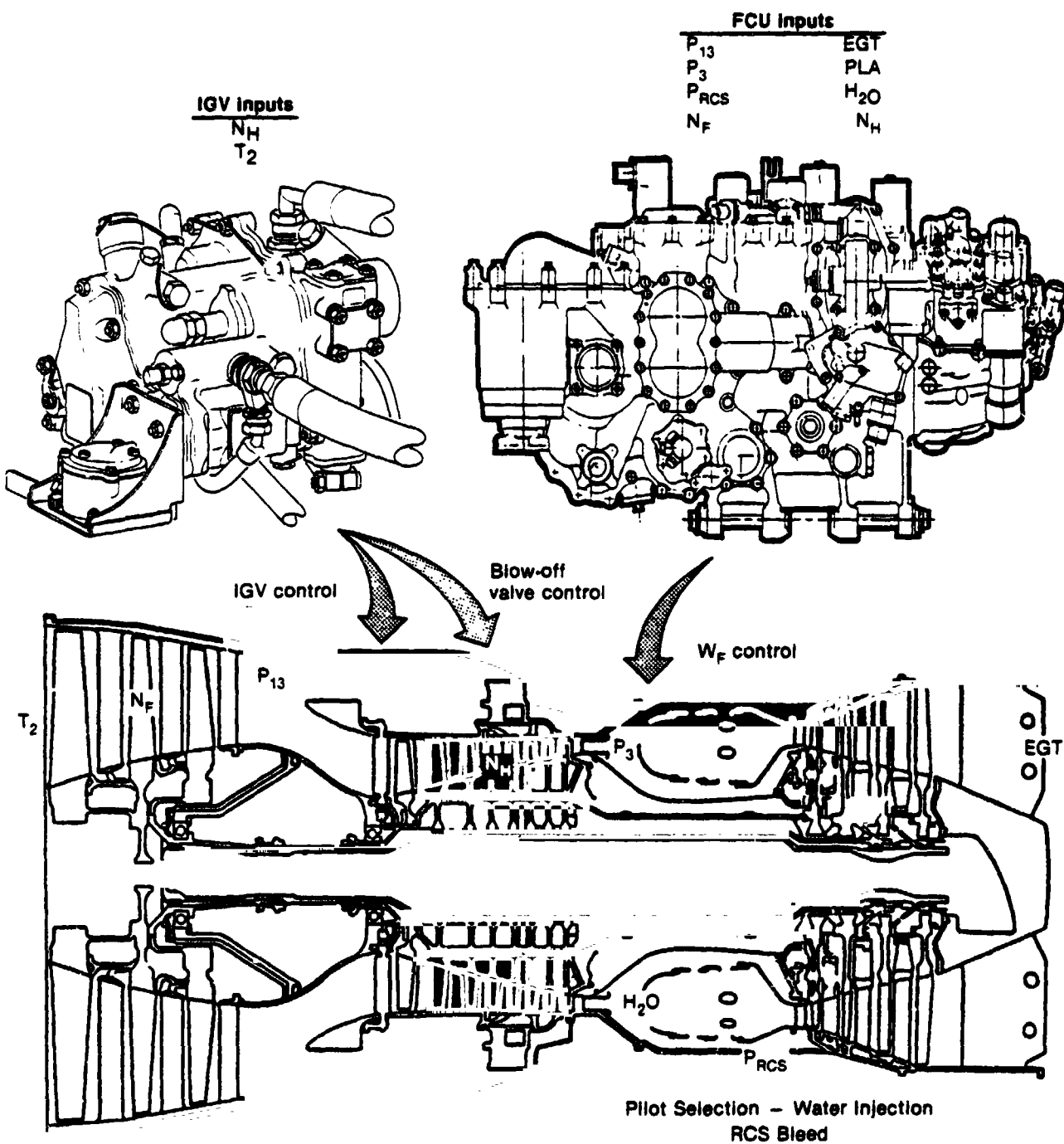
**FIGURE 2.6-6
ENGINE CONTROL DESCRIPTION**

The Pressure Ratio Limiter (PRL) maintains stable engine operation at high altitude/low speed conditions by limiting maximum engine speed, and therefore maximum airflow. Corrected fan speed is limited to a maximum of 101% through limitation of the pressure ratio across the HP compressor. This is achieved by the PRL, which senses fan and HP delivery pressure, bleeding fuel from downstream of the main metering valve back to pump inlet. A signal from the air data computer renders the PRL inoperative at altitudes below 10,000 ft where corrected speed limiting is neither needed nor desired.

The Compressor Pressure Limiter (CPL) senses HP compressor exit pressure and operates at approximately 255 psig to restrict the P_3 pressure signal to the ACU, thus controlling the metered fuel supply. The effect is to limit the maximum combustion chamber pressure and also the LP shaft torque to values which permit the design cyclic fatigue life to be achieved on these items.

In case of emergency, the limiters, with the exception of CPL, can be overridden by the pilot. A switch on the throttle quadrant cuts the pressure ratio and exhaust gas temperature limiters out of the control circuit. The switch can be actuated either by hand or by pushing the throttle hard against the forward throttle stop. Once the limiters have been overridden, it is necessary for the pilot to manually control engine speed and temperature through the throttle.

o __Inlet Guide Vane Control__ - The Inlet Guide Vane (IGV) Control regulates the HP compressor variable inlet guide vanes. They are operated on a linear schedule against corrected compressor speed from +40° to -2°. The IGV control uses fuel as its hydraulic medium but is otherwise completely separate from the main fuel system.

o __Blow Off Valve Control__ - The Blow Off Valve (BOV) Control regulates the HP compressor bleed valves on the 5th stage which bleed approximately 10% of the core airflow into the plen . chambe These are closed by a rotary valve mounted on the IGV operating shaft. The BOV closes/opens at 18° IGV angle which corresponds to approximately 70% HP RPM/55% fan RPM. With the BOV open, additional HP compressor surge margin is obtained at low speeds to assist starting and acceleration.

o __Water Injection__ - Water can be injected into the combustion chamber to augment thrust for V/STOL operation. The control system resets to higher speed and temperature limits since the use of water allows increased turbine inlet gas temperatures without increasing metal temperature above the corresponding dry value. The water flow rate is approximately 350 pounds per minute.

o __Manual Fuel Control__ - In the event of a malfunction in the primary fuel control, the pilot can select manual fuel control operation. In this mode all governing, acceleration, deceleration, and limiting functions are bypassed and fuel flow is directly and mechanically controlled by the power lever. All limits must be pilot observed.

2.6.2.2 Nozzle Control System - The vectored thrust feature of the Pegasus engine enables the pilot to rotate the engine gross thrust vector to the optimum angle for a given flight condition. Thrust vectoring is accomplished through the simultaneous rotation of the four nozzles within the range of 0° to 98.5° relative to the engine centerline. This rotation is initiated by, and is proportional to, the movement of the nozzle control lever. This movement is transmitted via pulley and cable to duplicate air motors which are driven by sixth stage compressor bleed air. The air motors drive the nozzles through a system of shafts, gears, and chains. The nozzle control lever is the only additional cockpit control required for V/STOL operation; the only additional cockpit instrument is the gauge which displays the angular position of the nozzles.

2.6.2.3 Operating Limits - The YF402-RR-404 engine control and time limits are shown in Figure 2.6-7. The time limitations shown are cumulative and include any time spent at higher power settings. The pilot must manually control the throttle so as not to exceed the fan speed limits at high ambient temperatures while using the Short Lift ratings at zero or low bleed rates. The Normal Lift and Maximum Continuous ratings also require pilot control over engine speed and temperature. Selection of dry limits by the fuel control is dependent upon the operating mode of the aircraft, i.e., V/STOL or conventional flight. This information is supplied by electrical signals taken from the nozzle and main landing gear positions. Wet limits are actuated by pilot selection of water injection. Below 10,000 ft the pilot must manually control engine speed to stay within corrected speed limits since the PRL is inoperative.

For flight test purposes, the YF402-RR-404 engines have been cleared to operate at Combat EGT levels for wingborne flight and for extended periods within Normal Lift Dry for hover. Combat EGT levels of 650°C or 675°C are available for a maximum of 2.5 minutes in wingborne flight. This is achieved through the use of special EGT Limiter datum temperature selector

Rating	Fan speed limit (% N_F)	Corrected fan speed limit (% $N_F/\sqrt{\theta T_2}$)	Maximum exhaust gas temperature limit (°C)	Compressor discharge pressure limit (psig)	Cumulative time limit*
Short lift (wet)	107.0	106.5	745	255	15 sec
Short lift	103.5		715		15 sec
Normal lift (wet)	104.5		720		1-1/2 min
Normal lift**	100.0		695		2-1/2 min
Maximum thru	95.5	101.0 above 10,000 ft	610		15 min
Maximum cont	89.0		540		None

*Includes time at all higher ratings
**May also be used in flight as a combat power setting

QP21-0092-24

FIGURE 2.6-7
YF402-RR-404 ENGINE OPERATING LIMITS

plugs, which substitute either 650°C or 675°C for the normal Max Thrust
limit of 600°C. When either of the special plugs is installed, the Max Thrust
EGT limitation must be manually controlled by the pilot. In addition, when
operating in the Combat EGT regime, the fan speed must be limited to 100%
at airspeeds between 250 to 450 knots, and to 95.5% at airspeeds above
450 knots. An engine life penalty is also assessed ~ each flight using
Combat EGT.

For the purposes of achieving steady state conditions during sustained
performance hover activity, the YF402-RR-404 has been cleared to operate for
4 minutes at exhaust gas temperatures below 685°C, in lieu of the normal 2.5
minute limitation within Normal Lift Dry (NLD). Four minutes at 685°C
results in the same number of Engine Life Recorder counts as does 2.5 minutes
the NLD EGT limit of 695°C, therefore no engine life penalty is associated
with this extension.

2.6.2.4 <u>Engine Starting</u> - The YAV-8B propulsion system is completely self-
sufficient for engine starting. An engine mounted gas turbine starter
(GTS) is started using internal battery power. The YAV-8B incorporates an
improved Lucas GTS, which is derived from the Lucas Mk I and Mk II GTS units
used on the AV-8A. The aircraft boost pumps are actuated by switches on
the righthand instrument panel. Opening the LP fuel valve then allows
fuel to be delivered to the engine LP fuel pump. Moving the START switch
to ON opens a solenoid valve to deliver fuel to the GTS and arms the starting
circuits. The momentary movement to the START position initiates the GTS
and engine starting cycle.

The GTS is started by a 3.0 horsepower electrical motor powered by an
aircraft battery. The electric motor automatically disengages when the
GTS reaches self-sustaining speed. For engine starting, the GTS power turbine
drives the engine through the auxiliary gearbox. Rotation of the HP spool
allows fuel to be delivered to fuel-actuated engine accessories such as
the IGV control. After the GTS has started, the HP fuel valve must be
opened by advancing the engine throttle to the IDLE position. This allows
fuel to be delivered through the fuel control units to the engine combustor.
By the time the GTS output shaft and the HP rotor of the engine have acceler-
ated to 3200 RPM, the engine is self-sustaining and starter assist is no longer
required. The GTS is then automatically shut down by shutting off its
fuel supply. The engine continues to accelerate up to its idle speed of
approximately 25% fan speed.

In order to shut down the engine, the throttle is simply retarded to
the cutoff position, which closes the HP fuel valve and stops the fuel flow.

2.6.2.5 <u>V/STOL Operation</u> - In the V/STOL flight mode, the EGT limiter is
reset from the wingborne flight limit to the lift rating limit. The thrust-
vectoring exhaust nozzles are down and compressor bleed air is provided to
the aircraft reaction control system.

Whenever the nozzles are deflected more than 16° below the aft position or the main landing gear is locked down, the exhaust gas temperature limiter is reset to the Short Lift Dry value to allow operation at higher engine speed. Thrust augmentation is available by water injection into the combustor if the fan speed is at least 95%. Selection of water injection by the pilot turns on the water pump and resets the fan speed governor to a higher limit. The EGT limiter is reset to a higher value as soon as the water begins to flow. Automatic reversion to the Short Lift Dry rating will occur if the water supply is exhausted, the fan speed drops below 75%, or the pilot shuts off the water injection system switch.

Automatic engine control within the applicable speed and temperature limits is provided only in the Short Lift ratings; the pilot must manually control the engine to the Normal Lift speed and temperature limits.

Rotation of the nozzles beyond 36° fully opens a butterfly valve in the aircraft reaction control system duct that makes compressor discharge bleed air available for attitude control during takeoff and landing. Maximum airflow is available for nozzle deflections beyond 15°. When the lift ratings are used, total thrust (including the thrust from the reaction control system) is maintained approximately constant over a range of bleed rates. (The extent of this range is dependent upon ambient temperature and power setting). This is accomplished by increasing fuel flow and the turbine inlet temperature as the bleed rate is increased. An air-bleed-reset within the fuel control unit provides the additional fuel flow during acceleration whenever bleed air is being extracted. As bleed is increased, the exhaust gas temperature will eventually reach a selected limit. Further increases in bleed then cause a reduction in thrust at the limiting temperature. When the nozzles are rotated aft, reaction control bleed is shut off. Also, when the nozzles are rotated aft to their conventional flight positions and the main landing gear is retracted, the EGT limiter resets to conventional flight limits and the engine is controlled to the Maximum Thrust rating.

2.6.2.6 Conventional Flight Operation - Engine operation in the conventional flight mode is similar to that of other engines. The highest power setting in normal operation is a 15 minute Maximum Thrust rating. The YF402-RR-404 engines have been cleared to a 2.5 minute Combat rating for flight test. Thrust vectoring may be used as an aid to aircraft maneuvering, within the flight envelope restrictions. The nozzle system can be rotated through 98.5° to obtain reverse thrust either in flight or on the ground.

2.6.3 AIR INDUCTION SYSTEM - The air induction system for the YAV-8B is the direct result of an inlet development program which follows a minimum change philosophy. The basic AV-8A inlet concept has been retained with modifications incorporated to achieve desired performance and distortion improvements. The inlet development program was directed toward an increase in V/STOL total pressure recovery and reduction in high speed distortion at high positive and negative angles of attack. Extensive inlet model testing at static, low speed and high speed conditions, combined with full scale test results at NASA Ames Research Center facilities, has shown that these objectives have been achieved with the YAV-8B inlet.

2.6.3.1 Physical Description - The YAV-8B inlet is a subsonic bifurcated pitot
type and incorporates two side inlet ducts each of approximately 190° circular
arc at the highlight plane. The ducts merge two inches ahead of the engine
face. The main lip incorporates a large contraction ratio (highlight area
divided by lip throat area, 1.24) where the lip throat is defined as the
junction between a 2:1 quarter-ellipse lip and the internal duct lines.
This lip shape is being used on the YAV-8B inlet because of its excellent
V/STOL and high speed performance characteristics.

A large auxiliary inlet around the periphery of each cowl provides
additional inlet area for takeoff and low speed operation. The double-
door auxiliary inlet configuration is shown in Figure 2.6-8. Each auxiliary
inlet contains seven passages which converge to form a continuous slot
before entering the main inlet duct. The passages are separated by fore-
and-aft struts which connect the front and rear sections of the inlet cowl.
Each auxiliary inlet passage incorporates two free floating blow-in-doors
hinged at their leading edges. The door external surface is flush with
the aircraft moldline in the closed position.

The boundary layer bleed system, shown in Figure 2.6-9, is similar to
that of the AV-8A. A flush bleed slot is located on the inboard wall of
each inlet, immediately aft of the entry plane. The slot is covered by
a two piece door (split into upper and lower halves) which is hinged at
its leading edge and is spring-loaded closed. Boundary layer air from each
slot is ducted upward to an exit at the rear of the canopy, from which it
discharges overboard at an angle of approximately 45°.

The inlet plan and side views previously shown in Figure 2.6-8 illustrate
the short highly curved nature of the inlet ducts. The duct length is
roughly equal to the engine face diameter due to constraints set by the
overall airframe layout. Figure 2.6-10 presents the inlet design parameters.

2.6.3.2 Operation - The YAV-8B inlet has two separate and distinct operating
modes, i.e., V/STOL and conventional flight operation. These modes are
determined by the positions of the auxiliary inlets and the boundary layer
bleed doors. Static pressure differential across these components
determines their positions and hence the operating mode. The auxiliary inlet
doors are free-floating, their positions determined only by static pressure
different. The spring-loaded boundary layer bleed doors are positioned
by a static pressure differential and an opposing spring force.

o V/STOL Operation - The engine airflow required for vertical or short
takeoff is supplied at high total pressure recovery through use of a
large inlet contraction ratio and auxiliary inlets. The auxiliary inlets
increase available flow area, thus maintaining low velocity past the main
inlet lips and minimizing total pressure loss. During V/STOL operation the
free-floating auxiliary inlet doors open due to the pressure differential
caused by the duct static pressure being less than ambient pressure. The
combined effects of spring force and pressure differential hold the boundary
layer bleed doors closed. Figure 2.6-11 illustrates inlet operation in the
V/STOL regime.
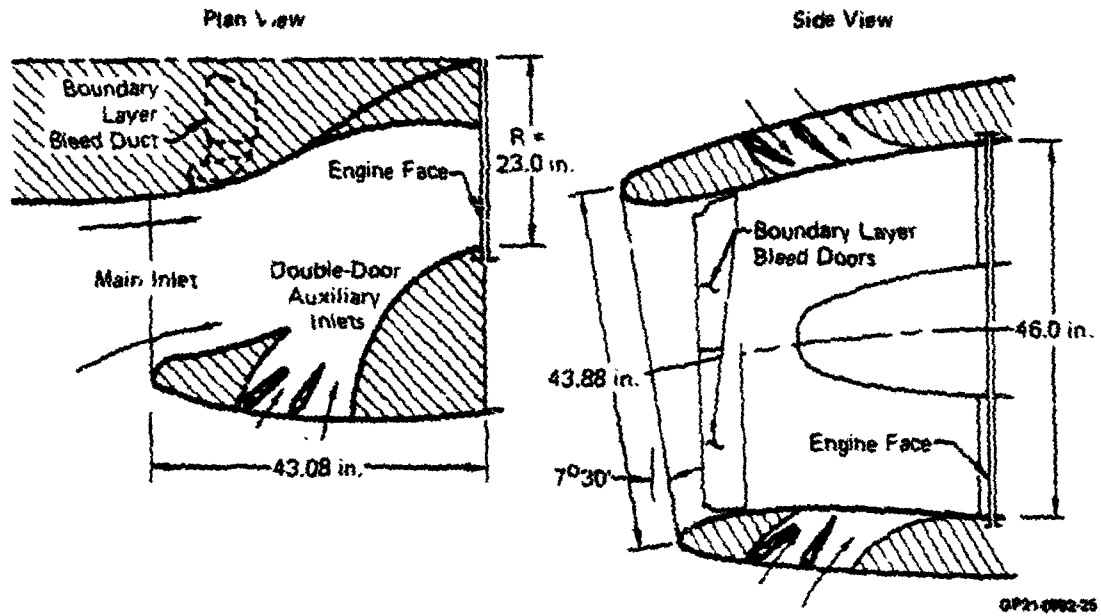
**FIGURE 2.6-8
GENERAL INLET ARRANGEMENT**
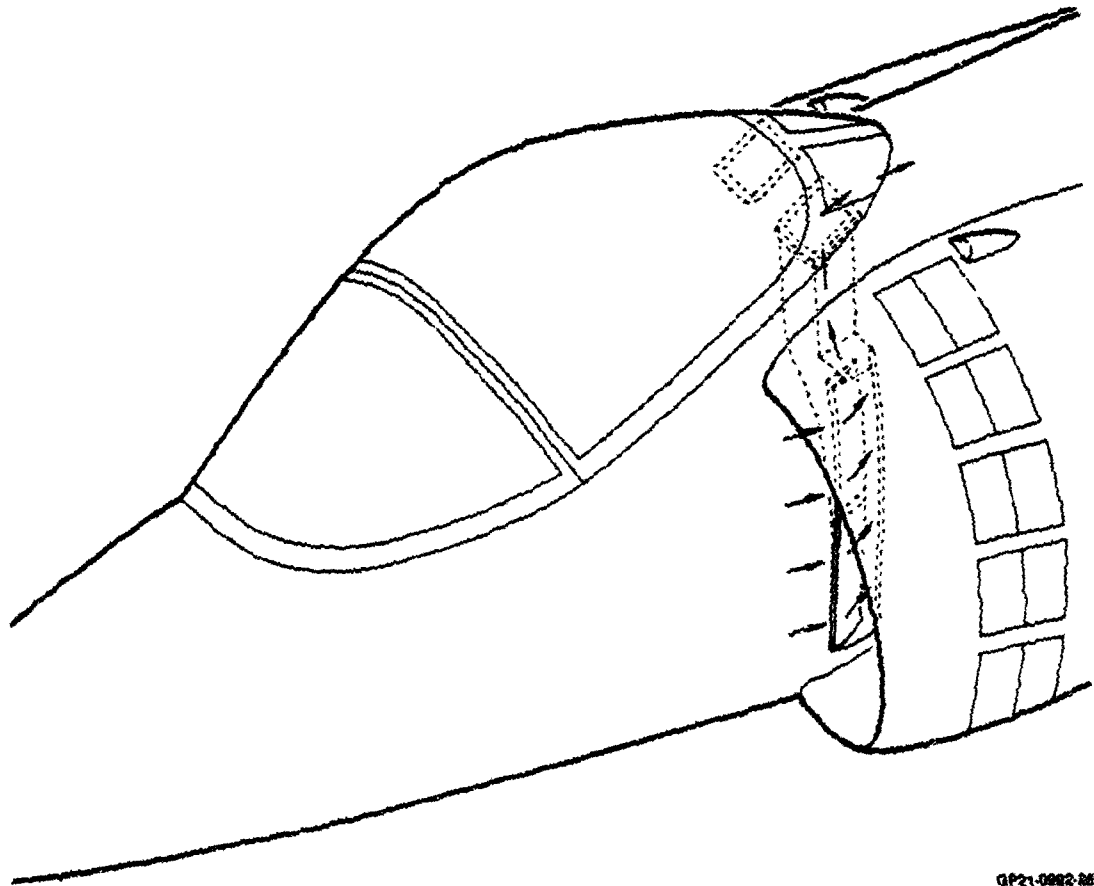
**FIGURE 2.6-9
BOUNDARY LAYER BLEED SYSTEM**

		YAV-8B
Minimum duct area	(ft^2)	9.7
Lip shape		2:1 ellipse
Highlight area	(ft^2)	12.53
Mean lip contraction ratio		1.24
Auxiliary throat area	(ft^2)	8.41
Auxiliary entry area	(ft^2)	12.38
Auxiliary contraction ratio		1.49
Maximum cowl area	(ft^2)	17.78

GP21-0883-7

**FIGURE 2.6-10
INLET DESIGN PARAMETERS**

GP21-0883-28
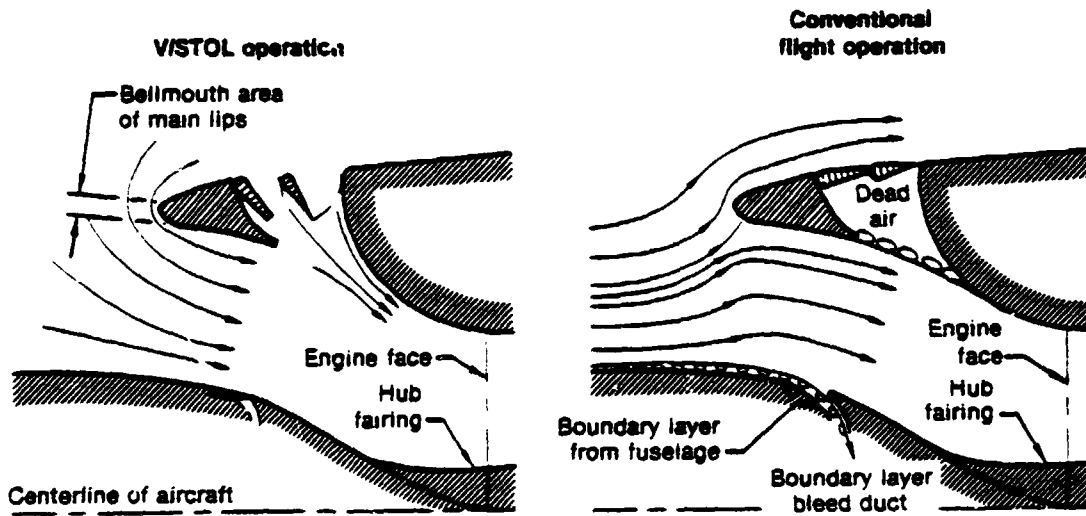
**FIGURE 2.6-11
INLET OPERATING MODES**

o <u>Conventional Flight Operation</u> - During conventional flight (cruise
or high speed) the auxiliary inlet doors are closed as a result of the inlet
duct pressure being higher than ambient. The boundary layer bleed doors
are positioned as a function of the duct static pressure which is established
by flight Mach number and engine power setting, the bleed exit static pressure
(usually ambient), and the opposing spring force. At cruise power settings
the reduced inlet mass flow ratio results in reduced inlet velocities with
resultant increased duct static pressure. As the spring force is overcome
by the pressure differential across the door(duct pressure minus bleed exit
pressure), the doors open to remove the boundary layer from the inlet flow.
The boundary layer bleed doors are free to operate individually in response
to static pressure gradients across the doors during operation at angles of
attack. The split upper and lower door configuration developed for the AV-8A
and retained for the YAV-8B is used to prevent recirculation of boundary
layer air from a high pressure region to a low pressure region, which would
cause separation and increased inlet pressure distortion. Figure 2.6-11
illustrates conventional flight operation.

3. YAV-8B NONLINEAR SIMULATION PROGRAM

The nonlinear program that has been developed to simulate the YAV-8B
aircraft is named YAV8B. The program computes six degree-of-freedom aircraft
motion plus a large number of aircraft performance parameters. The program is
written in FORTRAN in a manner to make it easy to use. Program organization,
structure and data card input format are described within this section.

3.1 PROGRAM STRUCTURE

The YAV8B program is structured into two primary categories: the
executive routines and the aircraft math model routines. For simplicity, all
computations are performed at the same iteration time. The program computes
aircraft motion as well as performance parameters. A great deal of flexibility
is available to the user with respect to which parameters are to be recorded.

Figure 3.1-1 diagrams the structure of the YAV8B program. The executive
(exec) routines include I50ØNCE, I50MS, AC07, CARDS and RTPDATA. The I50ØNCE and
I50MS routines are top level exec routines for the program. The AC07 routine
is the aircraft math model exec. The CARDS routine reads the input data from
the EXECUTE card deck and the RPTDATA routine is the exec for the output data
logic. The program computes in three different modes: INITIAL (first pass
initialization), IRESET (400 passes for dynamic stabilization), and OPERATE
(real time computation). The run time for each particular case can be
designated. The iteration time (DT) is defaulted to 50 milliseconds but can be
changed by the user.

Initial condition data, as well as the instructions for data printout,
are input to the program using the EXECUTE card deck. The EXECUTE card deck
loads the appropriate software files and executes the program. Dynamic
inputs to the aircraft controls, aircraft motion, etc. can be input to the
program with the I50MS card deck. The I50MS deck modifies the I50MS sub-
routine. Because the I50MS subroutine is a top-level exec routine, this is
a convenient location to math model a forcing function. A more detailed
description of user procedures is provided in Section 3.4. A sample case is
also provided in Section 3.4.

The aircraft math model flow diagram is shown in Figure 3.1-2. Each
subroutine in the aircraft math model is described in Section 3.3 along with
top-level flow charts. All of the subroutines for the aircraft math model
can be modified and changed by the user if required.

3.2 MATH MODEL EQUATIONS

The YAV8B program computes aircraft velocities, accelerations and
position at the aircraft c.g. The airframe is considered to be a rigid body.
The atmosphere data base is the U.S. Standard Atmosphere, 1962 - sea level to
100,000 feet. The following paragraphs describe some of the theory and math
model equations comprising the aircraft simulation model.

3.2.1 NUMERICAL METHODS - There are three general numeric methods used in
the YAV8B program that require some discussion. They are integration
techniques, digital filter techniques, and data table look-up methods. Each
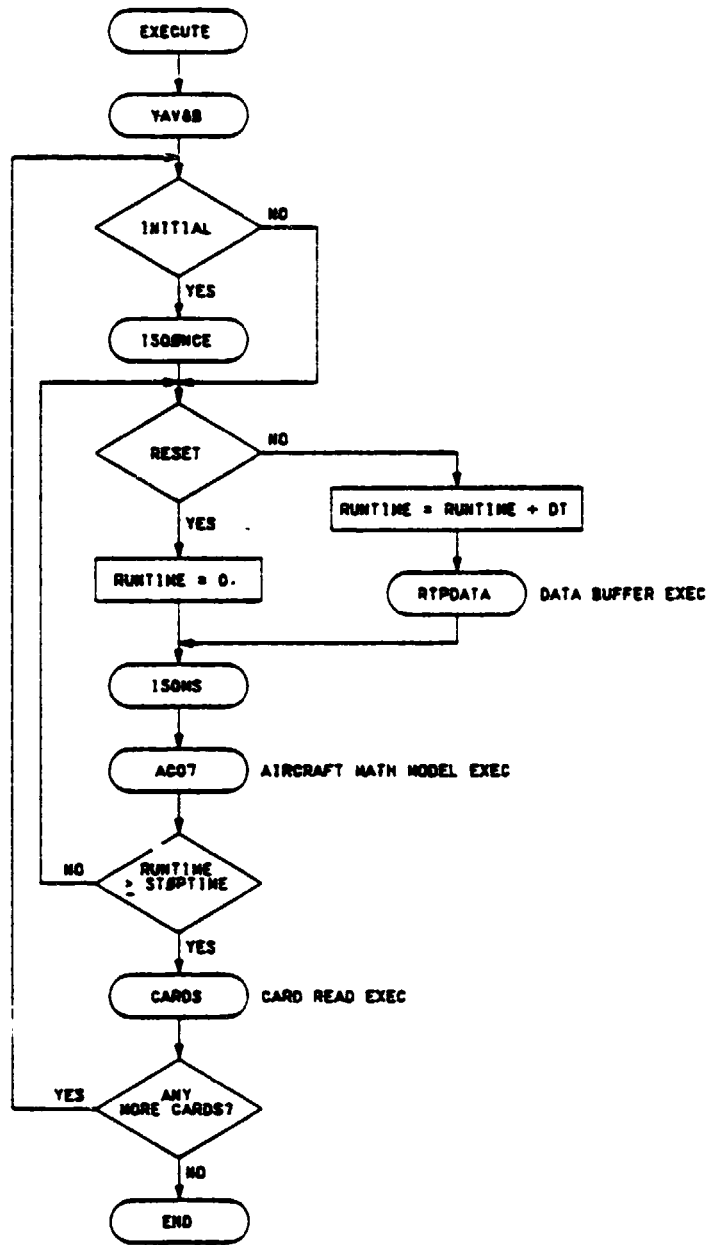
FIGURE 3.1-1
YAV8B PROGRAM STRUCTURE
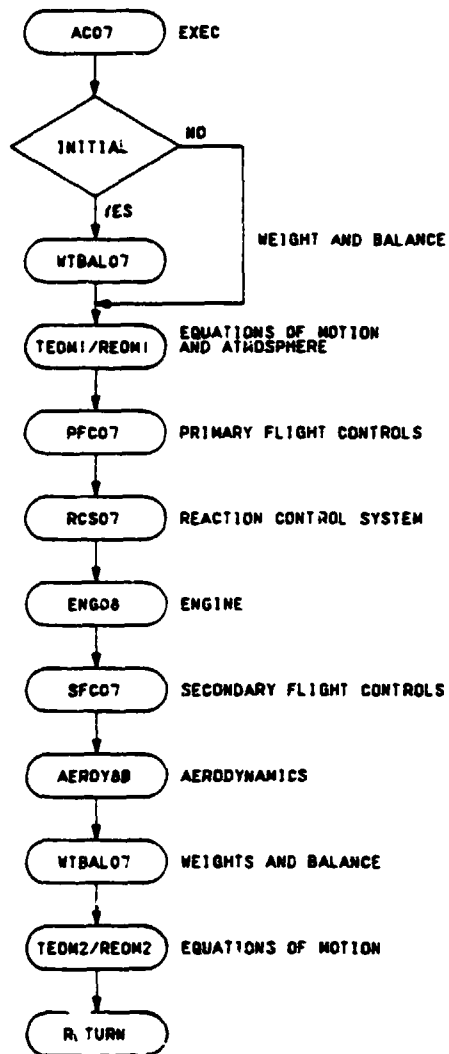
FIGURE 3.1-2
AIRCRAFT MATH MODEL FLOW DIAGRAM

method will be addressed briefly in order to familiarize the program user
with the techniques incorporated into YAV8B.

3.2.1.1 <u>Integration Techniques</u> - There are four types of integration schemes
used in the simulation program: Euler (rectangular), Tustin, Reddy Parabolic
and Adams third order. These methods fall into two general classes. The
first class is the predictor integration scheme. In this class, the most
currently available input is valid for the beginning of the integration inter-
val and the output is "predicted" for the end of the interval. The second is
the corrector integration scheme. This scheme is used when the input is
available at the same time that the output is desired. The Adams third order
method is used primarily in computations for the equations of motion. The
general form of these numerical integration methods are as follows:

o <u>Euler (Rectangular)</u>

$$X_n = X_{n-1} + \dot{X}_{n-1} * \Delta t, \quad \Delta t - \text{Sample period}$$ Zero Order Predictor

o <u>Tustin</u>

$$X_n = X_{n-1} + (.5 \dot{X}_n + .5 \dot{X}_{n-1}) * \Delta t$$ Linear Corrector

o <u>Adams Third Order</u>

$$X_n = X_{n-1} + (\frac{23}{12} \dot{X}_{n-1} - \frac{4}{3} \dot{X}_{n-2} + \frac{5}{12} \dot{X}_{n-3}) * \Delta t$$ Third Order Predictor

o <u>Reddy Parabolic</u>

$$X_n = X_{n-1} + (\frac{5}{12} \dot{X}_n + \frac{2}{3} \dot{X}_{n-1} - \frac{1}{12} \dot{X}_{n-2}) * \Delta t$$ Parabolic Corrector

3.2.1.2 <u>Digital Filtering Techniques</u> - Digital filters are needed to obtain
an acceptable model of hydraulic actuators in the control system model and
for other lead and lag filters used in the simulation model. Two methods are
used in the YAV8B program: Tustin's and Reddy's. The Tustin method is quite
good for modeling digital filters, as it has a simple relationship between the
Laplace transform and the Z transform operators S and Z:

$$\frac{1}{S} = \frac{\Delta t}{2} \frac{(Z + 1)}{(Z - 1)} \quad Z - \text{Z Transform operator}$$

The equivalent computer difference equation for C/R = 1/S would be:

$$C_n = C_{n-1} + \frac{\Delta t}{2} [R_n + R_{n-1}] \text{ Where } R_n \text{ is the present value of the input.}$$

Using the same method, the difference equation for the first order filter,
C/R = 1/τS+1, can be derived as:

$$C_n = \frac{1}{(1 + \frac{2\tau}{\Delta t})} (R_n + R_{n-1}) - \frac{(1 - \frac{2\tau}{\Delta t})}{(1 + \frac{2\tau}{\Delta t})} C_{n-1}, \quad \tau - \text{system time constant}$$

This difference equation would give the output sequence (C_n) of a first order
lag from the input sequence (R_n). Note that the coefficient terms involve only
the constants Δt and τ, and so are only computed once at the beginning of a run.

For better accuracy and stability, some filters with short time constants
are modeled using Reddy's method. For a first order transfer function and
linear input, the output at the end of each step is a constant times the
output at the beginning of each step plus other constants times values
of the input at the beginning and end of the step. A first order system
response to a linear input can be represented by the following recursion
formula:

$$C_n = C_{n-1} \ (e^{-\Delta t/\tau}) + R_n \ [1 - (\tau/\Delta t)(1 - e^{-\Delta t/\tau})]$$

$$+ R_{n-1} \ [\tau/\Delta t - (e^{-\Delta t/\tau})(1 + \tau/\Delta t)]$$

3.2.1.3 **Data Table Look-Up Techniques** - The method used in the table look-up
program, TBLKP, for even increments is simple and straightforward. It
requires the program to compute an index and a ratio. The index represents
the position in the table of dependent variables such that the corresponding
value of the independent variable is just below (or equal to) the input
variable. The input variable is bound by this value and the next value of
the independent variable. The ratio is the percentage distance of the input
variable between these two values.

For a single dimension table, the lookup function performs as shown:

RI = ((Input - low bound)(number of points - 1)/(high bound - low bound)) +1

Index = integer part of RI

Ratio = fractional part of RI

Once the index and ratio are found, it is only necessary to look up the
corresponding dependent variables and linearly interpolate:

Output = Table (Index) + [Table (Index + 1) - Table (Index)] x Ratio

The lookup method for a table with uneven breakpoints is similar, but
each set of breakpoints must be checked to determine which ones bracket the
input value.

Since the values of the independent variable will cover the allowable
boundaries, the table lookup program does not extrapolate outside the
boundaries of the tables. If an independent variable exceeds the boundary,
the corresponding dependent variable boundary value is used in the lookup.
Finally, to save additional time with either method, the index into the table
and the ratio between points is saved, so that if more than one table uses
the same breakpoints, the index and ratio need not be recomputed.

3.2.2 **EQUATIONS OF MOTION** - The parameters that determine the aircraft motion
are described by a set of six second-order differential equations, three to
describe the translational degrees of freedom and three to describe the
rotational degrees of freedom. This system of equations is used to describe
the aircraft state relative to a fixed coordinate reference frame.

The earth is modeled as a spherical surface, rotating relative to a fixed inertial frame. Rotation is about the polar axis with no "wobble". The acceleration due to gravity (g) is assumed to be constant and always acting perpendicular to the ground.

Four coordinate reference frames are used in describing the aircraft position, velocity and acceleration:

(1) Inertial Axes
(2) North-East-Down (NED), or local vertical
(3) Body Axes
(4) Stability Axes

The inertial coordinate frame is an orthogonal triad with its origin at the center of earth (see Figure 3.2-1). The first and second components (or x and y axes) define the equatorial plane and the z axis is positive toward the North Pole. The x axis orientation is initialized at the beginning of the mission to pass through the zero latitude and longitude point. The y axis passes through the point of latitude = 0°, longitude = +90°. After the mission begins, the rotation of the earth will cause an earth fixed longitude point to increase in inertial longitude (relative to the "fixed in space" inertial axes reference frame). It is in this axis system that accelerations and velocities are integrated to obtain aircraft position.

λ · Longitude, first rotation
L · Latitude, second rotation
O · Origin, earth center
X, Y, Z · Inertial coordinate triad

GP79-0269-344
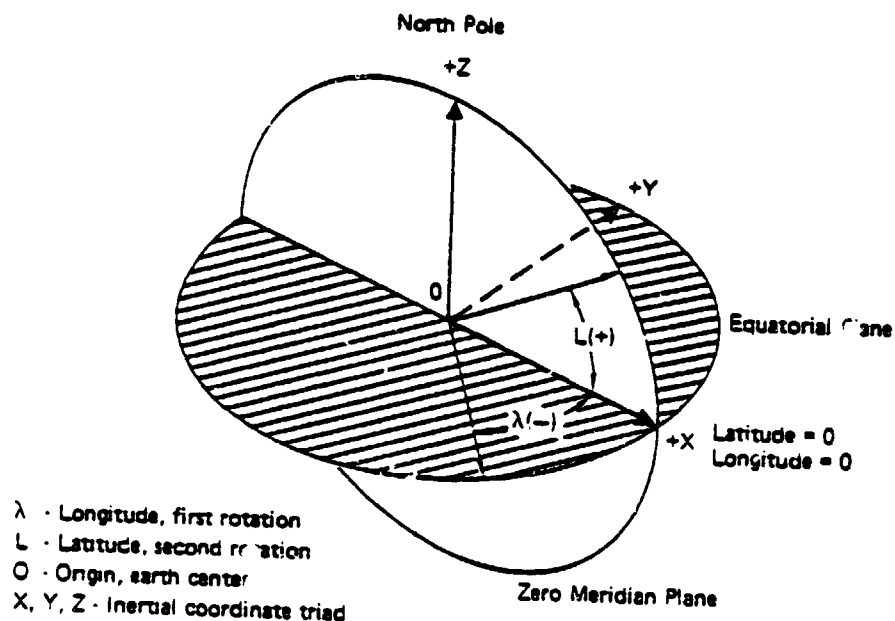
FIGURE 3.2-1
INERTIAL COORDINATE FRAME

The NED frame is centered at the aircraft c.g. The x axis is directed toward true North, the y axis is directed toward true East, and the z axis 's directed down perpendicular to the ground. Figure 3.2-2 illustrates this system. Aircraft translational velocities are transformed from inertial axis into this frame for the addition of wind and computation of ground speed and flight path angles. The aircraft Euler angles (pitch, roll, yaw) are defined from the body axes orientation relative to the NED reference frame.
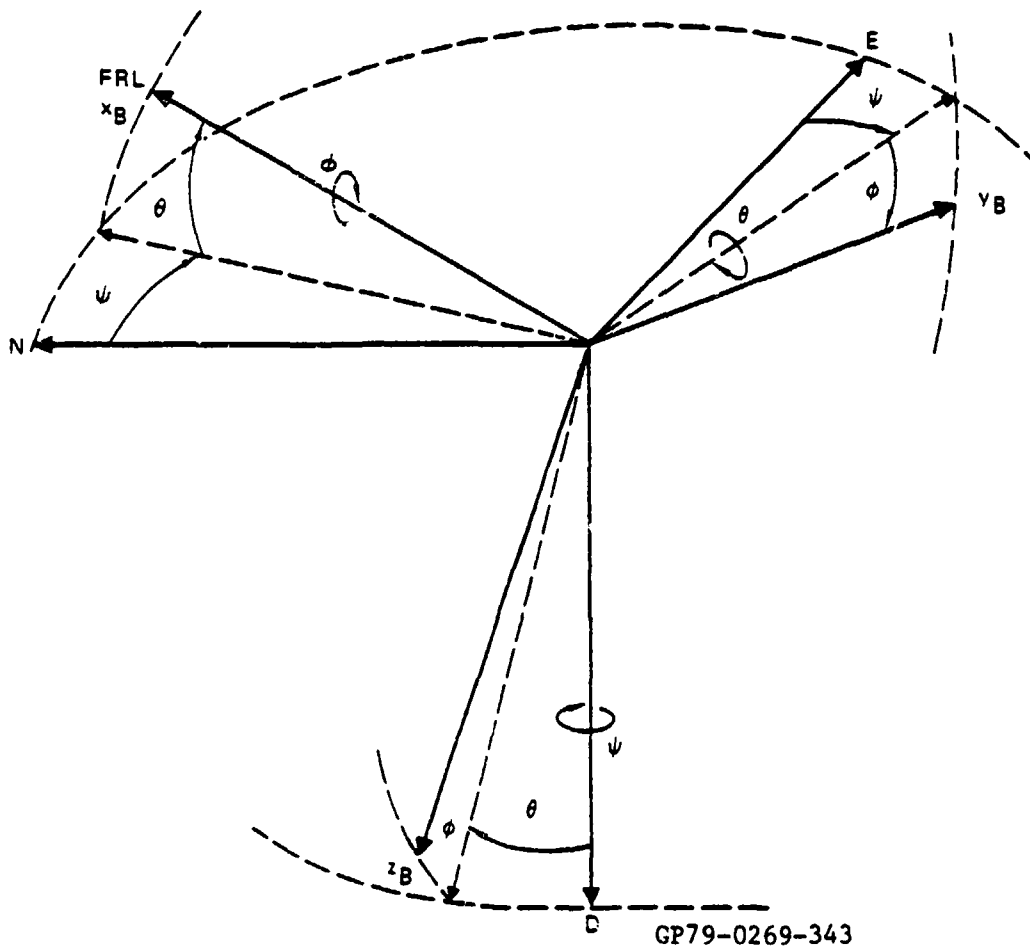
FIGURE 3.2-2
RELATIONSHIP OF BODY TO NED AXES

The equations of motion and their computational arrangement are illustrated in Figures 3.2-3 and 3.2-4.

The translational equations are a summation of the total aerodynamic, engine thrust, and RCS forces in the body axis coordinate system. Newton's Second Law of Motion is applied to compute the body axis accelerations and these are transformed to the inertial frame through a direction cosine matrix, as shown on Figure 3.2-3. The acceleration due to gravity is added

FIGURE 3.2-3
EQUATIONS OF MOTION SYSTEM
TRANSLATIONAL EQUATIONS
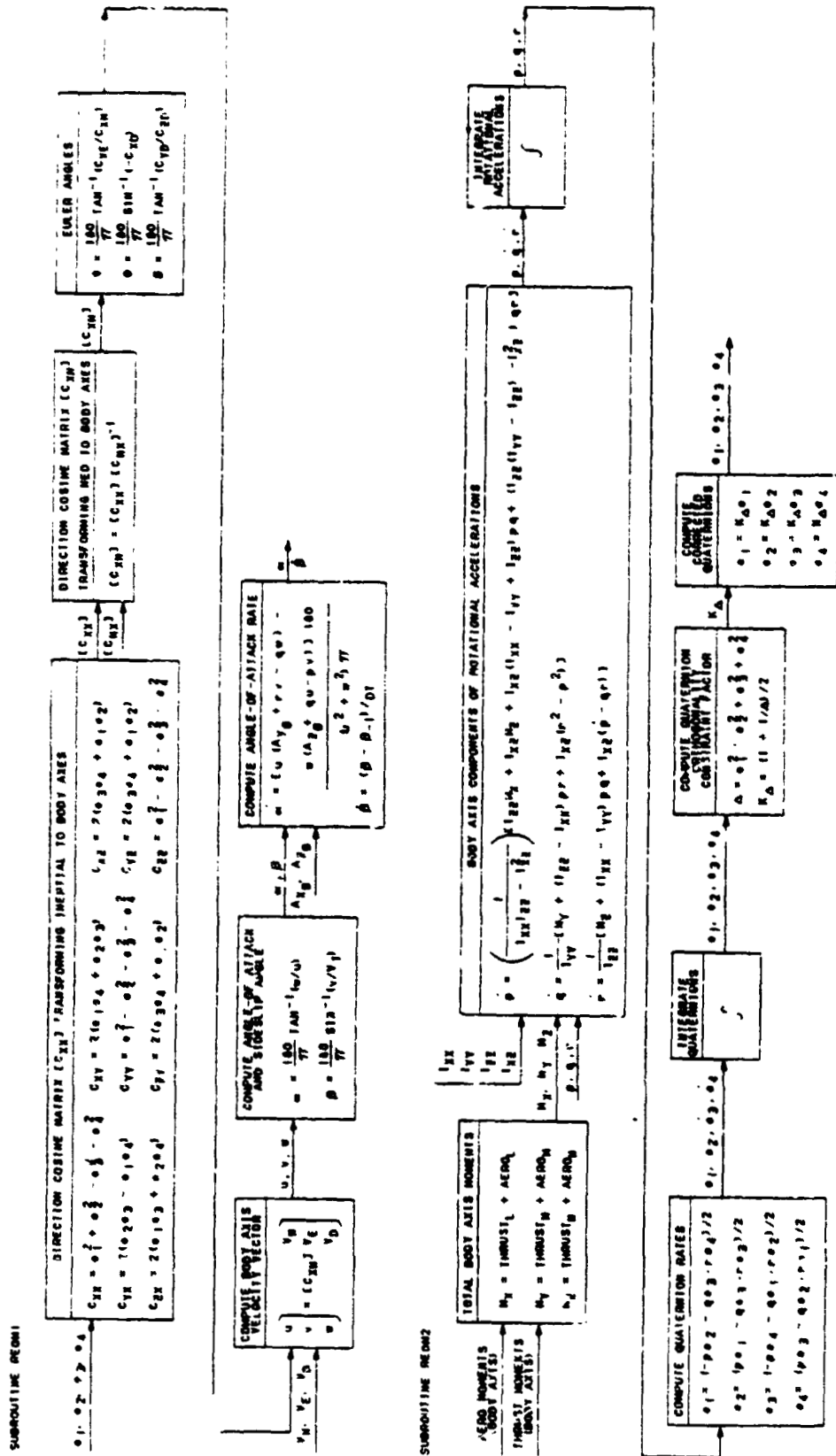
FIGURE 3.2-4
EQUATIONS OF MOTION SYSTEM
ROTATIONAL EQUATIONS

and the acceleration components are integrated to produce inertial velocity
and position components. These are transformed back to the NED axes for the
introduction of wind components and to the body axes for the computation of
the body axis velocity components and the velocity vector angles (α, β, γ, σ).

The rotational equations of motion are derived by summing the moments due
to aerodynamics, engine thrust, and RCS effects. The body axis rotational
accelerations are computed from these moments, the aircraft moments of
inertia, and the cross coupling terms. The body rates are determined by
integrating the rotational accelerations.

The attitude angles of the simulated aircraft are calculated using the
quaternion method. The quaternion method uses four parameters for specifying
the orientation of a coordinate system. The quaternion rates are calculated
from the body axis angular rates and then integrated to update the quater-
nions. The earth-to-body axis transformation matrix is computed directly
from the quaternions, thereby defining the aircraft orientation with respect
to the fixed frame. A correction factor is applied to compensate for inte-
grator drift and to ensure that the coordinate system remains orthogonal.
This correction factor is based upon the constraint that for an orthogonal
system, the sum of the squares of the quaternions must be unity. The quater-
nion method offers the advantage of allowing an all-attitude orientation that
is free from discontinuities.

3.2.3 AERODYNAMIC EQUATIONS - The aerodynamic forces and moments acting on
the aircraft are fully described by algorithms for three longitudinal and
three lateral-directional coefficients. The longitudinal terms are the
coefficient of lift (C_L) or normal force (C_N), drag (C_D) or axial force (C_A),
and pitching moment (C_m). The lateral-directional terms are the coefficients
of side force, (C_Y), rolling moment (C_l), and yawing moment (C_n).

3.2.3.1 Aerodynamic Reference Systems - The aerodynamic data base is divided
into two separate and distinct regions: low speed ($M \leq 0.3$) and high speed
($M \geq 0.5$). The data for the low speed region are derived in the body axis
system. The aircraft body coordinate system is shown in Figure 3.2-5a. It
has its origin at the aircraft's center of gravity. The x axis is directed
toward the nose of the aircraft coincident with the Fuselage Reference Line
(FRL). The y axis is directed toward the right wing of the aircraft (ortho-
gonal to the x axis). The z axis is directed downward, perpendicular to
the x_B - y_B plane.

The data for the high speed region are referenced to the stability axis
frame. Figure 3.2-5b illustrates the stability axis system. It has its
origin at the point of reference of the aerodynamic data. The x axis is
formed at the projection of the body axis on the velocity vector (rotated
through the aircraft angle of attack α). The y axis is directed out the
right wing of the aircraft and is oriented perpendicular to the aircraft
plane of symmetry. The z axis is directed downward, perpendicular to the
x-y plane.

(a) Body Coordinates

(b) Stability Axis Coordinates

GP21-0862-44
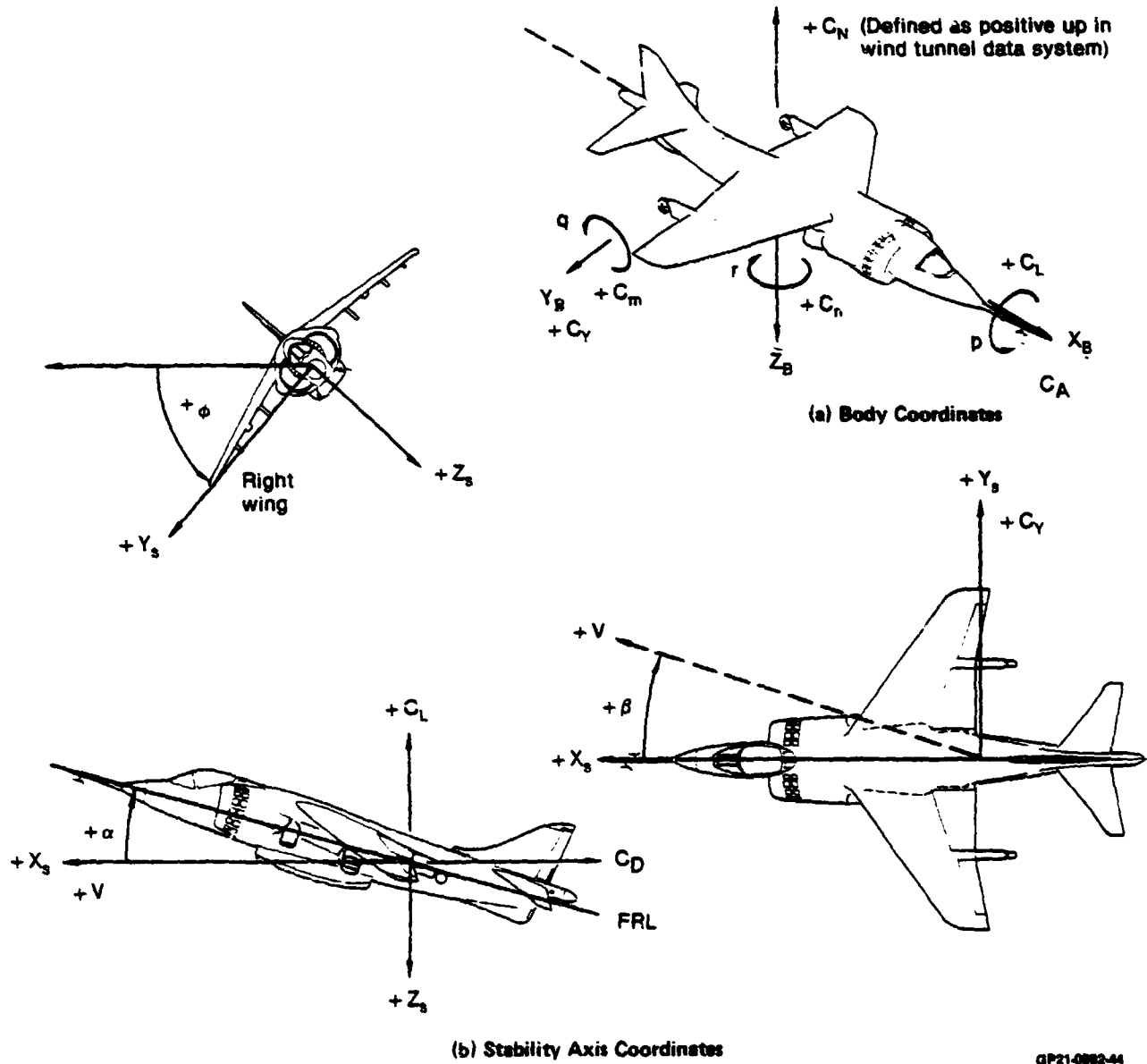
FIGURE 3.2-5
BODY AXIS AND STABILITY AXIS

For ground hover and low speed flight, another reference frame is used. This reference frame is a blend between the body axis and stability axis reference frame. The ground effects are introduced into the simulation for altitudes of approximately 70 feet or less. The longitudinal reference attitude for ground effects is as follows:

$$\alpha' = \alpha * K_1 + \theta * K_2 \text{ for } 0.05 < Veq < 0.10$$

Where $K_1 = (Veq - .05)/20.$ and $K_2 = (1 - K_1)$

for $Veq < 0.05$, $\alpha' = \theta$ and for $Veq > 0.10$, $\alpha' = \alpha$

The FORTRAN name for α' is THALP.

The parameter Veq is defined as the square root of the ratio of the freestream dynamic pressure to jet dynamic pressure:

$$\sqrt{\frac{\overline{q_\infty}}{\overline{q_J}}}$$

The lateral-directional reference angle is defined as below:

$$\beta' = Tan^{-1} (v'/u')$$

Where $u' = u/\cos \alpha$ and $v' = v * \cos \phi$

The FORTRAN name for β' is BETAP.

3.2.3.2 **Aerodynamic Algorithms** - Each component of the respective coefficient is summarized for the low speed and high speed data in the following equations. The FORTRAN name of each component is also included in parenthesis.

o **Low Speed Aero (M ≤ 0.3) - Body Axis System**

o **Normal Force**

$$F_N = [C_{N_o} + \Delta C_{N_{\delta_H}} + (\Delta C_{N_{\delta_{F_L}}} + \Delta C_{N_{\delta_{F_R}}}) + \Delta C_{N_{FJI}}$$

$$+ (\Delta C_{N_{\delta_{A_L}}} + \Delta C_{N_{\delta_{A_R}}}) + C_{N_{\delta_{GEAR}}} * \delta_{GEAR} + C_{N_{\delta_{LID}}} * \delta_{LID}$$

$$+ (C_{N_q} * q + C_{N_{\dot\alpha}} * \dot\alpha) * \frac{\bar{c}}{2V_T} + \Delta C_{N_{POWER}}] * \bar{q} * S + \Delta C_{N_{GE}}$$

Where:

C_{N_o} — Baseline normal force coefficient as a function of α, (CNBASE).

$\Delta C_{N_{\delta_H}}$ — Increment of normal force coefficient due to stabilator deflection as a function of α_{TAIL}, θ_J, Veq and altitude, (DCNSTAB).

$\Delta C_{N_{\delta_{F_{L,R}}}}$ — Increment of normal force coefficient due to left and right flap deflection as a function of α, θ_J and Veq, (CNFLAP).

$\Delta C_{N_{FJI}}$ — Increment of normal force coefficient due to flap-jet impingement as a function of δ_F, θ_J, α and Veq, (CNFJI).

$\Delta C_{N_{\delta_{A_{L,R}}}}$ — Increment of normal force coefficient due to left and right aileron deflection as a function of α, (DCNAIL).

$C_{N_{\delta_{GEAR}}}$ — $\partial C_N / \partial \delta GEAR$, where δ_{GEAR} is the normalized gear deflection, (DCNGEAR).

$C_{N_{\delta_{LID}}}$ — $\partial C_N / \partial \delta LID$, where δ_{LID} is the normalized LIDS deflection, (DCNLID).

$\Delta C_{N_{GE}}$ — Increment of normal force due to ground effects as a function of altitude, α, θ_J and engine thrust, (CNGE).

C_{N_q} — $\partial C_N / \partial q$, normal force coefficient due to pitch rate, (CNQ).

$C_{N_{\dot\alpha}}$ — $\partial C_N / \partial \dot\alpha$, normal force coefficient due to angle of attack rate, (CNALPD).

$\Delta C_{N_{POWER}}$ — Increment of normal force coefficient due to power effects as a function of α, θ_J and Veq, (DCNPOW).

o **Axial Force**

$$F_A = [C_{A_o} + \Delta C_{A_{\delta_H}} + (\Delta C_{A_{\delta_{F_L}}} + \Delta C_{A_{\delta_{F_R}}}) + \Delta C_{A_{FJI}}$$

$$+ (\Delta C_{A_{\delta_{A_L}}} + \Delta C_{A_{\delta_{A_R}}}) + C_{A_{\delta_{GEAR}}} * \delta_{GEAR} + C_{A_{\delta_{LID}}} * \delta_{LID}$$

$$+ \Delta C_{A_{POWER}}] * \bar{q} * S + \Delta C_{A_{GE}}$$

Where:

C_{A_o}	— Baseline axial force coefficient as a function of α, (CABASE).
$\Delta C_{A_{\delta_H}}$	— Increment of axial coefficient due to stabilator deflection, (DCASTAB).
$\Delta C_{A_{\delta_{F_{L,R}}}}$	— Increment of axial coefficient due to left and right flap deflection as a function of α and Veq, (CAFLAP).
$\Delta C_{A_{FJI}}$	— Increment of axial force coefficient due to flap-jet impingement as a function of δ_F, θ_J, and α, (CAFJI).
$\Delta C_{A_{\delta_{A_{L,R}}}}$	— Increment of axial force coefficient due to left and right aileron deflection as a function of α, (DCAAIL).
$C_{A_{\delta_{GEAR}}}$	— $\partial C_A / \partial \delta_{GEAR}$ where δ_{GEAR} is the normalized gear deflection, (DCAGEAR).
$C_{A_{\delta_{LID}}}$	— $\partial C_A / \partial \delta_{LID}$ where δ_{LID} is the normalized LIDS deflection, (DCALID).
$\Delta C_{A_{GE}}$	— Increment of axial force due to ground effects as a function of α, θ_J, altitude and engine thrust, (CAGE).
$\Delta C_{A_{POWER}}$	— Increment of axial force coefficient due to power effects as a function of θ_J, Veq and α, (DCAPOW).

C. ... .
OF POOR QUALITY

o **Pitching Moment**

$$PM = [C_{m_o} + \Delta C_{m_{\delta_H}} + (\Delta C_{m_{\delta_{F_L}}} + \Delta C_{m_{\delta_{F_R}}}) + \Delta C_{m_{FJI}}$$

$$+ (\Delta C_{m_{\delta_{A_L}}} + \Delta C_{m_{\delta_{A_R}}}) + C_{m_{\delta_{GEAR}}} * \delta_{GEAR} + C_{m_{\delta_{LID}}} * \delta_{LID}$$

$$+ (C_{m_q} * q + C_{m_{\dot\alpha}} * \dot\alpha) * \frac{\bar{c}}{2V_T} + \Delta C_{m_{POWER}}] * \bar{q} * S * \tilde{c} + \Delta C_{m_{GE}} + \Delta C_{m_{FP}}$$

Where:

C_{m_o}	– Baseline pitching moment coefficient as a function of α, (CMBASE).
$\Delta C_{m_{\delta_H}}$	– Increment of pitching moment coefficient due to stabilator deflection as a function of α_{TAIL}, θ_J, Veq and altitude, (DCMS'
$\Delta C_{m_{\delta_{F_{L,R}}}}$	– Increment of pitching moment coefficient due to left and right flap deflection as a function of α and Veq, (CMFLAP).
$\Delta C_{m_{FJI}}$	– Increment of pitching moment coefficient due to flap-jet impingement as a function of δ_F, θ_J, α and Veq, (CMFJI).
$\Delta C_{m_{\delta_{A_{L,R}}}}$	– Inc.. .ent c. ..itching moment coefficient due to left and right .i ... .eflection as a function of angle of attack, (DCMAIL).
$C_{m_{\delta_{GEAR}}}$	– $\partial C_m/\partial \delta_{GEAR}$ where δ_{GEAR} is the normalized gear deflection, (DCMGEAR).
$C_{m_{\delta_{LID}}}$	– $\partial C_m/\partial \delta_{LIDS}$ where δ_{LID} is the normalized LIDS deflection, (DCMLID).
$\Delta C_{M_{GE}}$	– Increment of pitching moment due to ground effects as a function of α, θ_J, altitude and engine thrust, (CMGE).
C_{m_q}	– $\partial C_m/\partial q$, pitching moment coefficient due to pitch rate, (CMQ).
$C_{m_{\dot\alpha}}$	– $\partial C_m/\partial \dot\alpha$, pitching moment coefficient due to angle of attack, (CM/
$\Delta C_{m_{POWER}}$	– Increment of pitching moment coefficient due to power effects as a function of α, Veq and θ_J, (DCMPOW).
$\Delta C_{m_{FP}}$	– Increment of pitching moment due to flat plate drag motion for u < 50 KTAS. Simulates aerodynamic damping in hover and low speeds, (TEMPX3).

o <u>Side Force</u>

$$SF = [C_{Y_o} + (\Delta C_{Y_{\delta_{A_L}}} + \Delta C_{Y_{\delta_{A_R}}}) + C_{Y_{\delta_R}} * \delta_R + \Delta C_{Y_{POWER}}] * \bar{q} * S$$

$$+ \Delta C_{Y_{GE}} + \Delta C_{Y_{PHI}} + \Delta C_{Y_{OGE}}$$

Where:

C_{Y_o} — Baseline side force coefficient. For u > 50 KTAS defined as $C_{Y_\beta} * \beta$, side force due to sideslip angle as a function of α, β, and average flap deflection, (CYBASE). For u < 30 KTAS, C_{Y_o} is 0.

$\Delta C_{Y_{\delta_{A_{L,R}}}}$ — Increment of side force coefficient due to left and right aileron deflection as a function of α, (DCYAIL).

$C_{Y_{\delta_R}}$ — $\partial C_Y/\partial \delta_R$, side force coefficient due to rudder reflection, (CYDR).

$\Delta C_{Y_{POWER}}$ — Increment of side force coefficient due to power effects as a function of Veq,α and β for u > 50 KTAS, (CYPOWER).

$\Delta C_{Y_{GE}}$ — Increment of side force due to ground effects as a function of α, altitude, engine thrust, θ_J and β', (SFIGE).

$\Delta C_{Y_{PHI}}$ — Increment of side force due to roll attitude in ground proximity (h < 70 ft.) as a function of altitude, Veq, ϕ, β', u, θ_J and engine thrust, (YDSFTP).

$\Delta C_{Y_{OGE}}$ — Increment of side force as a function of α, θ_J, engine thrust, and Veq for u < 30 KTAS, (SFOGE). For u > 50 KTAS, $\Delta C_{Y_{OGE}}$ is 0.

o <u>Rolling Moment</u>

$$RM = [C_{\ell_o} + (\Delta C_{\ell_{\delta_{A_L}}} + \Delta C_{\ell_{\delta_{A_R}}}) + C_{\ell_{\delta_R}} * \delta_R + \Delta C_{\ell_{POWER}} + \Delta C_{\ell_{\delta_F}}$$

$$+ \Delta C_{\ell_{FJI}} + (C_{\ell_r} * r + C_{\ell_p} * p) * \frac{b}{2V_T}] * \bar{q} * S * b + \Delta C_{\ell_{PHI}}$$

$$+ \Delta C_{\ell_{FF}} + \Delta C_{\ell_{GE}} + \Delta C_{L_{OGE}}$$

Where:

C_{ℓ_o} — Baseline rolling moment coefficient. For u > 50 KTAS defined as C_{ℓ_β} * β, rolling moment due to sideslip angle as a function of α, β and average flap deflection, (CLLBASE). For u < 30 KTAS, C_{ℓ_o} is 0.

$\Delta C_{\ell_{\delta_{A_{L,R}}}}$ — Increment of rolling moment coefficient due to left and right aileron deflection as a function of α, (DCLLAIL).

$C_{\ell_{\delta_R}}$ — $\partial C_\ell / \partial \delta_R$, rolling moment coefficient due to rudder deflection, (CLLDR).

$\Delta C_{\ell_{POWER}}$ — Increment of rolling moment coefficient due to power effects as a function of Veq, α and β for u > 50 KTAS, (CLLPOWR).

$\Delta C_{\ell_{\delta_F}}$ — Increment of rolling moment coefficient due to asymmetric flaps, (DCLLF).

$\Delta C_{\ell_{FJI}}$ — Increment of rolling moment coefficient due to flap-jet impingement, (DCLLFJI).

C_{ℓ_r} — $\partial C_\ell / \partial r$, rolling moment coefficient due to yaw rate as a function of α, (CLLR).

C_{ℓ_p} — $\partial C_\ell / \partial p$, rolling moment coefficient due to roll rate as a function of α, (CLLP).

$\Delta C_{\ell_{GE}}$ — Increment of rolling moment due to ground effects as a function of α, altitude, engine thrust, Veq, θ_J and β', (RMIGE).

$\Delta C_{\ell_{PHI}}$ — Increment of rolling moment due to roll attitude in ground proximity as a function of altitude, Veq, φ, β', u, θ_J and engine thrust, (DRMPHI).

$\Delta C_{\ell_{FP}}$ — Increment of rolling moment due to flat plate drag motion for u < 50 KTAS. Simulates aerodynamic damping in hover and low speeds, (TEMPX5).

$\Delta C_{R_{OGE}}$ — Increment of rolling moment as a function of β', α, Veq, θ_J and engine thrust, (RMOGE). For u > 50 KTAS, $\Delta C_{\ell_{OGE}}$ = 0.

o **Yawing Moment**

$$YM = [C_{n_o} + (\Delta C_{n_{\delta_{A_L}}} + \Delta C_{n_{\delta_{A_R}}}) + C_{n_{\delta_R}} * \delta_R + \Delta C_{n_{POWER}} + \Delta C_{n_{\delta_F}} + \Delta C_{n_{FJI}}$$

$$+ (C_{n_r} * r + C_{n_p} * p) * \frac{b}{2V_T}] * \bar{q} * S * b + \Delta C_{n_{PHI}} + \Delta C_{n_{FP}} + \Delta C_{n_{GE}} + C_{n_{OGE}}$$

Where:

C_{n_o} — Baseline yawing moment coefficient. For u > 50 KTAS defined as $C_{n_\beta} * \beta$, yawing moment due to sideslip angle as a function of α, β and average flap deflection, (CLNBASE). For u < 30 KTAS, C_{n_o} is 0.

$\Delta C_{n_{\delta_{A_{L,R}}}}$ — Increment of yawing moment coefficient due to left and right aileron deflection as a function of α, (DCLNAIL).

$C_{n_{\delta_R}}$ — $\partial C_n / \partial \delta_R$, yawing moment coefficient due to rudder deflection, (CLNDR).

$\Delta C_{n_{POWER}}$ — Increment of yawing moment coefficient due to power effects as a function of Veq, α and β for u > 50 KTAS, (CLNPOWR).

$\Delta C_{n_{\delta_F}}$ — Increment of yawing moment coefficient due to asymmetric flaps. (DCLNF).

$\Delta C_{n_{FJI}}$ — Increment of yawing moment coefficient due to flap-jet impingement, (DCLNFJI).

C_{n_r} — $\partial C_n / \partial r$, yawing moment coefficient due to yaw rate as a function of α, (CLNR).

C_{n_p} — $\partial C_n / \partial p$, yawing moment coefficient due to roll rate as a function of α, (CLNP).

$\Delta C_{n_{GE}}$ — Increment of yawing moment due to ground effects as a function α, altitude, engine thrust, Veq, θ_J and β', (YMIGE).

$\Delta C_{n_{PHI}}$ — Increment of yawing moment due to roll attitude in ground proximity (altitude < 70') as a function of altitude, Veq, ϕ, β', u, θ_J and engine thrust, (DYMPBI).

$\Delta C_{n_{FP}}$ — Increment of yawing moment due to flat plate drag motion for u < 50 KTAS. Simulates aerodynamic damping in hover and low speeds, (TEMPX6).

$\Delta C_{n_{OGE}}$ — Increment of yawing moment as a function of β', α, Veq, θ_J and engine thrust, (YMOGE). For u > 50 KTAS, $\Delta C_{n_{OGE}} = 0$

o __High Speed Aero (M $\geq$ 0.5) - Stability Axis System__

   o __Lift__

$$F_L = [C_{L_o} + (\Delta C_{L_{\delta_{F_L}}} + \Delta C_{L_{\delta_{F_R}}}) + (\Delta C_{L_{\delta_{A_L}}} + \Delta C_{L_{\delta_{A_R}}}) + \Delta C_{L_{POWER}}] * \bar{q} * S$$

$$+ \Delta C_{L_{STAB}}$$

Where:

   C_{L_o} - Baseline lift force coefficient as a function of α
              and M, (CLBASE).

   $\Delta C_{L_{\delta_{F_{L,R}}}}$ - Increment of lift force coefficient due to left and
              right flap deflection as a function of α and M,
              (DCLFL and DCLFR).

   $\Delta C_{L_{\delta_{A_{L,R}}}}$ - Increment of lift force coefficient due to left and
              right aileron deflection as a function of M, (DCLAL
              and DCLAR).

   $\Delta C_{L_{POWER}}$ - Increment of lift force coefficient to power effects
              as a function of θ_J, α and Veq, (DCLPOW).

   $\Delta C_{L_{STAB}}$ - Increment of lift force due to stabilator deflection
              as a function of α and M, (CLSTAB).

   o __Drag__

$$F_D = [C_{D_o} + (\Delta C_{D_{\delta_{F_L}}} + \Delta C_{D_{\delta_{F_R}}}) + (\Delta C_{D_{\delta_{A_L}}} + \Delta C_{D_{\delta_{A_R}}}) + \Delta C_{D_{STAB}}$$

$$+ C_{D_{\delta_R}} * |\delta_R| + \Delta C_{D_{STOW}} + C_{D_{\delta_{GEAR}}} * \delta_{GEAR} + C_{D_{\delta_{LID}}} * \delta_{LID}] * \bar{q} * S$$

Where:

   C_{D_o} - Baseline drag coefficient as a function of α, M and
              C_{L_o}, (CDBASE).

   $\Delta C_{D_{\delta_{F_{L,R}}}}$ - Increment of drag force due coefficient due to left and right
              flap deflection as a function of α and M, (DCDFL and DCDFR).

   $\Delta C_{D_{\delta_{A_{L,R}}}}$ - Increment of drag force coefficient due to left and right
              aileron deflection as a function of α and M, (DCDAL and DCDAR).

$\Delta C_{D_{STAB}}$ — Increment of drag force coefficient due to stabilator deflection as a function of α and M, (CDSTAB).

$C_{D_{\delta_R}}$ — $\partial C_L / \partial \delta_R$, drag force coefficient due to rudder deflection as a function of α and M, (CDDR).

$\Delta C_{D_{STOW}}$ — Increment of drag force coefficient due to pylons and gun pods, (HCDSTOW).

$C_{D_{\delta_{GEAR}}}$ — $\partial C_D / \partial \delta_{GEAR}$, where δ_{GEAR} is the normalized gear deflection.

$C_{D_{\delta_{LID}}}$ — $\partial C_D / \partial \delta_{LID}$, where δ_{LID} is the normalized LIDS deflection.

o **Pitching Moment**

$$PM = [C_{m_o} + (\Delta C_{m_{\delta_{F_L}}} + \Delta C_{m_{\delta_{F_R}}}) + (\Delta C_{m_{\delta_{A_L}}} + \Delta C_{m_{\delta_{A_R}}})$$

$$+ \Delta C_{m_{STAB}} + (C_{m_q} * q + C_{m_{\dot\alpha}} * \dot\alpha) * \frac{\bar c}{2V_T} + \Delta C_{m_{POWER}} + \Delta C_{m_{STING}}] * \bar q * S * \bar c$$

Where:

C_{m_o} — Baseline pitching moment coefficient as a function of α and M, (CMBASEH).

$\Delta C_{m_{\delta_{F_{L,R}}}}$ — Increment of pitching moment coefficient due to left and right flap deflection as a function of α and M, (DCMFL and DCMFR).

$\Delta C_{m_{\delta_{A_{L,R}}}}$ — Increment of pitching moment coefficient due to left and right aileron deflection as a function of α, (HCMDAL and HCMDAR).

$\Delta C_{m_{STAB}}$ — Increment of pitching moment coefficient due to stabilator deflection as a function of α and M, (DCMST).

C_{m_q} — $\partial C_m / \partial q$, pitching moment coefficient due to pitch rate as a function of M, (CMQH).

$C_{m_{\dot\alpha}}$ — $\partial C_m / \partial \dot\alpha$, pitching moment coefficient due to angle of attack rate as a function of M, (CMALPDH).

$\Delta C_{m_{POWER}}$ — Increment of pitching moment coefficient due to power effects as a function of α, V_{eq} and θ_J, (HCMPOW).

$\Delta C_{m_{STING}}$ — Increment of pitching coefficient due to sting interference correction to wind tunnel data, (CMSTING).

o <u>Side Force</u>

$$SF = [C_{Y_\beta} * \beta + \Delta C_{Y_\beta} * \beta + (\Delta C_{Y_{\delta_{A_L}}} + \Delta C_{Y_{\delta_{A_R}}}) + C_{Y_{\delta_R}} * \delta_R/15$$

$$+ C_{Y_r} * r * \frac{b}{2V_T}] \bar{q} * S$$

Where:

C_{Y_β} – $\partial C_Y/\partial\beta$, side force coefficient due to sideslip angle as a function of α and M, (HCYB).

ΔC_{Y_β} – Increment of C_{Y_β} due to flaps as a function of M, α and flap deflection, (HCYBF).

$\Delta C_{Y_{\delta_{A_{L,R}}}}$ – Increment of side force coefficient due to left and right aileron deflection as a function of α, (HCYDAL and HCYDAR).

$C_{Y_{\delta_R}}$ – $\partial C_Y/\partial\delta_R$, side force coefficient due to rudder deflection as a function of M and α, (HCYDR).

C_{Y_r} – $\partial C_Y/\partial r$, side force coefficient due to yaw rate as a function of M, (HCYR).

o <u>Rolling Moment</u>

$$RM = [C_{\ell_\beta} * \beta + \Delta C_{\ell_\beta} * \beta + (\Delta C_{\ell_{\delta_{A_L}}} + \Delta C_{\ell_{\delta_{A_R}}}) + C_{\ell_{\delta_R}} * \delta_R/15$$

$$+ (C_{\ell_r} * r + C_{\ell_p} * p) * \frac{b}{2V_T} + C_{\ell_{POWER}}] * q * S * b + \Delta C_{\ell_{\delta_F}}$$

Where:

C_{ℓ_β} – $\partial C_\ell/\partial\beta$, rolling moment coefficient due to sideslip angle as a function of M and α, (HCLLB).

ΔC_{ℓ_β} – Increment of C_{ℓ_β} due to flaps as a function of M, α and flap deflection, (HCLLBF).

$\Delta C_{\ell_{\delta_{A_{L,R}}}}$ – Increment of rolling moment coefficient due to left and right aileron deflection as a function of α and M, (HCLDAR and HCLDAL).

$C_{\ell_{\delta_R}}$ $- \partial C_\ell / \partial \delta_R$, rolling moment coefficient due to rudder deflection as a function of α and M, (HCLLDR).

C_{ℓ_r} $- \partial C_\ell / \partial r$, rolling moment coefficient due to yaw rate as a function of M and α, (HCLLR).

C_{ℓ_p} $- \partial C_\ell / \partial p$, rolling moment coefficient due to roll rate as a function of M and α, (HCLLP).

$\Delta C_{\ell_{\delta_F}}$ - Increment of rolling moment due to asymmetric flaps, (HDCLLF).

$\Delta C_{\ell_{POWER}}$ - Increment of rolling moment coefficient due to power effects, (HCLLBF * BETA).

o **Yawing Moment**

$$YM = [C_{n_\beta} * \beta + (\Delta C_{n_{\delta_{A_L}}} + \Delta C_{n_{\delta_{A_R}}}) + \quad \delta_R/15$$

$$+ (C_{n_r} * r + C_{n_p} * p) * \frac{b}{2V_T}] * \bar{q} * S * b + \Delta C_{n_{\delta_F}}$$

Where:

C_{n_β} $- \partial C_n / \partial \beta$, yawing moment coefficient due to sideslip angle as a function of M and α, (CNB).

$\Delta C_{n_{\delta_{A_{L,R}}}}$ - Increment of yawing moment coefficient due to aileron deflection as a function of M and α, (CNDAR and CNDAL).

$C_{n_{\delta_R}}$ $- \partial C_n / \partial \delta_R$, yawing moment coefficient due to rudder deflection as a function of M and α, (CNDR).

C_{n_r} $- \partial C_n / \partial r$, yawing moment coefficient due to yaw rate as a function of M and α, (CNR).

C_{n_p} $- \partial C_n / \partial p$, yawing moment coefficient due to roll rate as a function of α and M, (CNP).

$\Delta C_{n_{\delta_F}}$ - Increment of yawing moment due to asymmetric flaps, (HCDNF).

3.2.3.3 Center of Gravity Effects - The effects of center of gravity displacement are included in the moment equations. All of the forces are referenced to a point on the aircraft at Fuselage Station 346.6, waterline Station 96.0 and coinciding with the X-axis of the aircraft. Incremental distances from the reference point to the center of gravity are computed and used in the following equations:

o Pitching Moment

$$PM = PM - F_N * (346.6 - CG_{FS})/(12) + F_A * (CG_{WL} - 96.)/(12)$$

o Rolling Moment

$$RM = RM - SF * (CG_{WL} - 96.)/(12) + F_N * CG_{BL}/(12)$$

o Yawing Moment

$$YM = YM + SF * (CG_{FS} - 346.6)/(12) + F_A * CG_{BL}/(12)$$

3.2.3.4 Reference Axes Transformations - The aerodynamic force and moments are derived in the body axis system for use in the equations of motion. The following equations transform the high speed aero forces and moments from the stability to body axis system.

o L-Body Force (Positive down)
$$F_{Z_B} = -F_{LIFT} * COS\alpha - F_{DRAG} * SIN\alpha$$

o X-Body Force (Positive forward)
$$F_{X_B} = -F_{DRAG} * COS\alpha + F_{LIFT} * SIN\alpha$$

o X-Body Rolling Moment (Positive right wing down)
$$RM_{X_B} = RM_{STAB} * COS\alpha - YM_{STAB} * SIN\alpha$$

o Z-Body Yawing Moment (Positive nose right)
$$YM_{Z_B} = YM_{STAB} * COS\alpha + RM_{STAB} * SIN\alpha$$

3.2 4 ENGINE AND REACTION CONTROL SYSTEM FORCE AND MOMENT EQUATIONS - All engine and RCS forces and moments are resolved in the body axis system (Figure 3.2-5) for use in the equations of motion. The engine forces and moments include inlet momentum effects and scrub and boundary layer drag increments.

3.2.4.1 Engine Thrust Geometry - Figure 3.2-6 shows the relative geometry of the effective thrust center with respect to the moment reference center used for the aerodynamic data. The following equations define the resulting engine thrust forces and moments about the aircraft c.g. in the body axis system.
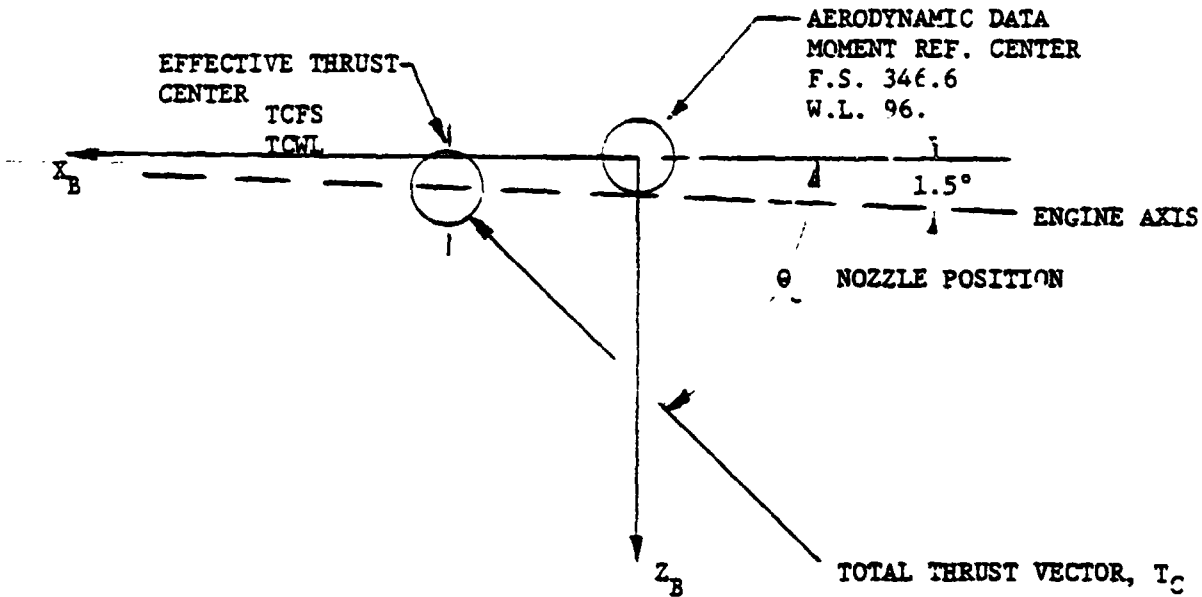
FIGURE 3.2-6

ENGINE THRUST GEOMETRY

o <u>X-Body Force (Positive forward)</u>

$$FT_{X_B} = T_C * COS\ (\theta_J + 1.5°)$$

o <u>Y-Body Force (Positive out right wing)</u>

$$FT_{Y_B} = 0.$$

o <u>Z-Body Force (Positive down)</u>

$$FT_{Z_B} = -T_C * SIN\ (\theta_J + 1.5°)$$

o <u>Pitching Moment</u>

$$PM_B = T_C * ((346.6 - TCFS)/12.) * SIN\ (\theta_J + 1.5°)$$
$$+ T_C * ((96. - TCWL)/12.) * COS\ (\theta_J + 1.5°) - FT_{Z_B} *$$
$$((CGFS - 346.6)/12.) + FT_{X_B} * ((CGWL - 96.)/12.)$$

o <u>Yawing Moment</u>

$$YM_B = FT_{X_B} * CGBL/12. + FT_{Y_B} * ((CGFS - 346.6)/12.)$$

o <u>Rolling Moment</u>

$$RM_B = -FT_{Z_B} * CBGL/12. - FT_{Y_B} * ((CGWL - 96.)/12.)$$

Where:

T_C is the total thrust vector.
TCFS is the thrust center fuselage station location.
TCWL is the thrust center waterline station location.

3.2.4.2 Ram Drag and Inlet Effects - Incremental forces and moments at the inlet are derived from ram drag forces as a function of inlet flow angle and from air mass flow as a function of aircraft body rates. The following equations summarize these inlet contributions at the aircraft c.g. The force application point on the inlet is defined as F.S. 220.63, W.L. 90.77 and B.L. 27.

o X-Body Force

$$FI_{X_B} = -\text{Ram Drag} * \text{COS}\beta * \text{COS}\alpha - \frac{\dot{m}}{g} * q * \Delta Z$$

o Y-Body Force

$$FI_{Y_B} = -\text{Ram Drag} * \text{Sin}\beta + \frac{\dot{m}}{g} * p * \Delta Z - \frac{\dot{m}}{g} * r * \Delta X$$

o Z-Body Force

$$FI_{Z_B} = -\text{Ram Drag} * \text{COS}\beta * \text{SIN}\alpha + \frac{\dot{m}}{g} * q * \Delta X$$

o Pitching Moment

$$PMI = \text{Ram Drag} * \text{COS}\beta * ((\text{SIN}\alpha * \Delta X) - (\text{COS}\alpha * \Delta Z))$$
$$- \frac{\dot{m}}{g} * q * (\Delta X^2 + \Delta Z^2)$$

o Yawing Moment

$$YMI = \text{Ram Drag} * ((\text{COS}\beta * \text{COS}\alpha * CGBL/12.) - (\text{SIN}\beta * \Delta X))$$
$$+ \frac{\dot{m}}{g} * p * \Delta X * \Delta Z - \frac{\dot{m}}{g} * r * (\Delta X^2 + \Delta Y^2)$$

o Rolling Moment

$$RMI = \text{Ram Drag} * ((\text{SIN}\beta * \Delta Z) - (\text{COS}\beta * \text{SIN}\alpha * CGBL/12.))$$
$$- \frac{\dot{m}}{g} * p * (\Delta Z^2 + \Delta Y^2) + \frac{\dot{m}}{g} * r * \Delta X * \Delta Y$$

Where:

$$\text{Ram Drag} = \frac{\dot{m}}{g} * V_T \sim \text{lb}_f$$

$$\Delta X = (CGFS - 220.63)/12. \sim \text{ft.}$$

$$\Delta Y = (27. - CGBL)/12. \sim \text{ft.}$$

$$\Delta Z = (CGWL - 90.77)/12. \sim \text{ft.}$$

3.2.4.3 RCS Thrust Geometry - The relative geometry of the YAV-8B RCS is shown in Figure 3.2-7. To compute the pitch and roll forces due to the RCS requires accounting for the off-axis orientation of the pitch and roll valves. The following equations are used to derive the RCS forces and moments in the body axis system at the aircraft c.g.:

o X-Body Force

$$FT_{X_{RCS}} = FT_{FPV} * SIN (7.63°) - FT_{RPV} * SIN (8°)$$
$$- COS (5°) * SIN (7°) * (FT_{RVWD} + FT_{RVWU})$$

NOTE: Subscripts defined in Figure 3.2-7.

o Y-Body Force

$$FT_{Y_{RCS}} = FT_{YV} - SIN (5°) * COS (7°) * ((FT_{RVWD} + FT_{RVWU})_{RT}$$
$$- (FT_{RVWD} + FT_{RVWU})_{LT})$$

o Z-Body Force

$$FT_{Z_{RCS}} = FT_{FPV} * COS (7.63°) + FT_{RPV} * COS (8°)$$
$$+ COS (5°) * COS (7°) * (FT_{RVWD} + FT_{RVWU})$$

o Pitching Moment

$$PM_{RCS} = FT_{RPV} * (COS (8°) * (\frac{605.51 - CGFS}{12.}) + SIN (8°) * (\frac{114.63 - CGWL}{12.}))$$
$$+ FT_{FPV} * (COS (7.63°) * (\frac{137.48 - CGFS}{12.}) + SIN (7.63°) * (\frac{CGWL - 70.36}{12.}))$$
$$- COS (5°) * SIN (7°) * (\frac{83.89 - CGWL}{12.}))$$
$$+ (FT_{RVWD} + FT_{RVWU}) * ((COS (5°) * COS (7°) * (\frac{432.45 - CGFS}{12.})$$
$$- COS (5°) * SIN (7°) * (\frac{83.89 - CGWL}{12.}))$$

o Yawing Moment

$$YM_{RCS} = FT_{YV} * (\frac{CGFS - 599}{12.}) - ((FT_{RVWD} + FT_{RVWU})_{RT}$$
$$- (FT_{RVWD} + FT_{RVWU})_{LT}) * (SIN (5°) * COS (7°) * (\frac{432.45 - CGFS}{12.})$$
$$+ COS (5°) * SIN (7°) * (\frac{177.84 - CGBL}{12.}))$$
$$+ (FT_{FPV} * SIN (7.63°) - FT_{RPV} * SIN (8°)) * CGBL/12$$

Yaw Valve (YV)
FS 599.0
WL 120.5
BL 0

Fuselage Datum
WL 96.00

Rear Pitch Valve (RPV)
FS 605.51
WL 114.63
BL 0

Front Pitch Valve (FPV)
FS 137.48
WL 70.36
BL 0

7.63°

8°

7°

Roll Valve (RV)
FS 432.45
WL 83.89
BL 177.84

(RVWU)$_{RT}$

5°

5°

(RVWD)$_{LT}$

177.84
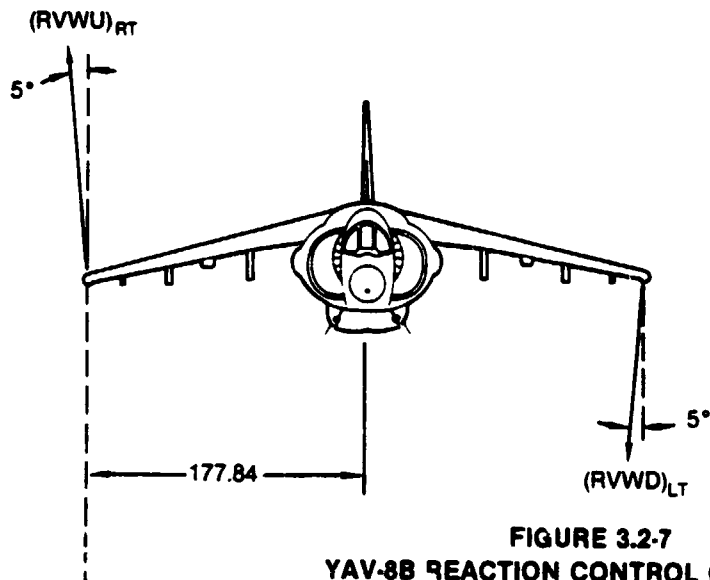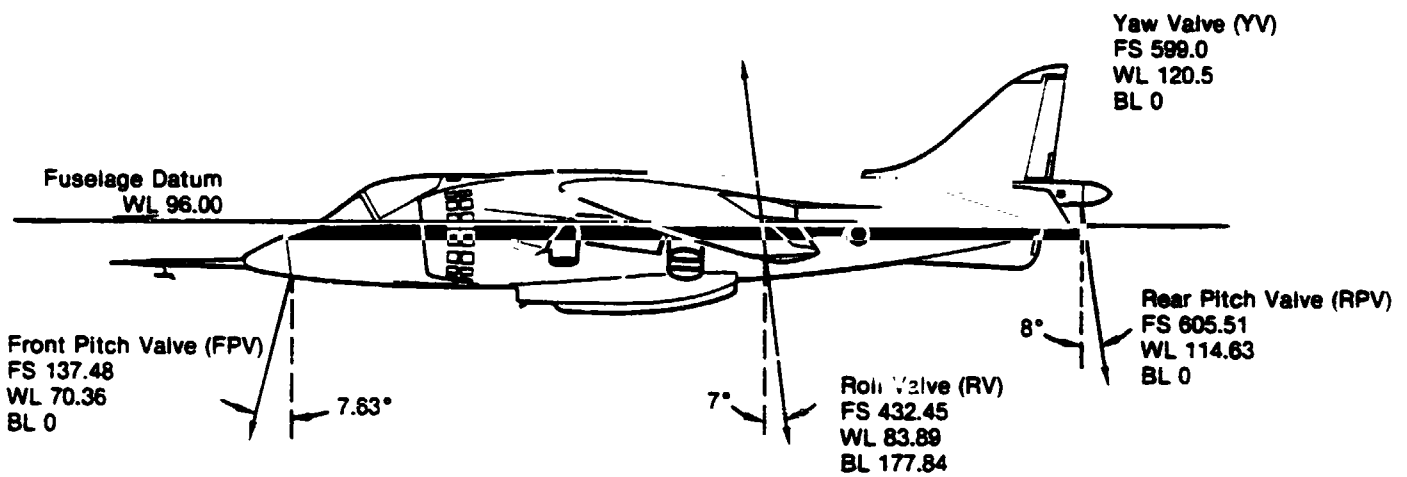
All dimensions in inches
FS · Fuselage station
WL · Water line
BL · Butt line

GP21-0982-46

FIGURE 3.2-7
YAV-8B REACTION CONTROL GEOMETRY

o <u>Rolling Moment</u>

$$RM_{RCS} = ((FT_{RVWD} + FT_{RVWU})_{RT} - (FT_{RVWD} + FT_{RVWU})_{LT}) *$$

$$(SIN (5°) * COS (7°) * (\frac{CGWL - 83.89}{12.}) + COS (5°) * COS (7°)$$

$$* (\frac{177.84 - CGBL}{12.})) - (FT_{FPV} * COS (7.63°) + FT_{RPV} * COS (8°)) *$$

$$CGBL/12 + FT_{YV} * (\frac{120.5 - CGWL}{12.})$$

3.2.5 <u>WEIGHT AND BALANCE EQUATIONS</u> - The total weight of the aircraft is computed by summing aircraft dry weight (including the pilot), fuel weight, and water weight. Because the weight distribution in the aircraft is constantly changing due to fuel transfer and water usage, the center of weight moment for each factor is computed in all three body axes. In addition the moments of inertia and the cross product of inertia, I_{XZ}, are computed as a function of these factors.

The body axis coordinates of the center of gravity of each fuel tank and the water tank are stored in the subroutine, WTBAL07, data tables as a function of fuel and water remaining. The weight moment of the dry weight aircraft about the aircraft reference point in each axis is stored as well. With the relative aircraft geometry determined, the body axis coordinates of the center of gravity are computed:

$$M_{X_{FUEL}} = Tank (1) * X_{TANK 1} + Tank (2) * X_{TANK 2} + \ldots$$

$$M_{X_{H_2O}} = WATER * X_{H_2O}$$

$$X_{CG} = (M_{X_{DRY}} + M_{X_{FUEL}} + M_{X_{H_2O}})/WT , etc.$$

Similarly the y and z component of the center of gravity can be determined. The x component is referenced back to the wing leading edge and expressed as a percent of mean aerodynamic chord.

$$CGPC = ((X_{CG} - 336.3)/(99.792)) * 100$$

The moments of inertia and product of inertia are computed in a similar manner using the parallel axis theorem:

$$I_{XX_{FUEL}} = Tank (1) * (Y^2_{TANK 1} + X^2_{TANK 1})/g + \ldots$$

$$I_{XX_{H_2O}} = WATER * (Z^2_{H_2O})/g$$

$$I_{XX} = I_{XX_{DRY}} + I_{XX_{FUEL}} + I_{XX_{H_2O}}$$

$$I_{XZ_{FUEL}} = \text{Tank (1)} * X_{TANK\ 1} * Z_{TANK\ 1}/g + \cdots$$

$$I_{XZ_{H_2O}} = \text{WATER} * X_{H_2O} * Z_{H_2O}/g$$

$$I_{XZ} = I_{XZ_{DRY}} + I_{XZ_{FUEL}} + I_{XZ_{H_2O}}$$

These inertias are used along with the aircraft mass to determine the aircraft mass matrix which is used in the equations of motion.

3.3 AIRCRAFT SUBROUTINES

The YAV8B Program includes 6 subroutines which comprise the necessary logic for math modeling the YAV-8B aircraft. The subroutines are the weights and balance routine (WTBAL07), the primary flight controls routine (PFC07), the reaction control system routine (RCS07), the engine routine (ENG08), the secondary flight control routine (SFC07) and the aerodynamics routine (AERØY8B). The sequential order of execution is shown in Figure 3.1-2.

A brief description of the inputs and outputs of each subroutine as well as top-level flow diagrams are provided to familiarize the program user with the purpose of each subroutine. A more complete description of necessary program input and output variables is given in the user's guide, Section 3.4. The flow diagrams are simplified in order to aid the program user to interpret the program listings. Although the listings contain many useful comments, the flow diagrams can be useful if it becomes necessary to modify or change existing logic. A more detailed description of the math model equations for the aerodynamic algorithms, the engine and RCS force and moment calculations, and the weights and balance breakdown is given in Section 3.2.

3.3.1 WTBAL07 SUBROUTINE - The WTBAL07 Subroutine (weights and balance) computes current values of the moments of inertia, center of gravity location, weight and mass of the YAV-8B. This subroutine interfaces with the engine subroutine (ENG08) which determines the remaining internal fuel and water. The WTBAL07 subroutine is not designed to include stores configurations although it could be modified to simulate external stores on the aircraft.

The total weight of the aircraft is computed by summing aircraft dry weight, fuel weight and water weight. The moments of inertia about each body axis and the cross product of inertia, I_{XZ}, are continuously computed as a function of the remaining fuel and water. The center of gravity location is determined by computing the weight moment of each factor (dry weight of aircraft, fuel weight and water weight) along the respective body axis and dividing by the gross weight. A selective bias in the weight moment for each axis is included if it is necessary to simulate a c.g. offset. This moment bias also will alter the respective moment of inertia.

The inputs to this subroutine fuel weight, water weight, and gear and LIDS positions. The location, inertias, gross weight and mass. The c.g. the body axis system. Figure 3.3-1 depicts the logic subroutine.
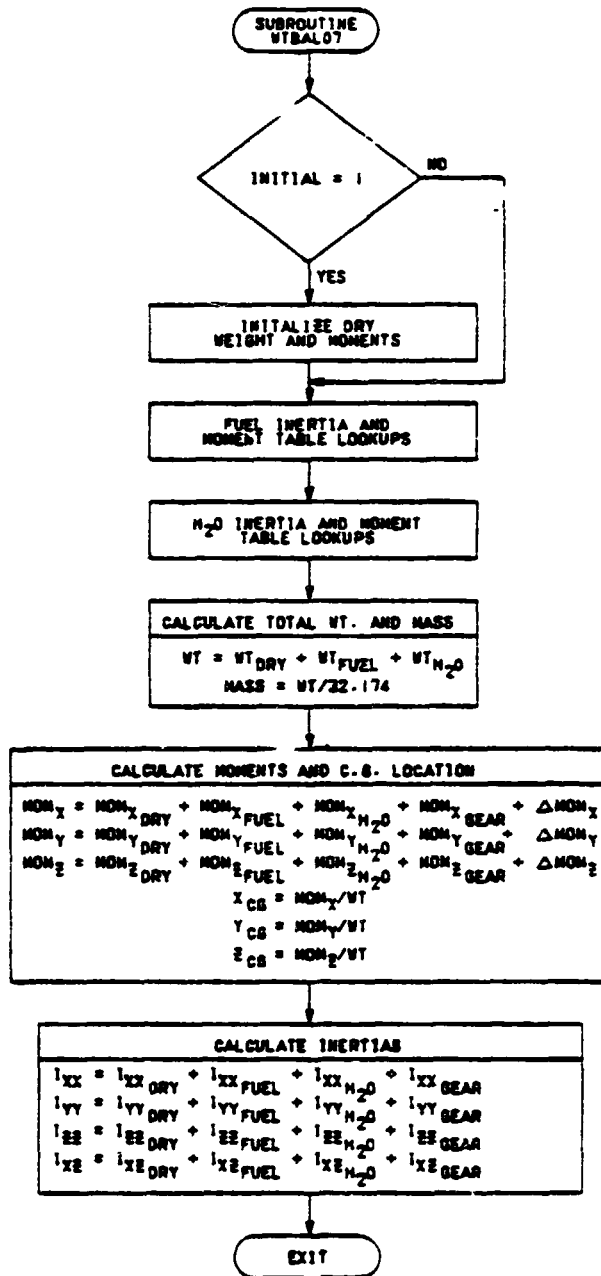
FIGURE 3.3-1
SUBROUTINE WTBAL07 FLOW DIAGRAM

3.3.2 PFC07 SUBROUTINE - The YAV-8B primary flight control system consists of conventional ailerons, rudder, and stabilator, with a Reaction Control System (RCS) which acts about all three axes during hover and transition. Longitudinal control of the YAV-8B is maintained by a combination of stabilator and reaction controls. Likewise, conventional ailerons, in combination with reaction controls, provide lateral control. Both longitudinal and lateral controls operate directly through mechanical linkage to the control stick. The directional control system is a combination of rudder and reaction controls as a function of rudder pedal position. The stabilator and ailerons can be trimmed by electro-mechanically moving the control stick. A limited authority Stability Augmentation System (SAS) provides rate stabilization.

The PFC07 subroutine computes the control surface deflections and the RCS area openings. The control actuators are represented by first order transfer functions. The closed loop technique used for real time digital simulation of these actuators is based on equations derived from a predictive method known as the "Reddy" method, (see Section 3.2.1.2). The math model includes rudder hinge moment limits applied to the total rudder travel.

A simplified flow diagram of the PFC07 subroutine is shown in Figure 3.3-2. Typical inputs include percent stick and rudder pedal, body rates, dynamic pressure and lateral acceleration. Outputs from the subroutine are surface deflections and RCS valve area openings.

3.3.3 RCS07 SUBROUTINE - The Reaction Control System (RCS) is used during hover and transition between full wingborne flight and fully jet-borne flight. The system is fully activated when the nozzles are rotated below 15 degrees. It uses high pressure compressor bleed air, which is fed to the aircraft extremities and ejected through variable shutter valves connected to the aerodynamic surfaces (stabilator, rudder, etc.).

The RCS07 subroutine computes the RCS pressure dynamics and mass flow characteristics. The RCS model in this subroutine is based on modified Rolls-Royce engine data and MCAIR determined aircraft installation losses. Included in the model is the RCS geometry for computing the resulting forces and moments in the body axis system (see Section 3.2.4).

The inputs to the subroutine are the valve areas (calculated in the PFC07 subroutine), compressor discharge temperature and pressure and nozzle deflection. Other inputs include aircraft c.g. location and ambient pressure and temperature. The outputs are the total mass flow rate, the individual valve thrust values and the resulting forces and moments. The forces and moments are added to the engine produced forces and moments in the FNG08 subroutine. The forces and moments are in the body axis system. Figure 3.3-3 shows the logic flow used in the RCS07 subroutine.
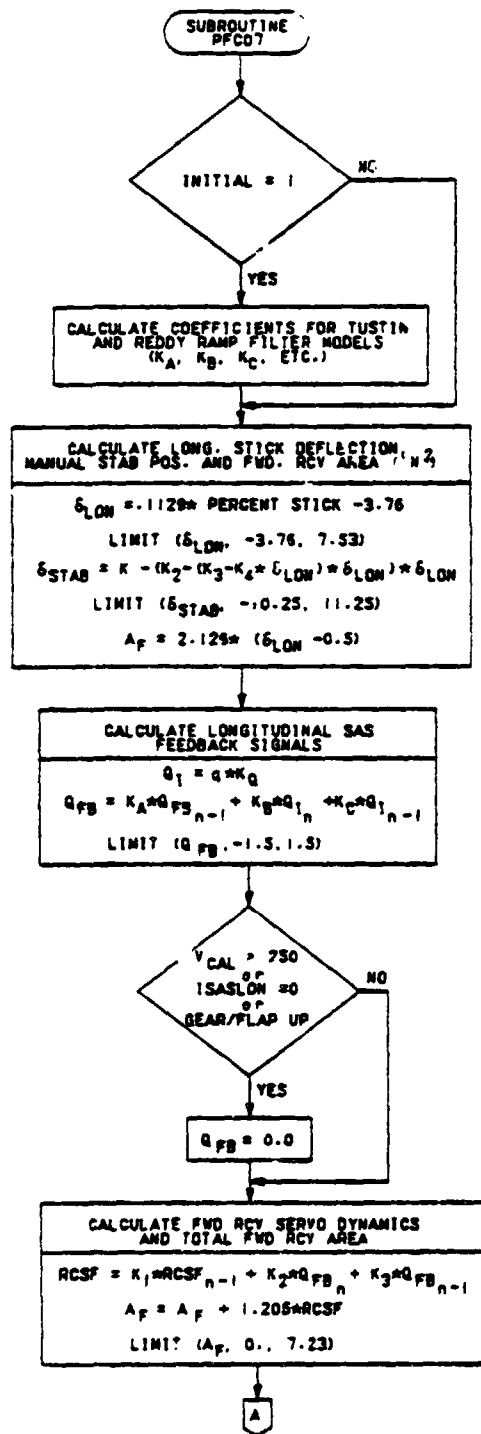
FIGURE 3.3-2
SUBROUTINE PFC07 FLOW DIAGRAM
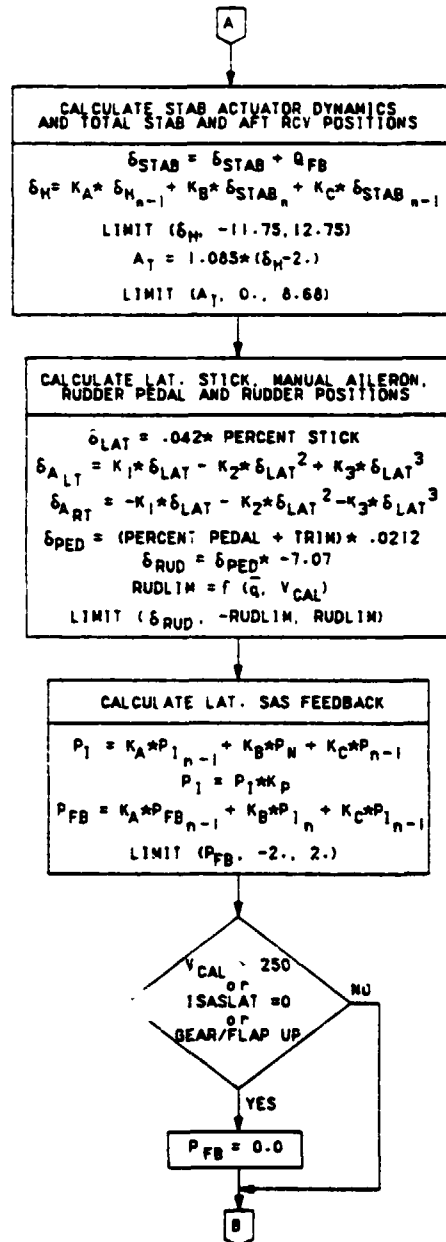
FIGURE 3.3-2 (CONTINUED)
SUBROUTINE PFC07 FLOW DIAGRAM

FIGURE 3.3-2 (CONTINUED)
SUBROUTINE PFC07 FLOW DIAGRAM

```
                    ┌─┐
                    │C│
                    └┬┘
                     ▼
┌─────────────────────────────────────────┐
│   CALCULATE AILERON SERVO DYNAMICS,      │
│  AILERON POSITIONS AND WING COV AREAS    │
├─────────────────────────────────────────┤
```

$$\delta_{A_{LT}} = \delta_{A_{LT}} - P_{FB}$$

$$\delta_{A_{RT}} = \xi_{A_{RT}} + P_{FB}$$

$$\delta_{A_L} = K_A * \delta_{A_{L_{n-1}}} + K_B * \delta_{A_{LT_n}} + K_C * \delta_{A_{LT_{n-1}}}$$

$$\delta_{A_R} = K_A * \delta_{A_{R_{n-1}}} + K_B * \delta_{A_{RT_n}} + K_C * \delta_{A_{RT_{n-1}}}$$

$$\delta_{A_L} = \delta_{A_L} + DROOP$$

$$\delta_{A_R} = \delta_{A_R} + DROOP$$

$$LIMIT \ (\delta_{A_L}, \ -27., +12.)$$

$$LIMIT \ (\delta_{A_R}, \ -27., +12.)$$

$$A_{DWN_{LT}} = .778 * (\delta_{A_L} - DROOP)$$

$$LIMIT \ (A_{DWN_{LT}}, \ 0., \ 5.05)$$

$$A_{UP_{LT}} = (\delta_{A_L} - DROOP + 10.5) * .477$$

$$LIMIT \ (A_{UP_{LT}}) \ -3.1, \ 0)$$

$$A_{UP_{LT}} = | A_{UP_{LT}} |$$

$$A_{DWN_{RT}} = .778 * (\delta_{A_R} - DROOP)$$

$$LIMIT \ (A_{DWN_{RT}}, \ 0., \ 5.05)$$

$$A_{UP_{RT}} = (\delta_{A_R} - DROOP + 10.5) * .477$$

$$LIMIT \ (A_{UP_{RT}}) \ -3.1, \ 0.)$$

$$A_{UP_{RT}} = | \ _{RT} |$$

```
                    ┌─────────┐
                    │  EXIT   │
                    └─────────┘
```
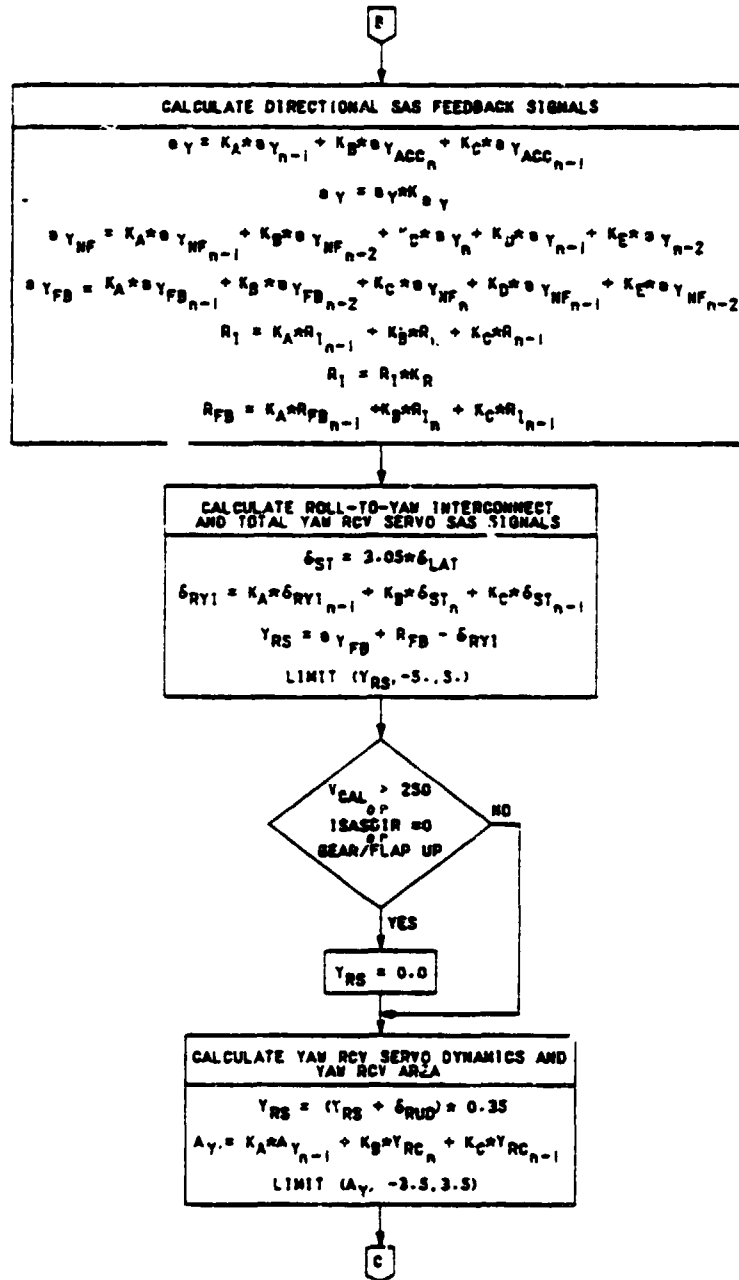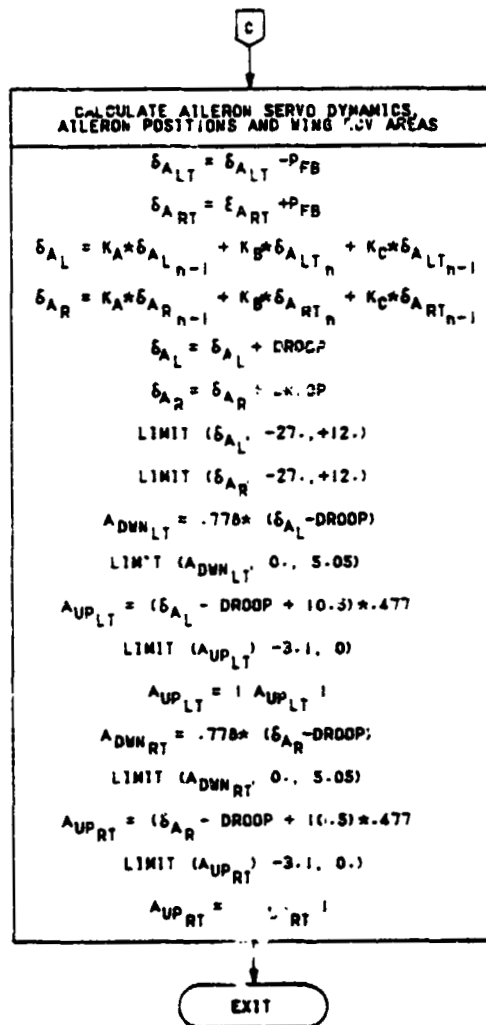
FIGURE 3.3-2 (CONTINUED)
SUBROUTINE PFC07 FLOW DIAGRAM
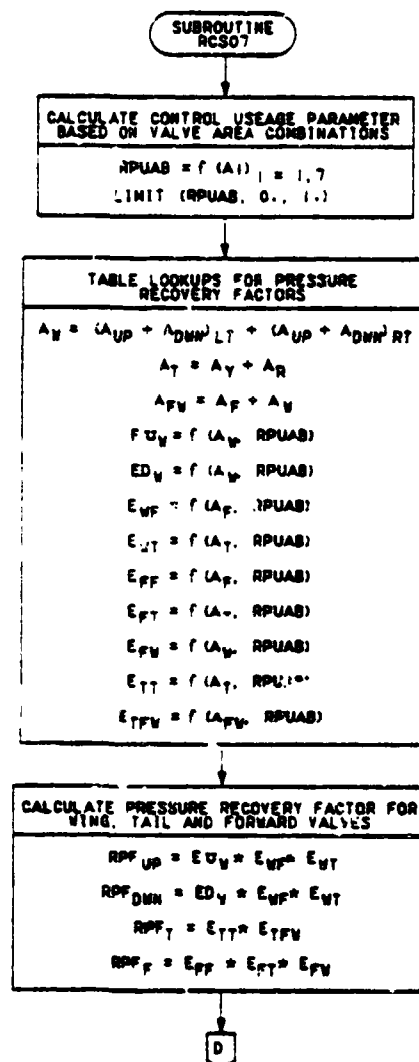
FIGURE 3.3-3
SUBROUTINE RCS07 FLOW DIAGRAM

ORIGINAL PAGE IS
OF POOR QUALITY

D

CALCULATE PRESSURES AND MASS FLOW RATES
FOR # 6   TAIL AND FRONT VALVES

$$P_{UP} = RPF_{UP} * P_3$$

$$P_{DWN} = RPF_{DWN} * P_3$$

$$P_T = RPF_T * P_3$$

$$P_F = RPF_F * P_3$$

$$\dot{m}_{UP} = f(A_W) * P_{UP}/\sqrt{T_3}$$

$$\dot{m}_{DWN} = f(A_W) * P_{DWN}/\sqrt{T_3}$$

$$\dot{m}_T = f(A_T) * P_T/\sqrt{T_3}$$

$$\dot{m}_F = f(A_F) * P_F/\sqrt{T_3}$$

CALCULATE TOTAL RCS MASS FLOW

$$RACF = (\theta_J - 2.)/13.$$

$$\dot{m}_{MAX} = 4.09 * RACF * P_3/\sqrt{T_3}$$

$$\dot{m}_{RCS} = \dot{m}_{UP} + \dot{m}_{DWN} + \dot{m}_T + \dot{m}_F$$

$$LIMIT (\dot{m}_{RCS}, -\dot{m}_{MAX}, \dot{m}_{MAX})$$

CALCULATE VALVE THRUSTS

$$T_T = -(P_T - P_{AMB}) * f(A_T, A_W) * .95 * RACF$$

$$T_F = -(P_F - P_{AMB}) * f(A_F) * .95 * RACF$$

$$T_{DWN} = -(P_{DWN} - P_{AMB}) * f(A_W)$$

$$T_{UP} = -(P_{UP} - P_{AMB}) * f(A_W)$$

CALCULATE BODY AXIS RCS FORCES
AND MOMENTS ABOUT ACTUAL C.G.

EXIT

FIGURE 3.3-3 (CONTINUED)
SUBROUTINE RCS07 FLOW DIAGRAM

3.3.4 __ENG08 SUBROUTINE__ - The ENG08 subroutine computes YAV-8B engine performance. The program data is based on Rolls-Royce engine data and MCAIR aircraft installation losses for an "average" YF402-RR-404 engine. Engine performance was obtained using a Rolls-Royce steady state engine performance computer program. Installation losses include inlet total pressure recovery, inlet drag, boundary layer bleed drag, compressor bleed (for aircraft services and the reaction control system) and mechanical power extraction. Engine performance is corrected for atmosphere changes from standard day.

To give a representative engine, thrust, fuel flow, EGT, P_3, and fan RPM are assembled in data tables as functions of commanded throttle angle, aircraft Mach number, commanded nozzle angle and altitude. The steady state values are retrieved from the tables and modified for the type of day, water and bleed corrections. The results are used to compute:

   o Engine forces and moments (including the RCS values computed in RCS07)
   o Reaction control system bleed
   o Fuel depletion
   o Water depletion

Engine transients in RPM and EGT are modeled using first order time constants that vary with flight condition. The engine compressor discharge pressure limiter, EGT limiter and RPM limiter are also modeled. These are functional to limit fan speed and compressor discharge pressure. Selection of the limiters override causes all limiters except the compressor discharge pressure limiter to be bypassed.

There are a relatively large number of inputs to the ENG08 subroutine. Some of the more important inputs are percent throttle, altitude, atmosphere parameters, airspeed, c.g. location, initial fuel and water quantities, percent nozzle lever position and RCS forces and moments. Outputs include the total engine + RCS forces and moments in the body axis system, various engine performance parameters (RPM, EGT, etc.), nozzle position and remaining fuel and water quantities. A simplified flow diagram of the ENG08 routine is shown in Figure 3.3-4.

3.3.5 __SFC07 SUBROUTINE__ - The YAV-8B secondary flight control system includes flaps and drooped ailerons. The flaps are operated by an electro-hydraulic system consisting of an electronic flap controller and two dual tandem actuators. Flap positioning is provided by the flap controller in accordance with switch (mode) selection. There are two flap modes: up and down. The up mode provides either a constant 0 degree flap deflection or the capability to manually "beep" the flaps to any position from 0 to 25 degrees. The down mode schedules flap deflection as a function of nozzle position and airspeed. In addition the down mode switch also activates the aileron droop system, extending the ailerons to 15 degrees whenever the nozzles are 16 degrees or greater and the airspeed is less than 165 KIAS (with a $\pm$10 KIAS hysteresis).

Other secondary flight control systems modeled in the SFC07 subroutine include gear and LIDS deployment. Figure 3.3-5 outlines the SFC07 subroutine.

All extension and retraction rates, time delays surface load effects and essential logic characteristics relating to the YAV-8B secondary flight control systems are simulated. The inputs to the subroutine include nozzle position, flap mode selection, gear selection, LIDS selection switch, Weight-on-Wheels (WOW) switch and airspeed. Outputs are flap position, LIDS and gear positions and aileron droop position.
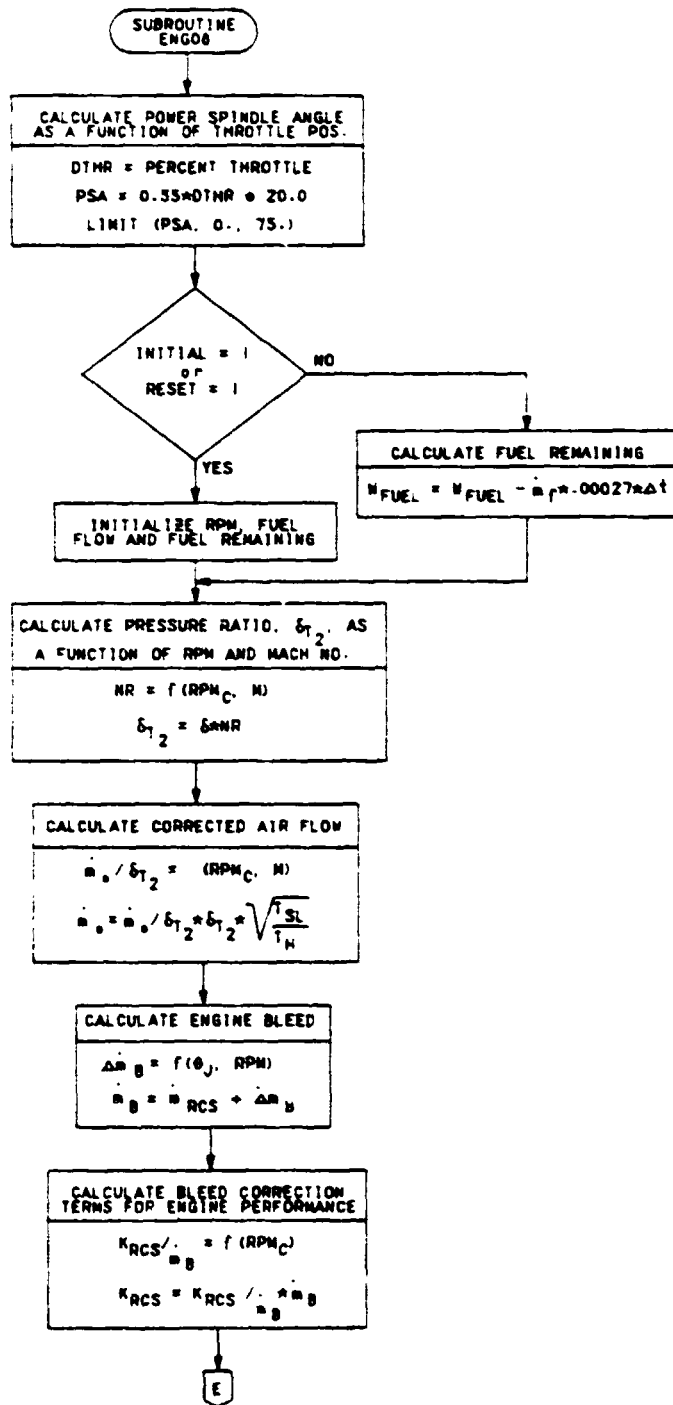
FIGURE 3.3-4
SUBROUTINE ENG08 FLOW DIAGRAM

FIGURE 3.3-4 (CONTINUED)
SUBROUTINE ENG08 FLOW DIAGRAM

F

CALCULATE FUEL FLOW ACCEL. AND DECEL. LIMITS
AND REQ'D INCREMENTAL CHANGE IN FUEL FLOW

$$\dot{m}_{f_{ACCEL}} = RPM \times 16.6 \times \delta_{T_2}$$

$$\dot{m}_{f_{DECEL}} = -\dot{m}_{f_{ACCEL}}$$

$$\Delta \dot{m}_f = (\dot{m}_{f_{COM}} - \dot{m}_{f_{SS}}) \times .465 \times \Delta t$$

LIMITER SWITCH OFF — YES / NO

CALCULATE TEMPERATURE AND RPM
LIMITER VALUES

$$TEMP\ LIM = f(\theta_J, \delta_{GEAR}, H_2O)$$

$$RPM\ LIM = f(M)$$

CALCULATE COMPRESSOR DISCHARGE
PRESSURE LIMITER VALUE

$$PRESS\ LIM = f(P_3, P_{ATM})$$

REDEFINE $\dot{m}_{f_{ACCEL}}$ IF APPLICABLE AND
LIMIT REQ'D CHANGE IN FUEL FLOW

$$\dot{m}_{f_{ACCEL}} = f(TEMP\ LIM,\ RPM\ LIM,\ or\ PRESS\ LIM)$$

$$LIMIT\ (\Delta \dot{m}_f,\ \dot{m}_{f_{DECEL}},\ \dot{m}_{f_{ACCEL}})$$

G

FIGURE 3.3-4 (CONTINUED)
SUBROUTINE ENG08 FLOW DIAGRAM

G

CALCULATE ENGINE RESPONSE

$$\dot{m}_f = \dot{m}_{f_{SS}} + \Delta\dot{m}_f$$

$$\Delta RPM/\Delta\dot{m}_f = f(RPM)$$

$$\Delta RPM = \Delta RPM/_{\Delta\dot{m}_f} \cdot \Delta\dot{m}_f * K(H)$$

$$\Delta RPM/_{\Delta t} = f(M, \text{ GROSS THRUST})$$

$$\Delta RPM_{LIM} = \frac{\Delta RPM}{\Delta t} \cdot \Delta t * K(H)$$

$$\text{LIMIT } (\Delta RPM, -\Delta RPM_{LIM}, \Delta RPM_{LIM})$$

$$RPM = RPM + \Delta RPM$$

$$RPM_C = RPM * \sqrt{\frac{T_{SL}}{T_M}}$$

CALCULATE GROSS THRUST, EGT AND COMPRESSOR DISCHARGE PRESSURE

$$F_G = (F_G(RPM_C, M) * K(H_2O) - K_{RCS}) * K(H) * K(\theta_J)$$

$$EGT = EGT(RPM_C, \delta_{T_2}) * K(M, T) * K(H) + K_{RCS} - PWEGTC - K(\theta_J)$$

$$P_3 = \frac{P_2}{\delta_{T_2}}(RPM_C, M) * \delta_{T_2} - K_{RCS}$$

CALCULATE THRUST FORCES AND MOMENTS IN BODY AXES

$$M_X = F_G * SIN\ \theta_J * \Delta Y + M_{X_{RCS}} + M_{X_{INLET}}$$

$$M_Y = F_G * SIN\ \theta_J * \Delta X + F_G * COS\ \theta_J * \Delta Z + M_{Y_{RCS}} + M_{Y_{INLET}}$$

$$M_Z = F_G * COS\ \theta_J * \Delta Y + M_{Z_{RCS}} + M_{Z_{INLET}}$$

$$FT_X = F_G * COS\ \theta_J + F_{X_{RCS}} + F_{X_{INLET}}$$

$$FT_Y = F_{Y_{RCS}} + F_{Y_{INLET}}$$

$$FT_Z = F_G * SIN\ \theta_J + F_{Z_{RCS}} + F_{Z_{INLET}}$$

CALCULATE NOZZLE POSITION

$$\theta_{J_{CON}} = .985 * \text{PERCENT NOZZLE} + 2.$$

$$\Delta\theta_J = (\theta_{J_{CON}} - \theta_J)/\Delta t$$

$$\text{LIMIT } (\Delta\theta_J, -98.5*\Delta t, 98.5*\Delta t)$$

$$\theta_J = \theta_J + \Delta\theta_J$$

EXIT

FIGURE 3.3-4 (CONTINUED)
SUBROUTINE ENG08 FLOW DIAGRAM

ORIGINAL PAGE IS
OF POOR QUALITY
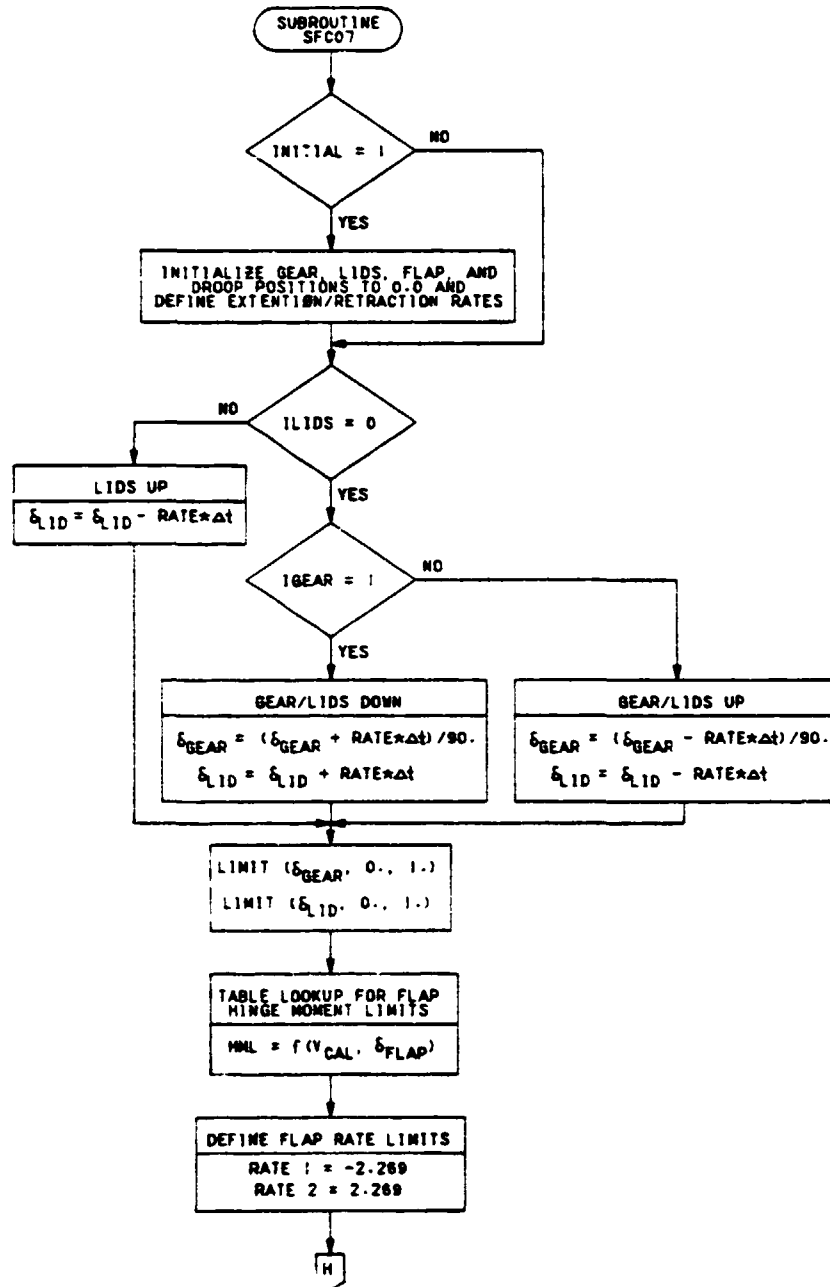
FIGURE 3.3-5
SUBROUTINE SFC07 FLOW DIAGRAM
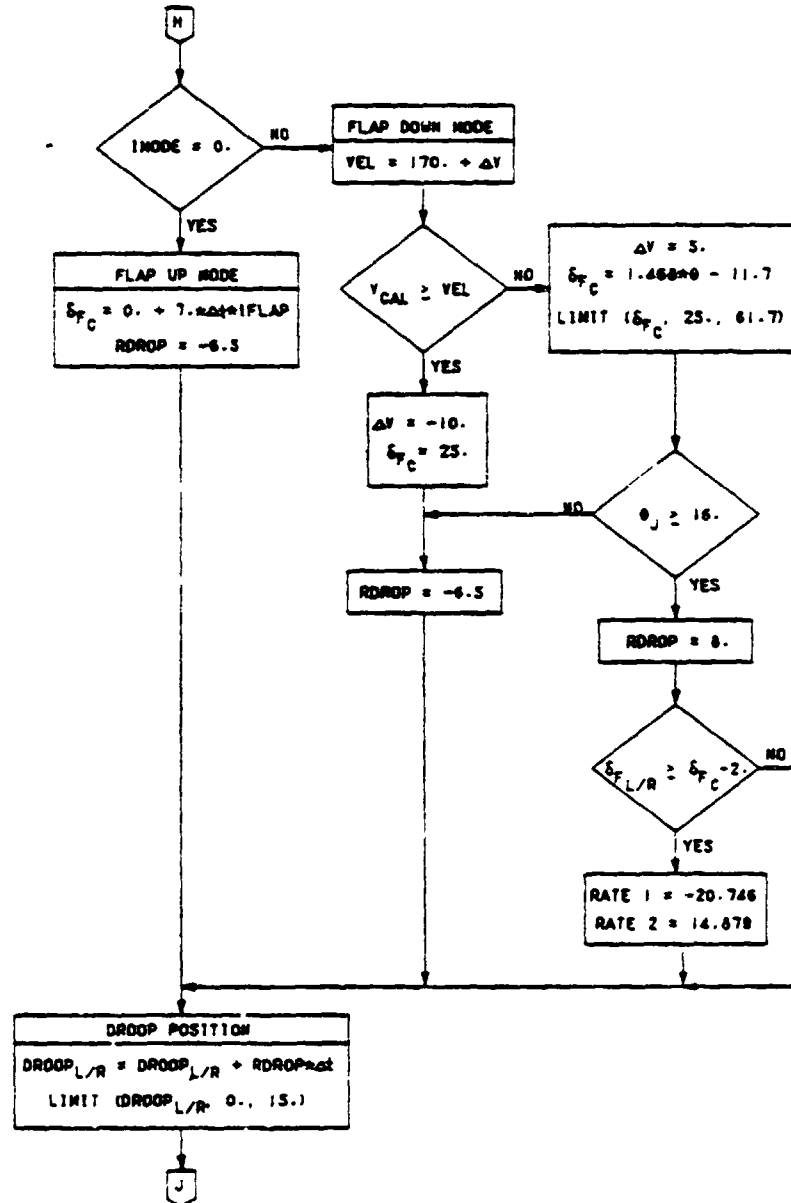
FIGURE 3.3-5 (CONTINUED)
SUBROUTINE SFC07 FLOW DIAGRAM

```
                                    ┌─┐
                                    │J│
                                    └─┘
                                     │
              ┌──────────────────────────────────────┐
              │   CALCULATE OUTPUT OF FLAP            │
              │   CONTROLLER RATE LIMITER             │
              ├──────────────────────────────────────┤
              │  R = (δ_F_c - DFB + BIAS)*100.        │
              │                                       │
              │  LIMIT (R, RATE 1, RATE 2)            │
              │       DFB = DFB + R*Δt                │
              │  LIMIT (DFB, -.65, 20.65)             │
              │       FTL = DFB*8.986                 │
              └──────────────────────────────────────┘
                                     │
              ┌──────────────────────────────────────┐
              │   CALCULATE FIRST STAGE OUTPUT        │
              │   OF FLAP ACTUATOR MODEL              │
              ├──────────────────────────────────────┤
              │  CM1 = FTL - DOUT*53.492              │
              │  LIMIT (CM1, -40., 40.)               │
              │  CM4 = 2.*CM1 - CM5*727.3             │
              │  CM5 = CM5 + CM4*.0603*Δt             │
              │  LIMIT (CM5, -.055, .055)             │
              │       DXL = f(CM5)                    │
              └──────────────────────────────────────┘
                                     │
              ┌──────────────────────────────────────┐
              │   CALCULATE FLAP HINGE                │
              │   MOMENT PARAMETER                    │
              └──────────────────────────────────────┘
                                     │
                  YES            ╱───────╲           NO
         ┌───────────────────◄  │ DXL ≥ 0 │  ►───────────────────┐
         │                      ╲───────╱                        │
         │                                                       │
  ┌──────────────────────┐                      ┌──────────────────────┐
  │   FLAP EXTENTION      │                      │   FLAP EXTENTION      │
  ├──────────────────────┤                      ├──────────────────────┤
  │ LIMIT (HML, -105500., │                      │ LIMIT (HML, -84400., │
  │        105500.)       │                      │        84400.)        │
  │ HMIN = 1. - HML*9.47  │                      │ HMIN = 1. + HML*1.18  │
  │        X 10^-6        │                      │        X 10^-5        │
  └──────────────────────┘                      └──────────────────────┘
                  │                                       │
                  └───────────────────┬───────────────────┘
                                      │
                            ┌──────────────────┐
                            │  HMLL = √HMIN     │
                            └──────────────────┘
                                      │
              ┌──────────────────────────────────────┐
              │   CALCULATE FINAL STAGE OUTPUT        │
              │   OF FLAP ACTUATOR MODEL              │
              ├──────────────────────────────────────┤
              │  DXL = DXL*HMLL                       │
              │  DOUT = DOUT + DXL*Δt                 │
              │  LIMIT (DOUT, 0., 3.353)              │
              │  δ_F_L/R = DOUT*61.7/3.353            │
              │  δ_FLAP = (δ_F_L + δ_F_R)*0.5         │
              └──────────────────────────────────────┘
                                      │
                              ╭──────────────╮
                              │    EXIT       │
                              ╰──────────────╯
```
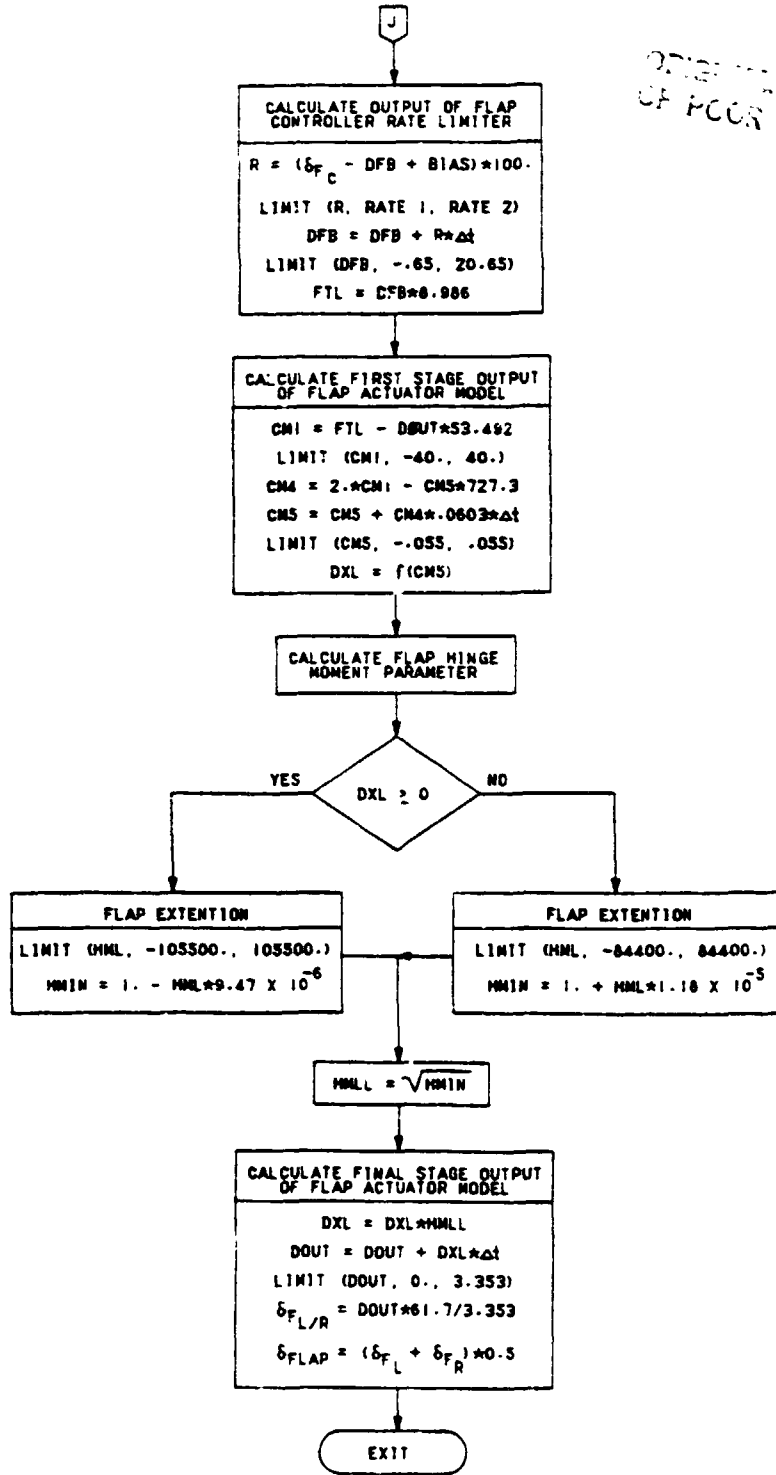
FIGURE 3.3-5 (CONTINUED)
SUBROUTINE SFC07 FLOW DIAGRAM

3.3.6 AERØY8B SUBROUTINE - The AERØY8B Subroutine computes all of the aero-
dynamic forces and moments acting on the simulated YAV-8B aircraft. These are
computed through the use of stability and performance characteristics. The
characteristics are stored in data tables and accessed through table look-up
routines. When combined with the aerodynamic reference dimensions of the
YAV-8B (e.g., wing area, mean aerodynamic chord, and wing span) and the
control surface positions, these coefficients are used to calculate total
forces and moments in the body axis system. The aerodynamic equations for
computing the total coefficients are given in Section 3.2.3. The aerodynamic
data cover the full range of aircraft performance, from hover to wingborne
flight. The aerodynamic forces and moments are primarily functions of air-
craft attitude, Mach number, power setting (with nozzles down) and control
surface position. The baseline coefficients represent the aircraft with five
bare pylons and the gun pods and LIDS onboard. Increments due to gear and
LIDS extension, flap deflection and power effects are included. Ground
effects for altitudes from 0 to approximately 70 ft. are also included in the
data base. The ground effects data include LIDS contributions.

The AERØY8B subroutine is divided into two distinct sections. The first
section is the low speed (M ≤ 0.3) region which includes ground effects. The
aerodynamic data for this section are referenced in the body axis system. The
second section is the high speed (M ≥ 0.5) region. The data here are
referenced in the stability axis system. For Mach numbers between 0.3 and
0.5, table lookups are done in both sections and a linear interpolation is
done to compute the respective total coefficient. The total aerodynamic
forces and moments are derived in the body axis system.

The hover (u < 30 KTAS) and low speed regimes for the YAV-8B require
special consideration when determining aerodynamic forces and moments (see
Section 3.2.3.1). The low speed baseline aerodynamic coefficients are input
for aircraft angles of attack between ± 180 degrees. The angle of attack
definition for the low speed table lookups is a blend of body axis pitch
attitude and true angle of attack. Likewise, in the lateral-directional
axis the technique for determining aerodynamic forces and moments in hover
differs from wingborne flight. For the aerodynamic table look-ups in hover
(u < 30 KTAS), the sideslip angle definition is a unique variable that is a
function of axial velocity, roll attitude and pitch attitude. For u > 50 KTAS,
the conventional definition of β is used. For u from 30 to 50 KTAS a blend
of the two definitions is used.

Power effects on the aerodynamic forces and moments are input as incre-
mental data. One of the parameters for determining the power effects is the
equivalent velocity ratio (Veq). This variable is defined as $\sqrt{13.0 * \bar{q}}$ Thrust.
This represents the square root of the ratio of freestream dynamic pressure
to the average nozzle exit dynamic pressure.

Some of the more significant inputs to the AERØY8B subroutine are the
control surface deflections, angle of attack, sideslip angle, gear and LIDS
positions, body attitudes and rates, Mach number, velocity components in the
body axis, dynamic pressure, thrust, nozzle position and flap position.
Outputs include the total aerodynamic forces and moments in the body axis
system and a large number of incremental aerodynamic coefficients. Figure
3.3-6 represents the functional flow diagram for the AERØY8B subroutine.
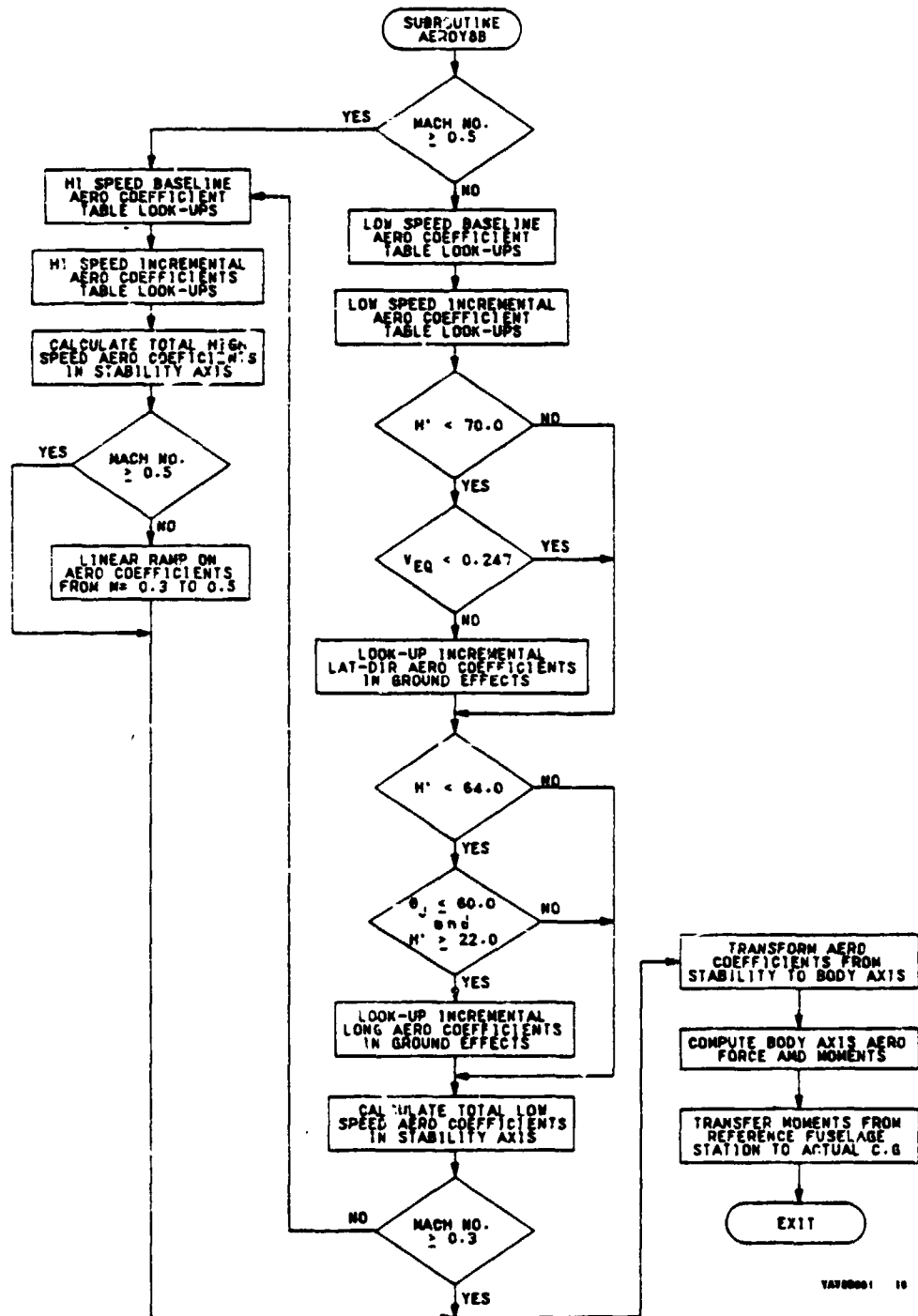
FIGURE 3.3-6
SUBROUTINE AEROY8B FLOW DIAGRAM

3.4 PROGRAM YAV8B USER'S GUIDE

Execution of program YAV8B is initiated by reading the EXECUTE deck into the computer. For most digital simulation runs, the EXECUTE, I50MS, and RTPD." card decks will contain the input variables required, depending on the c. _ ... · of a desired run. Each of these decks is described in this section, are the able look-up subroutine, program defaults and overrides, array structures nd subroutine modification capability.

3.4.1 VARIABLE ARRAY STRUCTURE

 - There are two primary arrays in the YAV8B prog for equivalencing program variables. These two arrays are the F array (FARRAY) and the A array. The F array is dimensioned as F (3000) whereas the A array is dimensioned as A (1000). The first 1000 locations of the F array are generally reserved for non-aircraft dependent variables such as program directives. The first location of the A array is equivalenced to F (1001). Thus, A (100) is equivalent to F (1100), etc. This array is generally used for aircraft dependent parameters such as aerodynamic coefficients, engine parameters, etc.

Throughout the following discussion, the user will be referred to variables assigned to the F or A arrays. Program variables are equivalenced to F or A array locations for ease in assigning the variables common storage locations. Each subroutine of the program contains equivalence statements defining the variables required for input or output. A listing of the F and A array equivalenced variables is given in Appendix B of Volume II. The array locations that have no assignment are available as spares.

3.4.2 EXECUTE DECK

 - The EXECUTE deck loads files, reads data cards necessary for program initialization, executes program YAV8B, and executes the program SPRINT to output the desired parameters for a simulation run. Figure 3.4-1 outlines the EXECUTE deck card sequence.

3.4.2.1 Load and Execute Card Sequence

  The load and execute card sequence for the EXECUTE deck is shown in Figure 3.4-2. The executive first gets the needed compiled files, described below:

FILE NAME	DESCRIPTION
YAV8B	MAIN PROGRAM; MUST BE LOADED FIRST
I50MS	TIMING SUBROUTINE
YAERØ	CONTAINS SUBROUTINES AERODAT AND AERØY8B
YENGN	CONTAINS SUBROUTINES YENGD AND ENGO8
YAVAC	CONTAINS SUBROUTINES AC07, RCS07, PFC07, SFC07, WTBAL07
EØM	EQUATIONS OF MOTION SUBROUTINES
ATMØS	STANDARD ATMOSPHERE TABLE AND ATMOSPHERE SUBROUTINE ATMØS
FMMPLY	MATRIX MULTIPLY AND TRANSPOSE SUBROUTINES
CARDS	SUBROUTINE CARDS TO READ DATA CARDS IN EXECUTE DECK
TBLKP	DATA TABLE LOOK-UP SUBROUTINES (FCALC, FSRCH) AND FUNCTIONS (F1A, F1B, etc.)
RTP	SUBROUTINE RTP TO BUFFER DATA INTO STORAGE LOCATION
RTPDATA	SUBROUTINE RTPDATA TO SPECIFY WHICH DATA IS BUFFERED; MUST BE LOADED BEFORE RTP
MSGABT	CONTAINS DIRECTIVES FOR PRINTING ERROR MESSAGES
SPRINT	PROGRAM TO PRINT DATA TO OUTPUT

NAMELIST OPTIONS

DATA CARDS

LOAD AND EXECUTE CARDS

JOB CONTROL CARDS

6
7
8
9

7
8
9

7
8
9

7
8
9
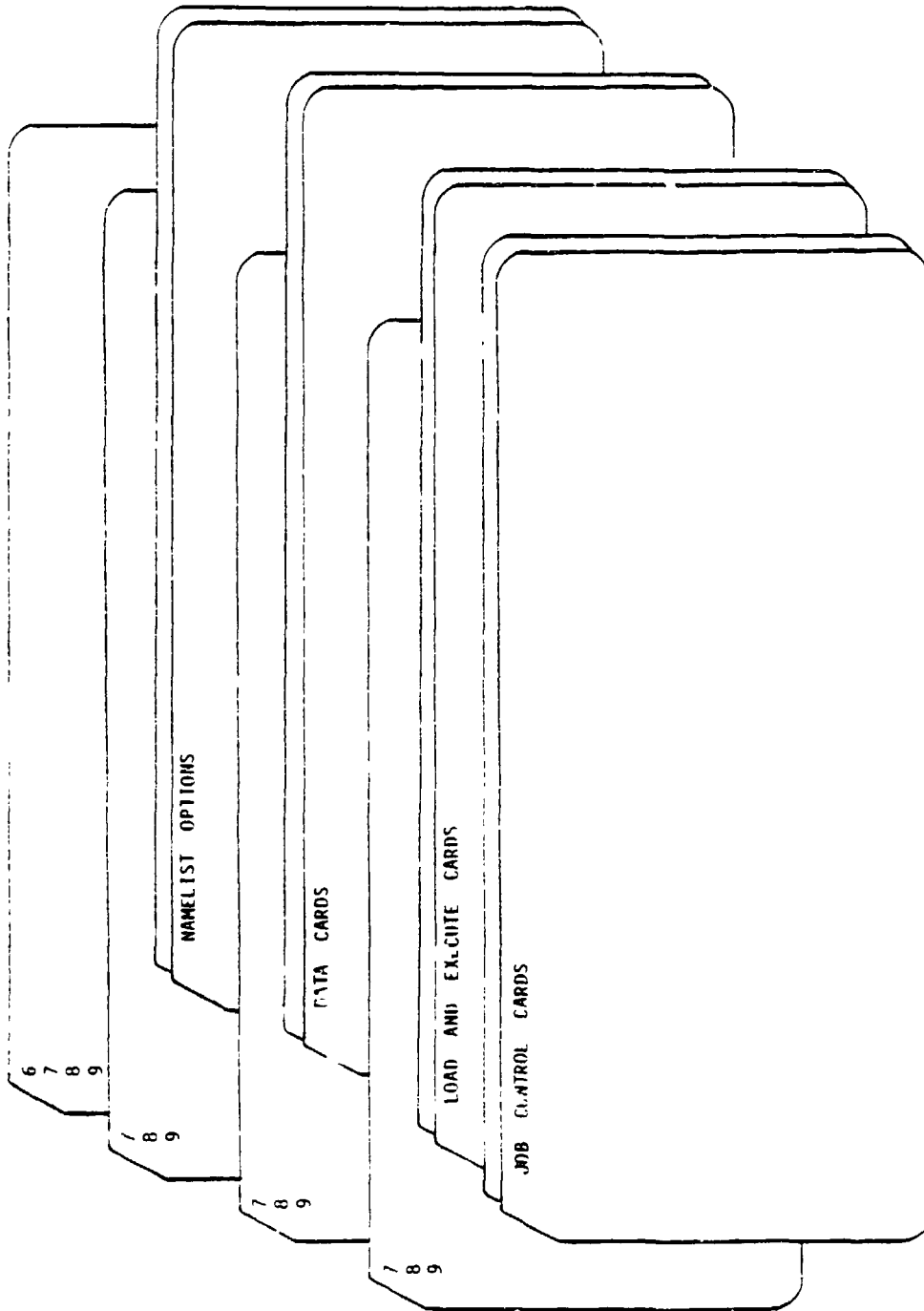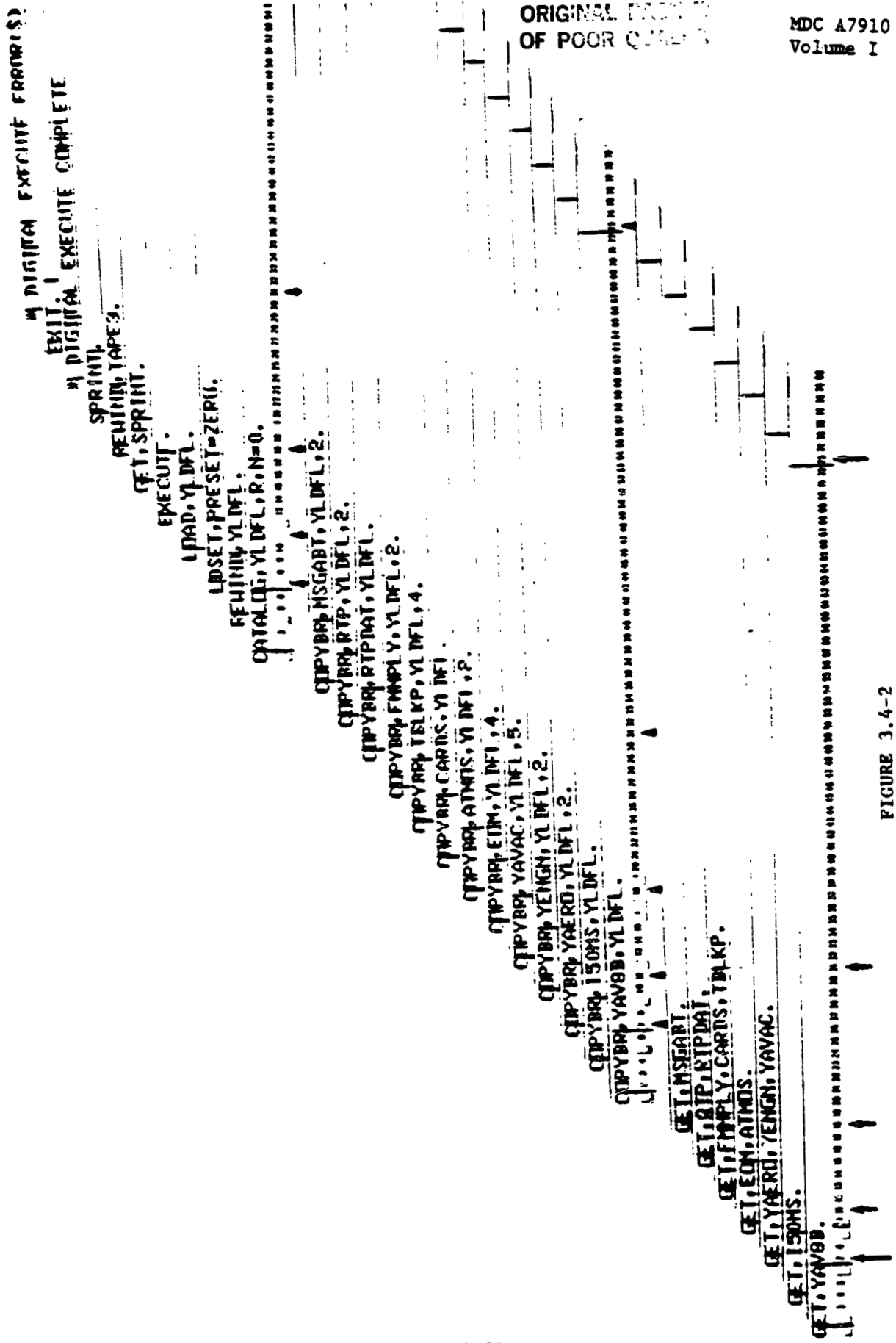
**FIGURE 3.4-1
EXECUTE DECK**

MDC A7910
Volume I

FIGURE 3.4-2

LOAD AND EXECUTE CARD SEQUENCE

These are loaded into temporary load file, YLDFL, after which the program
is executed. During execution, the RTPDATA and RTP subroutines are buffering
values of selected variables into temporary storage location TAPE3. Program
SPRINT buffers these data out of storage and into a format suitable for the
printer, based on a user's NAMELIST inputs (see section 3.4.2.3).

3.4.2.2 <u>Data Card Format</u> - Program YAV8B requires initial values of some
variables for execution. These data are entered through cards located behind
the first end-of-record in the EXECUTE deck. The data cards are read by
subroutine CARDS, which is called from program YAV8B. Card input format is
shown in Figure 3.4-3. Column 5 contains one of the following control or
data type identification numbers describing the data to be presented:

COLUMN 5 INPUT	INDICATION
1	INTEGER DATA
2	FLOATING POINT DATA
3	OCTAL DATA
4	ALPHANUMERIC DATA
5	CONTROL NUMBER INDICATING END OF A SET OF DATA CARDS
6	CONTROL NUMBER INDICATING END OF ALL SETS OF DATA CARDS
7	OPTIONAL ALPHANUMERIC DESCRIPTION OF TYPE 1 THROUGH 4 DATA; START 25 OR LESS CHARACTERS FOR COMMENTS IN COLUMNS 6, 31, AND 56

Up to three data points may be included on one data card for a given identi-
fication number. Types 1 through 4 cards require array locations of the
input variables (in the F array), and each specification must end in columns
10, 35, and 60. Input data itself is 20 or less characters ending in columns
30, 55, and 80.

The inputs shown in Figure 3.4-3 are generally what is required for a
simulation run. Only one data point per card has been input here for flexi-
bility in changing of single values. The data displayed is that used for a
YAV-8B conventional Dutch Roll case. Variable names corresponding to the
array locations of Figure 3.4-3 are defined below:

F ARRAY LOCATION	VARIABLE NAME	DESCRIPTION
150	TSTØPD	LENGTH OF RUN IN SECONDS
1011	H	ALTITUDE
1030	VT	TRUE AIRSPEED IN FT/SEC
1031	GAMMA	FLIGHT PATH ANGLE
1040	RMACH	MACH NUMBER
1103	THETA	PITCH ATTITUDE
1117	ALPHA	ANGLE OF ATTACK
1118	BETA	SIDESLIP ANGLE
1195	INSTD	NON-STANDARD DAY FLAG
1273	BSMØMX	INPUT FOR FUSELAGE STATION CG BIAS
1274	BSMØMY	INPUT FOR BUTT LINE CG BIAS
1275	BSMØMZ	INPUT FOR WATER LINE CG BIAS

ORIGINAL PAGE
OF POOR QUALITY

6			
5			
1	1959	62	
1	1882	0	
2	1819	495.	
2	1792	4888.	
2	1777	1.04	
2	1776	40.78	
1	1635	1	
1	1627	0	
1	1497	0	
1	1496	0	
1	1495	0	
2	1275	-1711.4	
2	1274	-911.	
2	1273	-5796.785	
1	1195	1	
2	1118	0.	
2	1117	5.5	
2	1103	5.5	
2	1040	.697	
2	1031	0.	
2	1030	685.	
2	1011	35200.	
2	150	8.0	

FIGURE 3.4-3
DATA CARD FORMAT

ARRAY LOCATION	VARIABLE NAME	DESCRIPTION
1495	ISASLØN	PITCH SAS SWITCH
1496	ISASLAT	ROLL SAS SWITCH
1497	ISASDIR	YAW SAS SWITCH
1627	IMØDE	FLAP MODE SWITCH
1635	IFLAP	MANUAL FLAP SWITCH
1776	PCTHR	PERCENT THROTTLE
1777	PCNØZ	PERCENT NOZZLE CONTROL
1782	PQFUEL	FUEL WEIGHT
1819	PWATER	WATER WEIGHT
1882	IGEAR	GEAR UP/DOWN FLAG
1959	ICASE	OPTIONAL CHECK CASE IDENTIFICATION NUMBER

3.4.2.3 NAMELIST options - Program SPRINT is used to print data from the local file TAPE3. The printout consists of start of run data, time history data, and end of run data. The user may select various control options over the following categories via NAMELIST input:

NAMELIST CONTROL CATEGORIES

o Run Selection

o Output Print Selection

o Parameter Selection

o Time to Print Selection

o Names Override

o Classification Override

o Low Core Execution

The data cards for the NAMELIST options are contained in the EXECUTE deck and follow the data cards described in the previous section. NAMELIST input options are available in each of these categories and are the following:

Run Selection

NRUNS
Number of consecutive runs to be printed, starting at the current file position. After NRUNS runs have been printed, the program will terminate with a STØP 1, unless a double end-of-file has been encountered before NRUNS has been satisfied. If this occurs, the program will terminate with a STØP 2. Parameter NRUNS is not used if IFILES(1) is non-zero.

IFILES(20)
File numbers of runs to be printed, starting at the current file position. File numbers must be in ascending order and no more than 20 separate runs may be specified by the user. A zero in the array terminates the sequence. After all runs have been printed, the program will terminate with a STØP 1, unless a

IFILES(20)   double end-of-file has been encountered before all runs
(Cont'd)   selected have been satisfied. If this occurs, the
               program will terminate with a STØP 2. Parameter IFILES
               overrides the parameter NRUNS.

Output Print Selection

IBLØCK   Format selection fo printing time history data. Legal
           values are as follows:

           Column Format (IBLØCK=0) prints the complete time
           history of ten parameters at a time in columns up to 441
           parameters out of a maximum of 881 parameters. If the
           data exceeds 441 parameters it can be read by using
           NPLIM for the first 441 parameters and then using NPLIM
           in conjunction with the IXR array for the remaining
           parameters; see IXJ array description.

           The Column Format requires more core since local files
           are used to sort the time history data for separate
           pages, and each file requires a separate buffer. If
           core is a problem the user should consider the Low Core
           Execution Optimum.

           Block Format (IBLØCK=1) prints all time history para-
           meters for one time pass in a block, ten per line. The
           maximum number of parameters that can be printed is 881.

           Block Format with Names (IBLØCK=2) prints all time
           history parameters for one time pass in a block, five
           per line with parameter names embedded within the block.
           The maximum number of parameters that can be printed is
           881.

           Column Format with Increased Accuracy (IBLØCK=3) prints
           the complete time history of five parameters at a time
           in columns up to 221 parameters out of a maximum of 881
           parameters. If the data exceeds 221 parameters the
           data can be read by using NPLIM for the first 221 para-
           meters and then using NPLIM in conjunction with the IXR
           array for the remaining parameters; see IXR array
           description for more details.

           This Column Format prints out the values of the para-
           meters to 8 decimal places. And if used in conjunction
           with the IXØCT array can print out the octal value of
           the parameter in 20 octal digits (where 20 octal digits
           = a 60-bit word).

Parameter Selection

NPLIM

Limit number of time history parameters to be printed.
If NPLIM is non-zero the first NPLIM parameters will be
printed. Normally, all the time history pointers and
names are printed on a start of run page. However, if
parameter NPLIM is used, then only the pointers and
names up to NPLIM will be printed. Also, for the
Column Format printout, less core will be required,
since only the sort file buffers needed for NPLIM
parameters will be allocated.

IP(176)

Page print selection array. Each array element is a
flag that corresponds to ten time history parameters
for the Column and Block Format Options. For the
Block Option with names each flag corresponds to five
parameters up to a maximum of 881. For the Column
Option with increased accuracy each flag corresponds to
five parameters up to a maximum of 221. If IP flags
are set to zero, the corresponding time history para-
meters will not be printed, but the pointers and names
will still appear on the start of run page.

IXR(881)

Parameter re-ordering array. For the Column Format
(IBLØCK=0) this array allows printing up to 441 time
history parameters in any desired order from a set of up
to 881 time history parameters. For the Column Format
(IBLØCK=3), this array allows printing up to 221 time
history parameters in any desired order from a set of
up to 881 time history parameters. For both Block
Formats this array allows printing up to 881 time
history parameters in any desired order. Each array
element corresponds to a parameter position. If any
array element is non-zero, the original time history
parameter corresponding to that element will be replaced
by the parameter number indicated by the value of the
array element. Only the parameters to be re-ordered
need specification in the IXR array. Also, for the
Column Format Option some time history parameters can
be duplicated to appear on more than one page, for
example, by specifying the parameter number in more than
one array position. This option can be used in combina-
tion with the namelist parameters NPLIM and IP.

NOTE: If the user wants Column Format (IBLØCK=0) and
has a tape with NP (442<NP<881) time history parameters,
the first 441 parameters may be printed by using NPLIM=
441. The remaining parameters (NP-441) may be printed
by using NPLIM=NP-440 and IXR(1)=-442, which will auto-
matically generate the correct IXR array. If the user
wants Column Format with Increased Accuracy (IBLØCK=3)
and has a tape with NP (222<NP<881) time history para-

IXR(881)
(Cont'd)

meters, a similar method is used to read the data in.
The first 221 parameters may be printed using NPLIM=221.
If NP ≤ 441, set NPLIM=NP-220 and IXR(1)=-222 and it
will automatically generate the correct IXR array for
this set of 221 parameters.

If NP ≤ 661. set NPLIM=NP-440 and IXR(1) =-442. Other-
wise, on this third pass leave NPLIM=221, set IXR(1)=-422
and it will generate the IXR array for parameters 442 to
661. For printing out the remaining parameters from
662≤NP≤881, set NPLIM=NP-550 and IXR(1) =-662.

IXØCT(881)

Parameter octal print array. This array allows for
printing of time history parameters in octal format.
Each array element is a flag that corresponds to a time
history parameter to be printed. That is, the second
array element is associated with the second time history
parameter to be printed, the third array element with
the third parameter to be printed, and so on. This
matchup is made regardless to whether or not the nth one
to be printed is actually the nth time history para-
meter or one that has been reordered using the IXR array.
To have the parameter printed out in octal, its related
IXØCT array element should be set high.

For the Column Format with Increased Accuracy (IBLØCK=3),
which prints out five parameters per page, the local re-
presentation is 20 characters long. For the Block Formats
and the Column Format with ten parameters per page
(IBLØCK=2,1,0) the octal representation is 10 characters
long. The maximum number of parameters printed out for
IBLØCK=0,1,2,3 is 441, 881, 881, and 221, respectively.
These limits hold for the IXØCT array also.

Time to Print Selection

DP

Print interval. Time history data will be printed once
every data pass that TIME exceeds or equals (within a
small tolerance) successive integral multiples of DP.
Thus if the parameter DP is less than or equal to the
smallest time increment, all the data will be printed.
If DP=0.0, all passes of data will be printed regardless
of the time increment. This could be useful if, because
of some error, TIME was equal to or less than a pre-
vious pass. If DP=0.0, the namelist parameters TSTART
and TSTØP are not operational.

TSTART(10)   Start/Stop times. Sections of time history data to be
TSTØP(10)   printed can be specified by use of the TSTART/TSTØP
                    arrays. The array elements, up to a limit of ten,
                    correspond to the sections to be printed. The start
                    time is specified by the TSTART element and the stop
                    time is specified by the TSTØP element. The stop time
                    must be greater than or equal to the start time, and
                    each start time must be greater than or equal to the
                    previous stop time. All array elements beyond those
                    desired must be zero.

LASTPAS   Print last pass of data. This parameter, when non-zero,
                    causes the last pass of time history data to be printed
                    regardless of the print interval or start/stop times.

Names Override

INAMES   Names override. When this parameter is non-zero, the
                    program will read data cards to input parameter names
                    up to a maximum of 881. If names are on the data tape,
                    they can be overridden using this option. If there are
                    no names on the data tape, they can be supplied via data
                    cards for the printout. Data cards must be in an (I10,
                    7A10) format immediately following the namelist cards.
                    The first field is for an index indicating the para-
                    meter number of the first name appearing in the second
                    field. Up to seven names may be input per card. All
                    the names on a card will be input in sequential order
                    starting with the index for the first name. A blank in
                    the name field will terminate input from that card. If
                    seven names are put on a card, the names on the follow-
                    ing card will be input sequentially even without index
                    specification. A blank card terminates the data card
                    input.

                    If the program is executed more than once in the same
                    job, the names need to be entered only from the first
                    namelist. If INAMES=2, names entered from a previous
                    namelist will be de-selected, and new names can be
                    entered by the user.

Classification Override

ICLASS   Classification override. The classification is normally
                    specified in the data tape start of run data, and will
                    print out automatically unless this override option is
                    specified by the user. Legal values and the resulting
                    printout are as follows:

                    ICLASS=1 - Printout will have no classification, blanks
                    will be printed instead of start of run classification
                    data.

ICLASS
(Cont'd)

ICLASS=2 - Printout will have "Confidential" classifi-
cation.

ICLASS=3 - Printout will have "Secret" classification.

Low Core Execution

LØWCORE

Small buffer option for Column Formats printout. For
these printouts (IBLØCK=0,3), each sort file has a
buffer which is defaulted to a length of 1002B for
maximum efficiency. If the parameter LØWCORE is set
non-zero, the buffer length is set to 102B, so there is
a core savings of 700B for every ten parameters to be
printed. The cost does not differ significantly, so
the normal option is recommended because the job runs
faster. The low core option can be used, however, when
the available core is limited. This option does not
apply to Block Formats (i.e. IBLØCK=1 or 2), which
always use less core since no file buffers are necessary.

Program SPRINT can be executed more than once in the same job in order
to change the NAMELIST parameters for a different run or series of runs. All
NAMELIST parameters not changed will retain their previously assigned values.
The only exception is the parameter INAMES. This parameter will not stay
non-zero on a subsequent execution so names do not have to be re-entered
unless desired by the user. However, the names will be retained unless the
parameter INAMES is set non-zero and new names are entered via data cards.

Figure 3.4-4 shows the NAMELIST options input for the YAV8B conventional
Dutch Roll simulation run. This set of cards is inserted behind the second
end-of-record card in the EXECUTE deck. A summary of NAMELIST parameters
is printed in the output for each run, and shown for this case in Figure
3.4-5. The column format has been selected, and one page of the time history
output for this run is shown in Figure 3.4-6. An example of block format
output can be seen in Figure 3.4-7.

3.4.3 I50MS DECK - Calls to the YAV8B aircraft subroutines and equations of
motion are made in the I50MS subroutine. Within this subroutine, both
dynamic time histories and static check cases can be modeled. In addition,
initialization of variables can be performed and miscellaneous parameters
can be defined. These features can be incorporated into the simulation with
the use of the I50MS modify card deck. This deck modifies the I50MS sub-
routine to include any pilot control input time histories and/or program
initializations.

3.4.3.1 Dynamic Time Histories - Any simulated pilot inputs during a time
history run are modeled in I50MS before the operate loop call to AC07, a
subroutine which calls the aircraft subroutines and equations of motion in
the proper sequence. The pilot inputs can include stick and rudder pedal
movements as well as throttle and nozzle changes. Any cockpit switches which
need to be activated during a run, such as flap mode switch or water switch,
can also be modeled.
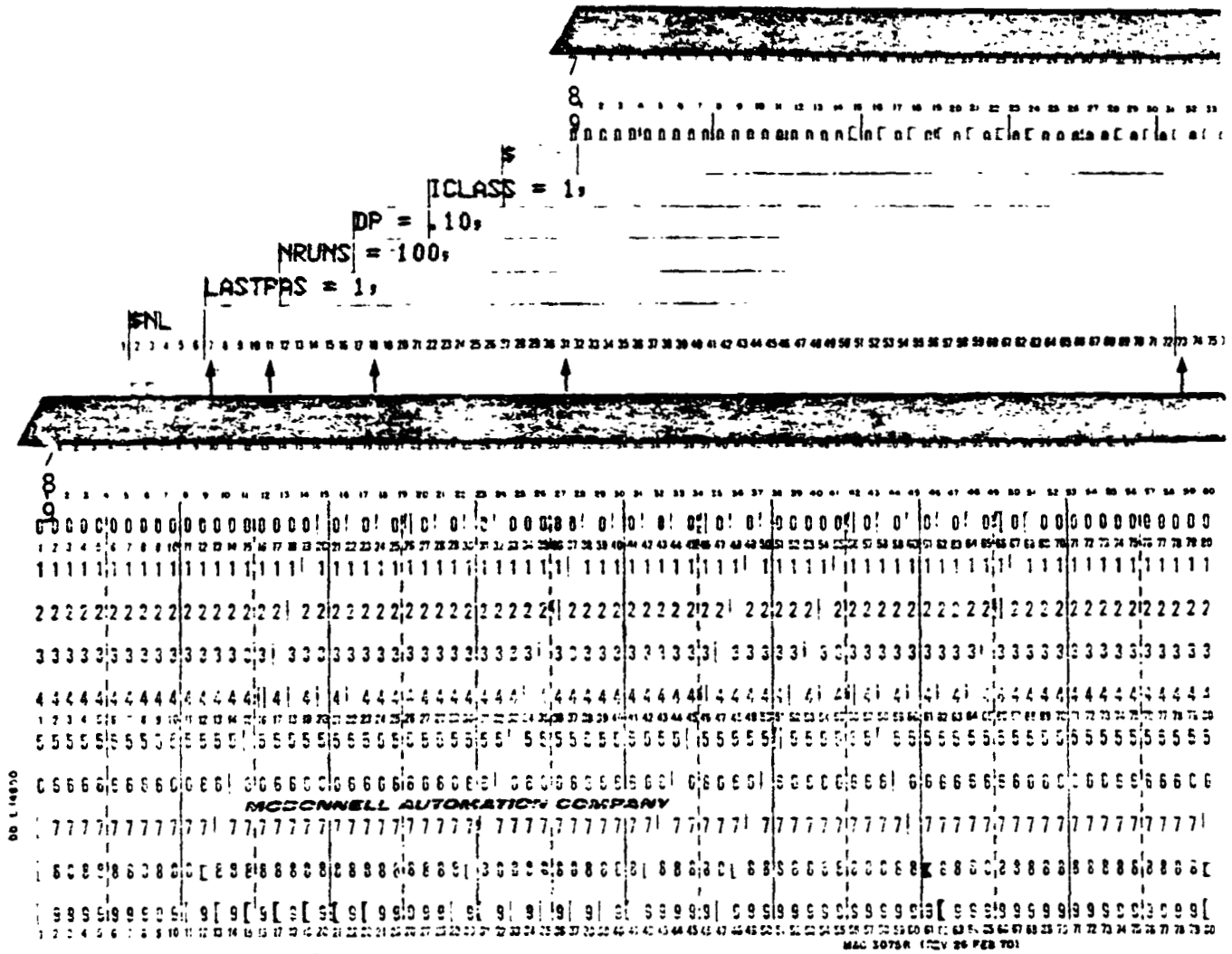
FIGURE 3.4-4
NAMELIST CARD SEQUENCE IN EXECUTE DECK

STANDARD PRINT -- NAMELIST OPTIONS

RUN SELECTION
NUMBER OF CONSECUTIVE RUNS .... NRUNS = 100
FILE NUMBERS OF RUNS DESIRED
(MAX.-20) .... EFILES = 0
IBLOCK = 0

PRINT SELECTION
COLUMN (IBLOCK=0)
BLOCK (IBLOCK=1)
TIME HISTORY (IBLOCK=2)
COLUMN WITH INCREASED (IBLOCK=3)
ACCURACY

PARAMETER SELECTION
LIMIT NO. OF PARAMETERS .... NPLIM
PAGE PRINT FLAGS .... IPP
PARAMETER RE-ORDERING .... IXR
PARAMETER PRINT INDICES .... IXOC

TIME ID PRINT
PRINT INTERVAL .... DP
START TIMES (MAX.-10) .... ISTART
STOP TIMES (MAX.-10) .... ISTOP
LAST PASS OF DATA PRINT FLAG ...... LASTPAS

NAMES OVERRIDE FLAG .... INAMFS
DATA YEARS FORMAT (110,7A10)

CLASSIFICATION OVERRIDE .... ECLASS
NORMAL (TAPE SORT) (CLASS=0)
-BLANK- (CLASS=1)
CONFIDENTIAL (CLASS=2)
SECRET (CLASS=3)

LOWCORE OPTION FLAG .... LOWCORE = 0

OLD TAPES ONLY
FIRST/LAST RUN INDICES .... ISDATA = 00, 00
(START OF RUN DATA
END OF RUN DATA

FIGURE 3.4-5
SPRINT NAMELIST OPTIONS SUMMARY

**FIGURE 3.4-6
SPRINT COLUMN (IBLOCK = 0) FORMAT**

FIGURE 3.4-7
SPRINT BLOCK (IBLOCK = 2) FORMAT

The simulation require, that stick inputs be made in percent of full stick deflection in both the longitudinal (100% full aft, 0% full forward) and lateral (-100% full left, 100% full right) axes. Rudder pedal is input in percent of total rudder pedal deflection (-100% full left pedal, 100% full right pedal). Varying throttle and nozzle control inputs are also made in percent for use in subroutine ENG08. See Figure 3.4-8 for commanded surface positions, RPM and nozzle angle as a function of percent stick, rudder, throttle and nozzle lever respectively.

Pilot control inputs to the program are normally modeled as functions of run time. Figure 3.4-9 shows the location in I50MS where control inputs have been made for a YAV-8B wingborne Dutch Roll case. Data tables have been utilized in storing both the percent stick and rudder pedal movement as a function of time. The format of the table look-up functions used to access these data tables is discussed in Section 3.4.5. It is acceptable to program step inputs of the controls as a function of time using IF statements in lieu of data tables. For example, this is the procedure to use when modeling changes in cockpit switch positions. However, the table look-up functions provide the capability of modeling more realistically the pilot control inputs due to linear interpolation between data points.

3.4.3.2 <u>Static Check Cases</u> - When the output of a simulation run is desired simply as a function of input and no control variations, the control input definitions can either be modeled as constants in the I50MS subroutine or defined in the EXECUTE deck data cards. It may at some time be desirable to isolate a particular subroutine in order to examine data or logic. The analysis of a particular subroutine can be simplified by excluding the equations of motion and any aircraft subroutines irrelevant to the topic of interest. This modification can be made by replacing the call to AC07 with a call to the desired subroutine(s) in the I50MS subroutine. These subroutines must be examined for necessary inputs, however, because some variables used in the logic will no longer be provided values when the irrelevant subroutines are excluded. Additional parameters can be initialized through data card inputs to the EXECUTE deck.

3.4.3.3 <u>Parameter Definition and Initialization Capabilities</u> - The user may define additional parameters of interest in the I50MS subroutine. Once equivalenced to available array locations, the parameters can be output in the RTPDATA subroutine (see Section 3.4.4). The advantage to defining a variable in I50MS is that the definition can be made after calculations within all subroutines have been completed for a given pass. The user can be assured that the variable is using current and not past values in its definition.

The entry point I50ØNCE is contained in I50MS, and provides an alternate means of initializing parameters for use in a simulation run. Greater flexibility is generally available in initializations made through the EXECUTE deck data cards. For necessary inputs which the user will not often be varying, however, entries made in I50ØNCE before the call to AC07 (or other subroutines) can eliminate having to handle more EXECUTE data cards than are needed.

FIGURE 3.4-8
YAV-8B PILOT CONTROL INPUT DEFINITIONS

```
                                        ****************************
*                                       **                        **
*                                       *   20/SEC SUBROUTINES    *
*                                       **                        **
*                                       ****************************
*
     CDT = FDT

     PDDEG = PD * 2TDD
     QDDEG = QD * DTDD
     RDDEG = PD * DTDD
     PDEG = P*RTDD
     QDEG = Q*RTDD
     RDEG = P*RTDD

     STLPDC=52.14
     STLAPC=0.0                                    ⎫
     CALL ESPCH(TIME,RQKTM25,13,ITHM25,1)          ⎬  control inputs
     RUDPC=F1B(TIME,13,BNDTM25,DELCS25)            ⎪
     IFLAP = 1                                     ⎭
     IF(DELAPL.GE.4.0) IFLAP = 0
●
     CALL ACO7
*


     ANZR = -AZ / G

     XTOT = AERDX + FTX
     YTOT = AERDY + FTY
     ZTOT = AERDZ + FTZ

     CDT = FDT

     RETURN                    ***********************************
●                              *
*                              *  ONE PASS INITIALIZATION
●                              *
*                              ***********************************
*
     ENTRY I50ONCE

     CDT = FDT

     PTRLO = 1.                              ONE PASS (INITIAL = 1)
*                                            INITIALIZATION CALLS
*

     CALL ACO7

     CDT = FDT
     RETURN
     END
```
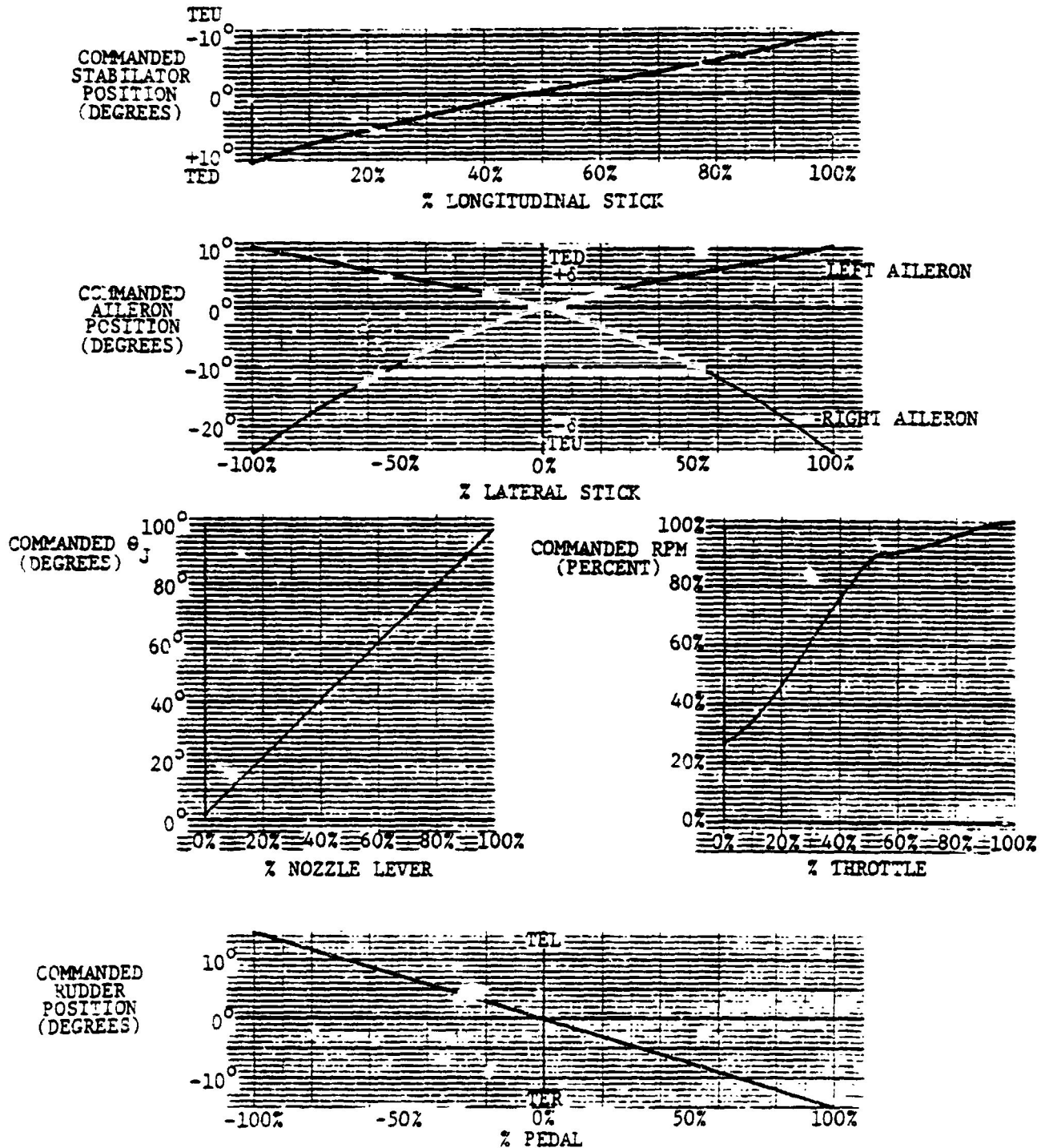
FIGURE 3.4-9
I50MS DYNAMIC INPUT LOGIC

3.4.4 <u>RTPDATA DECK</u> - Program variables in common arrays can be deleted from or added to the output listing by modifying the subroutine RTPDATA with the modify deck RTPDATA. Subroutine RTPDATA specifies which array locations will be buffered out during a simulation run. The user needs to know the array locations of variables desired to be a part of the output. The format for a variable print-out request is:

$$N=N+1 \quad \$ \quad IB(N)=INA + xxx \quad \$ \quad IN(N)=10H \; ccc,$$

where "xxx" is the array location of the output, and "ccc" represents a ten character name which will identify the data of location "xxx" in the print-out listing. INA in this statement specifies that the data is coming from the A array, which begins at $F(1001)$. If the variable address is defined in the F array and is less than 1000, INF should be used instead of INA.

The capability exists for the user to output start of run data, time history data, and/or end of run data. Start of run and end of run variables are printed only once in the output, while time history variables can be recorded throughout the simulation run. The same statement format shown above is utilized for any of these three cases. Placement of a variable print-out statement within subroutine RTPDATA will determine the order that the variable name and its value are printed. An example of the output variables in RTPDATA specified for a YAV-8B wingborne Dutch Roll case is shown in Figure 3.4-10. In this example, time history and start of run variables will be displayed, but no end of run output will be produced.

3.4.5 <u>DATA TABLE LOOK-UP FORMAT</u> - Data tables such as those containing aero-dynamic and engine performance data are accessed using subroutines and functions contained in file TBLKP. The appropriate interpolation ratio, index, and data point selections are based on given independent variable values and inputs provided in the TBLKP functions and subroutine calls.

3.4.5.1 <u>Data Table Structure</u> - The aerodynamic and engine data tables are defined in subroutines AERØDAT and YENGD respectively. The tables may be one-, two-, or three-dimensional. The order of the data within the tables is important when using a table look-up function. The first dimension of a data table is a function of the first independent variable, the second dimension likewise is a function of the second independent variable, etc. Figure 3.4-11 displays the structure for three-dimensional table CNFLAPT.

```
*********************************
*
*  TIME HISTORY DATA
*  POINTERS AND NAMES
*
*********************************
```

```
IB(1) = 151
IB(2) = 7C
N = 2
INA = 1000
```

```
N=N+1 S IB(N)=INA +  959 S IN(N)=10H CASE
N=N+1 S IB(N)=INA +   40 S IN(N)=10H MACH
N=N+1 S IB(N)=INA +   11 S IN(N)=10H ALT
N=N+1 S IB(N)=INA +   39 S IN(N)=10H QBAR
N=N+1 S IB(N)=INA +  251 S IN(N)=10H GW
N=N+1 S IB(N)=INA +  782 S IN(N)=10H FUEL
N=N+1 S IB(N)=INA +  819 S IN(N)=10H WATER
N=N+1 S IB(N)=INA +  253 S IN(N)=10H FSCG
N=N+1 S IB(N)=INA +  255 S IN(N)=10H WLCG
N=N+1 S IB(N)=INA +  254 S IN(N)=10H BLCG
N=N+1 S IB(N)=INA +  256 S IN(N)=10H IXX
N=N+1 S IB(N)=INA +  257 S IN(N)=10H IYY
N=N+1 S IB(N)=INA +  258 S IN(N)=10H IZZ
N=N+1 S IB(N)=INA +  259 S IN(N)=10H IXZ
N=N+1 S IB(N)=INA +  883 S IN(N)=10H GEAR
N=N+1 S IB(N)=INA +  639 S IN(N)=10H LID
N=N+1 S IB(N)=INA +  117 S IN(N)=10H ALPHA
N=N+1 S IB(N)=INA +  118 S IN(N)=10H BETA
N=N+1 S IB(N)=INA +   31 S IN(N)=10H GAMMAV
N=N+1 S IB(N)=INA +  478 S IN(N)=10H STKLON
N=N+1 S IB(N)=INA +  503 S IN(N)=10H DH
N=N+1 S IB(N)=INA +  479 S IN(N)=10H STKLAT
N=N+1 S IB(N)=INA +  505 S IN(N)=10H DAL
N=N+1 S IB(N)=INA +  506 S IN(N)=10H DAR
N=N+1 S IB(N)=INA +  637 S IN(N)=10H DFLAPL
N=N+1 S IB(N)=INA +  638 S IN(N)=10H DFLAPR
N=N+1 S IB(N)=INA +  480 S IN(N)=10H PEDAL
N=N+1 S IB(N)=INA +  513 S IN(N)=10H DR
N=N+1 S IB(N)=INA +  788 S IN(N)=10H THETAJ
N=N+1 S IB(N)=INA +  805 S IN(N)=10H NFC
N=N+1 S IB(N)=INA +  804 S IN(N)=10H NF
N=N+1 S IB(N)=INA +  825 S IN(N)=10H INAIR
N=N+1 S IB(N)=INA +  769 S IN(N)=10H FGTOT
N=N+1 S IB(N)=INA +  412 S IN(N)=10H VE
N=N+1 S IB(N)=INA +  315 S IN(N)=10H DRAGSCB
N=N+1 S IB(N)=INA +  750 S IN(N)=10H DRAGIBL
N=N+1 S IB(N)=INA +  812 S IN(N)=10H DRAGRAM
N=N+1 S IB(N)=INA +  657 S IN(N)=10H TOTBLD
N=N+1 S IB(N)=INA +  104 S IN(N)=10H PHI
N=N+1 S IB(N)=INA +  103 S IN(N)=10H THETA
```

FIGURE 3.4-10
RTPDATA VARIABLE OUTPUT FORMAT

```
◄──────────────── DIMENSION 1 ────────────────►
     DATA (CNFLAPT(I),I=1,64)/
     .8*0.0,
   . 0 208.   0.195,   0 183,   0.160,   0.133,   0.125,   0.120,
   . 0.120
   . 0.360,   0.345,   0.330,   0.305,   0.268,   0.235,   0.218,
   . 0.203,
   . 0.455,   0.448,   0.438,   0.430,   0.380,   0.330,   0.280,
   . 0.248,
   . 0.500,   0.505,   0.505,   0.505,   0.490,   0.405,   0.308,
   . 0.243,
     .8*0.0,
   . 0.198,   0.185,   0.178,   0.153,   0.130,   0.125,   0.120,
   . 0.120
   . 0.357,   0.133,   0.318,   0.295,   0.263,   0.235,   0.218,
   . 0.203/
     DATA (CNFLAPT(I),I=65,120)/
   . 0.448,   0.440,   0.428,   0.410,   0.378,   0.330,   0.280,
   . 0.228,
   . 0.508,   0.508,   0.508,   0.508,   0.495,   0.405,   0.308,
   . 0.243,
     .8*0.0,
   . 0.168,   0.160,   0.155,   0.143,   0.130,   0.125,   0.120,
   . 0.120,
   . 0.308,   0.298,   0.293,   0.272,   0.255,   0.235,   0.218,
   . 0.203,
   . 0.405,   0.400,   0.393,   0.370,   0.350,   0.330,   0.280,
   . 0.228,
   . 0.470,   0.470,   0.470,   0.470,   0.465,   0.405,   0.308,
   . 0.243/
```

(DIMENSION 2 and DIMENSION 3 axis labels appear along the left margin)

8 x 5 x 3 TABLE

DIMENSION 1 INDEPENDENT VARIABLE = CORRECTED ANGLE OF ATTACK
DIMENSION 2 INDEPENDENT VARIABLE = FLAP DEFLECTION
DIMENSION 3 INDEPENDENT VARIABLE = NOZZLE ANGLE

FIGURE 3.4-11
DATA TABLE STRUCTURE

3.4.5.2 Functions – The format for a one-dimensional table look-up with no previously calculated ratios or indices is:

XOUT = F1A(RIN,NUMPTS,BOUNDS,VALUES)

where RIN is input independent variable
      NUMPTS is number of points
      BOUNDS is minimum and maximum values of input variable, defined in
             subroutine DATA statements, and
      VALUE is table of output function values corresponding to each breakpoint.

For a two- or three-dimensional table look-up, the arguments have the same
meaning, but RIN will need to be specified as a temporary array whose elements
are in two (or three) independent variables:

TEMP(1)=RIN1
TEMP(2)=RIN2
XOUT=F2A(TEMP,NUMPTS,BOUNDS,VALUES)

Here also NUMPTS becomes a two-dimensional array defined in subroutine data statements and expressed as: DATA NUMPTS number in dimension 1, number in dimension 2 . BOUNDS becomes a four- rather than two-dimensional array, defining the endpoints in both dimensions.

Whenever a table look-up function is used, the interpolation ratios and indices for each dimension of the function are stored in a temporary location. If the next logical function uses the same independent variable, number of points and boundaries as arguments, the previously calculated ratios and indices can be retrieved from storage for use in this interpolation. Seven different functions are available in TBLKP:

DIMENSION	FUNCTION	USE (RATIO MEANS RATIO AND INDEX)
$w = f(x)$	F1A	Find x ratio; calculate $f(x)$
	F1B	Calculate $f(x)$ using previous x ratio
$w = f(x,y)$	F2A	Find x,y ratios; calculate $f(x,y)$
	F2B	Use previous x ratio; find new y ratio; calculate $f(x,y)$
	F2C	Calculate $f(x,y)$ using previous x,y ratios
$w = f(x,y,z)$	F3A	Find x,y,z ratios; calculate $f(x,y,z)$
	F3D	Calculate $f(x,y,z)$ using previous x,y,z ratios

The breakpoints of all curves must be evenly spaced whenever an "A" function is used to calculate the ratios and indices. These functions do not extrapolate beyond the boundaries; they interpolate within the boundaries only. Out-of-bounds input arguments will receive the closest boundary value of the function. Previous ratios can be calculated by an "A" or "B" function, or by subroutines FSRCH or FCALC.

3.4.5.3 Subroutine FSRCH - When the breakpoints of a curve are unevenly spaced, a call to FSRCH will initiate a calculation of the interpolation ratio and index to be stored and subsequently used by one of the table look-up functions. Each dimension requires a unique call to FSRCH if more than one dimension has uneven breakpoints. The format for a call to FSRCH is:

   CALL FSRCH (RIN,BRKPT,NUMPTS,IPREV,IDIM)

where   RIN is input independent variable,
       BRKPT is array name of uneven breakpoints defined in DATA statement,
       NUMPTS is number of breakpoints in BRKPT array,
       IPREV is index position where search is to begin, and
       IDIM is for which dimension in the data table the search is being done (1,2, or 3).

The interpolation index for a given call to FSRCH is stored in IPREV, so that this index will be a starting point the next time this particular FSRCH call is made. IPREV must therefore be a unique name for all calls which do not have the same independent variable and breakpoint table specified in the call arguments.

3.4.5.4 Subroutine FCALC - FCALC assumes that breakpoints for a curve are evenly spaced. The format for a call to FCALC is:

    CALL FCALC (RIN,BOUNDS,NUMPTS,IDIM)

where   RIN is input independent variable,
        BOUNDS is low and high boundary of input variable,
        NUMPTS is number of points in direction considered, and
        IDIM is for which dimension in the data tables the search is being
             done.

An interpolation ratio and index are calculated and stored for use by one of the table look-up functions.

3.4.6 PROGRAM DEFAULTS AND OVERRIDES - Each subroutine comprising the YAV8B program may have a number of variables assigned with default values. The program user should be familiar with the more important variables with default values. The following paragraphs describe these variables for the YAV8B, ATMØS and aircraft routines. Overrides to the defaults can be incorporated in the data cards of the EXECUTE deck.

3.4.6.1 YAV8B - All variables defined in the DATA statements can be changed, but the following will be of chief interest to the user:

NPASSD	Number of passes in reset; currently defaulted to 400 for dynamic stabilization of the simulation.
FDT	Basic program update time increment in seconds: default value is .05.
CDT	Current update time increment in seconds; default value is .05.
TSTØPD	Run time limit; usually specified in the EXECUTE deck, but defaulted to 10 here in case user inadvertently excludes this input (in seconds).
DTBUF	Rate at which subroutine RTP will buffer data to storage; should coincide with value of CDT (in seconds).

3.4.6.2 ATMØS - The basic ATMØS subroutine defines temperature, speed of sound, pressure, and density as a function of altitude for a standard day. If a non-standard day model is desired, the user must modify the ATMØS subroutine to include the values for these atmospheric variables   In addition, a flag must be set to integer 1 in the EXECUTE data cards to bypass the standard day calculations in favor of the non-standard day inputs. This flag is INSTD, located in A(195) and specified as F(1195) on the data cards.

3.4.6.3 AERØY8B - No formal options exist in the aerodynamic subroutine to affect the logical sequence of computations. Any inputs necessary which are relative to cockpit controls or aircraft configuration are provided by other subroutines.

3.4.6.4 ENG08 - The engine routine has a number of switches to consider, which are summarized below:

F-ARRAY LOCATION	VARIABLE NAME	DEFAULT VALUE	DESCRIPTION
1781	IDEFUEL	1	Flag for fuel burn during run; default value inhibits fuel depletion
1835	IWATER	0	Water switch off
1831	IENGFØ	0	Engine normal; no flame-out
1874	ILIMØFF	0	All engine limiters on; when set to 1, EGT and RPM limiters are bypassed

3.4.6.5 RCS07 - No formal options exist in the reaction control system subroutine to affect the logical sequence of computations. Variable PTBLD is initialized to (1.) in I50ØNCE because it is used in the denominator of an equation here before it is defined by subroutine ENG08.

3.4.6.6 PFC07 - Stability augmentation system switches are defaulted off with a value of zero. The variables and locations are:

PITCH SAS	ISASLØN	F(1495)
ROLL SAS	ISASLAT	F(1496)
YAW SAS	ISASDIR	F(1497)

Although it is not necessary to include these flags as inputs in the EXECUTE data cards when the switches are off, they are included simply for user information.

3.4.6.7 SFC07 - The secondary flight controls subroutine has a number of options available which are summarized below:

F-ARRAY LOCATION	VARIABLE NAME	VALUE	DESCRIPTION
1882	IGEAR	0	Default; gear up
		1	Gear down
1628	ILID	0	Default; LIDS will extend and retract with gear
		1	Emergency LIDS retract
1627	IMØDE	0	Default; flaps in UP mode; movement of flaps must be commanded by IFLAP switch
		1	Down mode; flaps operate automatically as a function of nozzle position and airspeed; aileron droop activated in this mode; IFLAP ignored

F-ARRAY LOCATION	VARIABLE NAME	VALUE	DESCRIPTION
1635	IFLAP	0	Default; no manual flap movement
		-1	Retract flaps as long as IFLAP has this value
		1	Extend flaps, as long as IFLAP has this value, up to 25°
1900	IWØNW	0	Default; no weight on wheels
		1	Weight on wheels; should be set when aircraft is on the ground

If the flap mode switch is JP and the user wishes to extend the flaps less than 25°, logic must be inserted into I5OMS, before the call to AC07, to limit the duration of time that the IFLAP switch is set to 1.

3.4.6.7 WTBAL07 - A user may wish to bias the center of gravity to match a particular test configuration. This can be done by adding increments to the total moments used in the center of gravity calculations. The defaults for all biases are zero.

When a particular C.G. is desired, the total moment needed can be calculated for a given aircraft weight, i.e., for the fuselage station C.G.:

$$TØTMØMX=CGFS*WEIGHT$$

where   TØTMØMX=DRYMØMX + FUELMX + ... + BSMØMX

Since the moment contributions due to the dry aircraft (DRYMØMX), fuel (FUELMX), etc., and the total aircraft weight are known, the bias (BSMØMX) required for a particular C.G. location may be determined. The same procedure is followed for butt line and waterline C.G. biases, and the results for each are entered on EXECUTE data cards in the following locations:

BSMØMX	F(1273)
BSMØMY	F(1274)
BXMØMZ	F(1275)

These biases are added into the total moment calculations used to calculate the aircraft C.G. location in WTBAL07.

3.4.7 SUBROUTINE MODIFICATION - MØDIFY is a utility available on the Network Operating System (NOS) for Control Data Corporation (CDC) Cyber 170 Series Computer Systems; CDC Cyber 70 Series, Models 71, 72, 73, and 74 Computer Systems; and the CDC 6000 Series Computer Systems. MØDIFY is used to maintain and update subroutines that are on the decks of modify file YAVMØD. These decks and the subroutines defined in them are summarized below:

DECK ON YAVMØD	SUBROUTINES IN DECK
YAV8B	(Program) YAV8B
I50MS	I50MS
YAERØ	AERØDAT
	AERØY8B
YENGN	YENGD
	ENG08
YAVAC	AC07
	RCS07
	PFC07
	SFC07
	WTBAL07
ATMØS	STNDAY
	ATMØS
RTPDATA	RTPDATA

Figure 3.4-12 is an example of a modify card deck for incorporating changes into subroutine I50MS. Insert and delete cards are placed between the *DECK and *EDIT cards after the first end-of-record. The insert card will be of the format (beginning in column 1):

*INSERT or *I nnn

where nnn is a deck line number. Deck line numbers are those displayed to the right of subroutine statements, as shown in the listings of Volume II, Appendix A. Input cards following a given insert card will be placed by MODIFY in the I50MS deck immediately after nnn. The delete card will have the format (beginning in column 1):

*DELETE or *D nnn
or *D nnn, mmm

where nnn, mmm specifies the first and last deck line numbers of a group of lines to be deleted. Additional statements on cards following a given delete card are permitted, and these will replace the lines removed.

To make modifications to a deck other than I50MS in Figure 3.4-12, the user must replace the name I50MS on the FTN, REPLACE, *DECK, and *EDIT cards with that of the desired deck. Further details of the MODIFY utility can be found in Reference (7).

```
                                    /*EDIT ₫50MS
                                    /*DECK ₫50MS

                          /* YAV-BB I50MS ERROR(S)
                         /EXIT.
                        /* YAV-BB I50MS DONE
                       /REPLACE,I50MS.
                      /FTH,A,D,B=I50MS,R=2,OPT=2.
                     /MODIFY(P=YAVMOD,LO=ES)
                    /ATTACH,YAVMOD,NA.
                   /BANNERS(OP=DTSF)*YAV-BB*I50MS*MODIFY**

job control cards
```
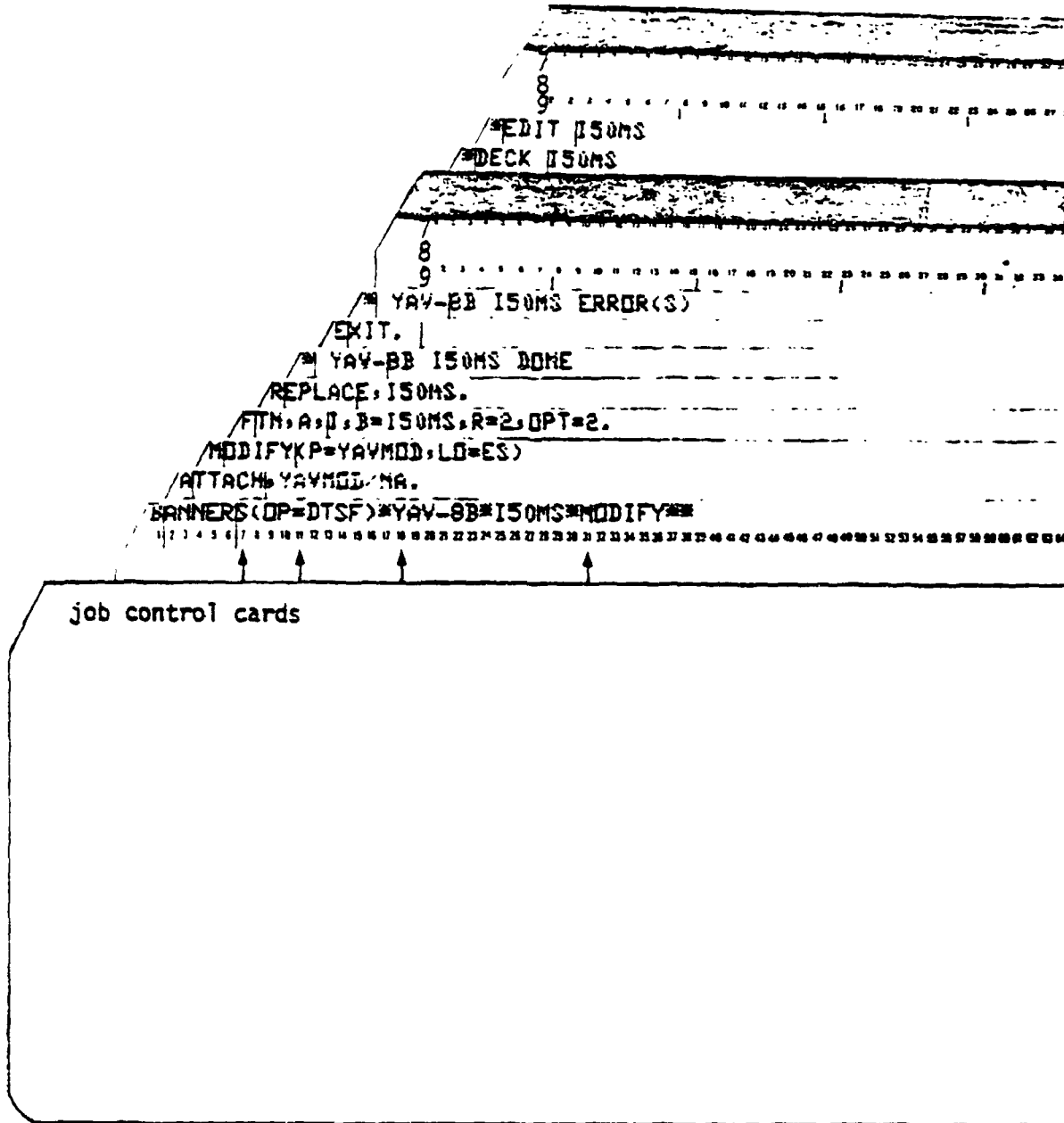
FIGURE 3.4-12
MODIFY CARD DECK FOR I50MS

4. YAV-8B LINEAR MATHEMATICAL MODEL

This section presents the linear mathematical model of the YAV-8B aircraft. The model is composed of small perturbation stability derivatives in the form traditionally used in the analysis of conventional aircraft. AV-8 project experience has shown that this form is adequate for control system design and handling qualities analysis in the V/STOL flight regime providing the linear analysis is supplemented by nonlinear six degree of freedom analyses. The nonlinear analyses can be obtained through real time pilot in the loop flight simulation or non-real time digital computer runs.

4.1 LINEARIZED EQUATIONS OF MOTION

The linearized equations of motion in stability axes are presented in Figure 4.1-1. The corresponding sign convention and nomenclature are presented in Figures 4.1-2 and 4.1-3. The variables in the equations are perturbation quantities from the initial condition.

4.2 TRIM CONDITIONS AND STABILITY DERIVATIVES

The stability derivatives presented in this section include the effects of aerodynamics, gross thrust and inlet momentum. These derivatives were obtained by perturbing the nonlinear model about a 3 degree of freedom wings level trim condition. Using a 3 degree of freedom trim ensures that the effectiveness of the RCS, which is a strong function of engine fan speed, is represented accurately in forming the control effectiveness derivatives. Figures 4.2-1 and 4.2-2 present the trim conditions and the corresponding stability derivatives used to generate the linear results that are compared to YAV-8B flight test data in Section 5. The corresponding weight and balance data are presented in Figure 5.1-5. Figures 4.2-3 to 4.2-5 present trim conditions and the corresponding stability derivatives for 24 flight conditions that characterize the YAV-8B throughout its flight envelope. The weight and balance data are presented in Section 2.3.

LONGITUDINAL

ΣF_X: $\quad \dot{u} + g\theta\cos\Gamma_o = X_u u + X_h h + X_q q + X_\alpha \alpha + X_{\delta_H} \delta_H + X_{\delta_{FRCS}} \delta_{FRCS} + X_{\delta_{ARCS}} \delta_{ARCS}$

ΣF_Z: $\quad V\dot{\alpha} - Vq + g\theta\sin\Gamma_o = Z_u u + Z_h h + Z_{\dot{\alpha}} \dot{\alpha} + Z_q q + Z_\alpha \alpha + Z_{\delta_H} \delta_H + Z_{\delta_{FRCS}} \delta_{FRCS} + Z_{\delta_{ARCS}} \delta_{ARCS}$

ΣM_{CG}: $\quad \dot{q} = M_u u + M_h h + M_q q + M_\alpha \alpha + M_{\dot{\alpha}} \dot{\alpha} + M_{\delta_H} \delta_H + M_{\delta_{FRCS}} \delta_{FRCS} + M_{\delta_{ARCS}} \delta_{ARCS}$

Altitude $\quad \dot{h} = V\theta\cos\Gamma_o - V\alpha\cos\Gamma_o + u\sin\Gamma_o$

LATERAL - DIRECTIONAL

ΣF_Y: $\quad V\dot{\beta} + Vr - g\phi\sin\Gamma_o - g\psi\cos\Gamma_o = Y_\beta \beta + Y_{\dot{\beta}} \dot{\beta} + Y_p p + Y_r r + Y_{\delta_A} \delta_{A_L} + Y_{\delta_R} \delta_R + Y_{\delta_{RRCS}} \delta_{RRCS} + Y_{\delta_{YRCS}} \delta_{YRCS}$

ΣL: $\quad \dot{p} - \frac{I_{xz}}{I_{xx}} \dot{r} = L_\beta \beta + L_{\dot{\beta}} \dot{\beta} + L_p p + L_r r + L_{\delta_A} \delta_{A_L} + L_{\delta_R} \delta_R + L_{\delta_{RRCS}} \delta_{RRCS} + L_{\delta_{YRCS}} \delta_{YRCS}$

ΣN: $\quad \dot{r} - \frac{I_{xz}}{I_{zz}} \dot{p} = N_\beta \beta + N_{\dot{\beta}} \dot{\beta} + N_p p + N_r r + N_{\delta_A} \delta_{A_L} + N_{\delta_R} \delta_R + N_{\delta_{RRCS}} \delta_{RRCS} + N_{\delta_{YRCS}} \delta_{YRCS}$

FIGURE 4.1-1
LINEARIZED EQUATIONS OF MOTION-STABILITY AXES
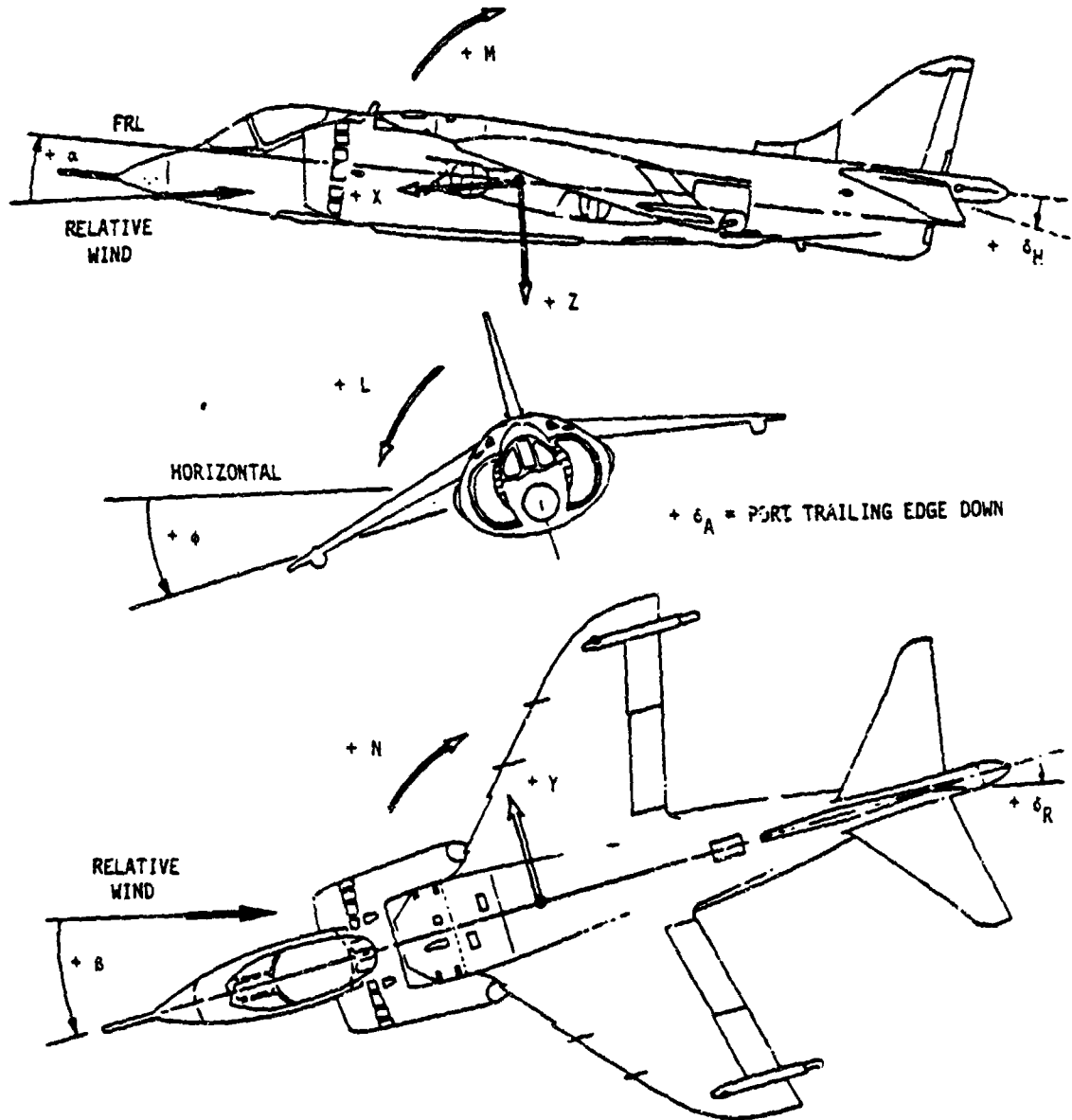
FIGURE 4.1-2
LINEARIZED MATHEMATICAL MODEL SIGN CONVENTIONS

VARIABLE	DEFINITION	UNITS
AND, U, L. R	Aircraft nose down, up, left, right	-
$\bar{c}$	Mean aerodynamic chord	in
FRL	Fuselage Reference Line	-
FS	Fuselage Station	in
g	Acceleration due to gravity	32.174 ft/sec^2
Gear	Landing Gear	-
h	Altitude	ft
I_{xx}	Moment of Inertia about X-axis	Slug-ft^2
I_{yy}	Moment of Inertia about Y-axis	Slug-ft^2
I_{zz}	Moment of Inertia about Z-axis	Slug-ft^2
I_{xz}	XZ Product of Inertia	Slug-ft^2
L	Rolling Moment (positive is RWD) or Left	ft-lb, -
LID	Lift Improvement Device	-
M	Pitching Moment (positive is ANU)	ft-lb
N	Yawing Moment (positive is ANR)	ft-lb
N_F	Engine Fan Speed	%
n_z	Load Factor	-
p	Rolling Velocity	rad/sec
q	Pitching Velocity	rad/sec
$\bar{q}$	Dynamic Pressure	psf
r	Yawing Velocity	rad/sec
RCS	Reaction Control System	-
RWD	Right wing down	-
TEU, D, L, R	Trailing Edge Up, Down, Left, Right	-
u	Forward speed	``/sec
V	Total freestream velocity	ft/sec
WL	Waterline	in
X	Force in X direction (positive is forward)	-
Y	Force in Y direction (positive is out right wing)	-
Z	Force in Z direction (positive is down)	-
α	Fuselage (WL) angle of attack	radian
β	Angle of sideslip	radian
Γ_o	Initial flight path angle	radian

FIGURE 4.1-3
LINEARIZED MATHEMATICAL MODEL AND STABILITY DERIVATIVES
NOMENCLATURE

VARIABLE	DEFINITION	UNITS
δ_A	Aileron deflection (positive is left aileron TED)	radian
δ_{AD}	Drooped aileron deflection (positive is TED)	radian
δ_{ARCS}	Aft RCS deflection in equivalent horizontal tail deflection for $\delta_H \geq 2^o \quad \delta_{ARCS} = \delta_H$ $\delta_H < 2^o \quad \delta_{ARCS} = 0$	radian
F	Trailing edge flap deflection (positive is TED)	deg
δ_{FRCS}	Forward RCS deflection in equivalent horizontal tail deflection for $\delta_H \geq 2^o \; \delta_{FRCS} = 0$ $\delta_H < 2^o \; \delta_{FRCS} = \delta_H$	radian
δ_H	Horizontal tail deflection (positive is TED)	radian
δ_R	Rudder deflection (positive is TEL)	radian
δ_{RRCS}	Roll RCS deflection in equivalent aileron deflection $\quad \delta_{RRCS} = \delta_{A\ LEFT}$	radian
δ_{YRCS}	Yaw RCS deflection in equivalent rudder deflection $\quad \delta_{YRCS} = \delta_R$	radian
ϕ	Roll angle (positive right wing down)	radian
θ	Pitch angle	radian
ψ	Yaw angle	radian

FIGURE 4.1-3
LINEARIZED MATHEMATICAL MODEL AND STABILITY DERIVATIVES
NOMENCLATURE (CONTINUED)

$$M_u = (\rho S V \bar{c} / I_{yy}) C_{M_u} \quad (1/\text{ft·sec})$$

$$L_\beta = (\rho S V^2 b / 2 I_{xx}) C_{\ell_\beta} \quad (1/\text{sec}^2)$$

$$M_h = (\rho S V \bar{c} / 2 I_{yy}) C_{M_h} \quad (1/\text{ft·sec}^2)$$

$$L_{\dot{\beta}} = (\rho S V b^2 / 4 I_{xx}) C_{\ell_{\dot{\beta}}} \quad (1/\text{sec})$$

$$M_\alpha = (\rho S V^2 \bar{c} / 2 I_{yy}) C_{m_\alpha} \quad (1/\text{sec}^2)$$

$$L_r = (\rho S V b^2 / 4 I_{xx}) C_{\ell_r} \quad (1/\text{sec})$$

$$M_{\dot{\alpha}} = (\rho S V \bar{c}^2 / 4 I_{yy}) C_{m_{\dot{\alpha}}} \quad (1/\text{sec})$$

$$L_p = (\rho S V b^2 / 4 I_{xx}) C_{\ell_p} \quad (1/\text{sec})$$

$$M_q = (\rho S V \bar{c}^2 / 4 I_{yy}) C_{m_q} \quad (1/\text{sec})$$

$$L_\delta = (\rho S V^2 b / 2 I_{xx}) C_{\ell_\delta} \quad (1/\text{sec}^2)$$

$$M_\delta = (\rho S V^2 \bar{c} / 2 I_{yy}) C_{m_\delta} \quad (1/\text{sec}^2)$$

$$N_\beta = (\rho S V^2 b / 2 I_{zz}) C_{n_\beta} \quad (1/\text{sec}^2)$$

$$X_u = (\rho S V / m) C_{X_u} \quad (1/\text{sec})$$

$$N_{\dot{\beta}} = (\rho S V b^2 / 4 I_{zz}) C_{n_{\dot{\beta}}} \quad (1/\text{sec})$$

$$X_h = (\rho S V / 2m) C_{X_h} \quad (1/\text{sec}^2)$$

$$N_r = (\rho S V b^2 / 4 I_{zz}) C_{n_r} \quad (1/\text{sec})$$

$$X_\alpha = (\rho S V^2 / 2m) C_{X_\alpha} \quad (\text{ft/sec}^2)$$

$$N_p = (\rho S V b^2 / 4 I_{zz}) C_{n_p} \quad (1/\text{sec})$$

$$X_{\dot{\alpha}} = (\rho S V \bar{c} / 4m) C_{X_{\dot{\alpha}}} \quad (\text{ft/sec})$$

$$N_\delta = (\rho S V^2 b / 2 I_{zz}) C_{n_\delta} \quad (1/\text{sec}^2)$$

$$X_q = (\rho S V \bar{c} / 4m) C_{X_q} \quad (\text{ft/sec})$$

$$Y_\beta = (\rho S V^2 / 2m) C_{y_\beta} \quad (\text{ft/sec}^2)$$

$$X_\delta = (\rho S V^2 / 2m) C_{X_\delta} \quad (\text{ft/sec}^2)$$

$$Y_{\dot{\beta}} = (\rho S V b / 4m) C_{y_{\dot{\beta}}} \quad (\text{ft/sec})$$

$$Z_u = (\rho S V / m) C_{Z_u} \quad (1/\text{sec})$$

$$Y_r = (\rho S V b / 4m) C_{y_r} \quad (\text{ft/sec})$$

$$Z_h = (\rho S V / 2m) C_{Z_h} \quad (1/\text{sec}^2)$$

$$Y_p = (\rho S V b / 4m) C_{y_p} \quad (\text{ft/sec})$$

$$Z_\alpha = (\rho S V^2 / 2m) C_{Z_\alpha} \quad (\text{ft/sec}^2)$$

$$Y_\delta = (\rho S V^2 / 2m) C_{y_\delta} \quad (\text{ft/sec}^2)$$

$$Z_{\dot{\alpha}} = (\rho S V \bar{c} / 4m) C_{Z_{\dot{\alpha}}} \quad (\text{ft/sec})$$

$$Z_q = (\rho S V \bar{c} / 4m) C_{Z_q} \quad (\text{ft/sec})$$

$$Z_\delta = (\rho S V^2 / 2m) C_{Z_\delta} \quad (\text{ft/sec}^2)$$

FIGURE 4.1-3
LINEARIZED MATHEMATICAL MODEL AND STABILITY DERIVATIVES
NOMENCLATURE (CONTINUED)

PARAMETER	UNITS	5.2-1	5.2-2	5.2-3	5.2-7	5.2-10	5.3-4	5.3-8
GROSS WEIGHT	LB	16450.0	16450.0	14690.0	20200.0	17070.0	16810.0	19230.0
ALTITUDE	FT	110.0	110.0	0.0	2800.0	4700.0	7000.0	35200.0
MACH	-	0.001	0.001	0.001	0.220	0.24	0.740	0.697
n_z	-	1.0	1.0	1.0	1.0	1.0	1.0	1.0
$\bar{q}$	PSF	.001	.001	.001	64.8	71.8	625.9	168.3
V	KTAS	0.7	0.7	0.7	145.6	152.9	478.0	406.1
θ_J	deg	79.0	79.0	79.0	45.0	61.0	0.0	3.0
α	deg	9.32	9.32	9.33	10.77	1.86	0.57	5.50
Γ_o	deg	0.0	0.0	0.0	-5.2	0.0	0.0	0.0
β	deg	0.0	0.0	0.0	0.0	0.0	0.0	0.0
ϕ	deg	0.0	0.0	0.0	0.0	0.0	0.0	0.0
N_F	%	96.0	96.0	93.8	71.9	87.9	79.8	76.7
δ_H	deg	2.85	2.85	2.41	5.43	5.51	0.67	-0.69
δ_F	deg	61.7	61.7	61.7	25.0	25.0	5.0	5.0
δ_{AD}	deg	15.0	15.0	15.0	0.0	0.0	0.0	0.0
δ_{SB}	deg	NA	NA	NA	NA	NA	NA	NA
Gear	-	DOWN	DOWN	DOWN	DOWN	DOWN	UP	UP
LID	-	DOWN	DOWN	DOWN	DOWN	DOWN	UP	UP

FIGURE NUMBER

FIGURE 4.2-1

TRIM CONDITIONS FOR TIME HISTORIES OF SECTION 5

PARAMETER	UNITS	FIGURE NUMBER 5.2-1	5.2-2	5.2-3	5.2-7	5.2-10	5.3-4	5.3-8
X_u	1/sec	-.02314	-.02314	-.02421	-.05251	-.05845	-.02764	-.01375
X_h	1/sec²	0.	0.	0.	0.	0.	0.	0.
X_u	ft/sec	.00045	.00045	.00049	7.50101	-1.28891	26.23723	2.16491
X_α	ft/sec	-.00136	-.00136	-.00149	-.25248	-.05474	0.	0.
X_q	ft/sec	.03132	.03172	.03374	-.30764	-.07401	-.00773	.00276
$X_{\delta H}$	ft/sec²	-.00004	-.00004	-.00004	-2.01663	-.45907	-10.10234	.38332
$X_{\delta FRCS}$	ft/sec²	0.	0.	0.	0.	0.	0.	-.04076
$X_{\delta ARCS}$	ft/sec²	-.44996	-.44996	-.45982	-1.21706	-.63233	0.	0.
Z_u	1/sec	-.00785	-.00785	-.00819	-.21130	-.11886	-.11522	-.11062
Z_h	1/sec²	0.	0.	0.	0.	0.	0.	0.
Z_α	ft/sec	-.02982	-.02982	-.03232	-79.82455	-129.40479	-1265.01374	-299.50798
$Z_{\dot\alpha}$	ft/sec	-.00826	-.00826	-.00908	-1.32704	-1.68769	-4.74021	-1.23647
Z_q	ft/sec	.24600	.24600	.25120	-1.57690	-1.97096	-7.11780	-1.89026
$Z_{\delta H}$	ft/sec²	-.00024	-.00024	-.00027	-10.59964	-14.15394	-190.99274	-42.82959
$Z_{\delta FRCS}$	ft/sec²	0.	0.	0.	0.	0.	0.	-.17473
$Z_{\delta ARCS}$	ft/sec²	-10.08967	-10.08967	-11.48248	-3.56754	-6.65651	0.	0.
M_u	1/ft-sec	.00050	.00050	.00044	-.00131	-.00040	-.00180	-.00039
M_h	1/ft-sec²	0.	0.	0.	0.	0.	0.	0.
M_α	1/sec	.00517	.00517	.00469	-1.63402	-.68069	-28.41632	-5.07942
$M_{\dot\alpha}$	1/sec	-.00263	-.00263	-.00260	-.47449	-.50763	-1.30163	-.42639
M_q	1/sec	-.05076	-.05076	-.04635	-.64321	-.69371	-2.04286	-.68800
$M_{\delta H}$	1/sec²	-.00008	-.00008	-.00008	-3.73142	-4.25577	-53.02915	-14.58472
$M_{\delta FRCS}$	1/sec²	0.	0.	0.	0.	0.	0.	.05969
$M_{\delta ARCS}$	1/sec²	-6.98447	-6.98447	-6.53093	-2.11042	-3.57948	0.	0.

FIGURE 4.2-2
LONGITUDINAL STABILITY DERIVATIVES FOR
TIME HISTORIES OF SECTION 5

PARAMETER	UNITS	FIGURE NUMBER						
		5.2-1	5.2-2	5.2-3	5.2-7	5.2-10	5.3-4	5.3-8
$Y_{\delta A}$	ft/sec^2	-.00001	-.00001	-.00001	-2.46447	-4.34840	-17.55931	-3.63633
$Y_{\delta RRCS}$	ft/sec^2	-1.00661	-1.00661	-1.01513	-.33010	-.66086	0.	-.00893
$Y_{\delta R}$	ft/sec^2	.00013	.00013	.00014	4.48498	5.88645	41.92017	9.49418
$Y_{\delta YRCS}$	ft/sec^2	4.52141	4.52141	4.73450	1.18067	2.35936	0.	.04358
Y_{β}	ft/sec^2	-.02856	-.02856	-.03042	-32.83507	-48.74686	-365.15026	-85.34539
$Y_{\dot{\beta}}$	ft/sec	0.	0.	0.	0.	.00324	.02514	0.
Y_p	ft/sec	-.03307	-.03307	-.03567	-.01876		-5.85094	.04302
Y_r	ft/sec	-.25668	-.25668	-.26294	-.13871	-.21090	1.53703	.40988
$L_{\delta A}$	1/sec^2	.00019	.00019	.00019	7.42524	12.74662	135.05611	25.12207
$L_{\delta RRCS}$	1/sec^2	12.69730	12.69730	11.95021	3.09534	8.01053	0.	.39280
$L_{\delta R}$	1/sec^2	.00001	.00001	.00001	.03731	1.10894	9.51139	.74122
$L_{\delta YRCS}$	1/sec^2	-.44451	-.44451	-.42073	-.12999	.21745	0.	-.00028
L_{β}	1/sec^2	-.00290	-.00290	-.00298	-4.28536	-5.27269	-13.47119	-8.60165
$L_{\dot{\beta}}$	1/sec	0.	0.	0.	0.		0.	0.
L_p	1/sec	-.01983	-.01983	-.01991	-.87267	-1.46967	-5.85094	-1.28867
L_r	1/sec	-.02316	-.02316	-.02281	.27752	.25809	2.16419	.73352
$N_{\delta A}$	1/sec^2	0.	0.	0.	.46025	.80862	4.62761	.51576
$N_{\delta RRCS}$	1/sec^2	.00255	.00255	.00493	-.02540	.21273		.00159
$N_{\delta R}$	1/sec^2	-.00002	-.00003	-.00003	-1.17807	-1.33475	-10.86722	-2.89509
$N_{\delta YRCS}$	1/sec^2	-1.50765	-1.50765	-1.44172	-.41104	-.71774	0.	-.01444
N_{β}	1/sec	-.00443	-.00443	-.00417	2.96821	3.94821	18.06405	4.08138
$N_{\dot{\beta}}$	1/sec	0.	0.	0.	0.	0.	0.	0.
N_p	1/sec	-.00564	-.00564	-.00541	-.05918	-.00055	.00446	-.06499
N_r	1/sec	-.04680	-.04680	-.04095	-.22350	-.77487	-.99836	-.31488

FIGURE 4.2-2
LATERAL-DIRECTIONAL STABILITY DERIVATIVES FOR
TIME HISTORIES OF SECTION 5

ORIGINAL PAGE IS
OF POOR QUALITY
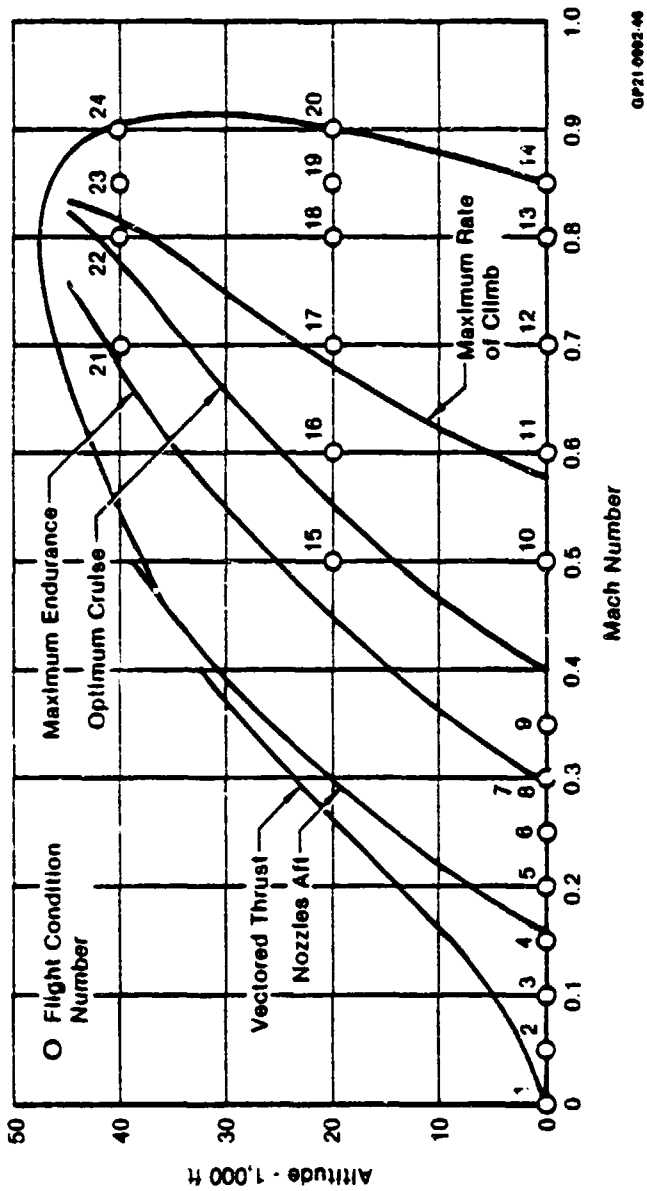
FIGURE 4.2-3

FLIGHT CONDITIONS FOR FULL FLIGHT ENVELOPE STABILITY DERIVATIVES

PARAMETER	UNITS	FLIGHT CONDITION NUMBER							
		1	2	3	4	5	6	7	8
GROSS WEIGHT	LB	16280	16280	16280	16280	16280	16280	16280	16280
ALTITUDE	FT	100.0	100.0	100.0	100.0	100.0	100.0	100.0	100.0
MACH	-	0.001	0.05	0.10	0.15	0.20	0.25	0.30	0.30
n_z	-	1.0	1.0	1.0	1.0	1.0	1.0	1.0	1.0
$\bar{q}$	PSF	.001	3.7	14.7	33.3	59.0	92.2	132.8	132.8
V	KTAS	.7	33.0	66.0	99.1	132.1	165.1	198.1	198.1
θ_J	deg	81.0	81.0	75.8	60.0	40.0	20.0	20.0	0.0
α	deg	7.30	4.52	4.00	3.83	1.94	4.03	0.72	0.47
Γ_o	deg	0.0	0.0	0.0	0.0	0.0	0.0	0.0	0.0
β	deg	0.0	0.0	0.0	0.0	0.0	0.0	0.0	0.0
ϕ	deg	0.0	0.0	0.0	0.0	0.0	0.0	0.0	0.0
NF	%	96.0	95.2	90.3	80.8	72.2	63.2	68.4	66.9
δ_H	deg	2.39	2.57	2.80	2.09	0.67	1.17	2.02	-0.66
δ_F	deg	61.7	61.7	61.7	61.7	47.0	25.0	25.0	25.0
δ_{AD}	deg	15.0	15.0	15.0	15.0	15.0	0.0	0.0	0.0
δ_{SB}	deg	NA	NA	NA	NA	NA	NA	NA	NA
Gear	-	DOWN	DOWN	DOWN	DOWN	DOWN	DOWN	DOWN	DOWN
LID	-	DOWN	DOWN	DOWN	DOWN	DOWN	DOWN	DOWN	DOWN

FIGURE 4.2-4
TRIM CONDITIONS
FULL FLIGHT ENVELOPE

PARAMETER	UNITS	FLIGHT CONDITION NUMBER							
		9	10	11	12	13	14	15	16
GROSS WEIGHT	LB	18158	18158	18158	18158	18158	18158	18158	18158
ALTITUDE	FT	100.0	100.0	100.0	100.0	100.0	100.0	20000.0	20000.0
MACH	-	0.35	0.50	0.60	0.70	0.80	0.85	0.50	.60
n_z	-	1.0	1.0	1.0	1.0	1.0	1.0	1.0	1.0
$\bar{q}$	PSF	180.8	369.0	531.3	723.2	944.6	1066.3	170.3	245.3
V	KTAS	231.2	330.3	396.3	462.3	528.4	561.4	307.0	368.4
θ_J	deg	2.0	2.0	2.0	2.0	2.0	2.0	2.0	2.0
α	deg	4.92	1.97	1.09	0.47	0.12	0.98	5.54	3.45
r_o	deg	0.0	0.0	0.0	0.0	0.0	0.0	0.0	0.0
β	deg	0.0	0.0	0.0	0.0	0.0	0.0	0.0	0.0
ϕ	deg	0.0	0.0	0.0	0.0	0.0	0.0	0.0	0.0
N_F	%	53.6	59.7	72.0	79.0	85.6	90.6	62.2	68.3
δ_H	deg	0.01	0.74	0.83	0.95	0.49	0.81	-0.84	-0.13
δ_r	deg	5.0	5.0	5.0	5.0	5.0	0.0	5.0	5.0
δ_{AD}	deg	0.0	0.0	0.0	0.0	0.0	0.0	0.0	0.0
δ_{SB}	-	NA	NA	NA	NA	NA	NA	NA	NA
Gear	-	UP	UP	UP	UP	UP	UP	UP	UP
LID	-	UP	UP	UP	UP	UP	UP	UP	UP

FIGURE 4.2-4 (CONTINUED)
TRIM CONDITIONS
FULL FLIGHT ENVELOPE

PARAMETER	UNITS	FLIGHT CONDITION NUMBER							
		17	18	19	20	21	22	23	24
GROSS WEIGHT	LB	18158	18158	18150	18158	18158	18158	18158	18158
ALTITUDE	FT	20000.0	20000.0	20000.0	20000.0	40000.0	40000.0	40000.0	40000.0
MACH	-	.70	.80	.85	.90	.70	.80	.85	.90
n_z	-	1.0	1.0	1.0	1.0	1.0	1.0	1.0	1.0
$\bar{q}$	PSF	333.8	436.0	492.2	551.9	134.8	176.1	198.8	222.9
V	KTAS	429.8	491.2	521.9	552.6	401.2	458.5	487.2	515.8
θ_J	deg	2.0	2.0	2.0	2.0	2.0	2.0	2.0	2.0
α	deg	2.16	1.30	0.94	1.01	6.80	4.47	3.71	3.58
Γ_o	deg	0.0	0.0	0.0	0.0	0.0	0.0	0.0	0.0
β	deg	0.0	0.0	0.0	0.0	0.0	0.0	0.0	0.0
ϕ	deg	0.0	0.0	0.0	0.0	0.0	0.0	0.0	0.0
NF	%	74.0	80.1	84.4	89.6	79.1	80.8	81.5	87.8
δ_H	deg	0.23	0.03	0.42	0.93	-1.27	-1.05	-0.81	-0.71
δ_F	deg	5.0	5.0	5.0	5.0	5.0	5.0	5.0	5.0
δ_{AD}	deg	0.0	0.0	0.0	0.0	0.0	0.0	0.0	0.0
δ_{SB}	-	NA	NA	NA	NA	NA	NA	NA	NA
Gear	-	UP	UP	UP	UP	UP	UP	UP	UP
LID	-	UP	UP	UP	UP	UP	UP	UP	UP

FIGURE 4.2-4 (CONTINUED)
TRIM CONDITIONS
FULL FLYING ENVELOPE

PARAMETER	UNITS	FLIGHT CONDITION NUMBER							
		1	2	3	4	5	6	7	8
X_u	1/sec	-.02308	-.03780	-.05886	-.09018	-.07249	-.05002	-.04071	-.04012
X_h	1/sec²	0.	0.	0.	0.	0.	0.	0.	0.
X_α	ft/sec²	.00041	.49982	2.40185	2.08548	4.66358	12.75305	13.43608	15.33057
X_δ	ft/sec	-.00107	-.03320	-.05873	-.08433	-.05704	-.14801	-.03192	-.02056
X_q	ft/sec²	.02151	-.03254	-.06841	-.10311	-.07456	-.18619	-.04584	-.03183
$X_{\delta H}$	ft/sec²	-.00003	-.04884	-.17289	-.37214	-.32179	-1.23069	-.31847	-.20517
$X_{\delta FRCS}$	ft/sec²	0.	0.	0.	0.	-5.19445	-4.29281	0.	0.
$X_{\delta ARCS}$	ft/sec²	.23063	.69511	.18533	-.68840	0.	0.	-1.61567	0.
Z_u	1/sec	-.00767	-.02663	-.1'212	-.19146	-.23381	-.21355	-.17585	-.14115
Z_h	1/sec²	0.	0.	0.	0.	0.	0.	0.	0.
Z_α	ft/sec	-.03056	-8.63061	-29.12989	-58.01804	-105.96188	-149.23892	-261.62280	-224.01700
Z_δ	ft/sec	-.00835	-.41967	-.83992	-1.26014	-1.68298	-2.09972	-2.32572	-2.52583
Z_q	ft/sec²	.24534	-.28708	-.84722	-1.42207	-1.99257	-2.55355	-3.08706	-3.09149
$Z_{\delta H}$	ft/sec²	-.00025	-.61737	-2.47115	-5.56123	-9.49384	-17.45852	-25.20064	-25.20181
$Z_{\delta FRCS}$	ft/sec²	0.	0.	0.	0.	-8.97689	-7.62326	0.	0.
$Z_{\delta ARCS}$	ft/sec²	-10.48198	-10.17959	-9.97046	-9.25184	0.	0.	-7.67142	0.
M_u	1/ft-sec	.00027	.00007	-.00134	-.00218	-.00298	-.06230	-.00157	.00029
M_h	1/ft-sec²	0.	0.	0.	0.	0.	0.	0.	0.
M_α	1/sec²	.00473	.11460	-.04995	-.46512	-.73862	-2.81489	-3.94402	-4.62889
M_δ	1/sec	-.00250	-.12486	-.24971	-.37457	-.49943	-.62428	-.74914	-.74914
M_q	1/sec	-.04729	-.20523	-.36374	-.51974	-.67705	-.83468	-.99904	-.99831
$M_{\delta H}$	1/sec²	-.00007	-.18591	-.74363	-1.67316	-2.85160	-5.25389	-7.56560	-7.56560
$M_{\delta FRCS}$	1/sec²	0.	0.	0.	0.	3.46904	2.52067	0.	0.
$M_{\delta ARCS}$	1/sec²	-6.83575	-6.63359	-5.69843	-4.56679	0.	0.	-3.20025	0.

FIGURE 4.2-5
LONGITUDINAL STABILITY DERIVATIVES
FULL FLIGHT ENVELOPE

ORIG... ...
OF PO... ...

PARAMETER	UNITS	FLIGHT CONDITION NUMBER
		1	2	3	4	5	6	7	8
$Y_{\delta A}$	ft/sec²	-.00001	.02697	.13919	.31317	.55675	-5.76406	-8.49692	-8.51139
$Y_{\delta RRCS}$	ft/sec²	-1.01957	-.99430	-.85532	-.66143	-.48815	-.36350	-.45730	0.
$Y_{\delta R}$	ft/sec²	.00013	.31711	1.26846	2.85403	5.07383	7.92786	11.41612	11.41612
$Y_{\delta YRCS}$	ft/sec²	4.76492	4.577A9	3.85579	3.16750	2.35433	1.74942	2.19860	0.
Y_β	ft/sec²	-.02871	-3.72\?7	-13.19956	-27.72350	-38.39084	-55.96326	-74.17628	-73.39457
$Y_{\dot\beta}$	ft/sec	0.	0.	0.	0.	0.	0.	0.	0.
Y_p	ft/sec	-.02289	-.01039	-.00752	-.00590	-.00081	-.00516	.0458	.00525
Y_r	ft/sec	-.25614	-.25548	-.23863	-.20705	-.18320	-.16098	-.17819	-.17392
$L_{\delta A}$	1/sec²	-.00019	.47099	1.87666	4.21673	7.33571	18.96115	26.67637	26.59589
$L_{\delta RRCS}$	1/sec²	13.28091	13.20824	11.37564	8.79886	6.47196	4.83427	6.01604	0.
$L_{\delta R}$	1/sec²	.00001	.04931	.21213	.48822	1.07670	1.32012	2.71077	2.76987
$L_{\delta YRCS}$	1/sec²	-.22989	.14287	.17021	.16309	.25029	.07967	.30985	0.
L_β	1/sec²	-.00211	-.54264	-2.50117	-5.99689	-5.83506	-5.25336	-3.71593	-3.41757
$L_{\dot\beta}$	1/sec	0.	0.	0.	0.	0.	0.	0.	0.
L_p	1/sec	-.01891	-.40754	-.80771	-1.20600	-1.60285	-2.00172	-2.38929	-2.38578
L_r	1/sec	-.01593	.07599	.15785	.23822	.28152	.40628	.38204	.37342
$N_{\delta A}$	1/sec²	0.	-.01260	-.05279	-.11513	-.13474	1.05851	1.65484	1.66506
$N_{\delta RRCS}$	1/sec²	.09409	.21156	.20135	.16062	.15839	.08507	.17254	0.
$N_{\delta R}$	1/sec²	-.00003	-.07415	-.79612	-.66594	1.17783	-1.85094	-2.64227	-2.64070
$N_{\delta VRCS}$	1/sec²	-1.48793	-1.42379	-1.19850	-.98438	-.73047	-.54379	-.68168	0.
N_β	1/sec²	-.00411	-.04373	.27731	1.25681	3.01798	4.89897	7.02223	7.03820
$N_{\dot\beta}$	1/sec	0.	0.	0.	0.	0.	0.	0.	0.
N_p	1/sec	-.00363	-.00648	-.00913	-.01199	-.00151	-.02106	.01112	.01396
N_r	1/sec	-.04146	-.10055	-.15848	-.21409	-.27164	-.32783	-.39300	-.39248

FIGURE 4.2-5 (CONTINUED)
LATERAL-DIRECTIONAL STABILITY DERIVATIVES
FULL FLIGHT ENVELOPE

PARAMETER	UNITS	FLIGHT CONDITION NUMBER
		9	10	11	12	13	14	15	16
X_u	1/sec	-.01841	-.07881	-.03528	-.03000	-.05989	-.09895	-.01653	-.01653
X_h	1/sec²	0.	0.	0.	0.	0.	0.	0.	0.
X_α	ft/sec²	11.05970	13.40382	22.93957	25.50322	26.97795	56.29080	7.92842	35.01464
X_δ	ft/sec	-.17002	0.	0.	0.	0.	0.	0.	0.
X_q	ft/sec	-.21519	-.00255	-.00631	-.09976	-.01304	-.01001	.00402	.00097
$X_{\delta H}$	ft/sec²	-3.16237	-2.09771	-12.45457	-13.28522	-6.35364	-7.45235	-1.11379	1.60778
$X_{\delta FRCS}$	ft/sec²	0.	0.	0.	0.	0.	0.	0.	0.
$X_{\delta ARCS}$	ft/sec²	0.	0.	0.	0.	0.	0.	0.	0.
Z_u	1/sec	-.16198	-.11129	-.10514	-.11441	-.09038	-.54034	-.13292	-.12276
Z_h	1/sec²	0.	0.	0.	0.	0.	0.	0.	0.
Z_α	ft/sec²	-293.23650	-664.16092	-967.70978	-1358.98241	-1920.19149	-2068.19315	-280.81606	-446.04434
Z_δ	ft/sec	-2.52272	-3.13436	-3.92704	-4.95218	-6.48011	-8.00595	1.55719	-1.95598
Z_q	ft/sec	-3.31355	-4.93993	-6.13200	-7.60479	-9.42146	-12.34684	-2.44495	-3.04464
$Z_{\delta H}$	ft/sec²	-40.34245	-87.17613	-136.65291	-200.50263	-274.67187	-323.67912	-40.24201	-61.33005
$Z_{\delta FRCS}$	ft/sec²	0.	0.	0.	0.	0.	0.	0.	0.
$Z_{\delta ARCS}$	ft/sec²	0.	0.	0.	0.	0.	0.	0.	0.
M_u	1/(ft-sec)	-.00120	-.00210	-.00183	-.00205	.00494	-.02454	-.00063	-.00114
M_h	1/(ft-sec²)	0.	0.	0.	0.	0.	0.	0.	0.
M_α	1/sec²	-5.53105	-12.40205	-18.41757	-26.78181	-33.65649	-34.63583	-6.83118	-7.97343
M_δ	1/sec	-.79807	-.98870	-1.24190	-1.56211	-2.04408	-2.52539	-.49120	-.61699
M_q	1/sec²	-1.11397	-1.63718	-2.03493	-2.51475	-3.10702	-3.72987	-.81513	-1.01132
$M_{\delta H}$	1/sec²	-12.69197	-27.35129	-42.89421	-62.93145	-86.19300	-101.56277	-12.62178	-19.23422
$M_{\delta FRCS}$	1/sec²	0.	0.	0.	0.	0.	0.	0.	0.
$M_{\delta ARCS}$	1/sec²	0.	0.	0.	0.	0.	0.	0.	0.

FIGURE 4.2-5 (CONTINUED)
LONGITUDINAL STABILITY DERIVATIVES
FULL FLIGHT ENVELOPE

FLIGHT CONDITION NUMBER

PARAMETER	UNITS	9	10	11	12	13	14	15	16
$Y_{\delta A}$	ft/sec^2	-8.38782	-9.77950	-13.90222	-18.74829	-24.35766	-27.95595	-3.88108	-6.64189
$Y_{\delta RRCS}$	ft/sec^2	0.	0.	0.	0.	0.	0.	0.	0.
$Y_{\delta R}$	ft/sec^2	13.23065	22.97510	33.08414	44.94291	58.73985	64.33045	10.40216	15.27221
$Y_{\delta YRCS}$	ft/sec^2	0.	0.	0.	0.	0.	0.	0.	0.
Y_β	ft/sec^2	-87.54961	-190.32207	-281.5168	-389.30816	-521.48015	-601.78432	-90.77561	-130.94543
$Y_{\dot\beta}$	ft/sec	0.	0.	0.	0.	.	0.	0.	0.
Y_p	ft/sec	.01570	.04910	.03733	.02551	.01752	.05095	.06076	.04764
Y_r	ft/sec	.10527	1.19963	1.42910	1.68731	1.94197	2.08835	.58124	.7053
$L_{\delta A}$	$1/sec^2$	27.23319	58.25566	83.68773	117.32015	162.62642	155.83428	26.72374	38.74602
$L_{\delta RRCS}$	$1/sec^2$	0.	0.	0.	0.	0.	0.	0.	0.
$L_{\delta R}$	$1/sec^2$	1.42398	3.68985	5.98119	8.60964	11.35212	11.94500	.90248	1.91964
$L_{\delta YRCS}$	$1/sec^2$	0.	0.	0.	0.	0.	0.	0.	0.
L_β	$1/sec^2$	-5.25868	-6.35429	-7.19123	-9.14053	-11.32757	-17.00421	-6.23711	-7.46459
$L_{\dot\beta}$	$1/sec$	0.	0.	0.	0.	0.	0.	0.	0.
L_p	$1/sec$	-2.16658	-3.72285	-4.55389	-5.35173	-6.21345	-6.68548	-1.83270	-2.25142
L_r	$1/sec$	.65476	1.50598	1.71879	1.94833	2.21937	2.58897	.98331	1.04095
$N_{\delta A}$	$1/sec^2$	1.46485	2.42233	3.94635	5.55190	6.79014	6.53071	.49636	1.25290
$N_{\delta RRCS}$	$1/sec^2$	0.	0.	0.	0.	0.	0.	0.	0.
$N_{\delta R}$	$1/sec^2$	-3.17451	-6.31819	-9.10400	-12.40000	-16.20340	-17.81851	-2.92014	-4.19877
$N_{\delta YRCS}$	$1/sec^2$	0.	0.	0.	0.	0.	0.	0.	0.
N_β	$1/sec^2$	5.41953	9.88420	14.82169	19.26549	25.09204	28.07313	4.48709	6.48874
$N_{\dot\beta}$	$1/sec$	0.	0.	0.	0.	0.	0.	0.	0.
N_p	$1/sec$	-.05381	-.04749	-.01881	.01133	.03604	-.01482	-.08519	-.06454
N_r	$1/sec$	-.44666	-.81175	-.98070	1.49929	-1.36987	-1.51394	-.40788	-.51084

FIGURE 4.2-5 (CONTINUED)
LATERAL-DIRECTIONAL STABILITY DERIVATIVES
FULL FLIGHT ENVELOPE

PARAMETER	UNITS	FLIGHT CONDITION NUMBER							
		17	18	19		21	22	23	24
X_u	1/sec	-.01732	-.02571	-.05138	-.18022	-.01372	-.01150	-.02760	-.07967
X_h	1/sec²	0.	0.	0.	0.	0.	0.	0.	0.
X_α	ft/sec²	16.88811	14.51112	27.25814	19.56186	2.78060	2.00150	-2.17767	-12.37480
X_δ	ft/sec	0.	0.	0.	0.	0.	0.	0.	0.
X_q	ft/sec	-.00149	-.00375	-.00505	-.00554	.00401	.00177	.00096	.00093
$X_{\delta M}$	ft/sec²	-12.98431	-.27809	-3.34295	-2.84277	-.13476	1.01493	2.39186	3.53818
$X_{\delta FRCS}$	ft/sec²	0.	0.	0.	0.	0.	0.	0.	0.
$X_{\delta ARCS}$	ft/sec²	0.	0.	0.	0.	0.	0.	0.	0.
Z_u	1/sec	-.10558	-.10935	.03135	.14466	-.11531	-.12449	-.02484	.07280
Z_h	1/sec²	0.	0.	0.	0.	0.	0.	0.	0.
Z_α	ft/sec²	-632.17232	-886.70396	1069.65392	-1025.26027	-219.45170	-377.55834	-422.08194	-507.13206
Z_δ	ft/sec	-2.46031	-3.21941	-3.97747	-4.80104	-1.06447	-1.39290	-1.7208	-2.07721
Z_q	ft/sec	3.77700	-4.67935	-5.63805	-6.66924	-1.62531	-2.01829	-2.43569	-2.88029
$Z_{\delta M}$	ft/sec²	-90.84896	-126.79328	-149.45095	-169.99789	-36.85793	-51.21255	-59.35425	-68.14082
$Z_{\delta ARCS}$	ft/sec²	0.	0.	0.	0.	0.	0.	0.	0.
M_u	1/ft-sec	-.00101	.00326	.00729	.23006	-.00051	-.00206	-.00066	.09381
M_h	1/ft-sec²	0.	0.	0.	0.	0.	0.	0.	0.
M_α	1/sec²	-11.76623	-15.48462	15.30934	-25.35701	-2.11569	-7.77561	-10.2?	-16.63632
M_δ	1/sec	-.77608	-1.01553	-1.25465	-1.51443	-.33578	-.43938	-.5?	-.65523
M_q	1/sec	-1.24956	-1.54385	-1.85290	-2.18807	-.54232	-.56914	-.?	-.94766
$M_{\delta M}$	1/sec²	-28.52161	-39.77884	-46.89415	-53.33928	-11.55765	-16.06025	-18.61588	-21.36701
$M_{\delta FRCS}$	1/sec²	0.	0.	0.	0.	0.	0.	0.	0.
$M_{\delta ARCS}$	1/sec²	0.	0.	0.	0.	0.	0.	0.	0.

FIGURE 4.2-5 (CONTINUED)
LONGITUDINAL STABILITY DERIVATIVES
FULL FLIGHT ENVELOPE

FLIGHT CONDITION NUMBER

PARAMETER	UNITS	17	18	19	20	21	22	23	24
Y_{δ_A}	ft/sec^2	-8.8719	-11.44490	-12.85130	-14.42113	-2.57071	-4.56300	-5.40421	-6.04786
$Y_{\delta_{RRCS}}$	ft/sec^2	0.	0.	0.	0.	0.	0.	0.	0.
Y_{δ_R}	ft/sec^2	20.60025	26.70811	29.70356	32.64435	7.86393	10.28863	11.78334	13.18525
$Y_{\delta_{YRCS}}$	ft/sec^2	0.	0.	0.	0.	0.	0.	0.	0.
Y_β	ft/sec^2	-179.74464	-240.49603	-277.74802	-318.87950	-72.35457	-97.18220	-112.78448	-179.28623
$Y_{\dot\beta}$	ft/sec	0.	0.	0.	0.	0.	0.	0.	0.
Y_p	ft/sec	.03734	.02873	.02457	.02795	.04447	.03516	.03219	.03355
Y_r	ft/sec	.83582	.96287	1.03833	1.10915	.34760	.40768	.44358	.47277
L_{δ_A}	$1/sec^2$	54.4?657	75.46063	71.90217	65.88496	21.66515	30.47904	29.38761	27.22524
$L_{\delta_{RRCS}}$	$1/sec^2$	0.	0.	0.	0.	0.	0.	0.	0.
L_{δ_R}	$1/sec^2$	3.12722	4.39626	5.53999	6.49397	.46004	.88628	1.47834	1.99852
$L_{\delta_{YRCS}}$	$1/sec^2$	0.	0.	0.	0.	0.	0.	0.	0.
L_β	$1/sec^2$	-7.61590	-8.05987	-7.72829	-8.75784	-9.41778	-7.38613	-7.66419	-8.44445
$L_{\dot\beta}$	$1/sec$	0.	0.	0.	0.	0.	0.	0.	0.
L_p	$1/sec$	-2.65445	-3.08354	-3.32157	-3.56269	-1.12366	-1.31544	-1.42180	-1.52747
L_r	$1/sec$	1.12724	1.23201	1.28186	1.37970	.71641	.70262	.68323	.71841
N_{δ_A}	$1/sec^2$	2.06?78	2.78256	3.02561	3.11177	.23038	.72925	.91301	.99826
$N_{\delta_{RRCS}}$	$1/sec^2$	0.	0.	0.	0.	0.	0.	0.	0.
N_{δ_R}	$1/sec^2$	-5.71624	-7.47044	-8.22731	-8.98816	-2.25129	-2.97430	-3.27276	-3.52595
$N_{\delta_{YRCS}}$	$1/sec^2$	0.	0.	0.	0.	0.	0.	0.	0.
N_β	$1/sec^2$	8.86219	11.54549	12.96997	14.39774	3.06305	4.54186	5.18239	5.72878
$N_{\dot\beta}$	$1/sec$	0.	0.	0.	0.	0.	0.	0.	0.
N_p	$1/sec$	-.04199	-.02044	.00598	-.00516	-.06099	-.05058	-.04495	-.04536
N_r	$1/sec$	-.59680	-.67387	-.75215	-.83329	-.24042	-.28614	-.32251	-.36111

FIGURE 4.2-5 (CONTINUED)
LATERAL-DIRECTIONAL STABILITY DERIVATIVES
FULL FLIGHT ENVELOPE

5. VALIDATION OF THE MATHEMATICAL MODEL

5.1 BACKGROUND

The YAV-8B mathematical model is based on AV-8A and YAV-8B wind tunnel test and flight test results. The model has been periodically refined since the first AV-8A air-to-ground attack simulations at MCAIR in 1972. The development of the V/STOL model commenced in 1974 with the definition of an engineering simulation of a hover, short takeoff and landing and transition mode for the AV-8A. During this period the coordinate system used for hover and the jet induced velocity parameter (Veq) were developed. Subsequent studies added data to simulate ground effects. To help validate the AV-8A simulation, John Farley, Chief Test Pilot for Hawker-Siddley, flew the simulator in hover using the motion base simulator. During 1975, additional improvements were made to the model including new air-to-ground weapon delivery modes and displays, improved ship and land-based landing aids, and continued use of the model for air-to-air combat. All the changes were evaluated by the USMC using the flight simulation facilities. Between early 1972 and late 1975, there were 13 contractual AV-8A simulations. AV-8A modeling was refined throughout each of these programs based upon additional test data and engineering analyses. This simulation capability and experience permitted MCAIR to design and conduct a preliminary AV-8B Simulation Evaluation in June, 1975.

This evaluation utilized a previously-developed simulation of the AV-8A aircraft modified with AV-8B lift, drag and pitching moment characteristics. Following this evaluation, the AV-8B simulation was further modified to include wind tunnel-derived AV-8B aerodynamic and flight control characteristics in conjunction with AV-8B weight and balance, and propulsion characteristics. During October and December 1975, a second simulation was conducted to demonstrate flying qualities and performance improvements estimated for the AV-8B. Two experienced USMC AV-8A pilots participated in this simulation and their comments and evaluation contributed to improvements in the refined AV-8B model.

Simulator modeling of the prototype AV-8B (YAV-8B) began in 1977. During 1978, the simulation was used for V/STOL flying quality evaluations and for pilot familiarization of the flight envelope prior to first flight of the YAV-8B.

The YAV-8B simulation was used very effectively during the entire prototype flight test program in the following areas of activity:

o Pilot familiarization prior to the first flights

o Determination of control time histories and flight profiles for maximum performance VTO's and STO's

o Determination of handling qualities and pitch transients during landing approaches and transitions to and from wingborne and jetborne flight

o Simulated control failures

o Flight trajectories following simulated engine flame-outs

o Handling qualities in wingborne flight

The YAV-8B simulator proved to be representative of the aircraft and very useful during each of these activities.

Prior to the YAV-8B engine/inlet compatibility testing in 1980, flight trajectories and approach/landing techniques following a simulated engine flame-out (SFO) were developed and practiced on the simulator. Landing profiles, flap angle, and the nozzle/power setting needed to represent engine windmilling were developed. During actual flight SFO practice, pilots reported that the flight SFO's were very close to those experienced in the YAV-8B simulator. Also, the aircraft settings (idle power/40° nozzle) chosen to simulate engine out conditions were representative of the actual engine out characteristics.

The YAV-8B mathematical model is based on extensive flight test and wind tunnel test results. Figure 5.1-1 summarizes the flight test conditions flown. A total of 364 flights were flown prior to the start of a store separation flight test program in 1982. A summary of both aerodynamic and propulsion wind tunnel test programs is presented in Figure 5.1-2. The aerodynamic tests consisted of both powered and unpowered tests on a 15% scale and full scale models over the entire Mach range. They covered the jetborne, semi-jetborne and wingborne modes of flight in and out of ground effect. Over 6600 hours of tests are shown. A similar wind tunnel test program was performed on the YAV-8B inlet to provide a firm data base for the propulsion performance package. Approximately 2000 hours of wind tunnel testing are shown.

The YAV-8B aircraft is equipped with both a noseboom angle of attack (AOA) probe and a production angle of attack indicator. The relationship between the noseboom AOA and the production AOA, in units, is shown in Figure 5.1-3. Note that the data fairing

$$\alpha_{FRL} = \theta - \gamma = .864 \ \alpha_{PRODUCTION} + 1$$

was used exclusively in this report to compare flight test and predicted angle of attack. Previously published reports such as Reference 1 used production angle of attack exclusively. A similar situation exists with respect to the pitot static system position error corrections shown in Figure 5.1-4. Reference 1 used the estimated values while this report uses a fairing approximately halfway between the estimated and tower flyby results to compute calibrated airspeed.

ORIGINAL PAGE IS
OF POOR QUALITY.
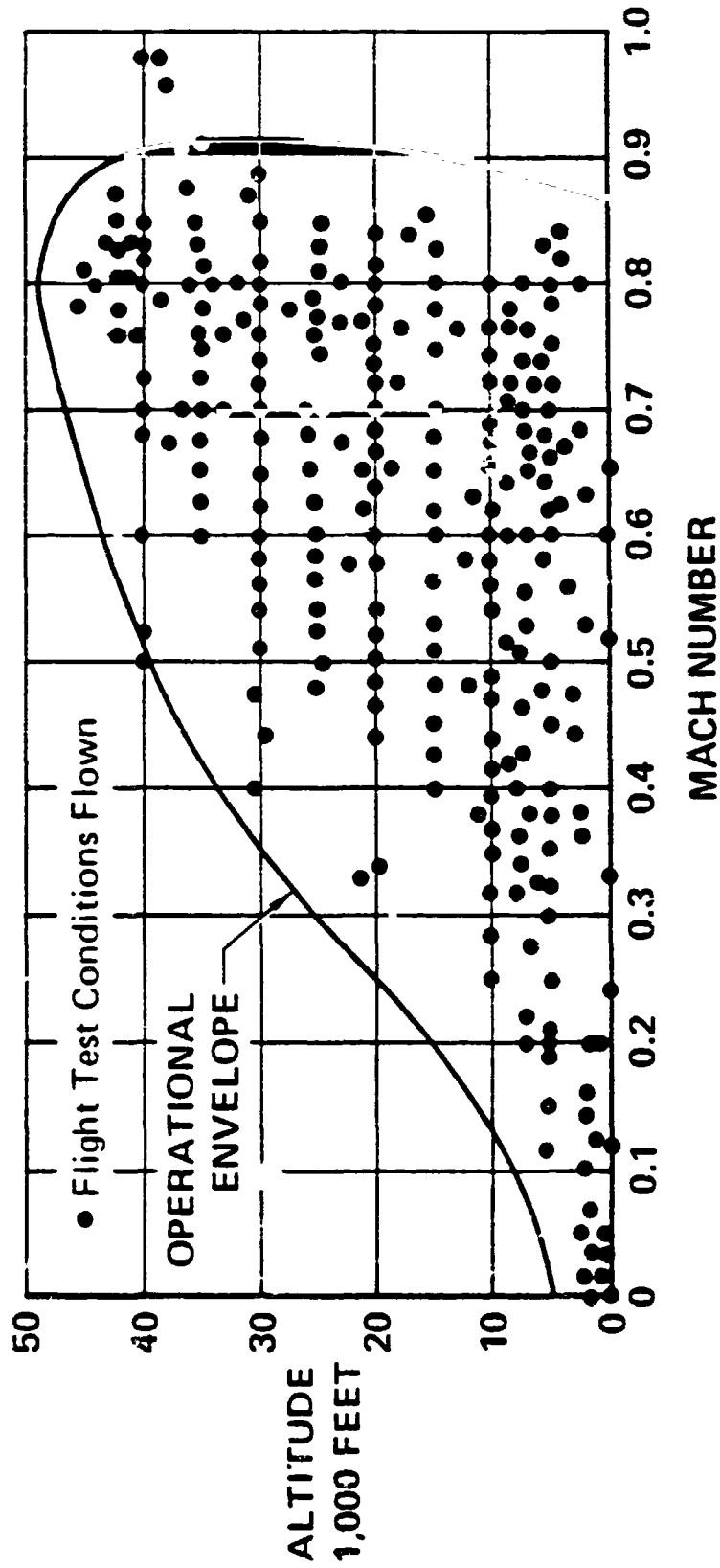
FIGURE 5.1-1
YAV-8B FLIGHT TEST ENVELOPE

DATE	MODEL	TUNNEL	MACH	RUNS	HOURS
Sept-Oct 73	AV-8A/AV-16A	AMES 11'	Transonic	475	276
Apr-Mar 74	AV-8A/AV-16A	ARA 9'x8'	Transonic	185	100
Aug-Oct 74	AV-8A	MSWT	Low Speed	516	583
Mar-Apr 74	YAV-8B	M/LSWT	Low Speed	590	645
June-July 75	YAV-8B	M/LSWT	Low Speed	455	542
June 75	YAV-8B	AMES 14'	Transonic	61	80
Aug-Oct 75	AV-8A	AMES 14'	Transonic	327	360
Oct 75	Inlet	MCAIR MFCF	Static	59	270
Nov 75	Inlet	MCAIR LSWT	Low Speed	116	164
Dec 75	Inlet	AMES 11'	Transonic	256	300
Dec 75-Jan 76	YAV-8B	AMES 11'	Transonic	269	252
Apr-May 76	AV-8A	MSWT	Low Speed	137	100
Aug-Sept 76	YAV-8B	AMES	Low Speed	144	316
Oct 76	Inlet	MCAIR MFCF	Static	34	172
Mar-Apr 77	AV-8A/YAV-8B	AMES 14'	Transonic	154	150
May-July 77	AV-8A/YAV-8B/AV-8B	M/LSWT	Low Speed	520	529
July 77	Inlet	AMES 11'	Transonic	317	272
Sept-Nov 77	AV-8A/YAV-8B	AMES 14'	Transonic	320	536
Feb-Mar 78	YAV-8B/AV-8B	M/LSWT	Low Speed	403	362
June 78	Inlet	MCAIR MFCF	Static	36	153
Oct 78	YAV-8B	AMES 14'	Transonic	140	160
Nov-Dec 78	AV-8C	MSWT	Low Speed	461	227
Jan-Feb 79	YAV-8B	AMES 14'	Transonic	305	161
Feb 79	YAV-8B	MSWT	Low Speed	81	50
Feb 79	Inlet	AMES 11'	Transonic	497	383
Feb-Mar 79	AV-8B	AMES 14'	Transonic	414	233
Mar 79	TAV-8B	AMES 14'	Transonic	225	184
Apr-May 79	TAV-8B/AV-8B/YAV-8B	LSWT	Low Speed	126	76
May 79	TAV-8B/AV-8B	MSWT	Low Speed	117	91
May 79	TAV-8B/AV-8B	LSWT	Low Speed	113	98
May 79	Inlet	AMES 11'	Transonic	213	228

TOTALS 8066 8053

FIGURE 5.1-2
YAV-8B RELATED WIND TUNNEL TESTS
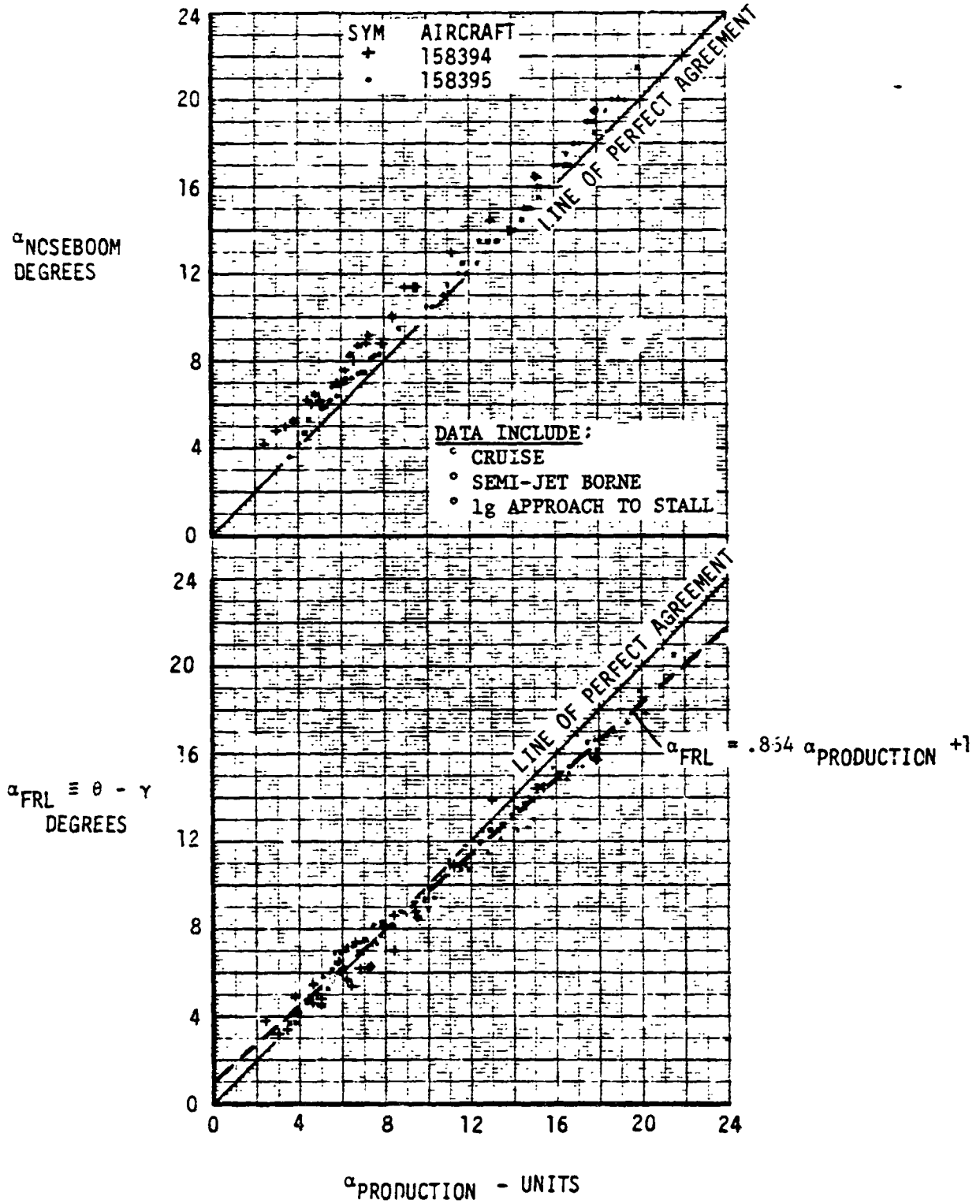
FIGURE 5.1-3
YAV-8B ANGLE OF ATTACK CALIBRATION

Tower Flyby Data
YAV-8B No. 1 Flight 42

Symbol	Gear	Nozzle	Flap
O	Up	Aft	5°
□	Down	VAR	VAR
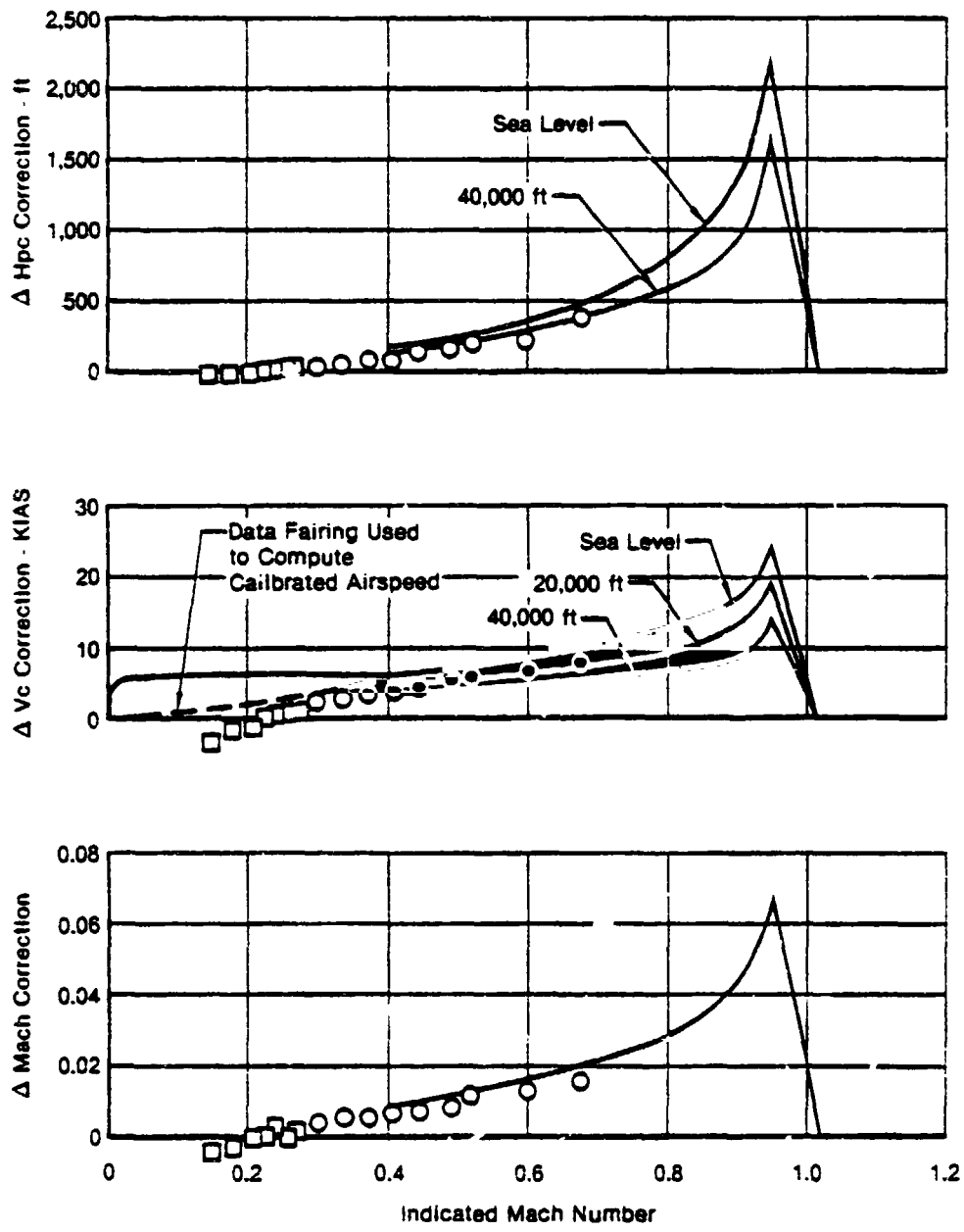
Note: Δ Corrections = True − Indicated

RP21-0982-47

FIGURE 5.1-4
YAV-8B PILOT STATIC SYSTEM ESTIMATED POSITION ERROR CORRECTIONS

The time history comparisons, presented in this section between flight
test results and predictions from the YAV-8B mathematical models, were
done using the weight and balance data presented in Section 2.3 adjusted to
the actual weight and c.g. location defined by the flight data. These weight
and balance data are presented in Figure 5.1-5.

5.2 JET BORNE AND SEMI-JET BORNE VALIDATION

A time history comparison of predicted and flight test results during
hover stability tests is presented in **Figures** 5.2-1 to 5.2-3. The predicted
include both nonlinear and linear mathematical models defined previously.

The predicted landing approach characteristics of Figure 5.2-4 show
good correlation with flight test results. The predicted data were obtained
by fixing nozzle angle and angle of attack and iterating on tail deflection,
fan speed and airspeed until a 3 degree of freedom wings level trim was
obtained.

A comparison of angle of attack stability for flap settings of 25° and
61.7° (STO) is presented in Figures 5.2-5 and 5.2-6. The predicted longitudinal
stability and trim tail deflections are representative of the actual aircraft.

Longitudinal dynamics in Semi-Jet Borne flight are compared in Figure
5.2-7 for both the nonlinear and linear mathematical models.

The predicted Semi-Jet Borne SAS on steady heading sideslip character-
istics shown in Figure 5.2-8 were obtained by using stability derivatives
and a three degree of freedom approximation at the flight test condition.

The predicted Semi-Jet Borne SAS on Dutch Roll characteristics are
compared to flight test data and the requirements of MIL-F-83300 in Figure
5.2-9. The Level 1 requirements are satisfied. A time history comparison
of Dutch Roll characteristics is presented in Figure 5.2-10.

5.3 WINGBORNE VALIDATION

A comparison of horizontal tail and angle of attack to trim at medium
and high altitudes is presented in Figure 5.3-1. The predicted data were
computed using the same Mach number, nozzle angle and fan speed as the flight
test data.

The predicted and flight test short period response characteristics are
compared in Figure 5.3-2 to 5.3-3. The short period frequency of Figure
5.3-2 shows the characteristics are within the Level 1 boundary. The damping

FIGURE NUMBER	GROSS WEIGHT LB	INERTIAS, SLUG-FT^2				CENTER OF GRAVITY, IN		
		Ixx	Iyy	Izz	Ixz	FUSELAGE STATION	BUTT-LINE	WATER LINE
5.2-1	16450	6610	30997	34814	1382	345.28	0	95.08
5.2-2	16450	6610	30997	34814	1382	345.28	0	95.08
5.2-3	14690	6300	28666	32313	1115	343.11	0	94.20
5.2-7	20200	9884	32239	39419	1634	349.9	0	97.7
5.2-1C	17070	7008	31249	35433	1393	346.67	0	96.8
5.3-3	16810	6291	31308	35436	1368	344.25	0	96.7
5.3-7	19230	9405	32089	39047	1510	349.11	0	97.7

FIGURE 5.1-5

YAV-8B INERTIA AND C.G. DATA FOR PREDICTED TIME HISTORIES
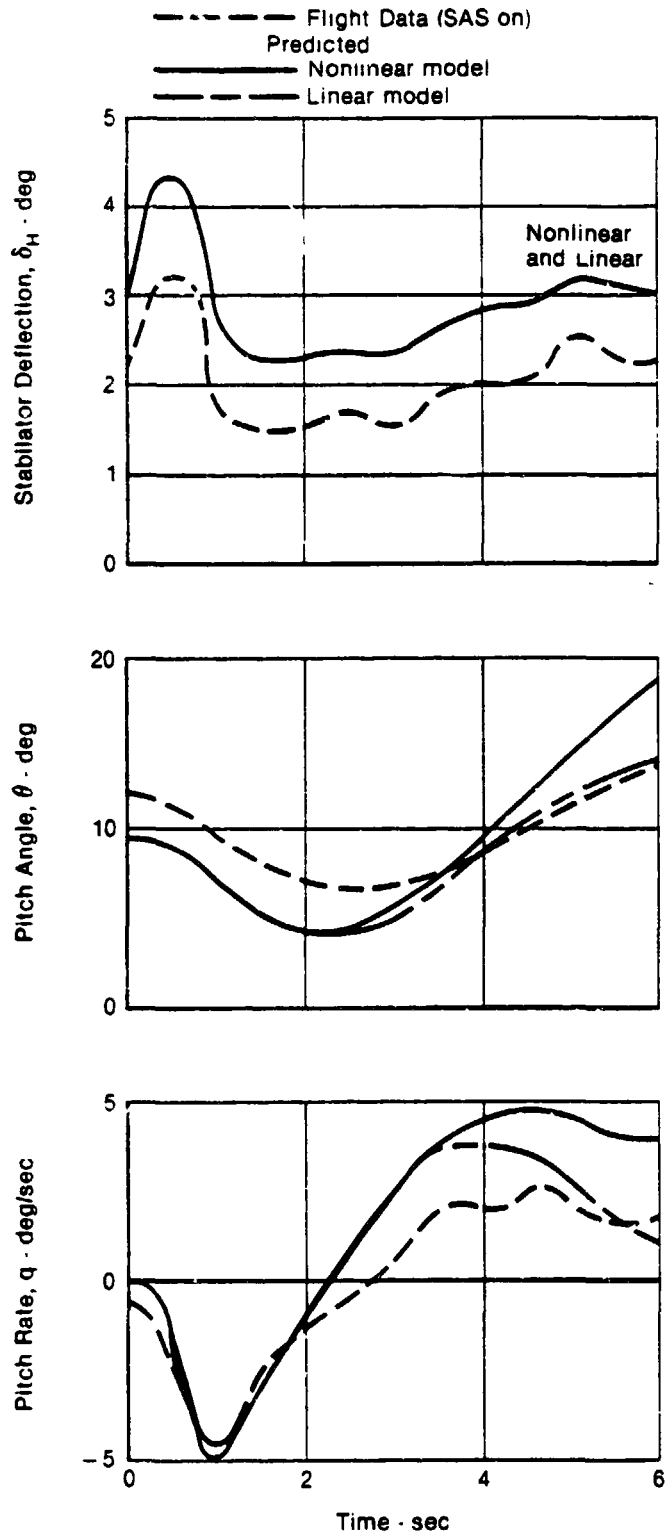
FIGURE 5.2-1
YAV-8B RESPONSE TO LONGITUDINAL STICK RAP IN HOVER
Gross Weight = 16,450 lb $N_F = 96\%$ $\theta_J = 79°$ $\delta_F = 61.7°$

Flight Data (SAS on)
Predicted
Nonlinear model
Linear model
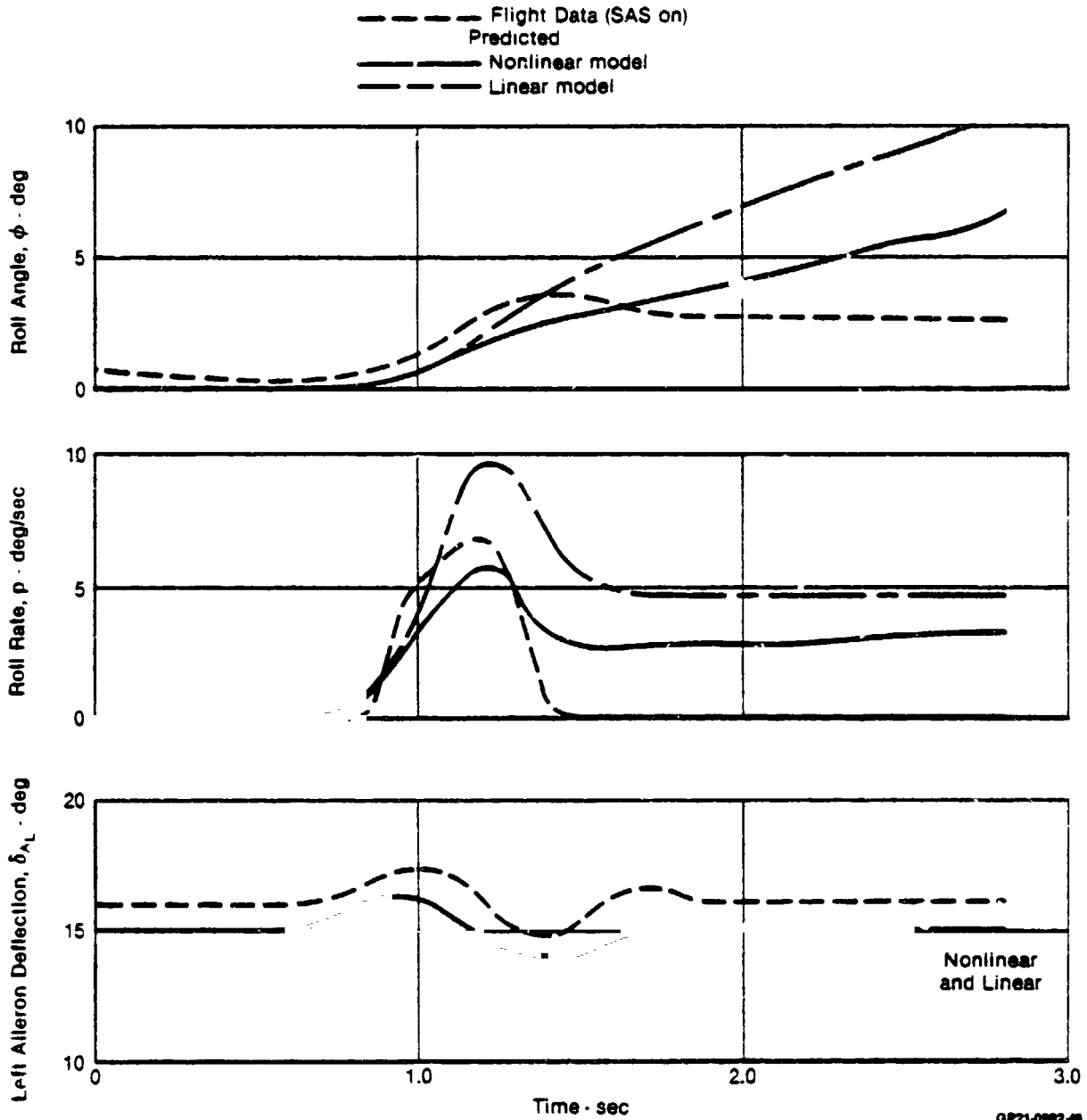
FIGURE 5.2-2
YAV-8B RESPONSE TO LATERAL STICK RAP IN HOVER
Gross Weight = 16,450 lb $N_F = 96\%$ $\theta_J = 79°$ $\delta_F = 61.7°$
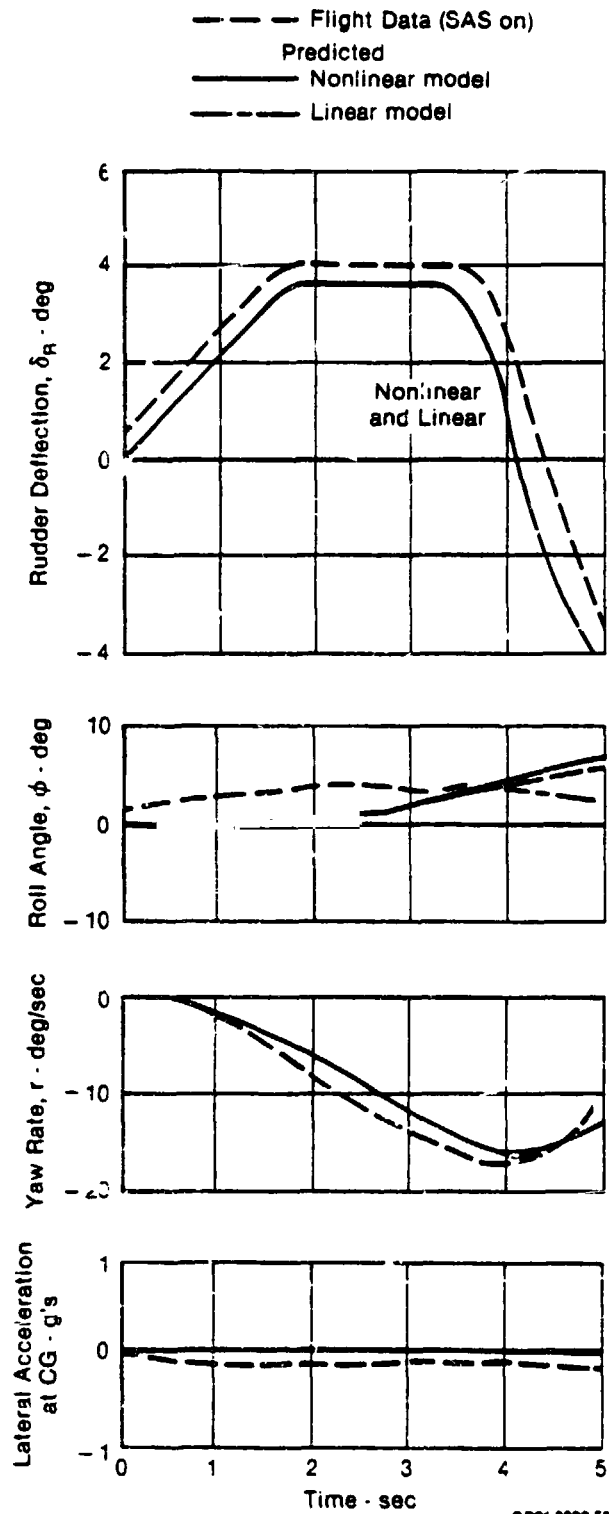
FIGURE 5.2-3
YAV-8B RESPONSE TO PEDAL INPUT IN HOVER
Gross Weight = 14,690 lb N_F = 92% θ_J = 79° δ_F = 61.7°
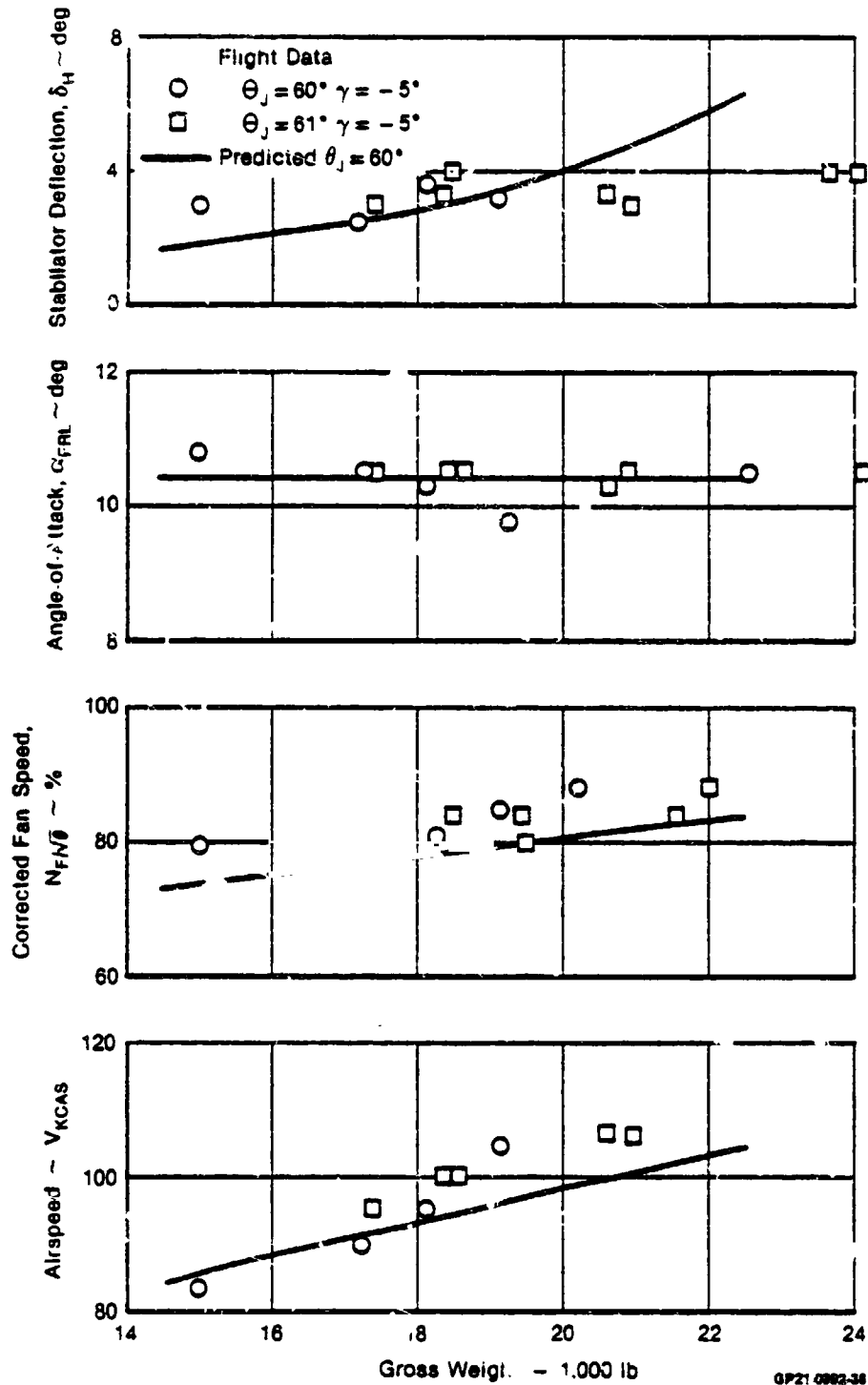
FIGURE 5.1-4
YAV-8B LANDING APPROACH CHARACTERISTICS
STOL Flap, Ailerons Drooped 15°

CRIGINAL
OF POOR QUALITY

Flight Data

Sym	θ_J (deg)	C.G. (%$\bar{c}$)	$N_F/\sqrt{\theta}$ (%)	V_{KCAS}	δ_F (deg)	'titude (ft)	T(°F)
□	52	12.2	79	100	25	1,600	64
△	63	13.2	66	130	25	3,000	59
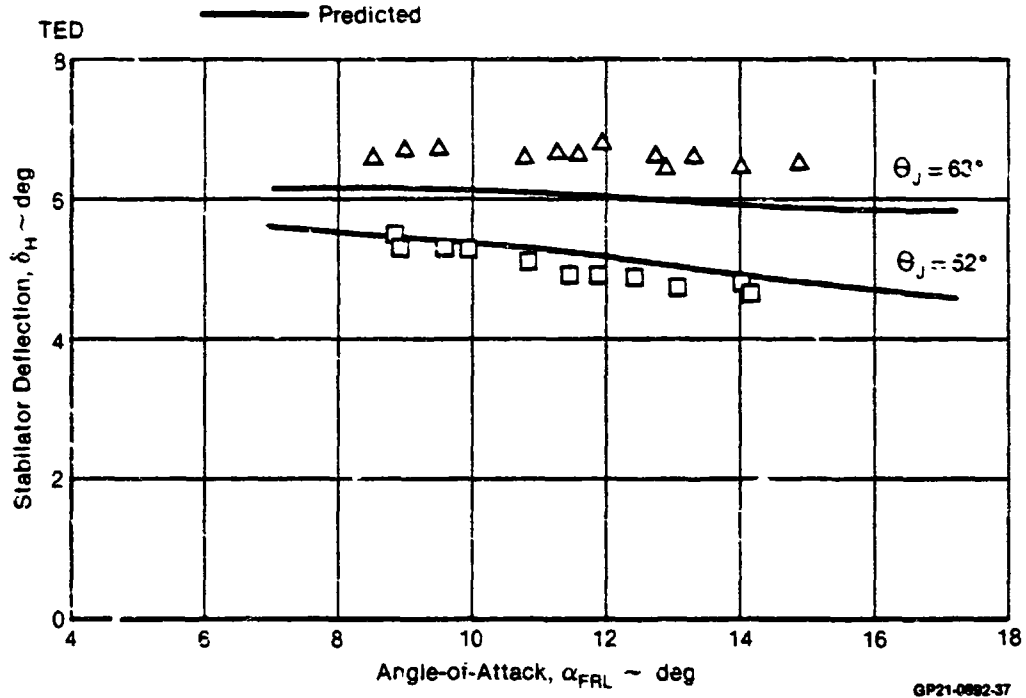
FIGURE 5.2-5
YAV-8B SEMI-JET BORNE ANGLE-OF-ATTACK STABILITY
25° Flap Ailerons Not Drooped

GP21-0692-37

— — — Flight Data

θ_J (deg)	C.G. (%c̄)	$N_F/\sqrt{\theta}$ (%)	V_{KCAS}	δ_F (deg)	Altitude (ft)	T(°F)
70	10.6	92	95	59	3500	45.0
50	10.3	84	130	61	3200	58.0
39	6.9	77	140	47	4000	61.0

— — — Predicted
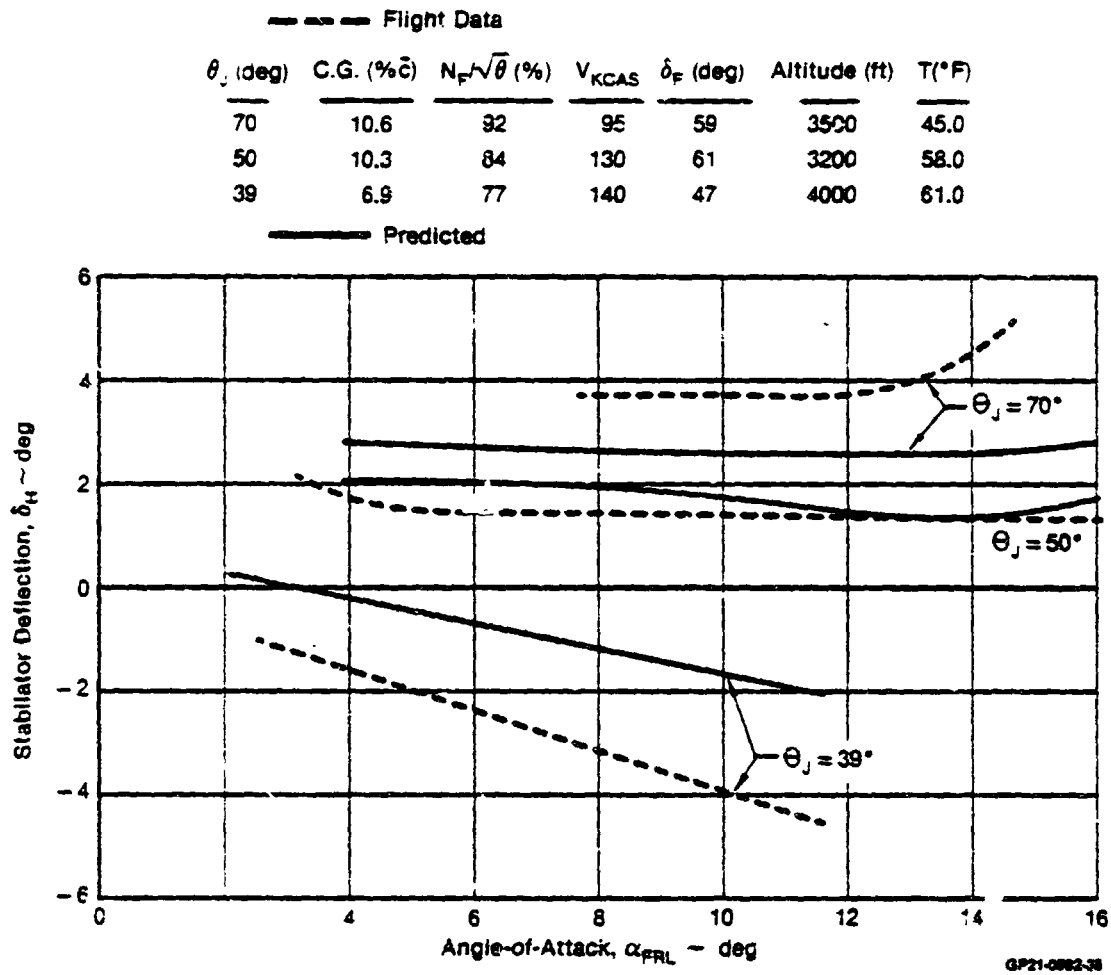
FIGURE 5.2-6
YAV-8B SEMI-JET BORNE ANGLE-OF-ATTACK STABILITY
STO Flap   Ailerons Drooped 15°
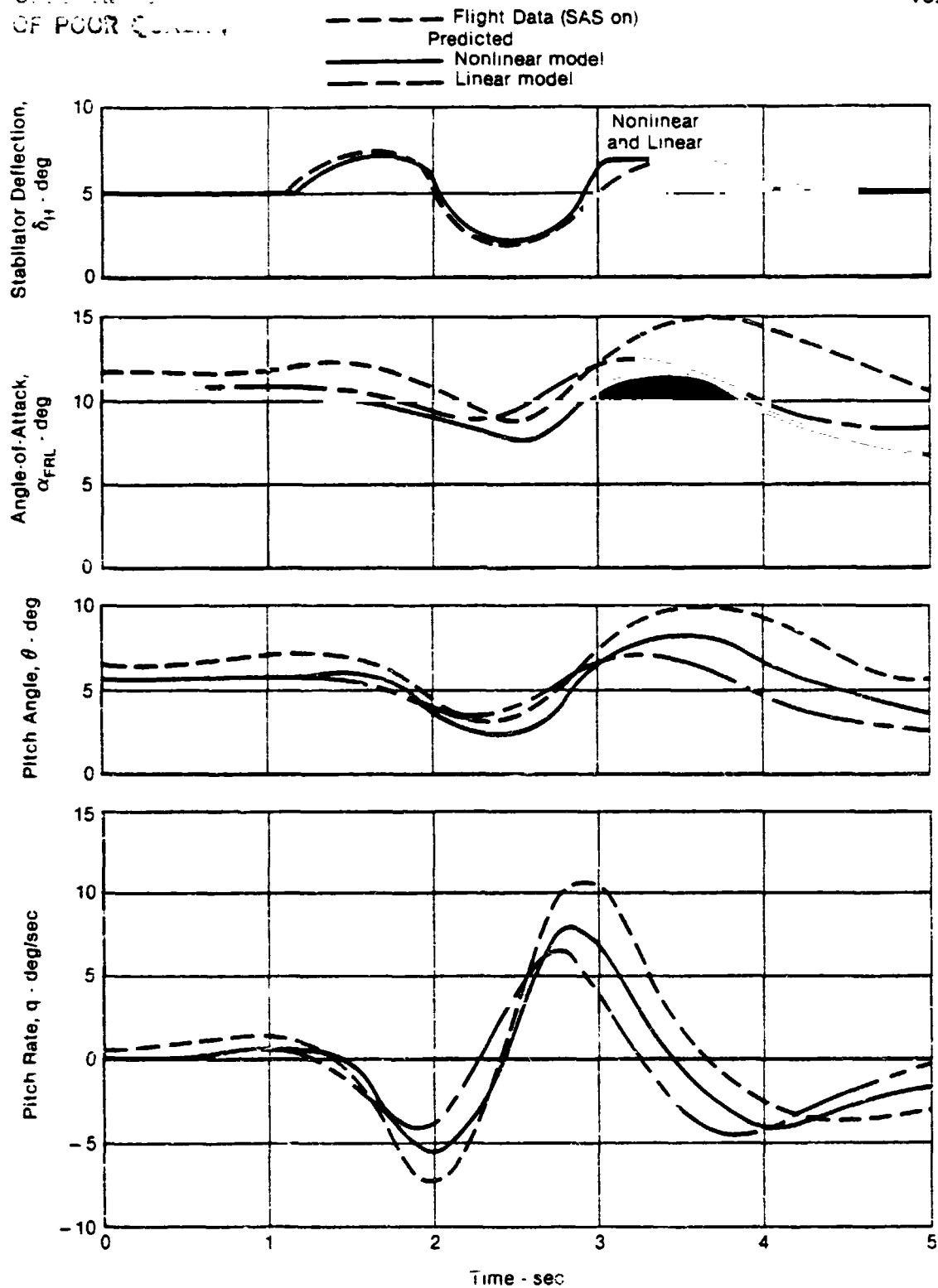
FIGURE 5.2-7

YAV-8B RESPONSE TO LONGITUDINAL DOUBLET IN SEMI-JET BORNE FLIGHT

Gross Weight = 20,200 lb $N_F = 73\%$ $\theta_J = 45°$ $\delta_F = 25°$

Mach 0.22   Altitude = 2,800 ft

GP21-0492-51

Flight Data

Sym	GW (lb)	α_{FRL} (deg)	θ_J (deg)	δ_F (deg)	N_F (%)
○	15,940	7.5	74	61	88
□	17,550	7.7	56	61	87
◇	20,930	8.6	37	41	74
——— Predicted					

FIGURE 5.2-8
YAV-8B V/STOL STEADY HEADING SIDESLIP CHARACTERISTICS
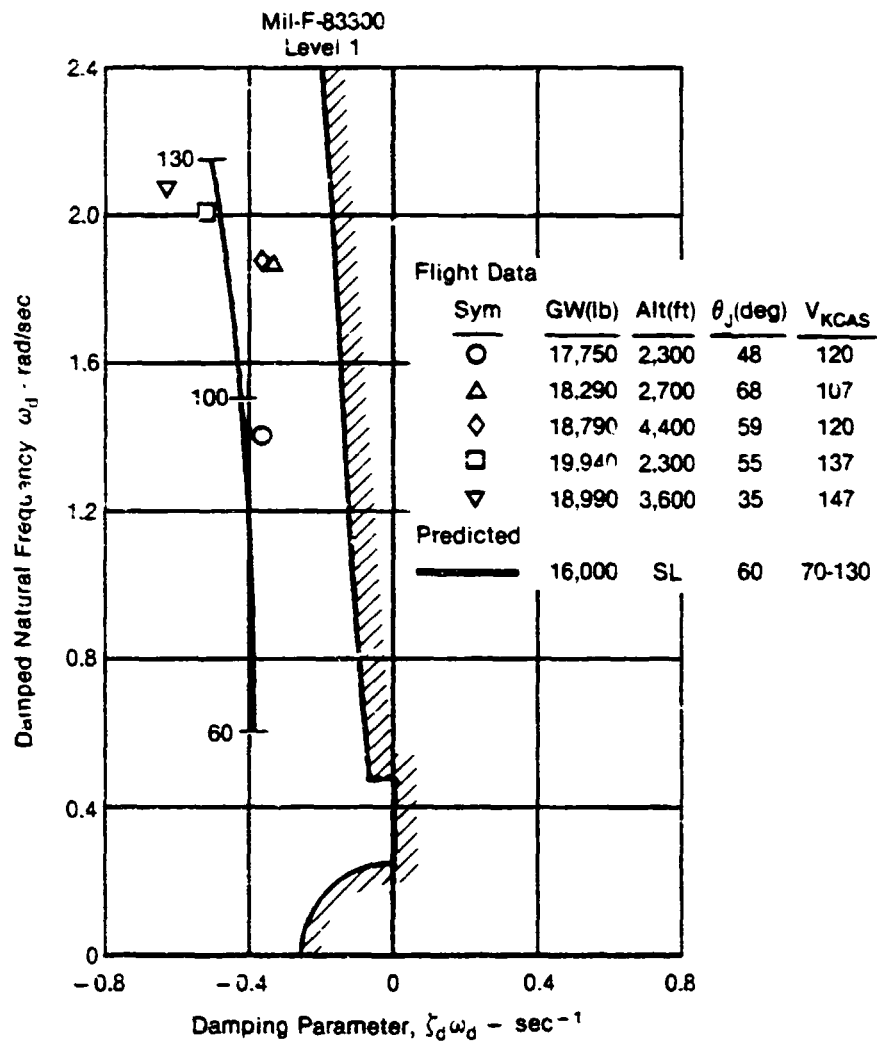
FIGURE 5.2-9
YAV-8B SAS ON DUTCH ROLL CHARACTERISTICS IN SEMIJETBORNE FLIGHT
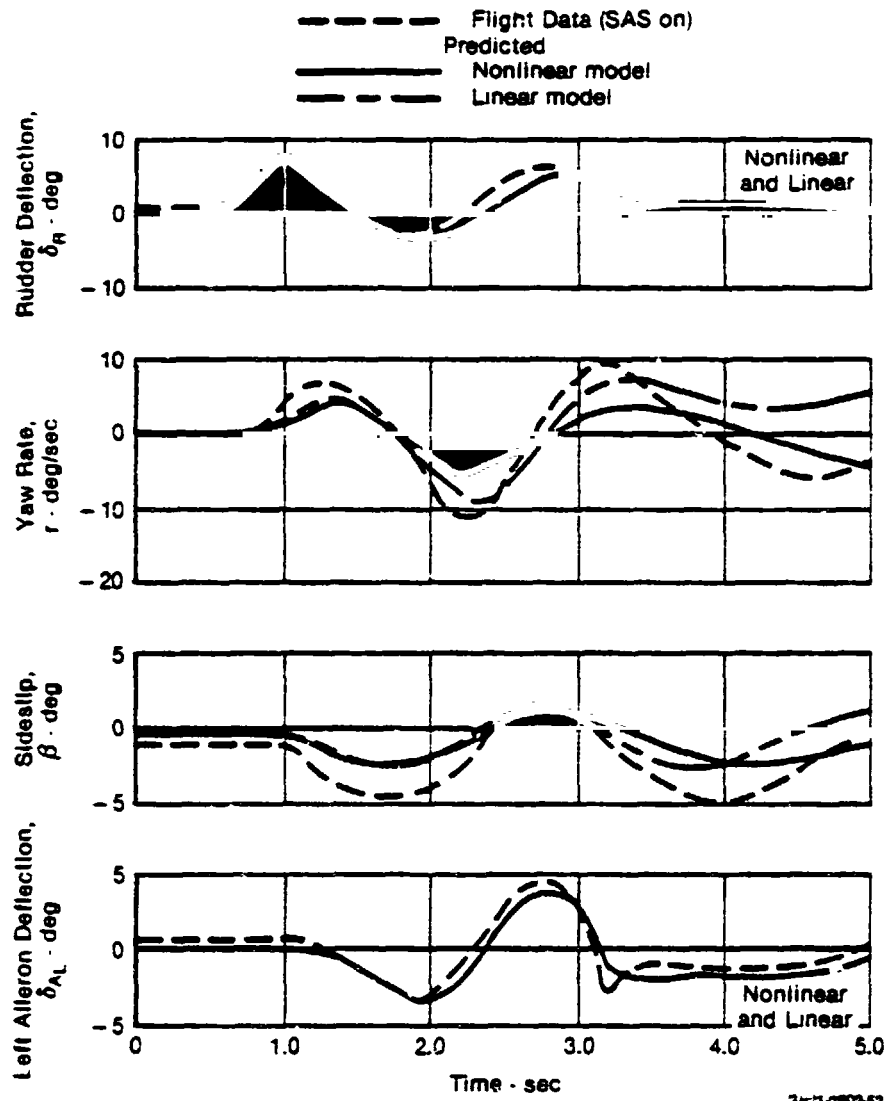
FIGURE 5.2-10
YAV-8B RESPONSE TO RUDDER IN SEMIJET BORNE FLIGHT
Gross Weight = 17,070 lb N_F = 88% θ_J = 61° δ_F = 25°
Mach 0.24 Altitude = 4,700 ft
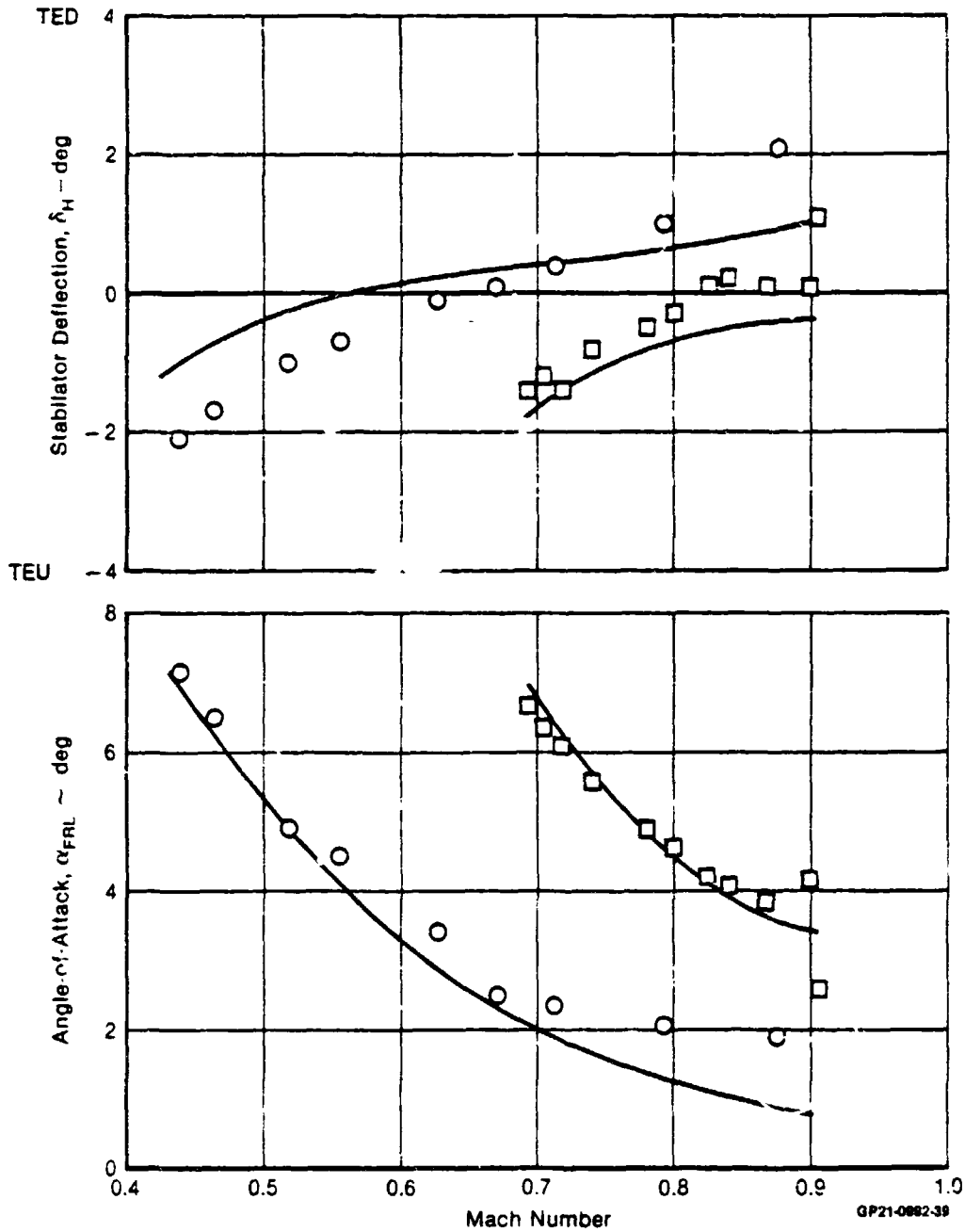
FIGURE 5.3-1
YAV-8B WINGBORNE TRIM CHARACTERISTICS
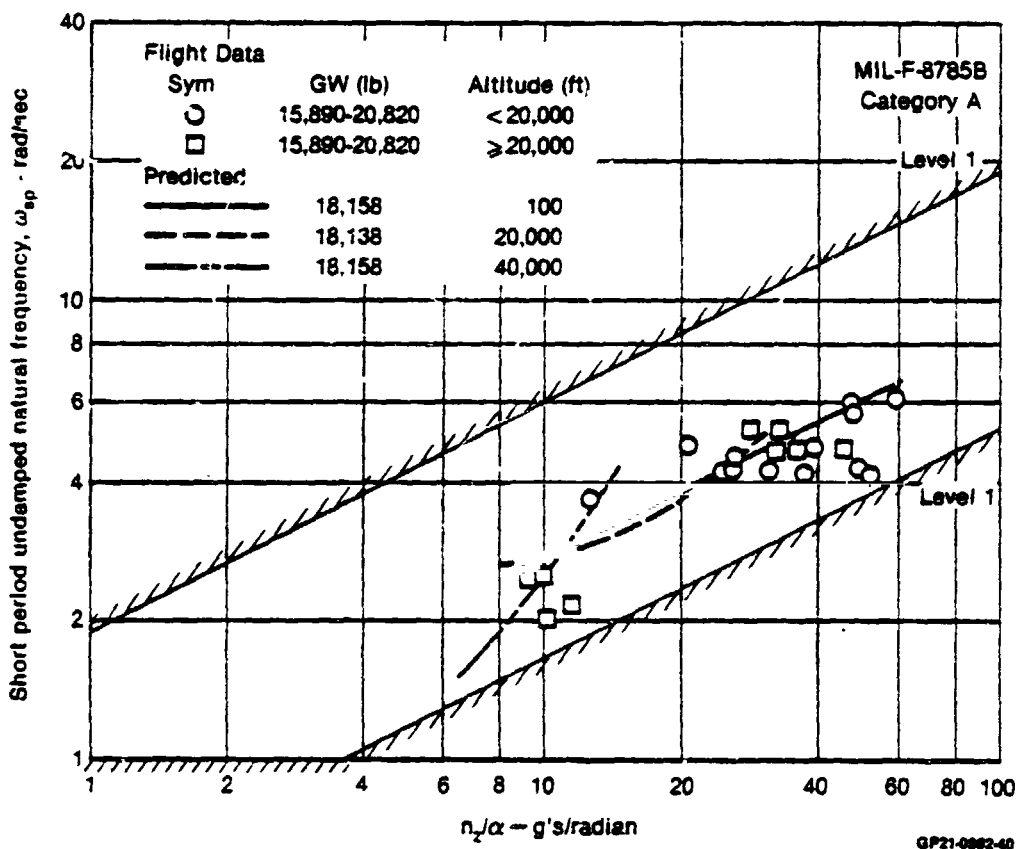
FIGURE 5.3-2
YAV-8B SHORT PERIOD FREQUENCY REQUIREMENTS
Wingborne Flight

ratios of Figure 5.3-3 are essentially Level 1 below 20,000 feet
and Level 2 above 20,000 feet. However, MIL-F-8785B states that above 20,000
feet the Level 1 damping requirements may be relaxed to the Level 2 require-
ments. The longitudinal maneuvering characteristics are compared for the
symmetrical pullup shown in Figure 5.3-4. The predicted characteristics
correlate well with the flight data.

Figure 5.3-5 summarizes roll rate capability and maximum sideslip angles
generated during 1g rolls. The flight data are primarily for low to moderate
altitudes. The predicted characteristics were computed for 7500 feet altitude
using a nominal gross weight, and nominal command input time history.

The comparison of steady heading sideslip characteristics presented in
Figure 5.3-6 indicate the predicted static lateral directional stability
and control characteristics are very representative of the actual aircraft.

The predicted Dutch Roll characteristics are compared to flight test data
and the requirements of MIL-F-8785B in Figure 5.3-7. The YAV-8B meets the
Level 1 requirements below 20,000 feet and Level 2 above 20,000 feet. A
time history comparison of Dutch Roll Characteristics is presented in
Figure 5.3-8. The predicted characteristics compare well with flight test
results.

5.4 PROPULSION SYSTEM VALIDATION

The validity of the propulsion system model is demonstrated by the
comparison of flight data and predicted performance in Figures 5.4-1 and
5.4-2. These flight data include wet and dry Vertical Takeoffs (VTO's) with
stick neutral (minimum RCS reaction control system bleed), hence these cases
are for a singular demand condition. The predicted engine acceleration
characteristics show similar slopes as that of the flight data. Absolute values
will not necessarily agree due to the following:

o Engine to Engine Variation: The propulsion system model represents
  an "average" YF402-RR-404 engine. Actual engines used in the YAV-8B
  exhibited higher Exhaust Gas Temperatures and higher fuel flow at
  steady state conditions than an "average" engine.

o Reaction Control Bleed: Bleed, which affects all engine parameters
  shown, is a function of control requirements which were not
  included in these cases.

o Fuel Control Unit (FCU) Variations: Engine acceleration character-
  istics are influenced by FCU settings which differ with each
  engine/FCU combination.

The stepwise characteristics of the measured fuel flow is due to the
low sampling rate of the flight data system and does not represent the true
schedule actually used by the engine/FCU.

Flight Data

Sym	GW (lb)	Altitude (ft)
O	15,890-20,820	1,800-8,700
□	17,030-20,140	20,790-20,940
△	18,470 - 19,950	35,100 - 37,750

Predicted

	18,158	100, 20,000, 40,000
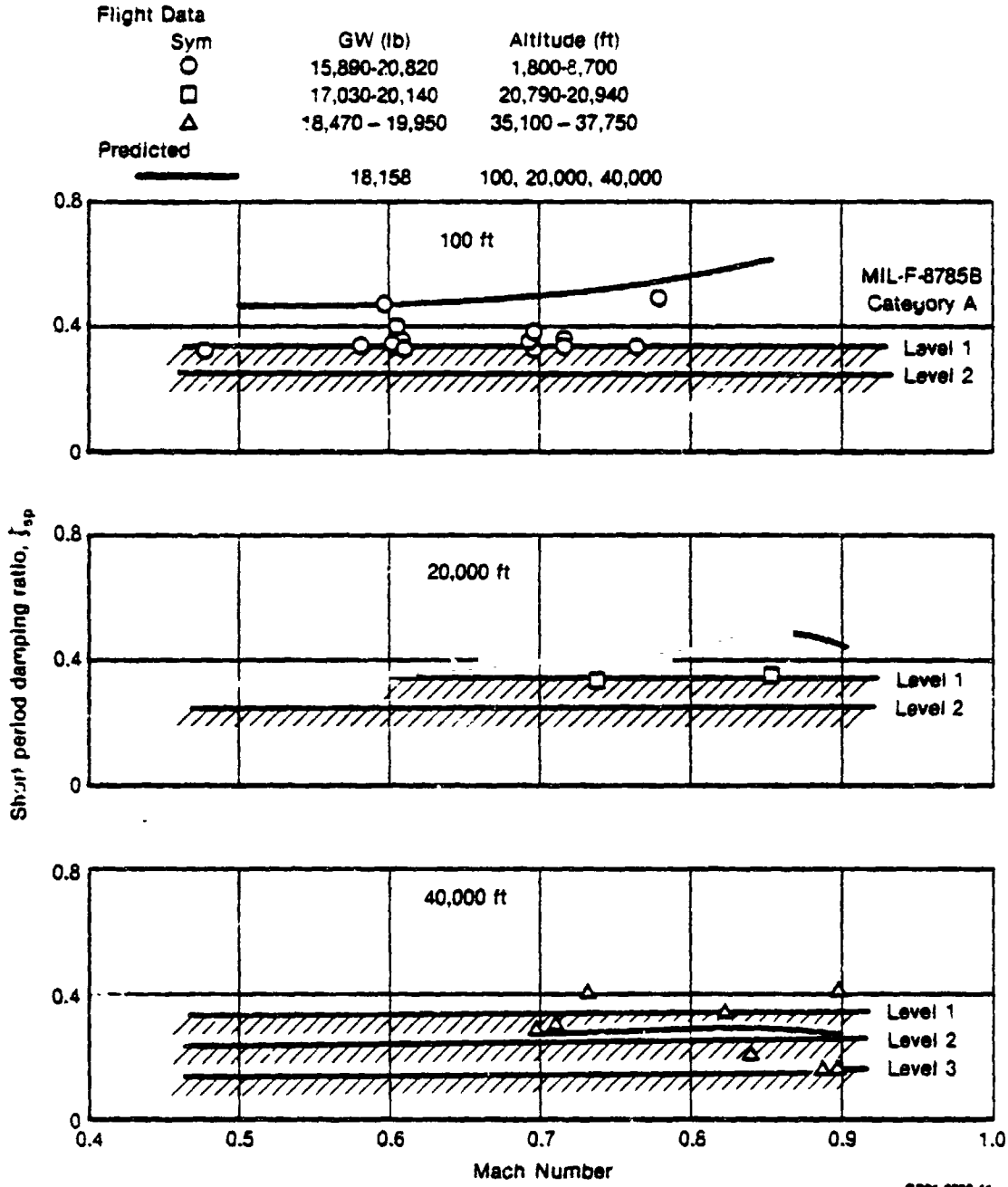
FIGURE 5.3-3
YAV-8B SHORT PERIOD MODE DAMPING RATIO
Wingborne Flight
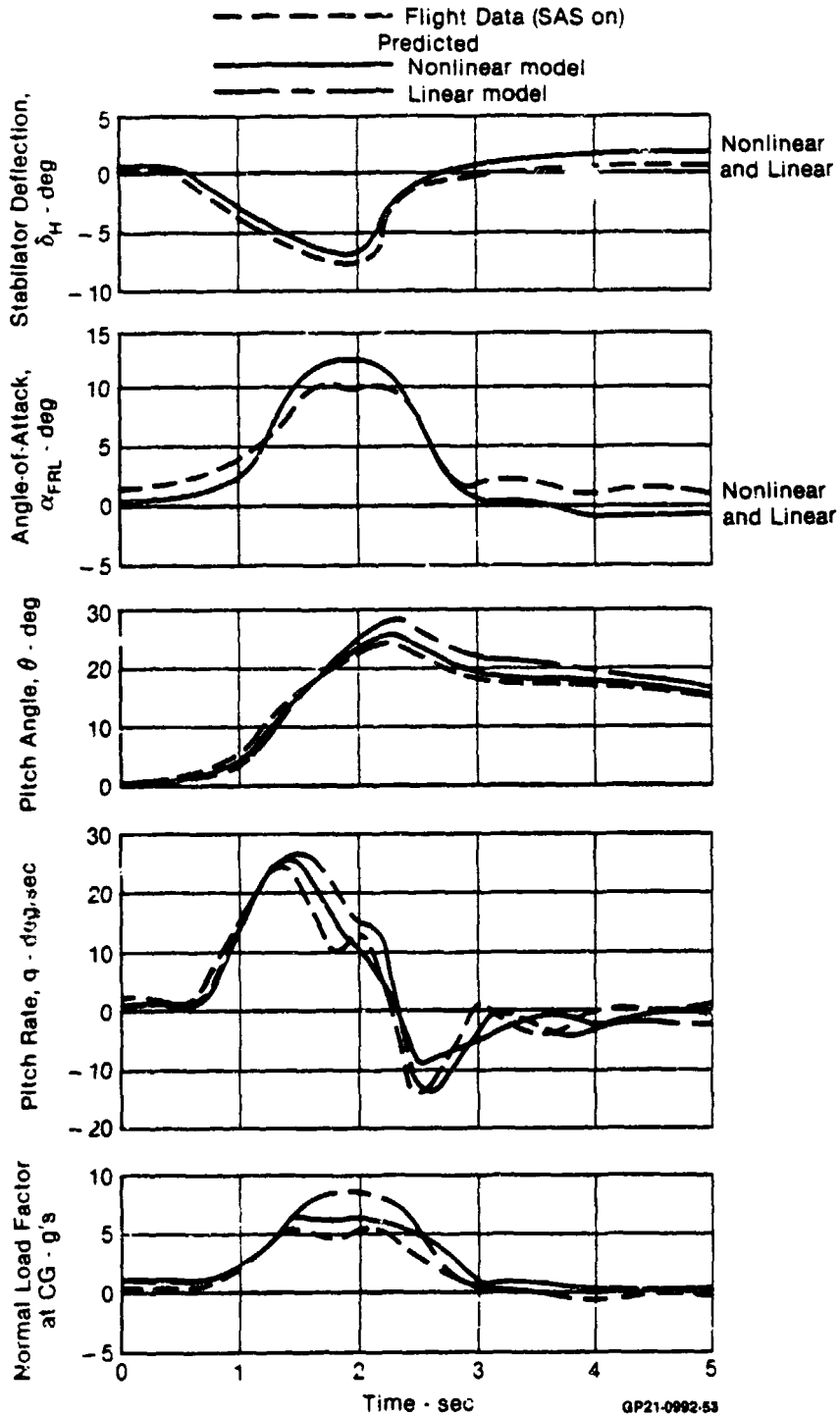
FIGURE 5.3-4
YAV-8B PULL-UP IN WINGBORNE FLIGHT
Gross Weight = 16,810 lb N_F = 80% θ_J = 0° δ_F = 5°
Mach 0.74   Altitude = 7,000 ft

Flight Data
Symbol   **Altitude**

○ 3,000 ft - 10,000 ft except as noted
□ 25° flap
Predicted
  7,500 ft, 18,158 lb
———————— Nonlinear model
— — ———— Linear model
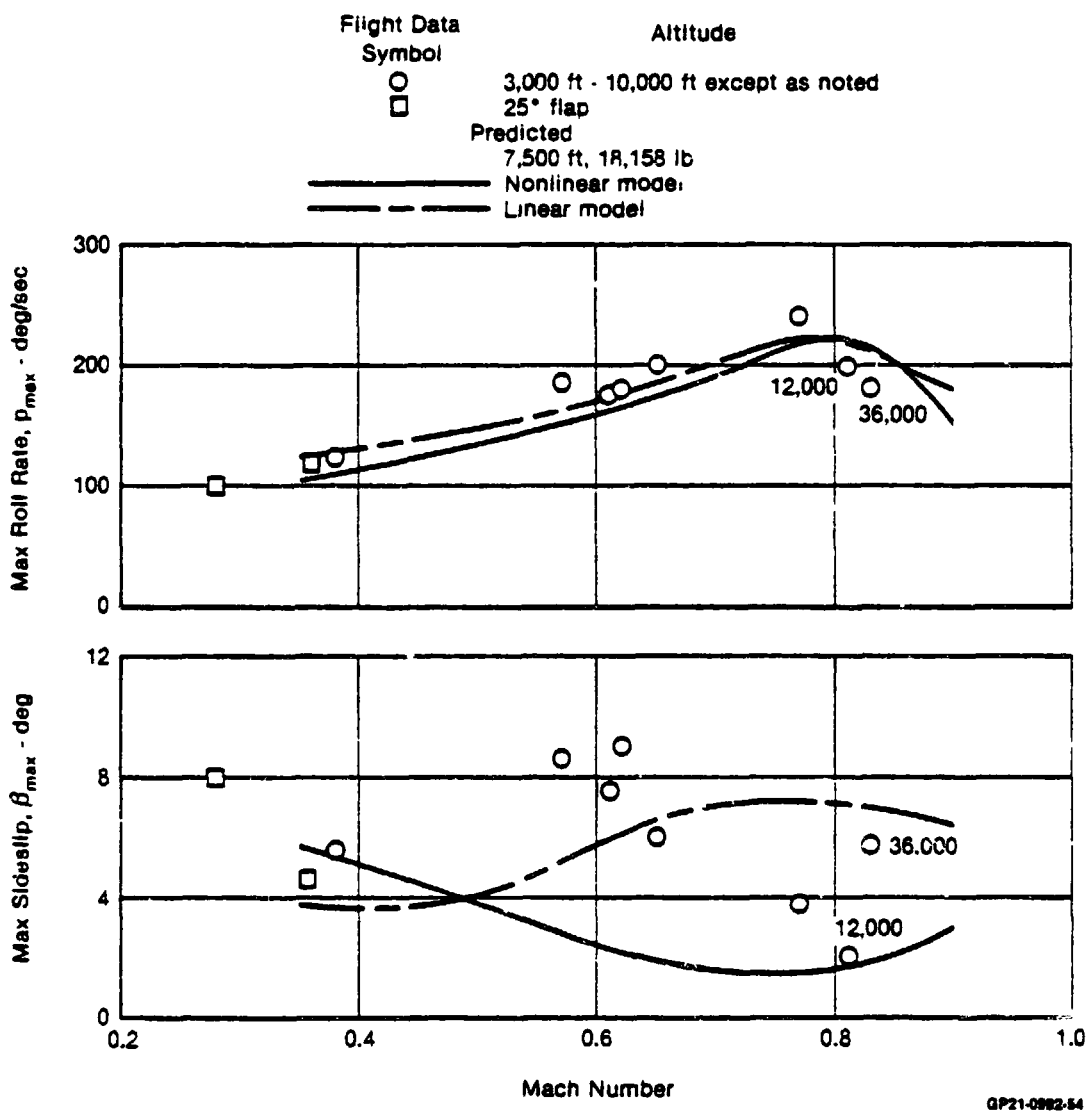
FIGURE 5.3-5
YAV-8B WINGBORNE 1 g ROLL PERFORMANCE
3.2 in. Lateral Stick Input

GP21-0992-54
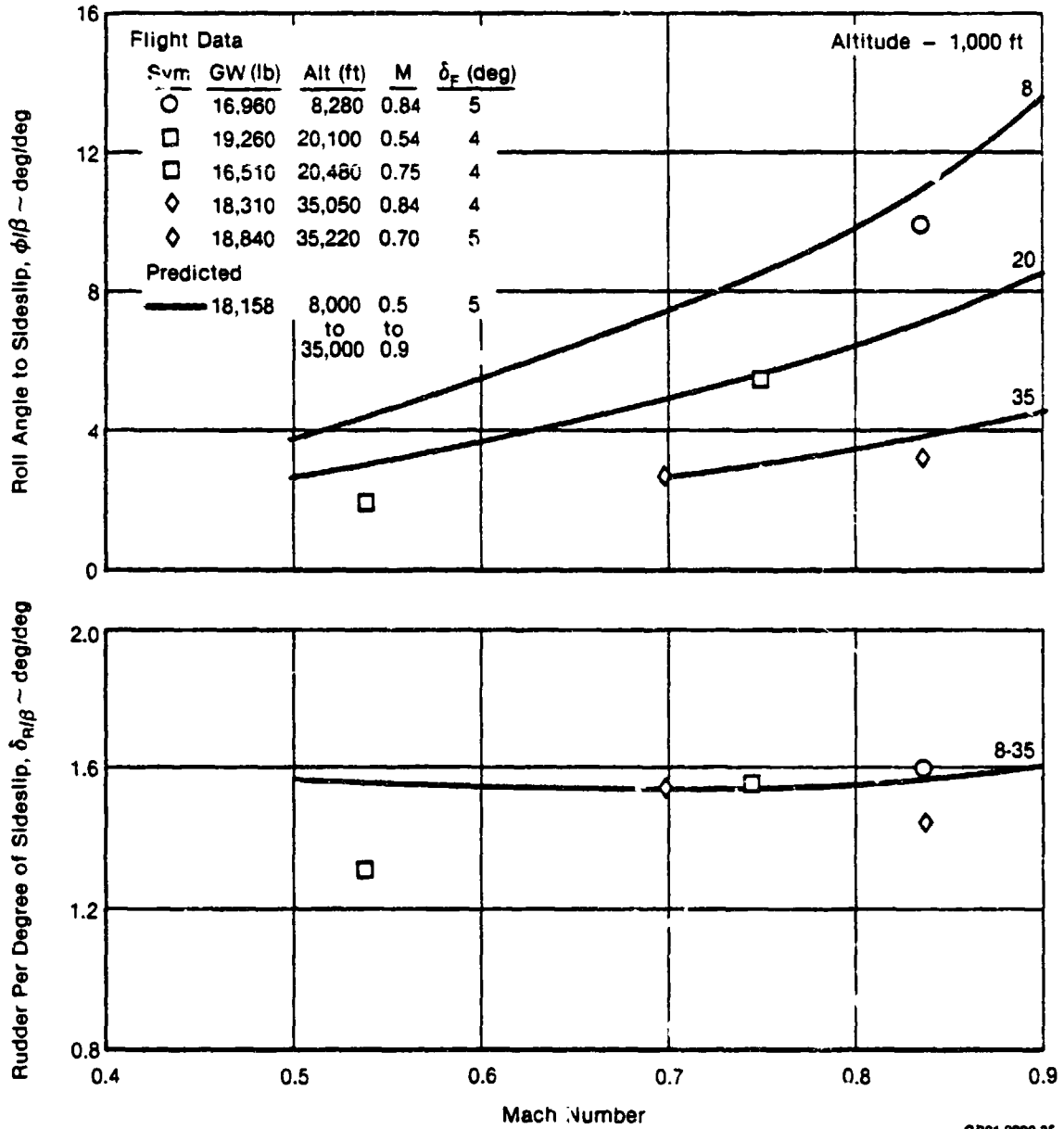
FIGURE 5.3-6
YAV-8B
WINGBONE STEADY HEADING SIDESLIP CHARACTERISTICS

GP21-0992-35

Flight Data

Sym	GW (lb)	Mach
O	15,540-22,340	0.275-0.87
□	15,890-19,950	0.55-0.86

Predicted

——————	18,158	0.35-0.85
— — — —	18,158	0.50-0.90
— · — · —	18,158	0.60-0.90

MIL-F-8785B
Category A
Level 2   Level 1

SL to 20,000 ft

MIL-F-8785B
Level   Level 1

20,000 to 40,000 ft

Dutch Roll Natural Frequency, ω_d - rad/sec

Dutch Roll Damping Ratio, ζ_{DR}

GP21-0902-2
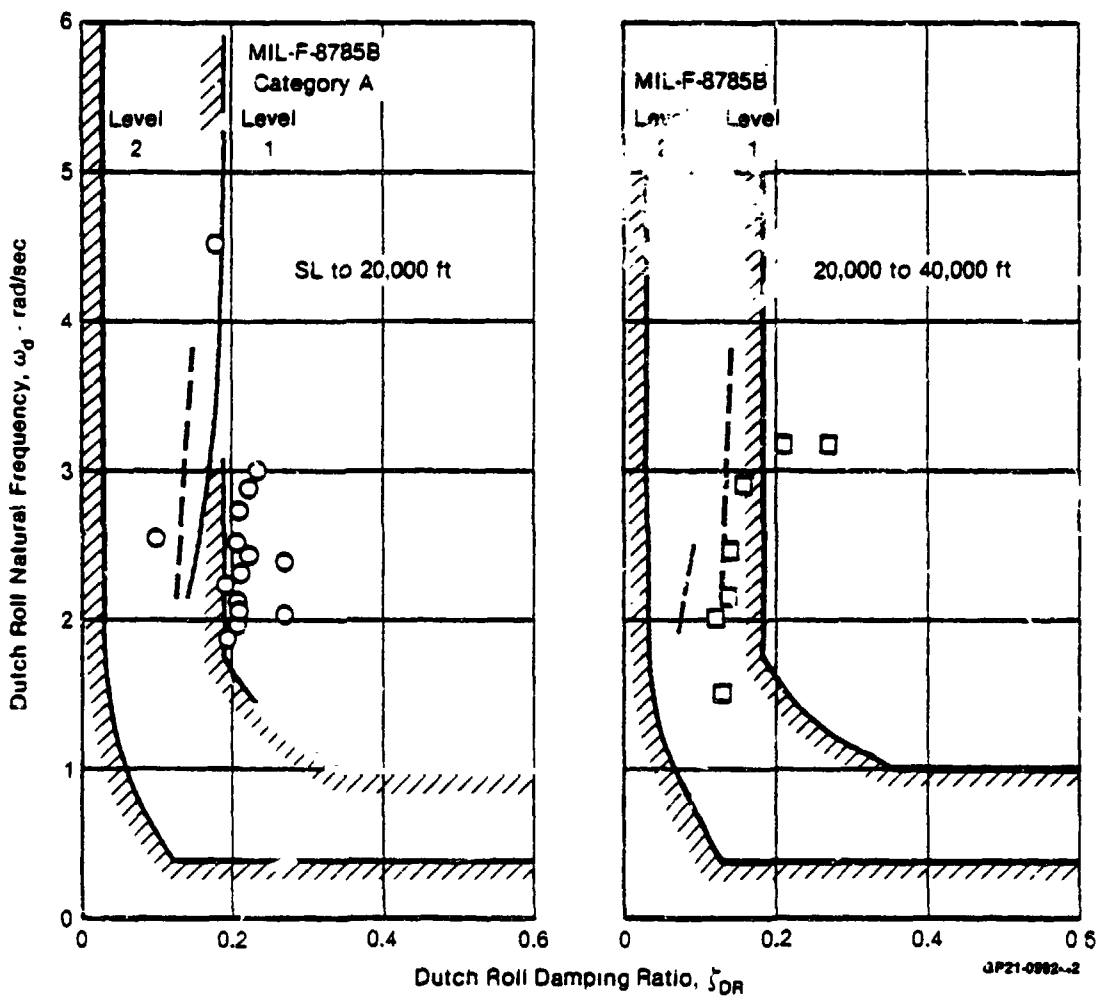
FIGURE 5.3-7
YAV-8B DUTCH ROLL FREQUENCY AND DAMPING
Wingborne Flight

5-26
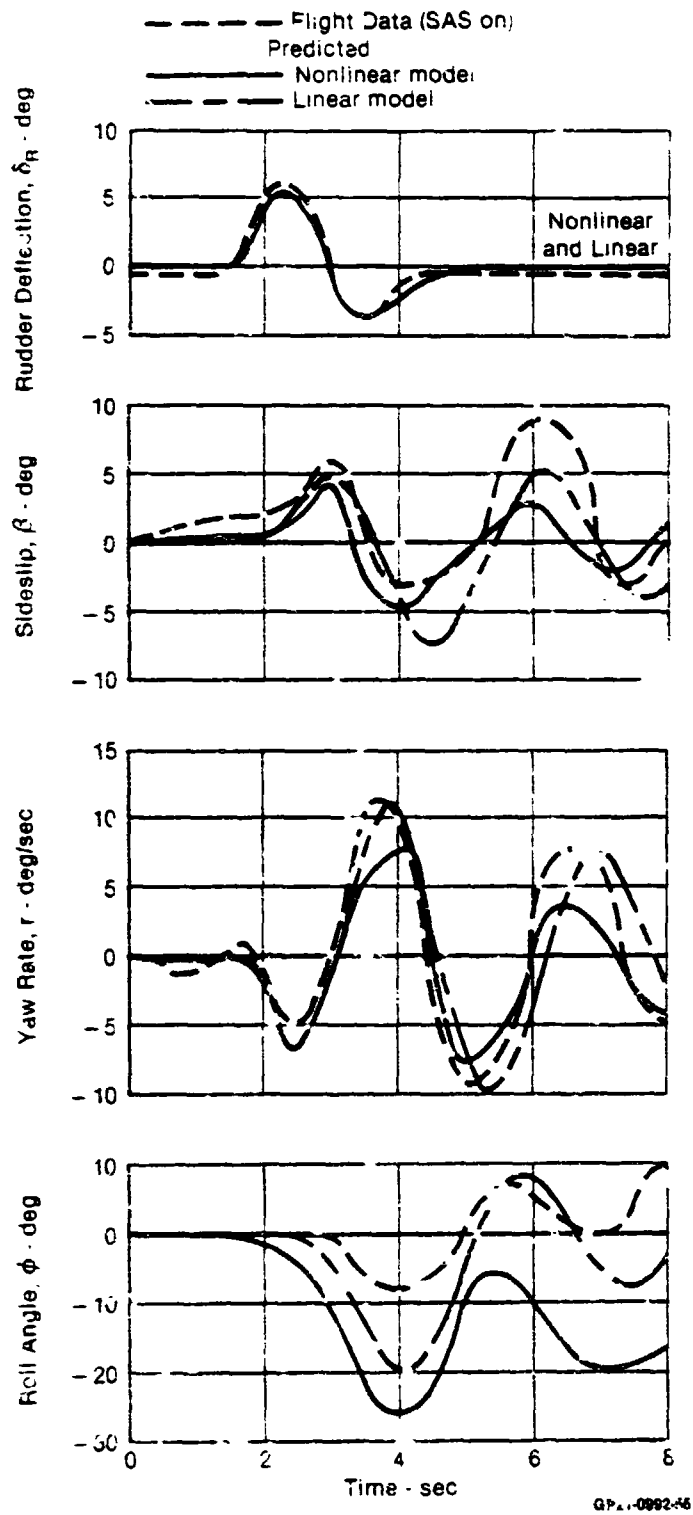
FIGURE 5.3-8
YAV-8B RESPONSE TO RUDDER INPUT IN WINGBORNE FLIGHT

Gross Weight = 19.200 lb $N_F = 77\%$ $\theta_J = 3°$ $\delta_F = 5°$
Mach 0.697   Altitude = 35,200 ft
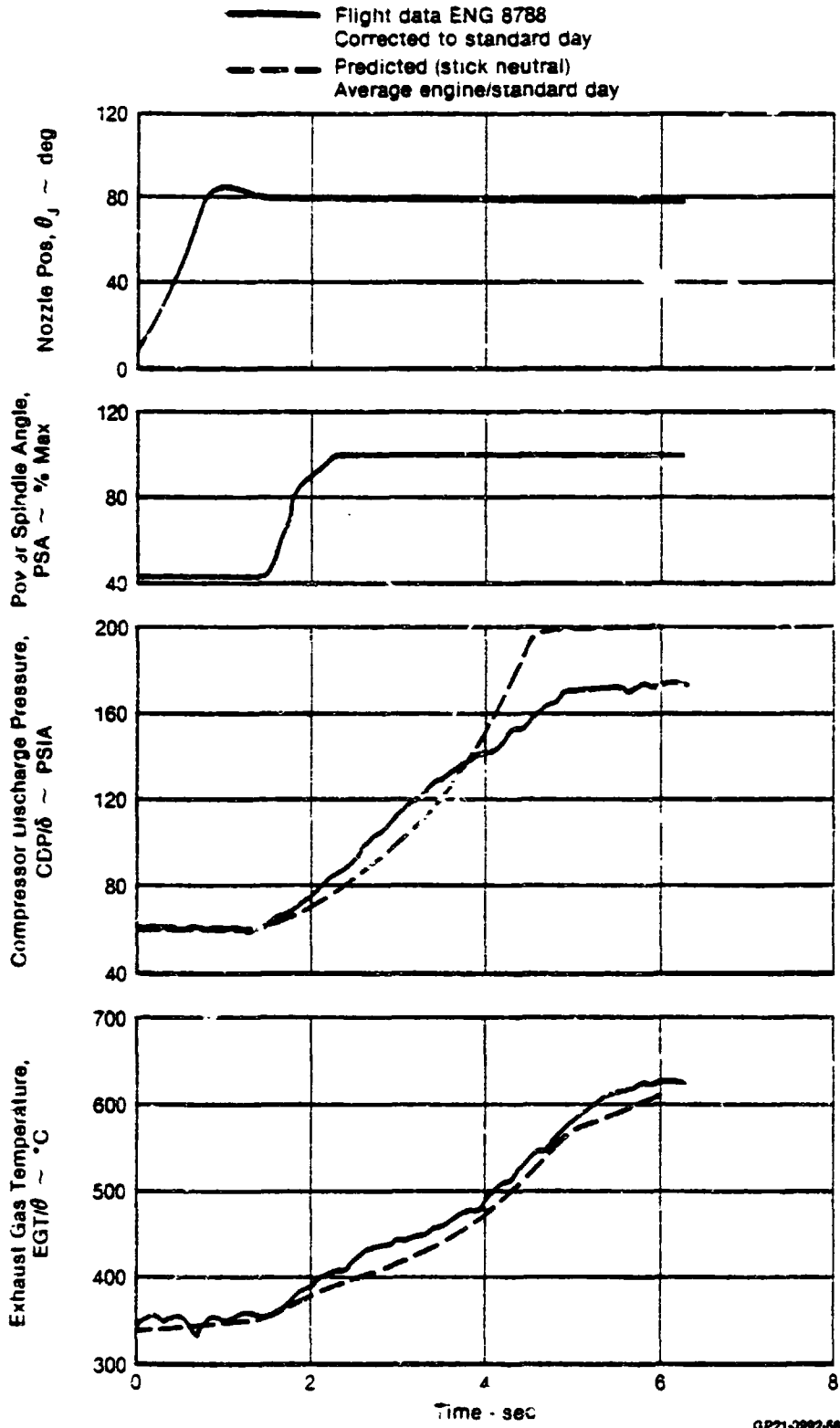
FIGURE 5.4-1
YAV-8B WET VTO

FIGURE 5.4-1 (Cont.)
YAV-8B WET VTO

ORIGINAL PAGE IS
OF POOR QUALITY
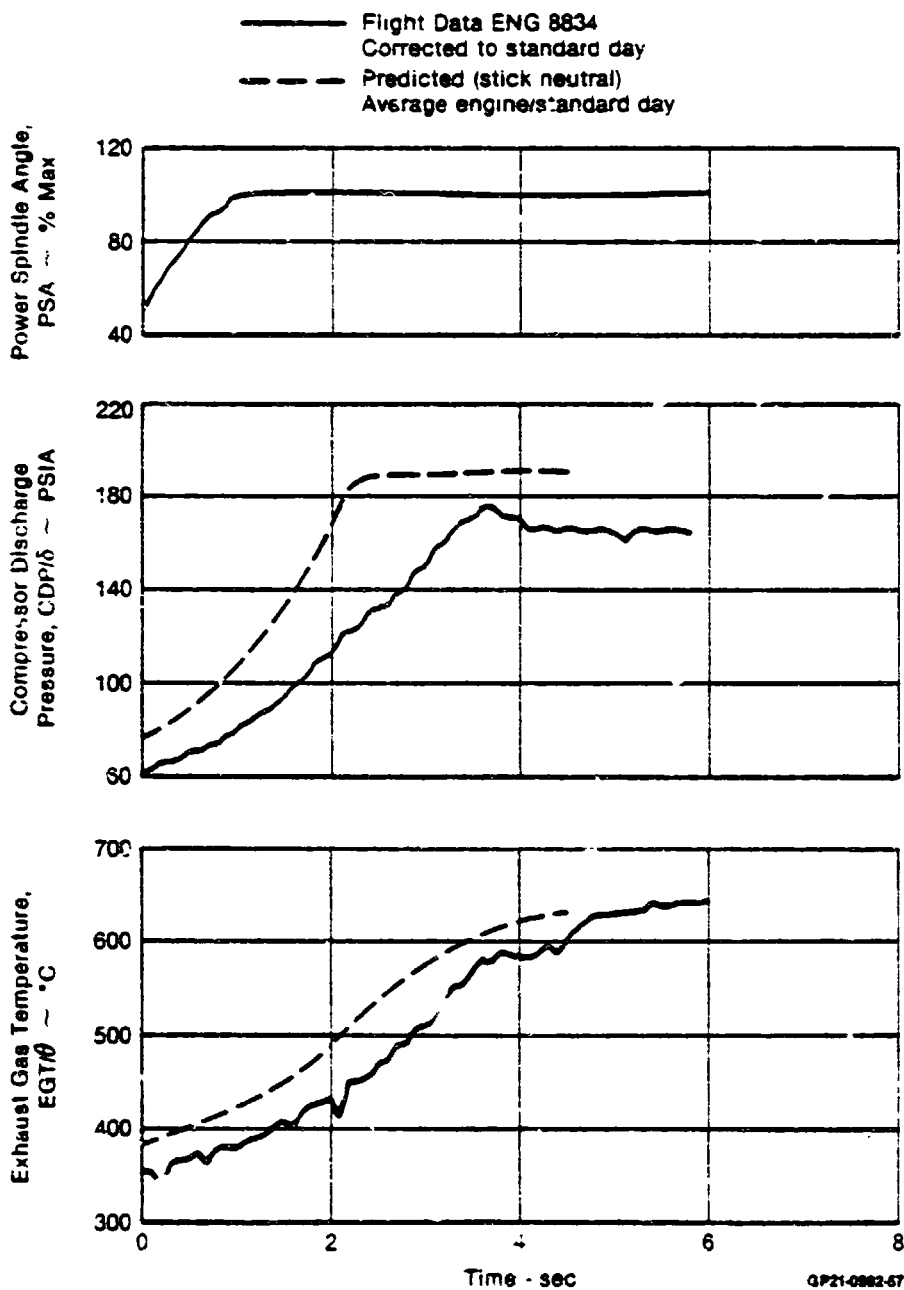
FIGURE 5.4-2
YAV-8B DRY VTO
Nozzle Angle = 77°
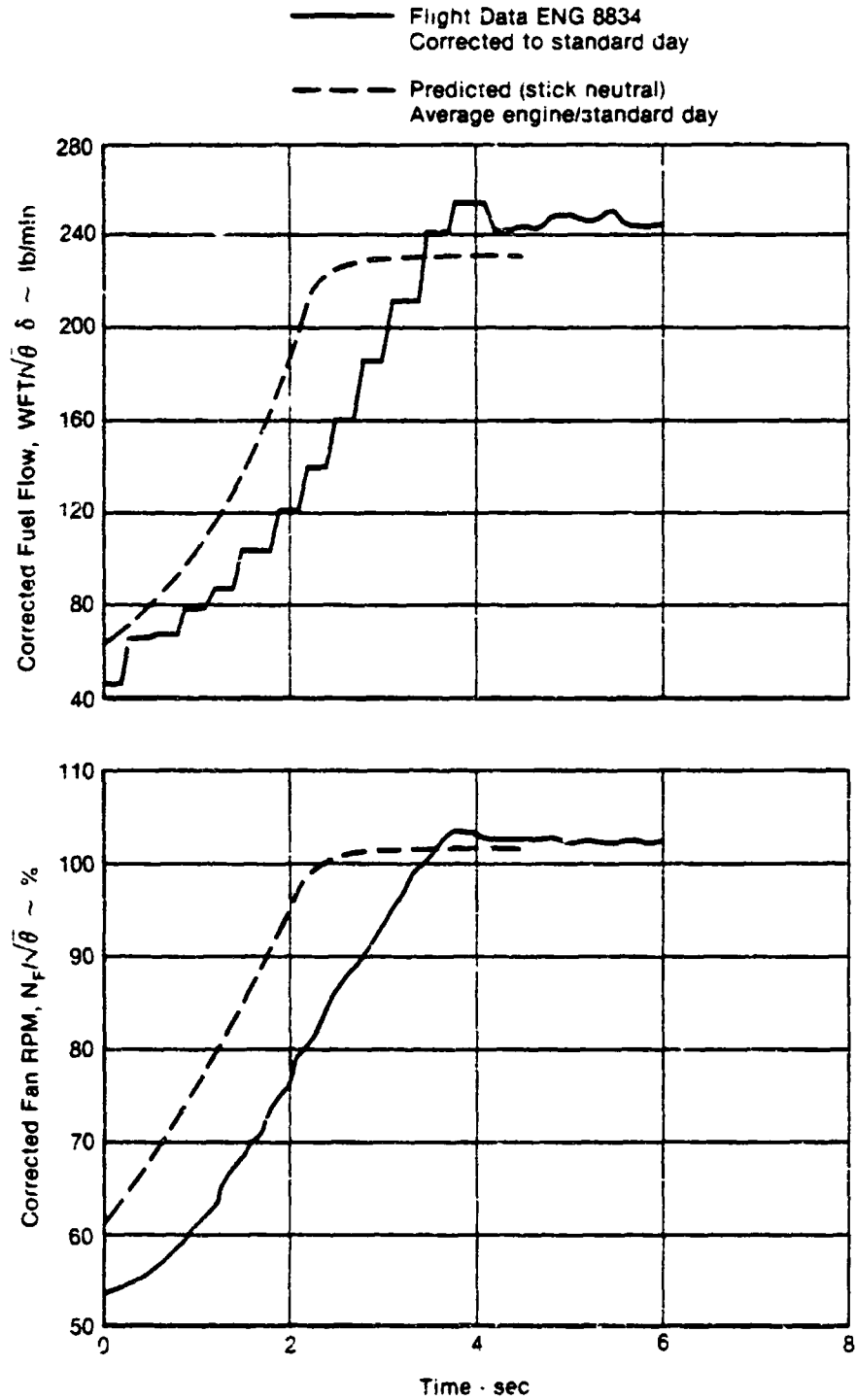
FIGURE 5.4-2 (Cont.)
YAV-8B DRY VTO

Nozzle Angle = 77°

GP21-0992-84

The simulator results during the dry VTO, Figure 5.4-2, appear to have a faster response than the actual engine. This discrepancy is due to a calibration error in the throttle position of the flight data. As a result, the initial engine fan speeds are offset.

5.5 CONTROL SURFACE ACTUATOR/SERIES SERVO VALIDA ON

A comparison of the frequency response characteristics of the control surface actuators and series servos is presented in Figures 5.5-1 to 5.5-4. The test data were obtained for small amplitude inputs while the predicted characteristics used the transfer functions presented in Section 2.5. Good agreement is shown for frequencies less than 1 Hertz, which are most pertinent to handling qualities analysis. Adequate gain margin and phase margins are shown.
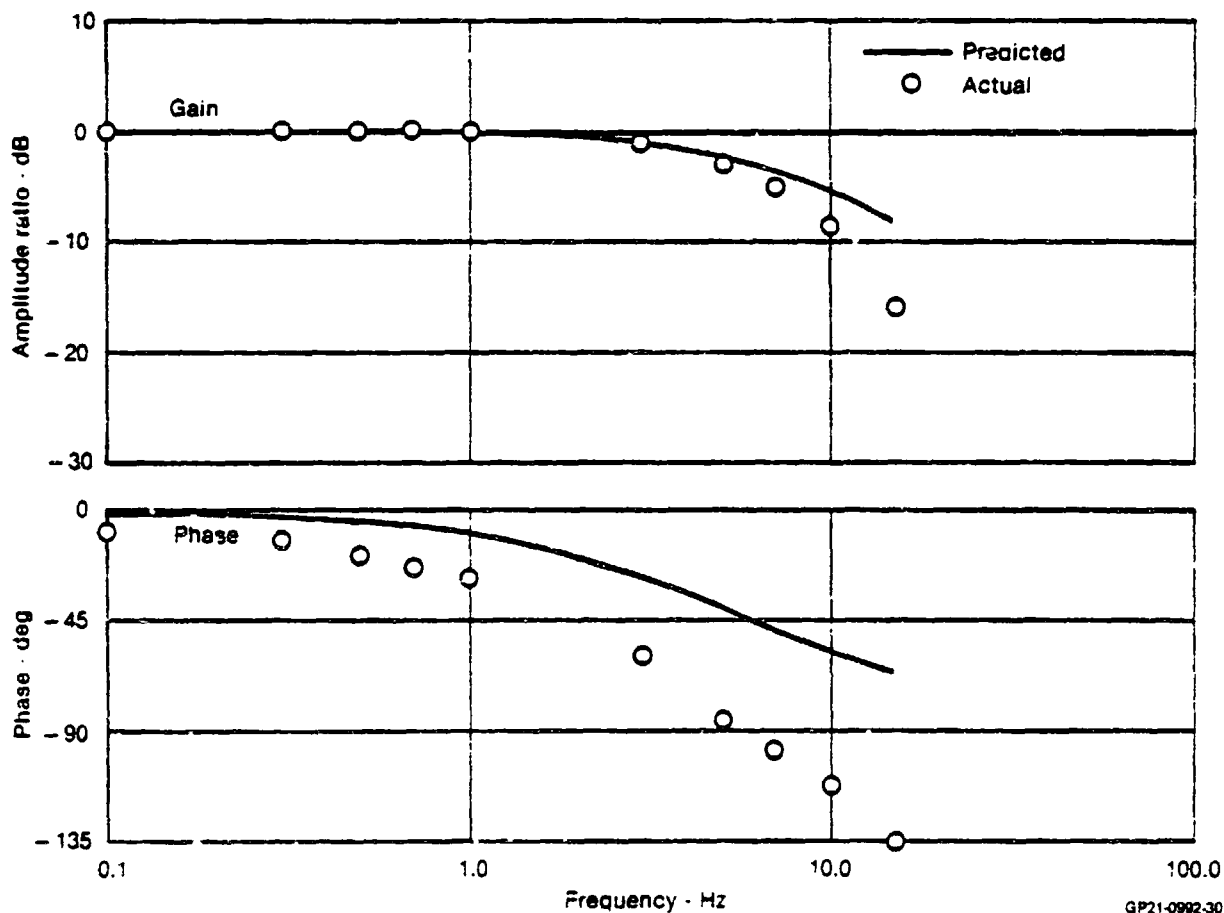

FIGURE 5.5-1
YAV-8B STABILATOR ACTUATOR — SAS MODE
Small Amplitude Frequency Response
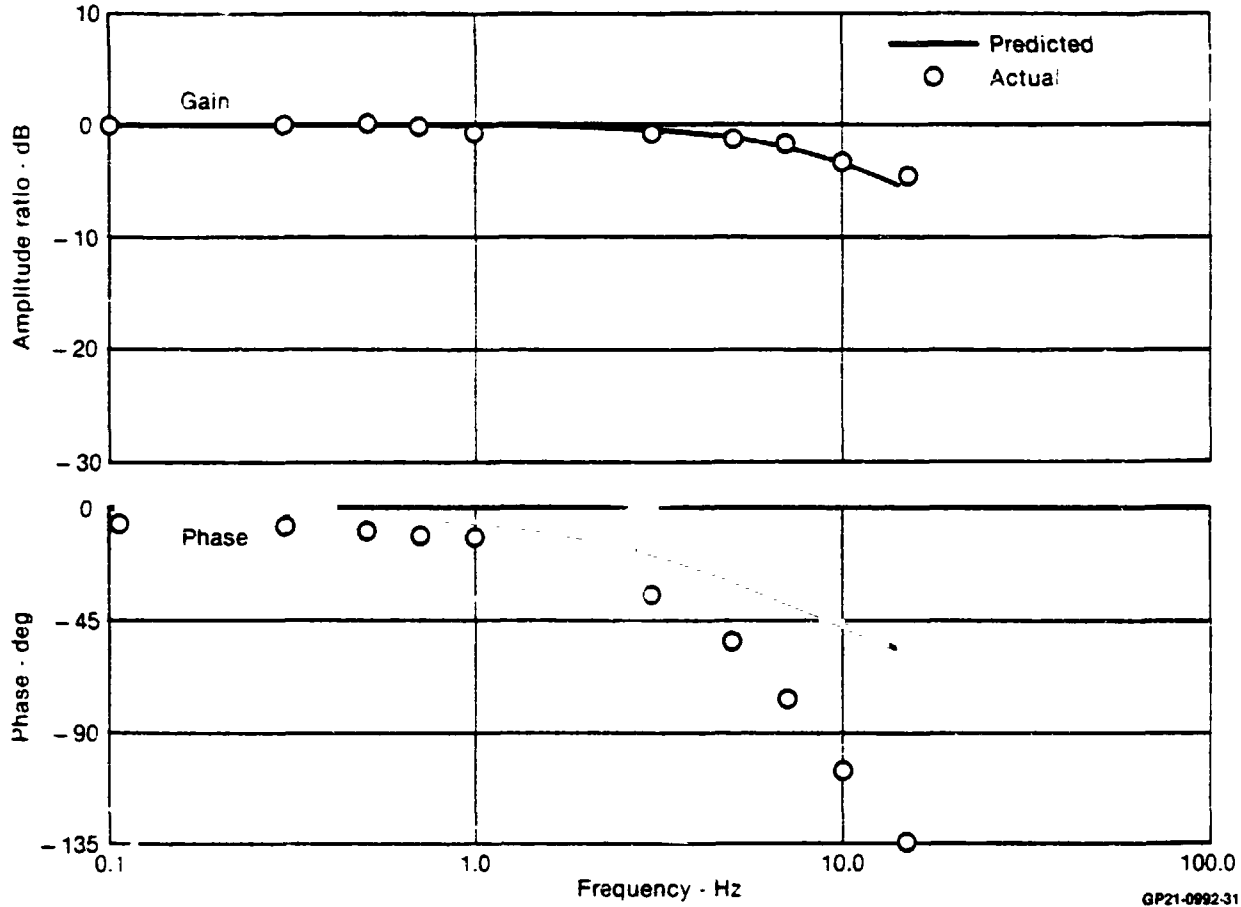
FIGURE 5.5-2
**YAV-8B FORWARD RCV SERIES SERVO**
Small Amplitude Frequency Response
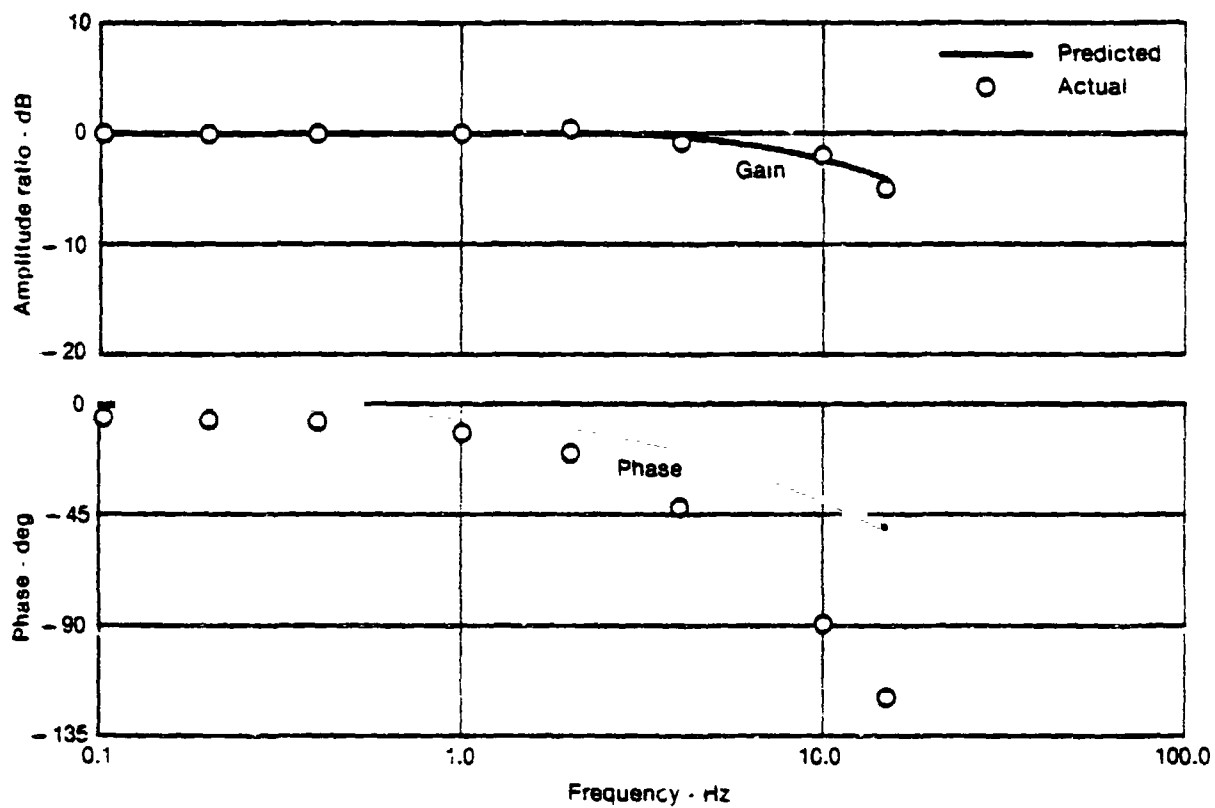
GP21-0092-32

FIGURE 5.5-3
**YAV-8B AILERON ACTUATOR – SAS MODE**
Small Amplitude Frequency Response
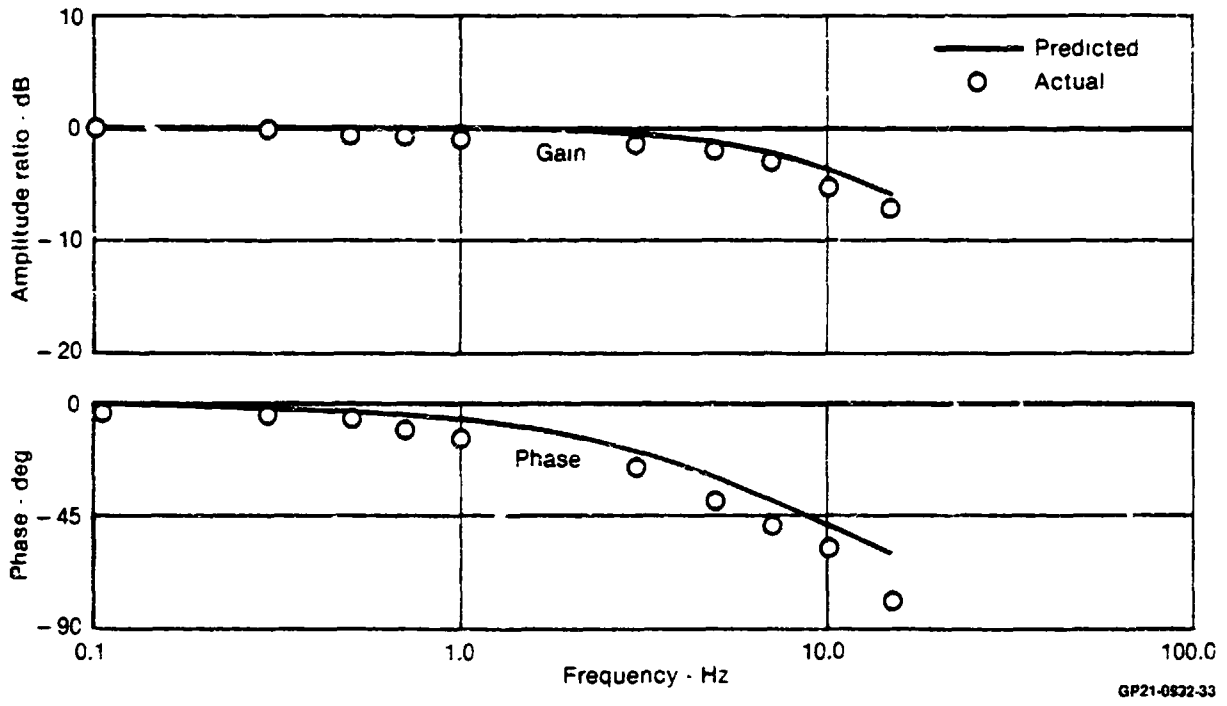
FIGURE 5.5-4
YAV-8B YAW RCV SERVO
Small Amplitude Frequency Response

6. PARAMETER ESTIMATION

The importance of determining the aircraft stability and control derivatives from flight test data has been recognized for many years. The flight determined derivatives are of much value to the flight test analyst. These results may be compared to other sources, such as wind tunnel test and theoretical calculations, to substantiate the predicted behavior of the aircraft. The extraction of stability and control derivatives from flight test data is a problem in parameter estimation.

Over the past 30 years, considerable work has been done in extracting the stability and control derivatives from flight test data. Various techniques have been investigated, some of which lend themselves to automation. As documented in References 2 and 3, techniques used by NASA include the Maximum Likelihood Parameter Estimation technique. To date, these efforts have concentrated on the conventional flight regime; however, with the acquisition of the YAV-8B, NASA intends to extend this investigation into the V/STOL flight regime.

This section contains suggestions on the forms of mathematical models to use in the estimation of V/STOL aircraft stability and control derivatives. In addition, some significant nonlinear effects, included and documented in the six degree of freedom mathematical model presented in Section 3, are discussed.

6.1 JET BORNE AND SEMI-JET BORNE

As discussed in Section 4, MCAIR uses the linearized representations of the aircraft in control system design and handling qualities analysis in the V/STOL flight regime. The comparisons to flight data of Section 5 show that the linearized model is representative of the actual aircraft. This form of the model was also used by CALSPAN in a study that assessed the feasibility of simulating the AV-8A in the terminal operation area, with the X-22A variable stability aircraft (Reference 4). A follow-on study that included flight test evaluation by 2 qualified AV-8A pilots concluded that the simulation was representative of the actual aircraft.

In hover and at very low speeds (≤ 35 KTAS) the simplifying assumptions detailed in the MIL-F-8330 Background Information and Users Guide (BIUG), Reference 5, may be applied to the linearized equations of motion. These assumptions include:

o Hover ($V_T = 0$)

o Vertical motion decoupled from pitching and horizontal translational motion

o Yawing motion decoupled from rolling and lateral translational motions

o Constant thrust magnitude and direction

Applying these assumptions to the linearized equations of Section 4, and recognizing that angle-of-attack, α, and sideslip angle, β, are no longer defined in hover, results in the simplified equations shown in Figure 6.1-1. This form of the equations was used to analyze the flight test and flight simulation data available when formulating the hover and low speed dynamic response requirements of Reference 6.

No matter which form of the equations is used, the following first order effects must be included in the formation of YAV-8B stability derivatives taken at fixed operating points in the V/STOL flight regime. Note that if the nonlinear model of Section 3 is used to establish a trim point and to formulate the stability derivatives, the following effects will be taken into account.

  o   Thrust level and control effectiveness   At low speeds the aero-
      dynamic controls are naturally ineffective and the primary source of
      control is the Reaction Control System (RCS). The effectiveness of
      this system is proportional to engine RPM as shown in Figure 6 1-2.

  o   Simultaneous demand and control effectiveness - The effect of multi-
      control usage is to reduce the effectiveness of the individual
      controls. This effect is shown in Figures 6.1-3 and 6.1-4 for the
      pitch RCS.

  o   Thrust vector application point - The application point of the thrust
      vector varies with engine RPM as shown in Figure 6.1-5.

One additional effect may be considered when evaluating the effectiveness of the RCS. AV-8B static tests using the individual Reaction Control Valves (RCV), showed the direction   of the RCV thrust vector to be a function of the valve opening. These AV-8B o   a have been combined with YAV-8B valve orientation geometry to produce the estimated variations shown in Figure 6.1-6. These variations are not included in the models defined in this report. Both the nonlinear and linear mathematical models u : the "design" RCV thrust vector angles.

6.2 WINGBORNE FLIGHT

The linearized equations of motion presented in Section 4 are applica-
ble to wingborne flight. The effects of Vectoring in Forward Flight (VIFF) should be invest-gated using stability derivatives based on perturbations from a trim point obtained using the nonlinear mathematical model.

LONGITUDINAL

$$\dot{u} + g\theta = X_u u + X_{\delta_H} \delta_H + X_{\delta_{FRCS}} \delta_{FRCS} + X_{\delta_{ARCS}} \delta_{ARCS}$$

$$\dot{q} = M_u u + M_q q + M_{\delta_H} \delta_H + M_{\delta_{FRCS}} \delta_{FRCS} + M_{\delta_{ARCS}} \delta_{ARCS}$$

LATERAL DIRECTIONAL

$$\dot{v} + g\phi = Y_v v + Y_{\delta_A} \delta_{A_L} + Y_{\delta_R} \delta_R + Y_{\delta_{RRCS}} \delta_{RRCS} + Y_{\delta_{YRCS}} \delta_{YRCS}$$

$$\dot{p} = -L_v v + L_p p + L_{\delta_A} \delta_{A_L} + L_{\delta_R} \delta_R + L_{\delta_{RRCS}} \delta_{RRCS} + L_{\delta_{YRCS}} \delta_{YRCS}$$

EQUATIONS FROM REFERENCE 5

FIGURE 6.1-1
SIMPLIFIED LINEAR EQUATIONS OF MOTION
HOVER
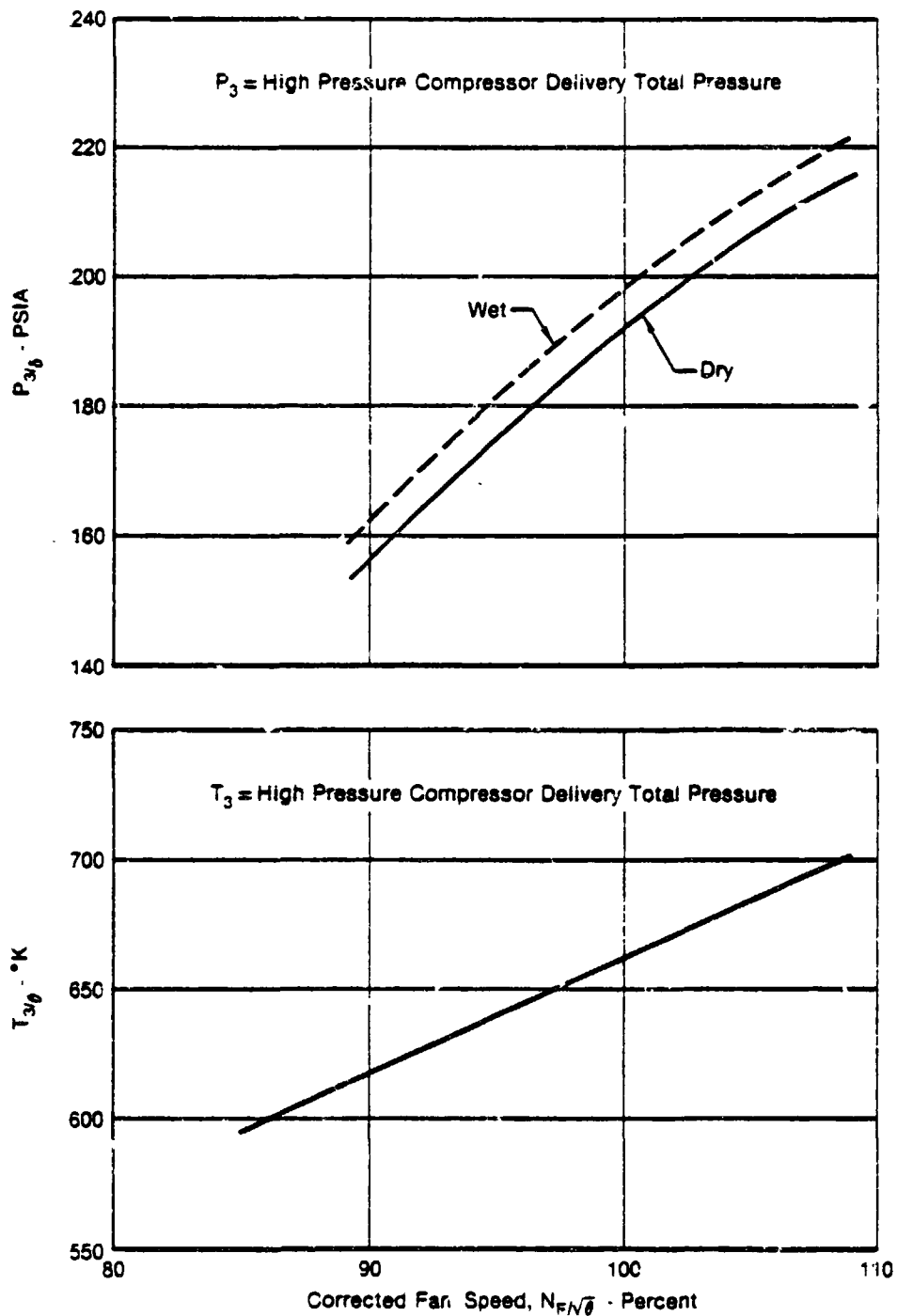
FIGURE 6.1-2
REACTION CONTROL SYSTEM BLEED AIR PRESSURE AND TEMPERATURE
YF402-RR-404 Installed Engine
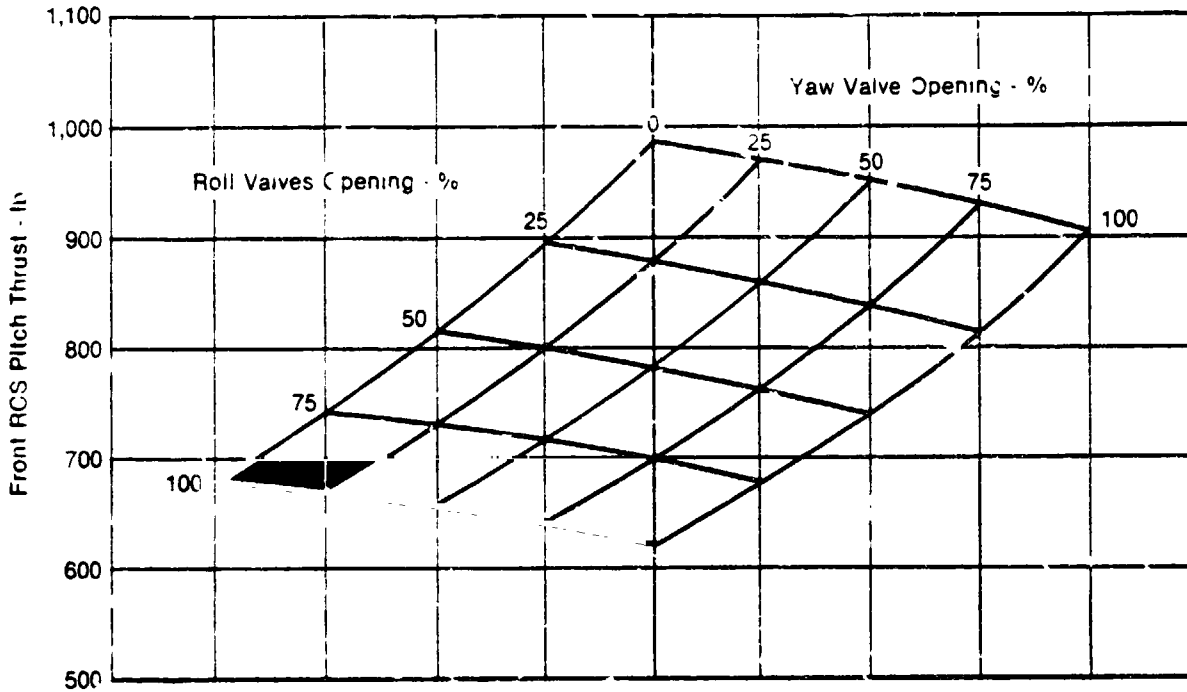
FIGURE 6.1-3
MAXIMUM RCS FRONT PITCH VALVE THRUST
Normal Lift Dry Full Nose Up Control Demand
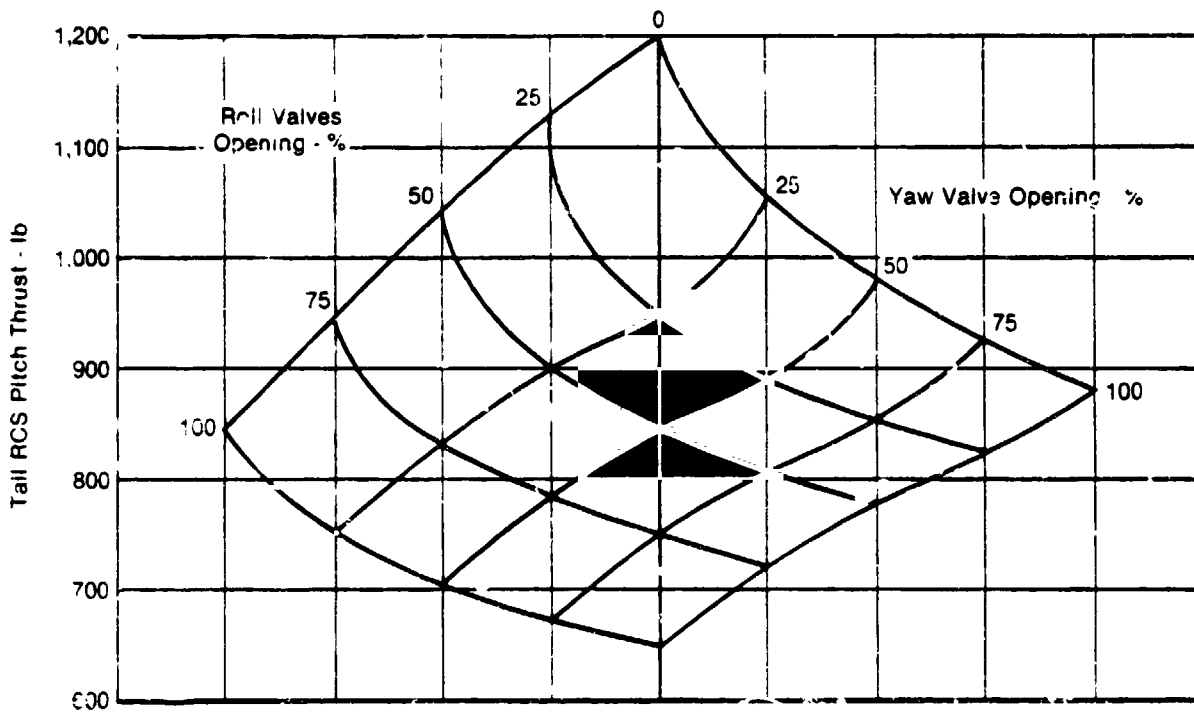
FIGURE 6.1-4
MAXIMUM RCS TAIL PITCH VALVE THRUST
NORMAL LIFT DRY   FULL NOSE DOWN CONTROL DEMAND
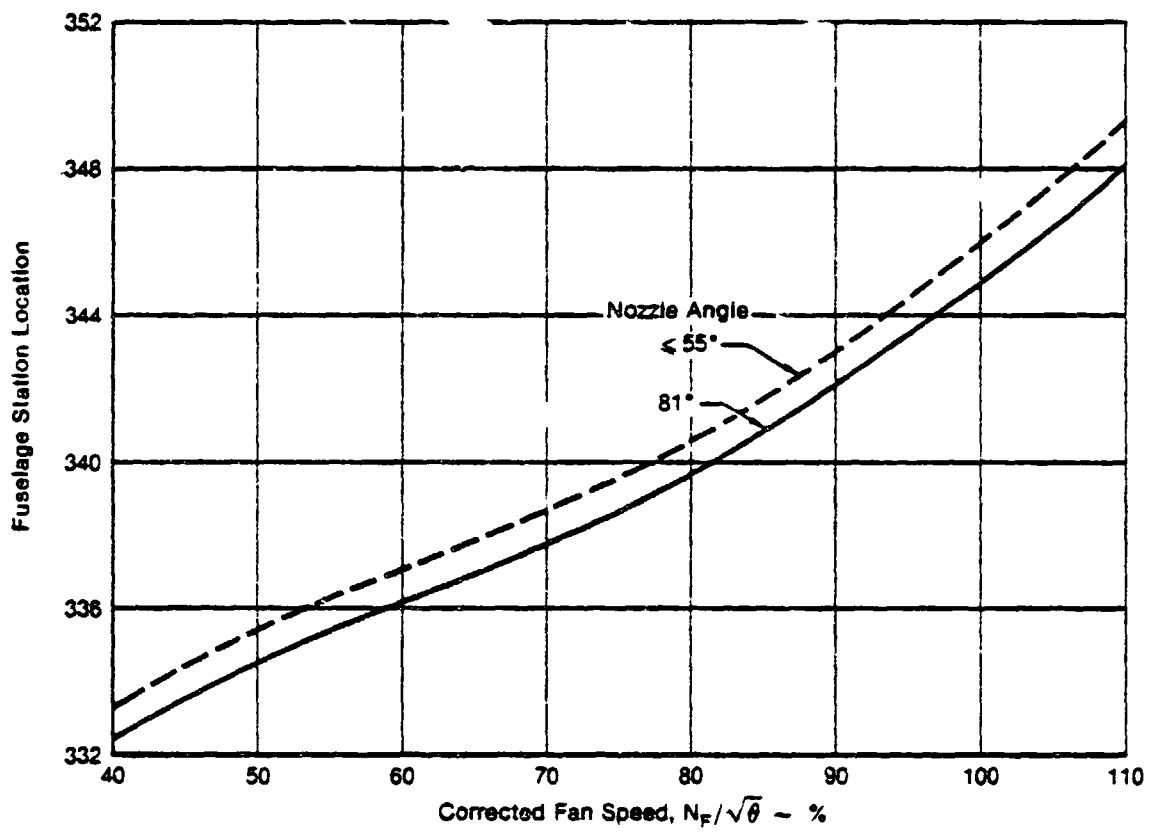
FIGURE 6.1-5
GROSS THRUST APPLICATION POINT

C - 3

ORIGINAL PAGE IS
OF POOR QUALITY
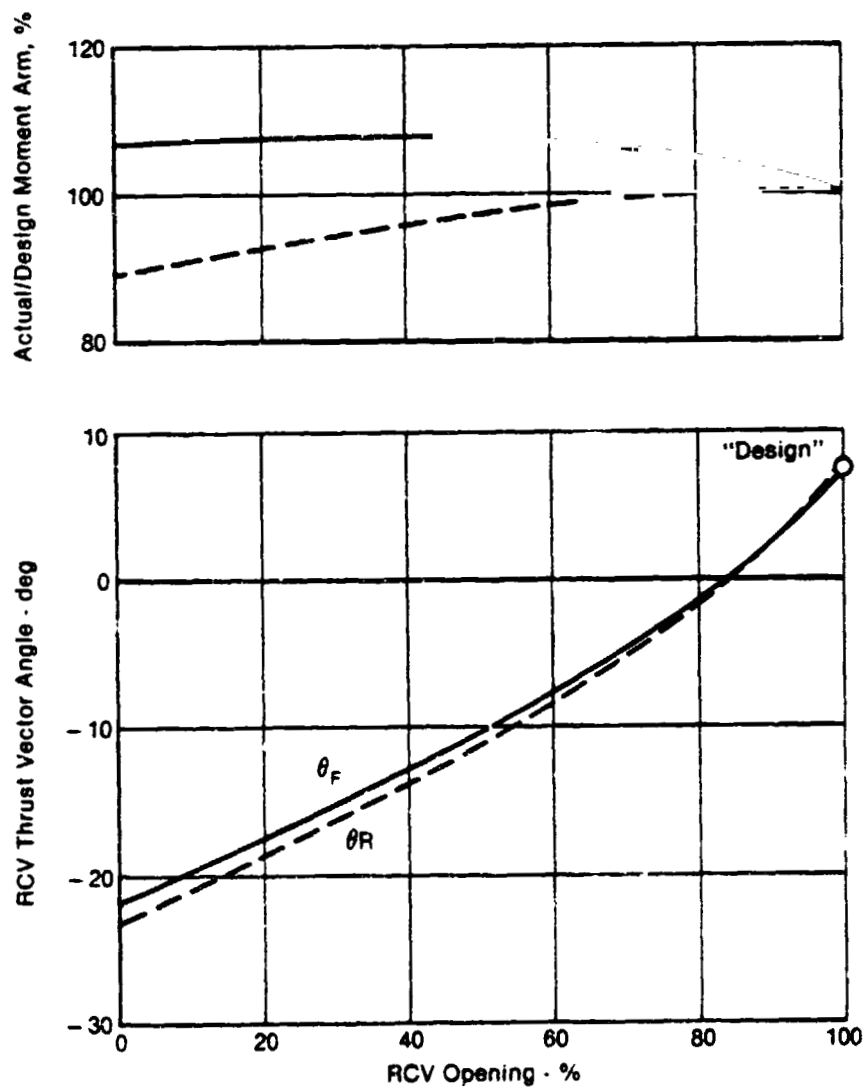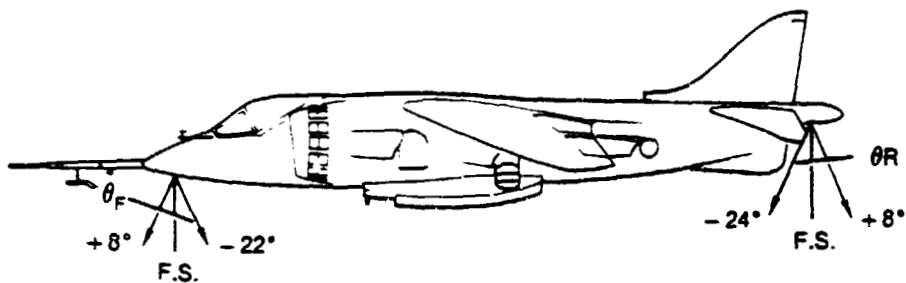
Note: Based on AV-8B Test Data

GP21-0082-82

**FIGURE 6.1-6
YAV-8B PITCH RCV THRUST VECTOR ANGLES**

7. CONCLUDING REMARKS

A six degree of freedom FORTRAN batch simulation of a nonlinear mathematical model of the YAV-8B aircraft has been produced and documented. The documentation includes top level flow charts, a discussion of program structure, subroutine interfaces, modeling equations, data format, a user's guide and plots of the over 17,000 data points used by the program. The model is based on the YAV-8B model used on the MCAIR manned flight simulator. The nonlinear model has been shown to be representative of the actual aircraft by comparison to both static and dynamic YAV-8B flight test data.

Two simplified models have been suggested for use in parameter estimation, one of which is the traditional longitudinal and **lateral-directional** 3 degree of freedom linearized model used in the analysis of conventional aircraft. A second model, applicable for hover and low speed analysis, is suggested. Aircraft stability derivatives, which characterize the aircraft throughout its flight envelope, are provded at 24 flight conditions. These derivatives were formulated by perturbing the nonlinear model after establishing control settings corresponding to a 3 degree of freedom 1 'g' wings level trim. These stability derivatives include the effects of aerodynamics, inlet momentum and gross thrust.

For reference a description of the major aircraft systems modeled in the FORTRAN program is included.

8. REFERENCES

1. MDC A4637, YAV-8B Aerodynamic Stability and Control and Flying Qualities
Report, 11 January 1980.

2. NASA TP1563, User's Manual for MMLE3, a General FORTRAN Program for
Maximum Likelihood Parameter Estimation, November 1980.

3. NASA TP1690, Programmer's Manual for MMLE3, a General FORTRAN Program for
Maximum Likelihood Parameter Estimation, June 1981.

4. CALSPAN Report No. AK-5876-F-1, A Study to Determine the Feasibility of
Simulating the AV-8A Harrier with the X-22A Variable Stability Aircraft,
July 1976.

5. AFFDL-TR-70-88, Background Information and User Guide For MIL-F-83300 -
Military Specification - Flying Qualities of Piloted V/STOL Aircraft,
March 1971.

6. MIL-F-83300, Military Specification - Flying Qualities of Piloted V/STOL
Aircraft, 31 December 1970.

7. Control Data Corporation Modify Reference Manual, Rev. F - CDC
Operating System: NOS1, 5 December 1980.

9. SYMBOLS AND ABBREVIATIONS

SYMBOL	DESCRIPTION	UNITS
ACU	Acceleration control unit	—
AND	Aircraft nose down	—
ANL	Aircraft nose left	—
ANR	Aircraft nose right	—
ANU	Aircraft nose up	—
AOA	Angle of Attack	deg
AR	Aspect ratio	—
Autostab	Autostabilization or SAS	—
A_{Yacc}	Lateral acceleration at the accelerometer location	ft/sec^2
b	Wing span	ft
B.L.	Butt Line	in
BOV	Blow off valve	—
C	Chord	in
$\bar{c}$	Mean aerodynamic chord	in
C_A	Coefficient of axial force (positive forward)	—
C_D	Coefficient of drag (positive aft)	—
C_L	Coefficient of lift (positive up)	—
C_1	Coefficient of rolling moment (positive RWD)	—
C_m	Coefficient of pitching moment (positive ANU)	—
C_N	Coefficient of normal force (positive up)	—
C_n	Coefficient of yawing moment (positive ANR)	—
C_Y	Coefficient of side force (positive out the right wing)	—
C.G.	Center of gravity	$\% \bar{c}$, in
$\cancel{\mathsf{L}}$	Centerline	—
CPL	Compressor pressure limiter	—
Ctr	Center	—
CR	Root chord	in
CT	Tip chord	in
DT	Iteration time	sec
e_1 to e_4	Quaternions	—
EGT	Exhaust gas temperature. Same as JPT	°C, °K
F_A	Force Axial (positive forward)	lb
FCU	Fuel control unit	—
FJI	Flap jet impingement	—
F_N	Force normal	lb
FOD	Foreign object damage	—
FP	Flat plate	—
FRL	Fuselage reference line. Same as W.L.	—
F.S.	Fuselage Station	in
Fwd	Forward	—
g	Acceleration due to gravity	32.174 ft/sec^2
GE	Ground effect	—
GTS	Gas turbine starter	—
GW	Gross weight	lb
h	Altitude	ft
HP	High pressure	—
HSA	Hawker Siddeley Aviation	—
HT	Horizontal tail	—
IGV	Inlet guide vane	—
Inbd	Inboard	—

9. SYMBOLS AND ABBREVIATIONS (CONTINUED)

SYMBOL	DESCRIPTION	UNITS
I_{xx}	Roll moment of inertia	slug - ft^2
I_{xz}	Product of inertia	slug - ft^2
I_{yy}	Pitch moment of inertia	slug - ft^2
I_{zz}	Yaw moment of inertia	slug - ft^2
JPT	Jet pipe temperature. Same as EGT	°C, °K
K_{AY}	Lateral acceleration feedback gain	deg/ft/sec^2
KCAS	Knots calibrated airspeed	knots
KIAS	Knots indicated airspeed	knots
K_p	Roll rate feedback gain	deg/deg/sec
K_q	Pitch rate feedback gain	deg/deg/sec
K_r	Yaw rate feedback gain	deg/deg/sec
KTAS	Knots true airspeed	knots
L	Left, Latitude	-, deg
LEMAC	Leading edge of the mean aerodynamic chord	in
LIDS	Lift improvement device system	-
LP	Low pressure	-
LSWT	Low speed wind tunnel (located at MCAIR)	-
Lt	Left	-
LVDT	Linear variable differential transformer	-
M	Mach number	-
$\dot{m}$	Mass flow	lb$_m$/sec
MAC	Mean aerodynamic chord	in
MCAIR	McDonnell Aircraft Company	-
MFCF	Mass flow calibration facility (located at MCAIR)	-
MSWT	Minispeed wind tunnel (located at MCAIR)	-
M_x	Rolling moment (positive is RWD)	ft - lb
M_y	Pitching moment (positive is ANU)	ft - lb
M_z	Yawing moment (positive is ANR)	ft - lb
NED	North, East, Down	-
N_F	Fan speed	%
N_H	High pressure compressor RPM	%
NLD	Normal lift dry	-
N_y	Lateral load factor	-
n_z	Normal load factor	-
0	Origin	-
Outbd	Outboard	-
OWE	Operating weight empty	lb
p	Roll rate	deg/sec
P_3	Compressor discharge pressure	lb/in^2
P_{13}	Fan delivery pressure	lb/in^2
PLA	Power lever angle	-
PM	Pitching moment (positive ANU)	ft - lb
PRL	Pressure ratio limiter	-
P_{RCS}	Reaction control pressure	lb/in^2
PSA	Power spindle angle	-
psia	Absolute pressure	lb/in^2
psig	Gauge pressure	lb/in^2

9. SYMBOLS AND ABBREVIATIONS (CONTINUED)

SYMBOL	DESCRIPTION	UNITS
q	Pitch rate	deg/sec
Q, $\bar{q}$	Dynamic pressure	lb/in^2
$\bar{q}_\infty$	Freestream dynamic pressure	lb/in^2
$\bar{q}_J$	Jet dynamic pressure	lb/in^2
R	Radius, Right	in, -
r	Yaw rate	deg/sec
RCS	Reaction control system	-
RCV	Reaction control valve	-
R_{EARTH}	Radius of the Earth	ft
RM	Rolling moment (positive RWD)	ft-lb
RPM	Revolutions per minute	-
RR	Rolls-Royce Limited	-
RT	Right	-
RWD	Right wing down	-
RWU	Right wing up	-
S	Wing area, Laplace transform	ft^2, -
SAS	Stability augmentation system	-
SF	Side Force (positive out the right wing)	lb
SFO	Simulated flame out	-
SLD	Short lift dry	-
SLW	Short lift wet	-
STO	Short takeoff	-
T,t	Temperature, thickness	°C, in
T_2	Temperature at engine face	°C, °K
T_3	Compressor discharge temperature	°C, °K
TED	Trailing edge down	-
TEL	Trailing edge left	-
TER	Trailing edge right	-
TEU	Trailing edge up	-
u	Velocity in X direction (positive forward)	ft/sec
v	Velocity in Y direction (positive out the right wing)	ft/sec
Veq	Equivalent velocity ratio $\sqrt{\bar{q}_\infty/\bar{q}_{JET}}$	-
VIFF	Vectoring in forward flight	-
V_s	Speed of sound	ft/sec
V/STOL	Vertical/Short Takeoff and Landing	-
V_T	Total velocity	ft/sec
VTO	Vertical takeoff	-
w	Velocity in Z direction (positive down)	ft/sec
W_D	Wind velocity, down component	ft/sec
W_E	Wind velocity, east component	ft/sec
W_F	Fuel flow	lb/min
WFT	Fuel flow	lb/min
W.L.	Waterline	in
W_N	Wind velocity, north component	ft/sec
W.R.P.	Wing reference plane (parallel to W.L.)	-
WOW	Weight on wheels	-
WT	Weight	lb

9. SYMBOLS AND ABBREVIATIONS (CONTINUED)

SYMBOL	DESCRIPTION	UNITS
Xcg	Fuselage station of c.g.	in
YM	Yawing moment (positive ANR)	ft-lb
Z	Z transform operator	-

GREEK SYMBOLS

α	Angle of attack	deg
$\dot{\alpha}$	Angle of attack rate	deg/sec
β	Sideslip angle	deg
Γ_o	Initial flight path angle	deg
γ	Flight path angle	deg
Δ	Incremental quantity	-
δ_A	Aileron deflection (positive is TED)	deg
δ_F	Flap deflection (positive is TED)	deg
δ_H	Horizontal tail (stabilator) deflection (positive is TED)	deg
δ_R	Rudder deflection (positive TEL)	deg
δ_θ	Longitudinal stick deflection	in
δ_ϕ	Lateral stick deflection	in
δ_ψ	Rudder pedal deflection	in
ζ_d	Dutch roll damping ratio	-
ζ_{sp}	Short period damping ratio	-
η	Fraction of semi-span	-
θ	Pitch angle	deg
θ_J	Nozzle deflection	deg
Λ_{LE}	Sweep angle of leading edge	deg
λ	Longitude	deg
ρ	Density of air	$slug/ft^3$
τ	Time constant	sec
ϕ	Roll angle	deg
ψ	Yaw angle	deg
Ω	Rate of rotation	deg/sec
ω_d	Dutch roll natural frequency	rad/sec
ω_{sp}	Short period natural frequency	rad/sec

APPENDIX A

CONTRACT STATEMENT OF WORK

1.0 INTRODUCTION

As part of its V/STOL research program, NASA intends to conduct flight investigations of the stability, control and handling qualities of highly augmented V/STOL aircraft. Specific plans include the flight tests of a YAV-8B aircraft modified to include an advanced avionics and flight control system for improved flying qualities and performance.

As an initial phase to this program, NASA will conduct flight tests of the YAV-8B vehicle in order to extract aerodynamic and propulsion characteristics, update existing simulation models, validate handling qualities and design criteria, and to improve V/STOL flight test techniques. This program will also include tests using a static test stand location at the Dryden Flight Research Center, where flight tests of the YAV-8B will take place.

In order to perform high quality parameter estimation and analysis of the YAV-8B characteristics, it is necessary to construct mathematical models of varying complexity and linearity from existing wind tunnel and flight test data. This procurement is intended to produce models and to compile existing data for the Harrier aircraft.

2.0 SCOPE

The contractor will assess existing wind tunnel, analytic, and flight data for V/STOL aircraft especially in VTOL-unique flight regimes in order to compile aerodynamic, propulsion, and system models. Detailed models of varying complexity will be derived for the YAV-8B aircraft for use in para- meter estimation as well as linear analysis programs. A simplified batch simulation of the YAV-8B, utilizing the best nonlinear representation of the airplane will be generated. Finally, flight data and wind tunnel predictions will be used to compare YAV-8B characteristics with flying qualities criteria and design guidelines.

3.0 CONTRACTOR TASKS

The contractor shall:

3.1 Assemble and compile sufficient available Harrier aerodynamic, pro- pulsion system, and flight control system data, as well as available flight test data to support completion of tasks 3.2 through 3.8.

3.2 Formulate the most complete model of the YAV-8B from the results of 3.1, to characterize the vehicle in hover, transition, cruise, and vectoring in forward flight (VIFF) flight conditions.

3.3 Produce a simplified FORTRAN batch simulation of the YAV-8B (including engine) using non linear equations of motion, capable of execution on the Dryden Cyber 73-28 computer.

3.4 Formulate linear models of the YAV-8B for distinct flight conditions in hover, transition, cruise, and VIFF modes of flight. Select a sufficient number of flight conditions to characterize the aircraft throughout its flight envelope.

3.5 Validate the models of 3.2 and 3.4 (with the exception of the VIFF mode), and the simulation program of 3.3 by generating time history responses and comparing them with actual flight data. Make adjustments to the models to correct gross discrepancies.

3.6 Recommend simplified (not necessarily linear) models appropriate for use in parameter estimation programs for each of the unique flight modes of 3.4.

3.7 Provide MCAIR Report MDC A4637, Revision C, dated 11 January 1980, "YAV-8B Aerodynamic Stability and Control and Flying Qualities Report" at no cost.

3.8 Provide MCAIR Report MDC A5032 Addendum No. 1 dated July 1981 "YAV-8B Bulletin No. 158394" at no cost.

4.0 REPORTING

The contractor shall provide the following documentation:

4.1 Tables, functional plots, and equations of motion for the non linear model of 3.2.

4.2 Linear coefficients and equations of motion for the models of 3.4.

4.3 Listing and tape of the FORTRAN program of 3.3. Also, a complete description of the software, including top-level flow charts, program structure, subroutine interfaces, and data format.

4.4 Time histories from non-linear and linear models for each of the flight conditions analyzed.

4.5 A Final Report in contractors format which documents all analysis and results of this procurement.

4.6 Monthly letter progress reports.